THERMO-HYDRO-MECHANICAL BEHAVIOR OF UNSATURATED CLAYEY SOILS VIA THERMO/SUCTION-CONTROLLED RING SHEAR TESTING

By

JAIRO EDMUNDO YEPES HEREDIA

Presented to the Faculty of the Graduate School of
The University of Texas at Arlington in partial fulfillment of
the requirements for the degree of

DOCTOR OF PHILOSOPHY

THE UNIVERSITY OF TEXAS AT ARLINGTON

December 2015

Acknowledgements

This research project was accomplished thanks to the knowledge, leadership and help of Dr. Laureano Hoyos. I would like to thank all my committee members: Dr Anand Puppala, Dr. Sahadat Hossain, and Dr. Xinbao Yu, for all their help and guidance.

I also would like to thank all my classmates and lab mates for all their support during these four years of research. Finally, I would like to thank my family for all the support during this difficult research process.

November 12, 2015

Abstract

THERMO-HYDRO-MECHANICAL BEHAVIOR OF UNSATURATED CLAYEY SOILS VIA THERMO/SUCTION-CONTROLLED RING SHEAR TESTING

Jairo Edmundo Yepes Heredia, PhD

The University of Texas at Arlington, 2015

Supervising Professor: Laureano R. Hoyos

There is a lot of geotechnical infrastructure made of compacted soil, or resting on unsaturated ground, which involves a wide range of deformations. Calculation of foundation settlement, for instance, requires a good estimation of soil stiffness at relatively small strains. Analysis of natural and engineered earth slopes, embankments, and soil bearing capacity, on the other hand, requires good estimations of shear strength, from peak to residual.

Besides, despite the critical importance of the thermo-mechanical behavior of unsaturated soils in many geotechnical applications, the effect of relatively high temperature on shear strength and stiffness properties of unsaturated soils is not yet well understood, as thermo-mechanical testing of soils is more complex than conventional isothermal testing. Thermally induced changes in shear strength and stiffness properties of surrounding soils may have a significant impact on key design parameters.

To date, however, there is hardly any comprehensive study at the laboratory scale that has focused on a thorough characterization of shear strength and stiffness behavior of unsaturated soils, controlling temperature and suction at the same time. This type of research, though crucially needed as justified above, has been deterred in the past by the lack of suitable testing tools and techniques. It is precisely in this context that a fully servo/thermo/suction-controlled ring shear play a fundamental role in the thorough characterization of this type of materials. The lack of experimental evidence of this kind has been the chief motivation for this research work.

In this work, a novel suction-controlled ring shear apparatus was enhanced and upgraded to investigate the thermo-hydro-mechanical behavior of unsaturated soils under large and small deformations respectively, including peak and residual shear strength response, and dynamic properties. A series of tests were conducted on both devices controlling suction and temperature at the same time.

In terms of the strength behavior of the soil, it was confirmed that the higher the suction, the higher the strength of the soil, both peak and residual, and the higher the net stress, the higher the shear strength. In terms of the shear strain behavior of the soil, the increase in suction generated an increase in the shear modulus. Also, an increase in net stress, also resulted in a shear modulus increase.

Regarding the temperature, it was demonstrated that at higher temperatures than the average (20°C), the shear strength of the soil depends on the net normal stress applied and the failure surface was found in a depth close to the middle point of the height of the sample.

Table of Contents

List of Illustrations

List of Tables

Chapter 1

Introduction

In the field of geotechnical engineering, projects related with foundations, tunneling, slope stability, pavement design, earth structures, among others, always have to deal with partially saturated soils, specially in tropical regions. These type of soils have not been deeply studied when a project is being designed. Here, two aspects affect the practice of geotechnical engineering. First, above water table, unsaturated soils have capillarity that generates suction in the soil, and subsequently, additional strength to the soils that is not still considered in the design. Second, unsaturated soils, particularly clayed soils, tend to be problematic. Wetting and drying processes, this is, season changes, generate volume changes in soils that affect geo-infrastructure. These two aspects have not been studied as to have a good estimate that can be considered in the practice of civil engineering.

Unsaturated soil mechanics is a field inside geotechnical engineering that has had slow advances. One of the reasons is that soil mechanics, since it was officially considered a field of civil engineering, did not consider this region above water table, where soil is unsaturated. Besides, considering suction stresses in the state of stresses of the soil was an issue as it meant a change in the principle of effective stresses, which represent the actual strength of the soil. Finally, demonstrating and validating the effect of suction in soils experimentally in the laboratory, was also difficult.

A vast majority of geotechnical infrastructure made of compacted soil, or resting on unsaturated ground, involves a wide range of deformations. Calculation of foundation settlement, for instance, requires a good estimation of soil stiffness at relatively small strains. Analysis of natural and engineered earth slopes, embankments, and soil bearing

capacity, on the other hand, requires good estimations of shear strength, from peak to residual. The accurate assessment of residual shear strength parameters at relatively low net normal stresses and low suction states is of critical importance in slope stability analyses involving potentially shallow failures triggered by rainfall at relatively high degrees of saturation. Accurate assessments of residual shear strength parameters at much higher suction states, on the other hand, is of paramount importance in natural slopes in fissured rocks with unsaturated clayey fills that can undergo significant shear strength changes upon wetting, or shallow fissured landslides that can also be activated by wetting. Residual shear strength of unsaturated soils, particularly clayey soils, can also be used as a macroscopic indicator of the nature of the micro-structural changes experienced by the soils when subjected to drying (Merchán et al. 2011). Clays also undergo significant volume and pore-size distribution changes when subject to hydraulic paths (Romero et al. 2005, 2011). These changes can have significant effects on shear strength properties: For instance, the aggregated microstructure induced by drying is expected to enhance the soil's dilatancy effects and, consequently, affect the peak-to-residual shear strength properties of clayey soils (Merchán et al. 2008).

Several authors started working with unsaturated soils, looking for a way to include suction in the state of stresses of soil and to validate it in the laboratory: Coleman (1962), Fredlund and Morgestern (1977), Alonso (1990), Rahardjo (1995), Hoyos (1998), among others.

They have worked with several theoretical and practical models to try to solve this problem. However, and, as it is common in the laboratory, both boundary conditions and limited application of stresses are always present, and can only consider certain types and ranges of stresses and deformations.

Then, it is very well know that projects related with foundations, slope stability, tunneling, earth dams, among others, involve a large range of stresses and deformations, and commonly happen in unsaturated soils.

Considering these factors, it is mandatory to look for a more precise estimation of strength and strain behavior of unsaturated soils. This is, peak and residual parameters, and stiffness of the materials that are subjected to suction stresses.

A considerable part of this project is to improve the understanding of the importance of residual strength in unsaturated soils. A lot of work has been done to understand residual strength of saturated soils in the practice of engineering (Skempton 1964, Lupini 1981, among others). Besides, work has also been done to test this residual strength in the laboratory through the ring shear device (Bromhead 1979, Stark 1993, Meehan 2007, among others).

Now, when it is about unsaturated soils, not a lot of work has been accomplished to study and measure residual strength. Recently the Bromhead ring shear apparatus was modified to test soils under suction stresses (Infante 2005, Vaunat 2007) via axis translation and vapor transfer technique respectively. The results showed an increase in residual strength with the increase of suction.

The research work preceding this project (Velosa 2011) developed a fully servo/suction-controlled ring shear apparatus, that helped getting more precise conclusions about the influence of suction in the peak and residual strength of soils. Results showed that both peak and residual strength of the soils tested, increased as the suction increased. These tests were performed using the axis translation technique.

On the other hand, despite the critical importance of the thermo-mechanical behavior of unsaturated soils in many geotechnical applications, the effect of relatively high temperature on shear strength properties of unsaturated soils is not yet well understood, as thermo-mechanical testing of soils is more complex than conventional isothermal testing. Particularly, shallow and drilled shaft foundations located above ground water table and used as an integral part of ground-source heat pump systems, also referred to as energy foundations, are a promising technology for increasing energy efficiency of heating and cooling systems in residential and commercial buildings (Brandl 2006, Laloui et al. 2006, Bourne-Webb 2009). Thermally induced changes in shear strength properties of surrounding soils may have a significant impact on key design parameters, including side (skin) shear resistance, and hence the overall mechanical performance of these energy foundations.

To date, however, there is hardly any comprehensive study at the laboratory scale that has focused on a thorough characterization of shear strength behavior of unsaturated soils, from peak to residual states, over a large range of shear deformations and for a wider range of controlled suction states and simultaneously controlled thermal conditions. This type of research, though crucially needed as justified above, has been deterred in the past by the lack of suitable testing tools and techniques. It is precisely in this context that a fully servo/thermo/suction-controlled ring shear apparatus will play a fundamental role in the thorough characterization of this type of materials. The lack of experimental evidence of this kind has been the chief motivation for this proposed research work.

This work used the same fully servo/suction-controlled ring shear apparatus, to measure peak and residual parameters in a high plasticity clay was tested.

Both apparatus were modified to adapt a temperature controller and measure the effect of both temperature and suction in strength and strain of the soil at the same time. Results and analysis of this behavior are shown in this project.

The following sections summarize the main objectives, the previous work, the experimental program, the main research tasks, and the broader scientific and educational impacts of the proposed research work.

1.1 Research Objectives

The principal and general objective of this research project is to study the strength behavior of high plasticity clay (CH) controlling suction and temperature at the same time. This includes tests in the ring shear apparatus mentioned previously. The main idea is to measure: peak and residual friction angle and cohesion in the ring shear apparatus.

Particularly, this project has the following objectives:

1. To perform tests in the ring shear apparatus using axis-translation technique, applying net stresses from 25 to 200 kPa and matric suction values from 25 to 300 kPa, at a temperature of 20°C. This is made to study the effect of suction and net stress at an average temperature.
2. To perform tests in the ring shear apparatus, using matric suction values from SWCC curve using constant water technique (C-W). For these tests, ranges of temperature from 20°C to 40°C will be considered. This way, temperature and

net stress can be controlled at the same time. The effect of these three variables in the strength of soil were be analyzed.

1.2 Thesis Organization

Chapter 2 reviews the basic and fundamental concepts used to perform this experimental work including: axis translation technique, C-W technique, peak and residual shear strength, shear modulus and damping, the effect of temperature in the strength behavior of soil. This chapter will also show some results of previous work the helped to develop this project.

Chapter 3 gives a detailed explanation of the devices used to measure unsaturated shear strength behavior of soils and the material used.

Chapter 4 explains changes made to the procedures followed to perform the tests, both preparing the sample and running the test.

Chapter 5 shows the changes made to the ring shear in order to be able to change the temperature to the soil sample and consequently to measure its effect in the strength behavior of soil.

Chapter 6 presents all the tests performed during this project. This includes: ring shear suction controlled tests via axis translation technique at an average temperature (20°C) using both multi-stage and single-stage testing procedures, ring shear suction controlled tests via C-W technique at different temperatures (20°C to 40°C), and a comparison between the results of axis translation and C-W techniques.

Chapter 7 analyses all the results in terms of the strength behavior of the material tested, peak and residual failure envelopes, and tau-matric suction envelopes.

Both of them considering axis translation and C-W technique, different temperatures. Finally, both techniques will be compared.

Chapter 8 considers all the results from the tests performed during this project, and will draw conclusions based on them. Some recommendations for upcoming projects will also be explained.

Chapter 2

Theoretical and Experimental Background

2.1 Introduction

Research work in unsaturated soils has been a matter of concern in the last few decades. One of the reasons is that in these conditions, the soil experiences an increase in shear strength and stiffness that has not been considered in the practice of geotechnical engineering, and this is a phenomenon that always occurs above the ground water level, specially in clayed soils.

Considering both peak and residual strength, and stiffness properties in unsaturated soils, is a topic that does not have as much reported research as other topics.

First, residual strength in saturated soils has been a matter of interest to many authors (Skempton 1965, Stark 1994, et al.), but in unsaturated soils, there is still a lot of research to be done.

In order to measure this peak and residual strength in the laboratory, the ring shear device has been used. As a first approach, a conventional Bromhead ring shear apparatus was used to consider residual strength as an important parameter in saturated soil behavior.

Then, a couple of modifications were done to this conventional Bromhead apparatus to be able to measure residual strength, now in unsaturated soils. (Infante 2005) modified it in order to measure residual strength in unsaturated soils under low suction values using axis-translation technique. (Vaunat 2006) reported a modified Bromhead apparatus to test soils under high suction values via vapor transfer technique. All of these was done to test clayed soils, and an important conclusion was drawn, the higher the suction, the higher the strength of the soil.

In this work, a novel suction-controlled ring shear apparatus, recently implemented by Hoyos (2012), will be further enhanced and upgraded to investigate the thermo-hydro-mechanical behavior of unsaturated soils under large deformations, including peak and residual shear strength response, for a wider range of controlled net normal stresses, suction states, and thermal conditions (which ranges will be reported in the following chapters). The proposed enhancements will render a fully servo/thermo/suction-controlled ring shear (RS) apparatus for simultaneous testing of unsaturated soils via axis-translation technique. A comprehensive series of thermo/suction-controlled RS tests will be accomplished on several statically compacted ring-shaped samples of high plasticity clay. Thermo/suction-controlled testing in the lower suction range will be accomplished via the axis-translation technique. A digital convection heater, featuring internal fan and thermocouple, will also be adapted to the main cell of the RS apparatus for measurement/control of thermal conditioning in the pore fluids of the test soil. The enhanced thermo/suction-controlled RS apparatus will be the first of its kind to ever be implemented at any geotechnical research institution in the world. The experimental data and related analyses will be of great interest to both the geotechnical and the geological engineering communities worldwide, facilitating the incorporation of more reliable material properties in analysis/design models of crucial geotechnical infrastructure, including earth slopes, slopes in fissured rocks with clayey fills, and thermo-active energy foundations. The enhanced device will constitute a major advancement in state-of-the-art instrumentation for integrated research and educational activities at the University of Texas at Arlington (UTA), facilitating the exposure of civil engineering graduates to advanced concepts of unsaturated soil mechanics and its applicability in the analysis and design of critical civil infrastructure resting on or made of unsaturated soil materials.

The experimental program will have the unlimited potential to advance our understanding of the thermo-hydro-mechanical behavior of compacted geomaterials over a whole range of shear deformations. However, the most exciting prospect of all is that the intended experimental work may reveal something completely unanticipated, opening new vistas on the fascinating nature of unsaturated soil behavior.

In general terms, this chapter explains the fundamental concepts of: peak and residual strength, shear modulus and damping, effect of temperature in strength and stiffness, and important conclusions from previous work.

2.2 Fundamental Concepts

In this section, the fundamental concepts that are the basis of this entire project are reviewed. These concepts include techniques used to perform all the experimental program and theoretical concepts used to analyze the results and to draw conclusions.

2.2.1 Axis Translation Technique

The axis-translation technique was the first approach performed in the laboratory to test unsaturated soils subject to high values of matric suction. In order to get a constant value of matric suction (Ua-Uw), pore water pressure (u_w) is kept close to atmospheric pressure, so the pore-air pressure (u_a) is the matric suction required. Then, in any equipment (ring shear, or others) used to test unsaturated soils, as long as pore-water pressure (u_w) can be kept close to atmospheric conditions, the pore-air pressure (u_a) applied will be the matric suction.

This way, the matric suction ($u_a - u_w$) can be controlled much higher than the cavitation limit for water under negative pressure. The origin of reference for the matric

suction variable is translated from a state of atmospheric water pressure and negative water pressure to the state of atmospheric water pressure and positive air pressure.

In other words, pore-air pressure (u_a) and pore-water pressure (u_w) are translated to the positive pressure range, so the matric suction (Ua-Uw) applied to the soil, remains constant, regardless the magnitude of the pore-air pressure (u_a) (Bishop, 1960; Fredlund, 1989).

Figure 2-1 shows the application of the axis-translation technique to an unsaturated soil sample undergoing a matric suction of 101 kPa. Pore-water pressure (u_w) is measured below a saturated high-air-entry value of 202 kPa which acts as an interface that separates air and water phases. The water phase is originally under 101 kPa tension. An air pressure of 202 kPa is then applied directly to the specimen in order to rise (Ua) to the same magnitude. As a result, pore-water pressure (u_w) is increased by an equal amount, with a final positive value of 101 kPa.

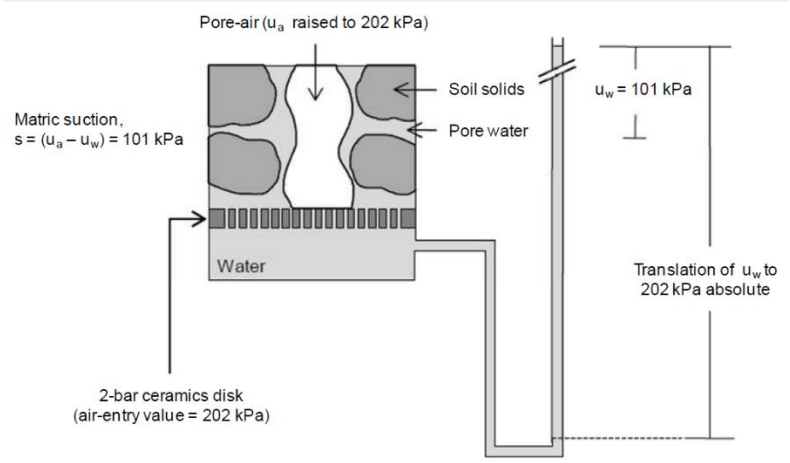

Figure 2-1. Concept of axis-translation technique (Velosa, 2011)

In spite of the translation of the reference pore-air pressure from 0 to 202 kPa, the matric suction (u_a – u_w) remains constant at 101 kPa.

As mentioned at the beginning of this section, if the pore-water pressure is kept in atmospheric conditions, the pore-air pressure (u_a) will be the matric suction that the soil experiences.

Even though the axis-translation is a good approach to test soils undergoing suction stresses, the technique has some limitations. Dineen (1997) defined limitations into two categories: equipment and materials. Equipment limitations are those related with the capacity of the device to resist high air pressures, the air pressure that the air supply can apply, and the limited air- entry value of the ceramic disks available.

Then, regarding the material limitations, the technique works well in those materials in which the air phase is continuous. If occluded air bubbles are present, high air pressures will cause the pore fluid to compress. This will develop pore pressure inside the specimen and a subsequent volume change. According to Booking and Fredlund (1980), the presence of occluded air bubbles will result in an overestimation of the matric suction.

In this project, the values of matric suction (Ua-Uw) used to test the soil samples via the axis translation technique were: 0, 25, 50, 75, 100, 200, and 300 kPa. Higher values of suction led the ring shear, for instance, to overcome the torque capacity (113 N-m).

2.2.2 Constant Water Technique

The constant-water technique is another approach to test unsaturated soils undergoing suction stresses. In this technique, the SWCC of the soil is the basis of its application.

For a certain value of matric suction ($u_a - u_w$), there will be a volumetric water content value (θ). Then, for a volumetric water content, a corresponding gravimetric water content (w) can be calculated.

This volumetric water content (w) is the value with which the soil sample will be prepared and tested. In this case, the test must be undrained, so the water content remains constant until the end of the test.

Shao-Kun and Mao-song (2013), defined SWCC as one of the most important tests to understand the behavior of unsaturated soils. They concluded that the key issue for the measurement of SWCC is how to control suction correctly and effectively. They used constant-water (C-W) technique to understand the behavior of Yunnan red clay in the south-west of China, getting a good approach. They found out that the effect of suction si more important in apparent cohesion than in friction angle. Figure 2-2 is an schematic of the application of this technique.

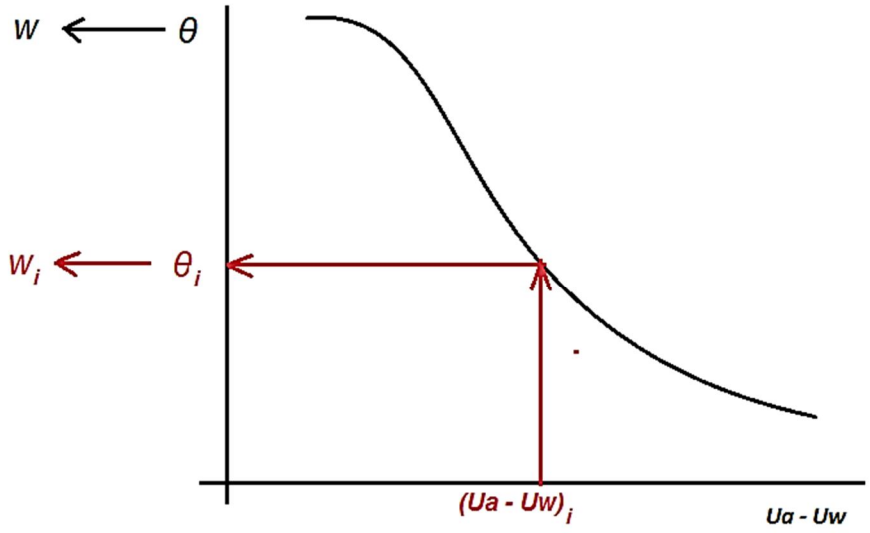

Figure 2-2. Schematics of the Constant-water technique

2.2.3 Unsaturated Peak and Residual Strength

When a shear stress is applied to the soil, shear strength will increase and shear strains will start to occur. At a certain point of application of shear stress, the soil will fail. This happens because the applied shear stress reached the strength of the soil, and it fails. This value is known as the “Peak Shear Strength”.

If after this failure point, shear stress is still applied, a decrease in shear strength will occur with a continuous increase in shear strain. At a certain application of shear stress, it will become constant with shear strain still increasing. When this happens, the soil reached residual state and the value of the shear stress will be the “Residual Shear Stress”. This concept applies both for saturated and unsaturated soils.

2.2.3.1 Shear strength

The shear strength of the soil represents one of the most important concepts in soil mechanics and geotechnical engineering. It defines the state of stresses at which the soil will fail. Therefore, it is very important to know the shear strength of the soil, specially in the practice of engineering.

Terzaghi (1936) proposed the principle of effective stresses for saturated soils, which main variable is the effective stress, σ’. This variable can be drawn in a τ - σ’ diagram, the Mohr-Coulomb theory, through Mohr circles. The equation proposed to get the shear strength of soils is:

$$\tau = c' + \sigma' \tan \varphi' \qquad (2\text{-}1)$$

Where:

τ = shear strength of soil

c' = effective strength parameter associated with cohesion

σ' = effective stress = $(\sigma - u_w)$

σ = total normal stress

u_w = pore water pressure

φ = effective strength parameter associated with the friction angle of the soil.

As mentioned before, the equation has been used for saturated soils. In the practice of geotechnical engineering, the soil is either dry or saturated, there is no middle point where a partial saturation can be present. The reality is that in situ, above the ground water level, there is soil that is partially saturated, but it is still not considered in engineering design and construction.

2.2.3.2 Unsaturated shear strength

There are plenty of practical problems that need to consider partially saturated soils, and calculate the unsaturated shear strength. The equation to calculate the effective stress now has to consider suction stresses, named the matric suction $(u_a - u_w)$. Bishop (1959) proposed the following equation to calculate the effective stress of unsaturated soils based on a modified effective stress variable, χ, which integrates both the matric suction (Ua-Uw) and the net normal stress $(\sigma - u_a)$, as follows:

$$\sigma' = (\sigma - ua) + \chi(ua - uw) \qquad (2\text{-}2)$$

Where:

σ = Total normal stress

u_a = Pore air pressure

u_w = Pore water pressure

χ = effective stress parameter that is a function of the degree of saturation of the soil.

The term $\chi(Ua-Uw)$ in equation 2-2, represents the interparticle stress due to suction. The term is often referred as suction stress. The figure ---- shows experimental work performed on different types of soils to correlate the effective stress parameter, χ, with the degree of saturation.

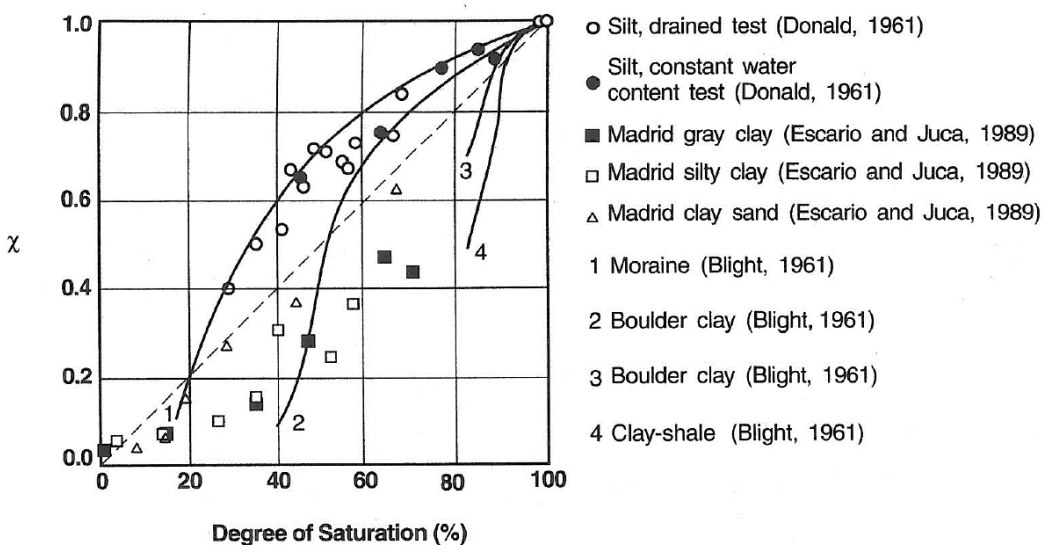

Figure 2-3. Experimental results showing the correlation between Bishop's effective stress parameter "χ" with the degree of saturation (Lu and Likos, 2004)

From figure 2-3, it is possible to conclude that Bishop's effective stress parameter, "χ" , increases approximately linearly with the degree of saturation. Bishop's effective stress equation has been criticized despite being widely used since its conception. Jenning and Burland (1962) mention that Bishop's equation is not very reliable because it does not consider volumetric changes the soil experiences during wetting processes.

Later, some authors proposed several approaches to try to describer properly the stress-strain behavior of unsaturated soils. Coleman (1962) suggested the use of two independent variables, the net normal stress (σ- u_a), and the matric suction (u_a – u_w), instead of only one effective stress variable.

Fredlund and Morgenstern (1977) through experimental work, demonstrated that both the shear strength and the volume change of unsaturated soils could be defined as a function of any two among three stress state variables: (σ- u_a), (u_a - u_w), and (σ- u_w). Finally, Fredlund (1978), considering this experimental results, proposed the following equation to describe the shear strength of unsaturated soils:

$$= c' + (\sigma - Ua)tan\varphi' + (ua - uw)tan\varphi^b \quad (2\text{-}3)$$

Where:

(σ-u_a) = Net normal stress

(u_a – u_w) = Matric suction

φ^b = internal friction angle associated with matric suction that describes the rate of increase in shear strength relative to matric suction

φ' = effective strength parameter associated with internal friction angle of soil that describes the rate of increase in shear strength relative to effective normal stress.

The first and second term in equation 2-3, as it is possible to infer, represents the Mohr-Coulomb theory for saturated soils. The last term represents the increase in shear strength with matric suction in unsaturated soils. Table 2-1 shows the results of experimental tests for a variety of soils in the literature, indicating the approximate range and variability of these shear strength parameters.

Table 2-1. Shear strength parameters measured for wide variety of soil types (Modified from Fredlund and Rahardjo, 1993)

TABLE 6.1 Shear Strength Parameters Measured for Wide Variety of Soil Types

Soil Type	c' (kPa)	ϕ' (deg)	ϕ^b (deg)	References
Compacted shale; w = 18.6%	15.8	24.8	18.1	Bishop et al. (1960)
Boulder clay; w = 11.6%	9.6	27.3	21.7	Bishop et al. (1960)
Dhanauri clay; w = 22.2%, ρ_d = 1580 kg/m^3	37.3	28.5	16.2	Satija (1978)
Dhanauri clay; w = 22.2%, ρ_d = 1478 kg/m^3	20.3	29.0	12.6	Satija (1978)
Madrid gray clay; w = 29%	23.7	22.5	16.1	Escario (1980)
Undisturbed decomposed granite	28.9	33.4	15.3	Ho and Fredlund (1982)
Tappen-Notch Hill silt; w = 21.5%, ρ_d = 1590 kg/m^3	0.0	35.0	16.0	Krahn et al. (1989)
Compacted glacial till; w = 12.2%, ρ_d = 1810 kg/m^3	10.0	25.3	7–25.5	Gan et al. (1988)

Source: Modified from Fredlund and Rahardjo (1993).

Figure 2-4 shows the failure surface for the extended Mohr-Coulomb criterion in a three dimensional space:

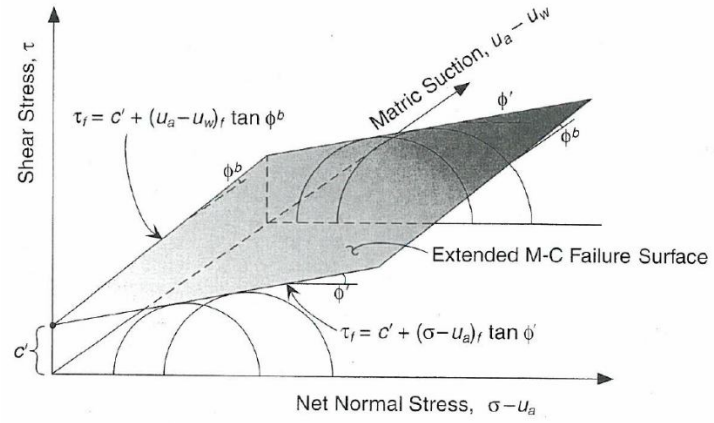

Figure 6.7 Extended Mohr-Coulomb failure surface for unsaturated soil.

Figure 2-4. Extender Mohr-Coulomb criterion for unsaturated soils (Lu and Likos, 2004)

The increase in shear strength due to matric suction, φ^b, was assumed to have a linear behavior when it was first proposed. This is a consequence of limited results published. Initial tests to measure shear strength in unsaturated soils were performed in a modified direct shear. Figure 2-5 shows a schematic of this device:

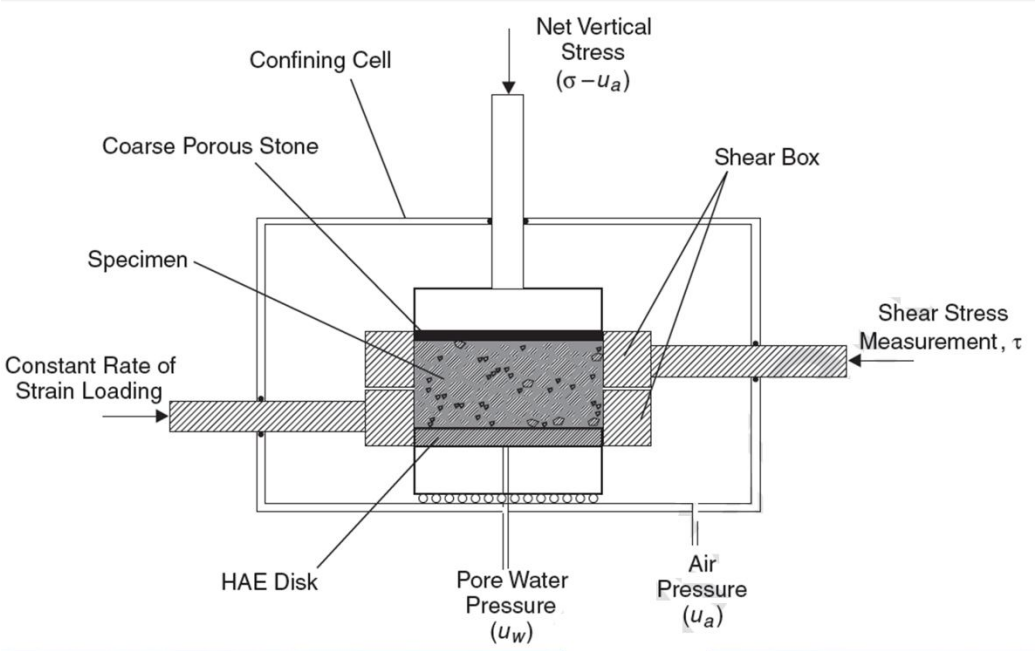

Figure 2-5. Schematic diagram of modified direct shear testing system for measuring shear strength of unsaturated soils (Lu and Likos, 2004)

Figure 2-6 shows results of direct shear tests on unsaturated Madrid gray clay performed by Escario (1980), in which it is possible to see the effect of matric suction on failure envelopes. From part (a) of the figure, $(\tau - \sigma)$ plane, it is possible to conclude that the shear strength of the soil increases with the increase in matric suction. The effect of suction in this case is mainly on cohesion, c'. The friction angle, φ', remains approximately constant.

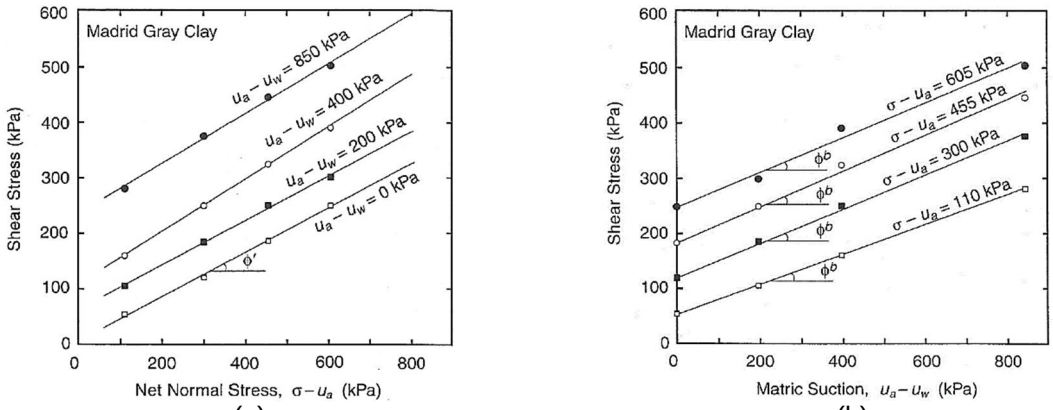

Figure 2-6. Direct shear testing results for unsaturated Madrid gray clay (data from Escario, 1980): (a) Peak shear stress as a function of net normal stress and (b) peak shear stress as a function of matric suction

After this initial conclusion that defines the friction angle associated with suction, φ^b, constant with the increase in matric suction, Fredlund and Rahardjo (1993) summarized results presented by other authors in the literature. They concluded that φ^b does not have a linear behavior. They demonstrated that φ^b is approximately equal to the friction angle, φ' , when soil is fully saturated, and is close to zero or may have negative values when matric suction has values that are close to residual saturation state.

Figure 2-7 show examples of experimental results that demonstrate the non-linear behavior in φ^b. In both figures, the data is in terms of peak shear stress as a function of matric suction, and they were performed using direct shear devices that were modified to control matric suction by axis translation.

The parameter φ^b defines the slope of the failure envelopes in a $(\tau - (ua - uw))$ plane. It is important to notice that an apparent softening behavior is observed for both soils where the value of φ^b either decreases (figure 2-7 (a)) or becomes negative (figure 2-7 (b)).

In figure 2-7 (a), Gan et al., (1988) performed tests in unsaturated glacial till. In figure 2-7 (b), Escario et al. (1989) confirmed this nonlinear behavior performing direct shear tests on Red silty clay and Madrid gray clay.

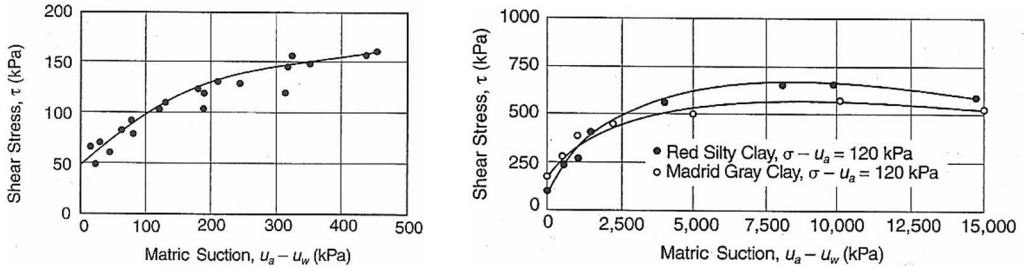

Figure 2-7. Examples of nonlinear behavior in relationship between shear strength and matric suction: (a) data from modified direct shear tests for unsaturated glacial till (Gan et al., 1988) and (b) data from modified direct shear tests for two clayed materials (Escario et al., 1989)

Recently, some authors (Rohm and Vilar, 1995, Pereira et al., 2006), have shown additional experimental data that show values of φ^b greater than φ' and an increase in φ' with matric suction.

2.2.3.3 Residual shear strength

When soils undergo shear stresses, their shear strength increases with increasing displacements, until it gets to a value where it fails. This is called the peak shear strength of the soil, which is the state of stresses where the applied shear stress reaches the strength of the soil.

After this point, the soils experience a decrease in strength with the continuous increase in displacement. There will be a point where the soils are not going to show more decrease in shear strength and it becomes constant, even if the displacement is still occurring. This shear strength is called the “residual shear strength”. At this point, a reorientation of soil particles will be carried out.

The residual shear strength is also defined in terms of the Mohr-Coulomb theory, but as a function of residual effective stress parameters. The following equation represents this residual behavior:

$$\tau_r = c'_r + (\sigma - uw) tan\varphi'_r \qquad (2\text{-}4)$$

Where:

τ_r = Residual shear strength

c'_r = Residual effective strength parameter associated with cohesion

φ'_r = Residual effective strength parameter associated with friction angle of the soil.

σ = Total normal stress

u_w = pore-water pressure

σ- u_w = Effective normal stress

In the practice of engineering, understanding in a proper way the concept of residual shear strength and its implications is very important for soils subjected to large deformations. Problems like long-term stability of slopes require a good estimation of residual strength. Randolph and Wroth (1982) mentioned that residual shear strength is the main strength present in the shaft of piles.

Skempton (1965) demonstrated through experimental work, that residual shear strength does not depend on the stress history of the soil, only in the nature of the soil particles.

2.2.3.4 Stress-strain behavior before residual shear strength

The stress-strain behavior of the soil is a function of the stress history of the soil. This behavior will be different if the soil is overconsolidated or normally consolidated. An overconsolidated clay will show an increase in shear stress at low shear strains until it gets the peak or the failure, and then it will show an important decrease in shear stress with a continuous increase in shear strain until it gets the critical state condition.

Critical state is the stress state that is reached when continuous shearing occurs at constant shear stress to normal effective stress ratio and constant volume. Then, at larger deformations, when particles already reoriented the strength decrease below the critical state and remains constant at residual stress.

In a normally consolidated clay, the peak is commonly lower than in overconsolidated clays, and the decrease in shear strength after the peak is not as dramatic before it gets to residual. This decrease in strength is a consequence of the orientation of particles in the direction of shearing.

Several authors have suggested ideas to explain the behavior of soil from peak to residual. Skempton (1964) defined that the magnitude of strength from peak to residual increases with the liquid limit. Lupini et al. (1981) and Skempton (1985) demonstrated that the reorientation of particles will only have an important influence in clayed soils that have platy clay minerals and that have a clay fraction greater than 20% (Skempton 1985).

Silts and sandy clays, even at large deformations, will show a peak strength that is low than normally consolidated clays and the drop to residual strength is a consequence of the water content increase (Skempton, 1985).

Considering all these ideas reported in the literature trying to correlate residual strength with clay fraction or plasticity index, several authors summarized and reported all these data, as it is possible to see in figure 2-8. In figure 2-8 (a) Lupini (1981) summarized them in terms of the residual friction angle, φ'_R, and the clay fraction, including experimental data reported by Skempton (1964) from direct shear tests. In figure 2-8 (b), Seycek (1978) shows results from authors suggesting that there is a better correlation between φ'_R and plasticity index.

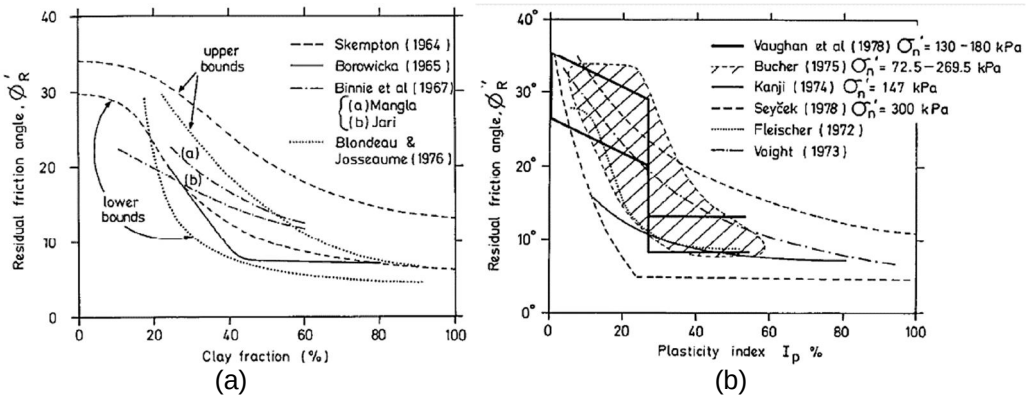

Figure 2-8. Correlations for residual friction angle with clay fraction and plasticity index.

Even though these correlations show a pattern, Lupini (1981) suggested that these correlations are not definitive, because they do not consider properties like mineralogy, pore-water chemistry, and particle shape.

These properties have an important influence in residual strength of soils. Besides, Stark and Eid (1994) defined that these correlations overestimate the drained residual friction angle.

2.2.3.5 Residual strength in the laboratory

There are two methods to assess the residual shear strength of soils: in the laboratory, and through a back analysis evaluation method. The second method is theoretical and require the assumption of some properties that can make the method produce uncertain results.

The most common methods to calculate residual shear strength are: modified direct shear, modified triaxial, and ring shear. Direct shear and triaxial tests were modified because they were initially created to assess only peak shear strength. On the other hand, ring shear was initially designed to measure both peak and residual shear strength.

Direct shear test is the most common method to calculate residual shear strength. Due to the limitation of the travel length of the shear box, large deformations are achieved by repeated reversals or by repeated uni-directional shears.

The advantages of the test are: availability of equipment, ease of operation, short duration of tests due to short drainage. The main disadvantage of the test is that the soil shears backward and forward until a minimum shear resistance, so the shearing is not continuous (Skempton, 1985).

Besides, the cross sectional area of the soil sample changes during shearing, producing local concentration of strains. Bromhead (1979), and Stark and Eid (1994) reported that these limitations among others yield higher residual strength values than those from ring shear.

Triaxial test is more complicated to modify in order to measure residual strength than direct shear. The major disadvantage of this equipment is that, to get large deformations, the sample has to suffer severe damage. Additional disadvantages are the corrections that need to be made due to: effect of rubber membrane, change in cross-sectional area of failure plane, and horizontal component of the ram load if the loading cap is not capable of lateral movement. Petley (1966) demonstrated that the deformation to get residual state could be reduced by smoothing the pre-cut shear surfaces with a piece of glass drawn over the surfaces in the direction of shear.

In any case, adapting the triaxial device to measure residual strength ends up being complicated, and for practical purposes, the test becomes unsuitable.

Ring shear test was specially developed to measure residual strength, although it can calculate both the peak and residual strength of soils. The ring shear device was actually designed to overcome several disadvantages of the conventional shear box.

The apparatus accommodates a ring-shaped specimen as shown in figure 2-9. The basic procedure of the test is as follows: an annular remoulded soil specimen is confined radially between concentric rings and vertically between porous annular discs with relatively rough surfaces. A net normal stress is applied until consolidation is achieved, and finally shearing is performed until soil sample gets peak and residual strength.

The two most important advantages of the ring shear are that it has an unlimited rotational shear displacement that can be applied to the soil sample continuously without having to stop and reverse the shearing movement as in the shear box, and that its cross-sectional area of contact on the shear plane remains constant.

This unlimited continuous displacement allows full orientation of the clay particles parallel to the direction of shearing and the development lf a true residual strength condition.

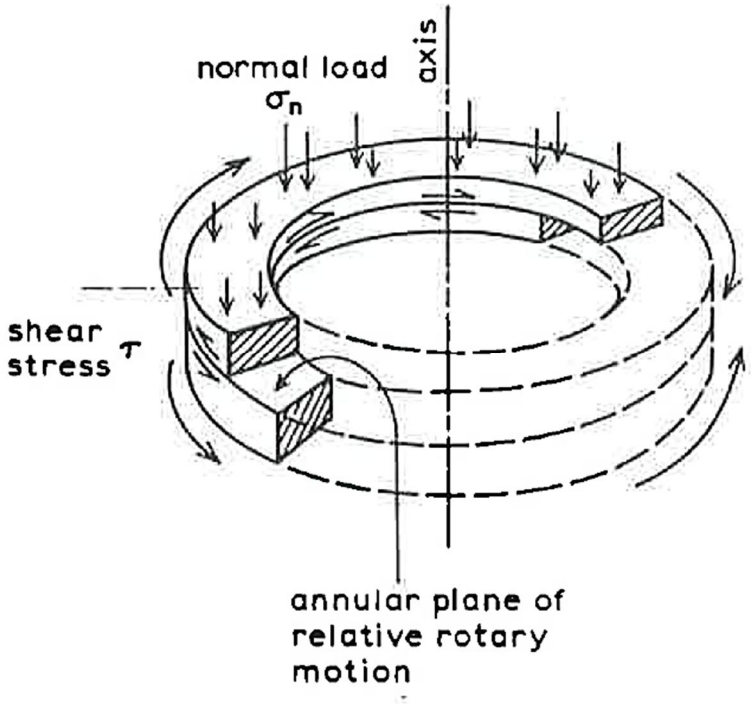

Figure 2-9. Principle of ring shear test (after Bishop et al., 1971)

Figure 2-10 shows two Squematics of approaches to the ring shear device explaining the procedure of the test and how the application of stresses is accomplished. Figure 2-10 (a) is an annular-split-ring device with the shear region at mid height developed in Imperial College of London and in Norwegian Geotechnical Institute. Figure 2-10 (b) presents an annular-solid-ring device with the shear region at the top of the specimen developed by Bromhead (1979).

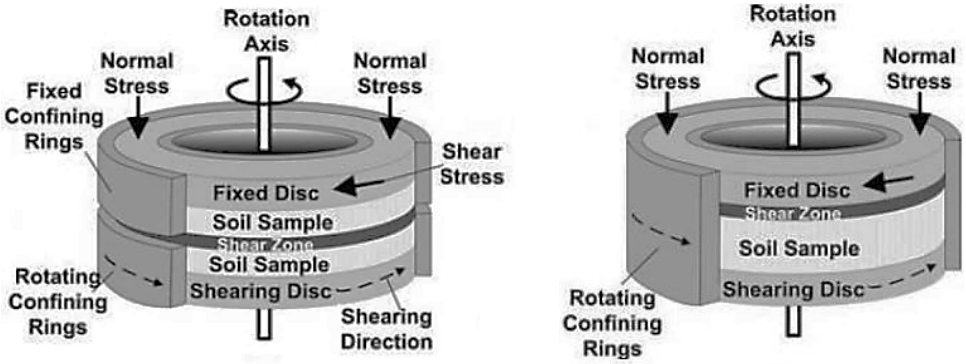

Figure 2-10. Ring shear mechanism

The Bromhead apparatus developed by Professor E.N. Bromhead at Kingston University (Bromhead 1979) is designed only to assess residual strength of cohesive soils, for which small remoulded samples are adequate. Figure 2-11 (a) and (b) shows a schematic diagram of how the Bromhead apparatus works. Vertical pressure is applied to the soil sample through the upper porous annulus by means of a lever-arm arrangement using hanger weights. The cell which contains the specimen can be removed and submerged in a water-bath during the test. The lower part of the cell is rotated by a motorised drive unit while the upper part is restrained by a matched pair of calibrated load rings, which enable the restraining torque to be assessed. Figure 2.12 shows a plan view of the Bromhead apparatus. This shows a schematic diagram of the torque arm positioning.

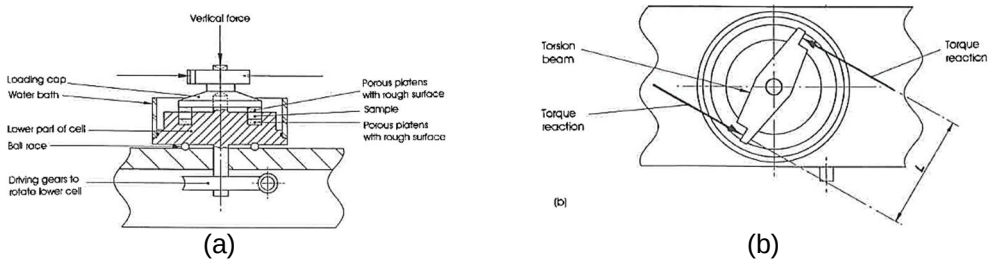

Figure 2-11. General arrangement of ring shear apparatus (Bromhead, 1979)

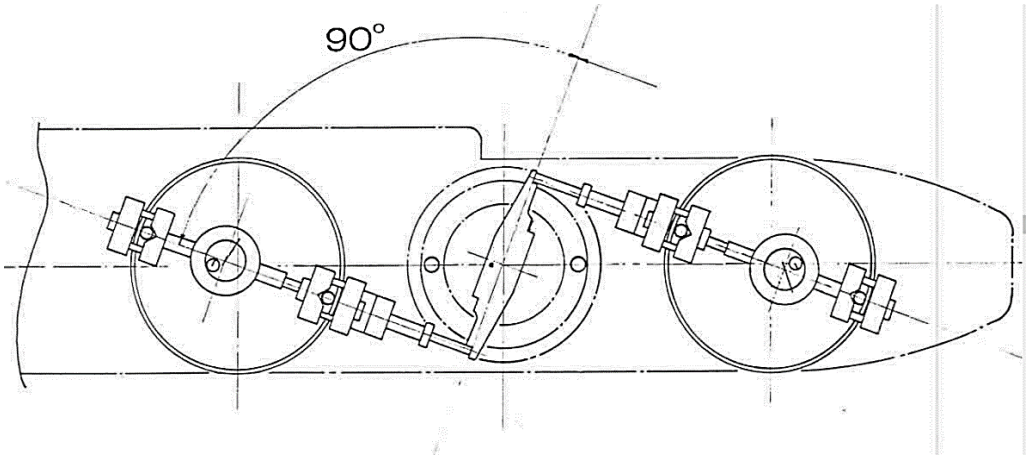

Figure 2-12. Diagrammatic view of torque arm positioning (Bromhead, 1979).

Figure 2-13, shows a typical result from Ring Shear testing in terms of peak strength, residual strength and displacement. Figure 2-13 (a) presents the increase in shear stress with the increase in rotational displacement until it reaches the strength of soil (peak strength), and then, with a continuous increase in rotational displacement, an important decrease in shear strength occurs. When this shear strength becomes constant, the residual shear strength is achieved. Figure 2-13 (b) shows the peak and residual failure envelopes. In this figure, it is possible to see three points that help plotting the envelopes. Each one of these points is one single curve like that in figure 2-13 (a).

Therefore, in order to get those three points and draw the failure envelopes, three curves like the one in figure 2-13 (a) need to be performed in the laboratory.

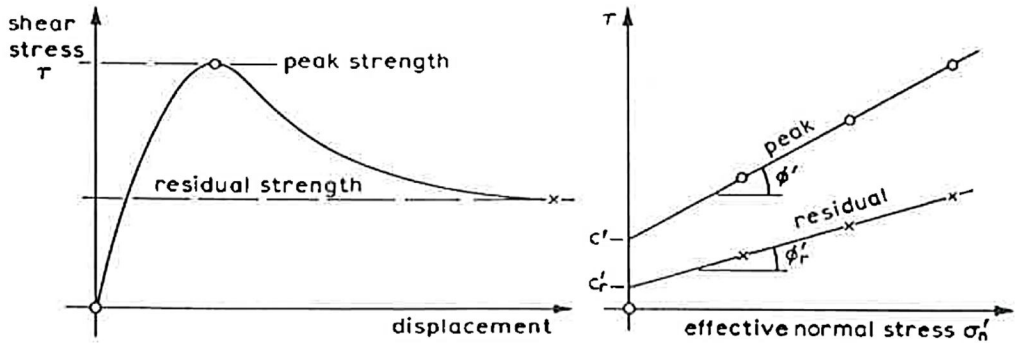

Figure 2-13. (a) Peak and residual shear strength (after Skempton, 1964)

The development of the ring shear device has several decades of hard research work. A.S.C.E. (1917), Streck (1928), Gruner and Haefeli (1934), Cooling and Smith (1936), Langer (1938), Tiedemann (1939) and Hvorslev (1939), were the first approaches to develop the ting shear device, which were mainly stress-controlled. Hvorslev (1947) designed a first approach to a both stress and strain controlled ring shear device.

Then, it was not until 1970 when the development of this device took place again. La Gatta (1970) from Harvard University, Bishop (1971) in Imperial College London and Norwegian Geotechnical Institute, and Bromhead (1979) in Kingston University, developed a ring shear device that could test annular or solid disc-shaped soil samples with either solid of split confining rings. Sample loss through squeezing between the confining rings is regulated by a precise gap control mechanism. Both the Harvard and the Imperial College/Norwegian Geotechnical Institute were strain-controlled.

Based on this important progress, ring shear became a widely known device and a reliable way to measure drained residual strength in clayed soils. The main advantage, as mentioned before, the unlimited continuous displacement that let the test guarantee that the residual state has been achieved.

Testing soils in these two proposed devices had problems related with availability because of the cost. Bromhead (1979) developed a ring shear device previously explained in this section, which was inexpensive and the time of the test was shorter. This was because consolidation occurred fast due to the thin, annular specimen, which had a short drainage path length. Then, Bromhead apparatus became the most used ring shear device used at that time.

Bromhead (1986), Stark and Vettel (1992), Meehan et al (2007), defined as a disadvantage the wall friction that there was between the inner and outer circumferences of the confined soil sample. This wall friction influences because it increases the shear plane.

Several authors in the last years have tried to develop different procedures to try to overcome the disadvantages of the test, like: soil extrusion, top platen intrusion and the wall friction previously mentioned.

Anyi (1988, 1989) adapted vanes into the porous stone and increased the thickness of the specimen from 5mm to 10mm, to try to find a failure plane at some depth inside the sample and not at the top, in order to avoid soil extrusion. Stark and Vettel (1992) proposed the “flush test” which limits the total settlement of the top porous stone due to consolidation and/or shearing to 0.75mm. They recommended only one sample per test and concluded that the flush test gives the lowest residual strength and agrees with insitu behavior.

Stark and Eid (1996) modified the Bromhead apparatus to have constant volume conditions. Results were in total agreement with direct shear results. Meehan (2007) compared results from single-stage and multi-stage tests using the Bromhead apparatus, and found differences of 10-15% in the secant residual friction angle, concluding that it was due to top platen intrusion and wall friction. In order to reduce wall friction they changed the inside and outside edges or the porous stone loading platen back to 45 degrees bevel. They also reported that both single and multi-stage yielded the same residual strength, so the modified platen eliminated wall friction.

Sadrekarimi and Olson (2009) from The University of Illinois designed a new ring shear device to perform constant volume or drained tests. This device has an additional load and torque cell that take into account wall friction developed along the confining rings, and they use quad-rings along the confining rings to avoid soil extrusion.

2.2.4 Effect of Temperature in Shear Strength Behavior of Soil

Thermal effects on saturated strength parameters: this topic has been studied for several decades. The study of the influence of temperature started around 50 years ago and it was not related directly with strength parameters, but with classification parameters.

The first approach to investigate in a direct form, the influence of temperature on strength, was studying the effect in the effective stress, particularly, the pore water pressure. When temperature increases with pore water pressure, the effective stress, and consequently the strength of soils decrease to a point where it can cause failure.

Moreover, Campanella and Mitchell (1968) demonstrated that the cyclic temperature change resulted in a hysteretic change in pore water pressure. Hueckel and

Baldi (1990) performed undrained triaxial tests at constant deviator stress and showed that a rise in pore water pressure due to monotonic heating caused failure to the soil specimen.

After this, researchers started to focus directly on measuring strength parameters. Sherif and Burrous (1969) and Maruyama (1969) studied the thermal effects on shear strength by performing unconfined compression tests on saturated normally consolidated clays. The results showed that by increasing temperature, pore water pressure increased and thus undrained shear strength decreased.

Thermo-hydro-mechanical models for unsaturated soils: Several models have been proposed to deal with this behavior. Philip and De Vries (1957) developed a model for coupled heat and moisture transfer in rigid porous media under the combined gradients of temperature and moisture.

Geraminegad and Saxena (1986) presented a de-coupled flow-deformation model, including the effect of matrix deformation on moisture, heat gas and flow through the porous media. They defined the mechanical behavior of the soil in terms of the stress state surface and the independent stress state variables in which the total stress tensor in excess of air pressure and suction are considered independent.

Khalili and Loret (2001) presented a theory for heat and mass transport through deformable unsaturated porous media. This work focused on fully coupled isothermal flow and deformation in variably saturated porous media to include thermal coupling effects.

In general terms, most of the models available in the literature end up in a conclusion that temperature affects soil strength.

Measurement of the influence of temperature in the laboratory: Several devices have been developed to take into account the effect of temperature in soil strength. Some of them are mentioned in this work. Most of them are triaxial devices or modified conventional triaxial devices and oedometers.

Mitchell and Campanella (1963) developed a temperature-controlled triaxial equipment to study creep in saturated clayed soils. A triaxial cell is placed in a heating chamber that has air pressure at an elevated temperature controlled by a thermostat. The temperature of the chamber is changed by circulating heated water through the triaxial cell until it reaches the required temperature. The equipment is capable of applying temperatures of 40°F to 140°F and is measured by a thermocouple. Figure 2-14 shows a schematic diagram of this equipment.

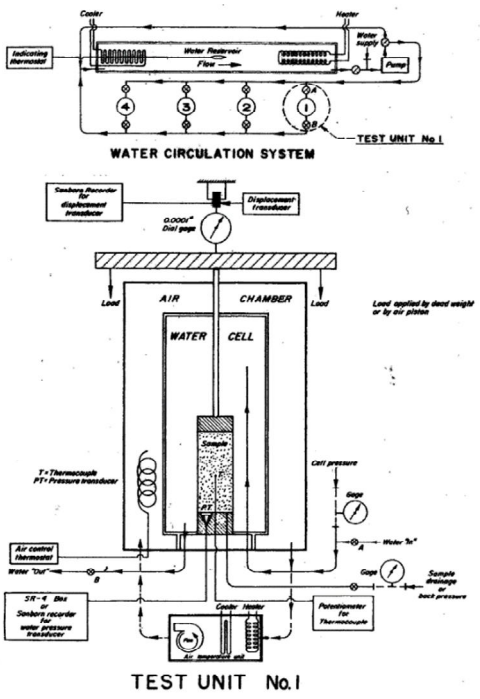

Figure 2-14. Temperature-controlled triaxial test system (Mitchell and Campanella, 1963)

Paaswell (1967) developed a temperature-controlled consolidometer for studying temperature to study its influence on clayed soils. The device is capable of heating the specimen and of measuring the temperature at certain points. A fixed ring consolidometer was used to locate the heater in the water bath that surrounds the specimen. Temperature was measured by thermocouples. Figure 2-15 shows the device.

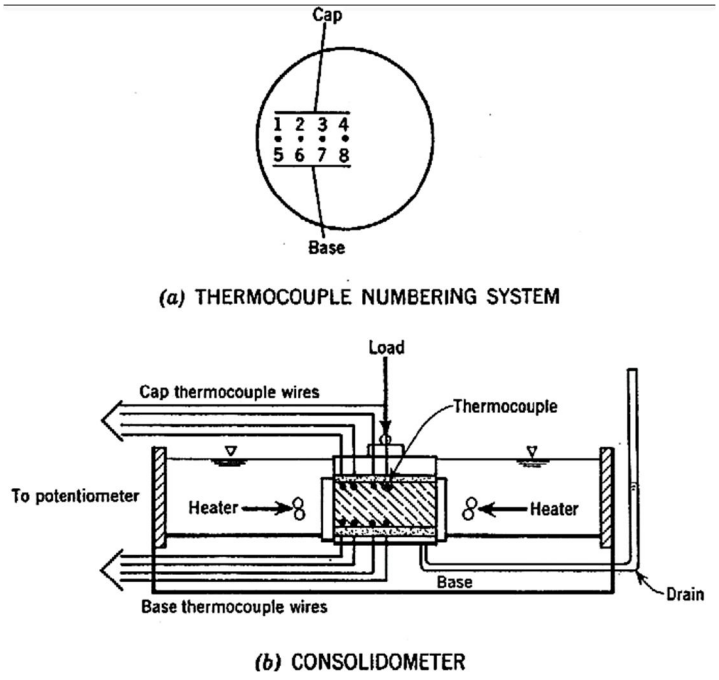

Figure 2-15. Scheme of the temperature controlled consolidometer (Paaswell, 1967)

De Bruyn and Thimus (1996) developed a high temperature triaxial cell. The sample is heated by fluid through a copper spiral which can apply temperatures up to 80°C. Sensors are located inside and outside the cell. The normal load is applied by external load transducers.

An advantage is that this transducer is not sensitive to temperature and confining pressure changes in the cell. Figure 2-16 shows a schematic diagram of this device.

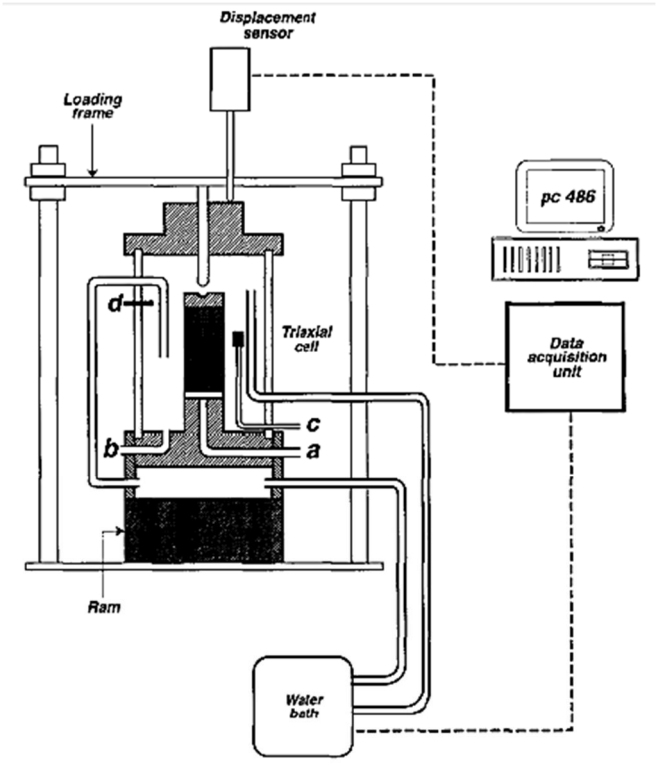

a: Pore-water pressure measurement

b: Confining pressure measurement

c: Temperature sensor (close to the specimen)

d: Temperature sensor (in confining liquid)

Figure 2-16. Diagram of high-temperature triaxial cell (De Bruyn and Thimus, 1996)

In the “previous work” section, other lately developed devices to study thermo-hydro-mechanical behavior of unsaturated soils are explained with their corresponding representative applications

2.2.5 Previous Work

2.2.5.1 Unsaturated peak and residual shear strength

Initial approaches to try to measure residual strength in soils started in the 1980's. Researchers modified devices like triaxial and direct shear to achieve this goal. These type of approaches were presented by Escario and Saenz (1986), Gan and Fredlund (1988), Yin (2003), among others. Nevertheless, these modifications to conventional devices had a limited shear deformation along the failure surface after peak failure condition was reached. This did not guarantee that residual condition was actually condition. Based on this limitation, a ring shear apparatus was developed by Bromhead (1979) and the modified to perform tests on unsaturated soils. The ring shear technique was developed to overcome certain disadvantages of the conventional direct shear box in the measurement of residual shear strength. The apparatus accommodates a ring-shaped specimen inside an annular space allowing application of unlimited rotational shear displacement to the specimen, without having to stop and reverse the shearing movement, while the area of contact on the shear plane remains constant. The ring shear testing technique has been utilized since the early 1930's to assess the residual strength of geomaterials or the interface strength between composite geomaterials (e.g., landfill liners, geosynthetics). The most recent works, including standards ASTM D6467 and ASTM D7608, for a wide variety of geotechnical applications, have been reported by Stark and Vettel (1992), Stark and Poeppel (1994), Stark and Eid (1994, 1997), Stark and Contreras (1996), Iverson et al. (1997), Kamai (1998), Jones and Dixon (1998), Watry and Lade (2000), Garga and Infante (2002), Wang and Kwong (2002), Wang and Sassa (2002), Mancktelow et al. (2002), De Gennaro et al. (2002), Shinohara and Golman (2002), Karakouzian and Hudyma (2002), Olsen (2002), Groger et al. (2003), Wang et al. (2003), and Stark et al. (2005), among several others.

Infante et al. (2005, 2007) modified the Bromhead ring shear apparatus to be able to test unsaturated soils under low suction states using axis-translation technique. The modifications allowed the device to measure air pressure and net normal stress independently, and the dimensions of the sample were increased. It allowed the measurement of unsaturated residual shear strength in soils under constant volume, consolidated drained test or constant water content conditions (matric suction values ranging from 0 to 500 kPa). Besides, the device is capable of studying changes in soil water characteristic curve (SWCC) during shearing process. They stated that the best way to predict shear strength is from SWCC at critical state (Infante et al., 2010).

Figure 2-17 shows a picture of the modified Bromhead ring shear apparatus whit the following components (explained by Velosa, 2011): (1) LVDR to measure vertical deformation, (2) load cells to measure the torque, (3) pressure transducer to monitor the pressure of the air phase, (4) rotational potentiometer to measure the angular displacement of the cell with respect to the top platen, (5) Load cell to measure the normal load, (6) Precise electronic balance to measure the water content change of the specimen.

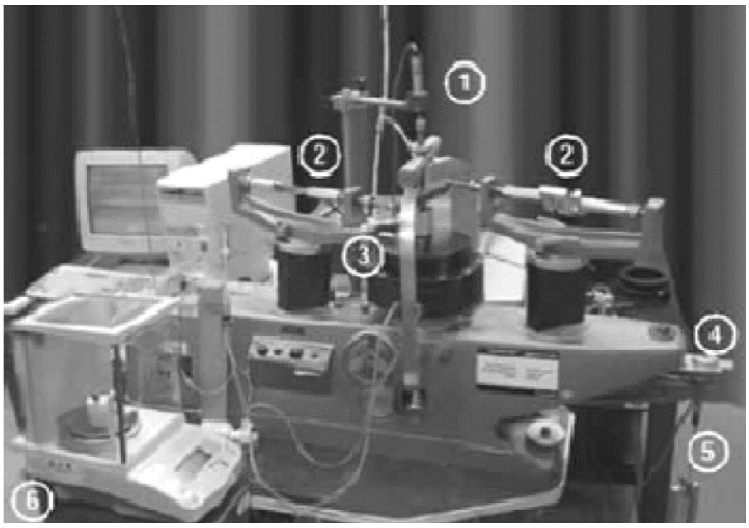

Figure 2-17. Modified Ring Shear apparatus (Infante et al., 2007)

Another approach to modify the Bromhead ring shear apparatus was developed by Vaunat et al. (2006, 2007). In this new modification the device was capable of measuring unsaturated residual strength under high suction states and now using vapor transfer technique. Clayed soils were tested and they concluded that the residual friction angle increased with the increase in suction stresses. They also stated that unsaturated residual strength of soil was independent of both the normal stress and the suction stress history. Figure 2-18 presents this last modified ring shear apparatus. In this case, the shear box was isolated by a glass-cap in order to apply the vapor transfer technique. The shear box was connected to a circuit of forced convection of vapor. Relative humidity was controlled through circulation of air above a solution saturated with different types of salts.

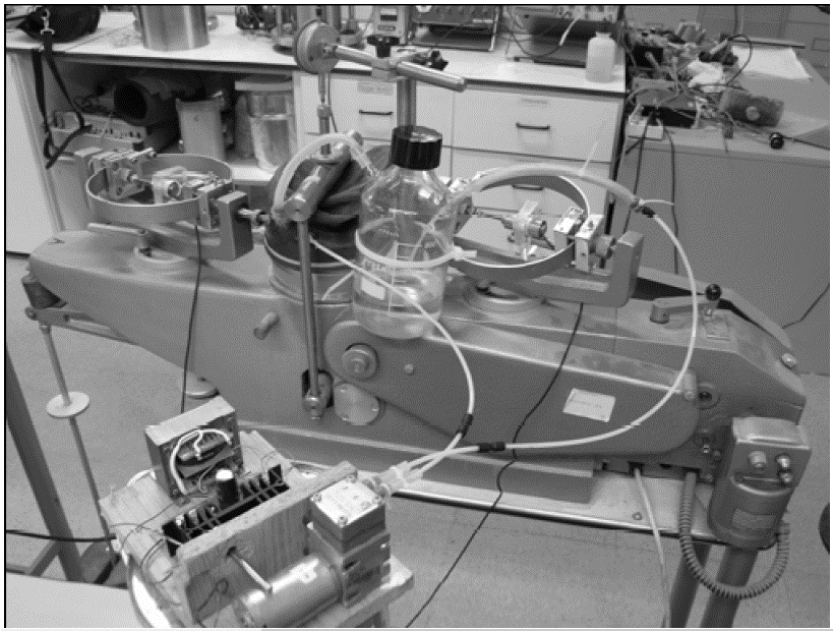

Figure 2-18. Modified Bromhead ring shear apparatus (Vaunat et al., 2006)

However, virtually none of these efforts has dealt directly with ring shear testing of clayey soils under controlled thermal and/or suction states; hence very scarce experimental data of this type have been reported in the literature.

Only a short handful of researchers have recently begun experimental trials with new test methodologies, including Vaunat et al. (2006, 2007), Infante Sedano et al. (2007), and Merchán et al. (2011).

The main focus of these pioneering efforts has been on adapting and expanding the testing capabilities of existing Bromhead-type devices for soil testing under controlled-suction states via either vapor-transfer or axis-translation technique.

Despite the crucial findings of these dedicated few, highlighting the key role played by matric suction, a comprehensive and thorough experimental effort has yet to be undertaken in order to obtain a thorough set of suction-dependent residual failure envelopes for soils tested at a wide range of suction states and thermal conditions; and to investigate the effects that both the original soil structure and the pre-shearing/thermal/suction histories may have on the residual shear strength properties of unsaturated soils.

The present research work is partly motivated by these research needs. Another important limitation of the Bromhead-type ring shear systems adapted in these previous efforts is that they only allow for suction-controlled testing through either axis-translation technique (Infante Sedano et al. 2007) or vapor-transfer technique (Merchán et al. 2011); while neither one features and independent thermally-controlled processing unit.

More recently, Hoyos et al. (2011) implemented a fully servo/suction-controlled RS apparatus suitable for soil testing at large deformations via axis-translation technique (which will be thoroughly explained in the following chapters). The general design of its core system is also similar to that of the original Bromhead device (Bromhead 1979). A full description of its development, including details of its main components, assembling, and performance verification against the original Bromhead apparatus, are presented by Hoyos et al. (2011). Recently, a series of suction-controlled RS tests were conducted on silty clayey sand (SM-SC) soil. Although not the ideal soil for ring shear testing, silty clayey sand was selected because of its relatively coarse nature, low plasticity, and poor gradation, which minimize the required time for pore-fluid equalization. The work was more intent on developing a novel servo/suction-controlled device, rather than simply adapt an existing Bromhead apparatus.

It turned out to be a 4-year effort, with much time required to design, test, modify, and calibrate the system, including software development/programming, after several preliminary test runs.

Figure 2-19 (a) shows a photo of the main cell and the rotational shear system, including pneumatic actuator for normal loads and electromechanical rotary actuator for torque loads. Figure 2-19 (b) shows the change of residual beta angle ϕ^b_r with matric suction for different net normal stresses. The data are fitted by second-degree polynomial functions. The residual beta angles start at a constant value of 22.09° ($\phi^b_r = \phi'_r$) under saturated state, s = 0; then increase ($\phi^b_r > \phi'_r$) until a suction state close to the air-entry value of the soil, s = 28 kPa (Hoyos et al. 2011); and finally decrease gradually ($\phi^b_r < \phi'_r$) to as low as zero, or even negative values, for higher suction values. This decrease is observed to be more dramatic at higher net normal stresses.

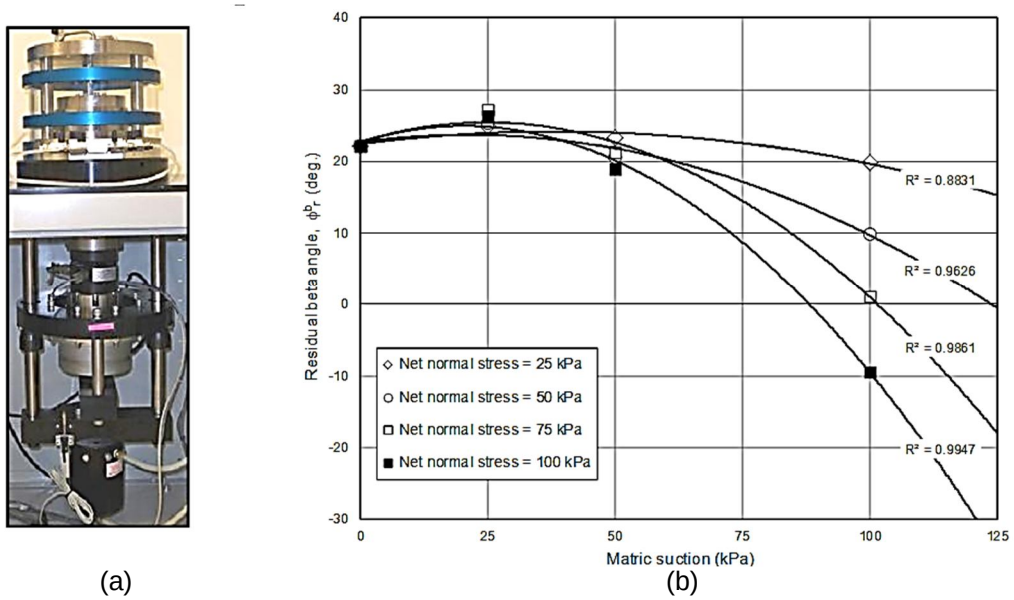

Figure 2-19. Preliminary ring shear testing on compacted SM-SC soil (Hoyos et al. 2011)

Figure 2-20, shows a picture of the servo/suction controlled ring shear apparatus and its basic components. Despite this device was thoroughly explained by Hoyos et al (2011), chapter 4 will give some insights of its components and performance.

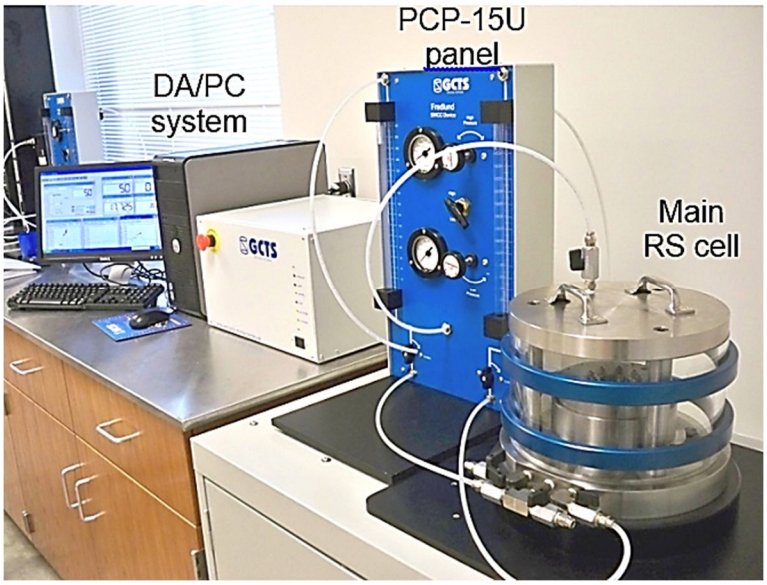

Figure 2-20. Servo/suction controlled ring shear apparatus (Hoyos et al., 2011)

Vanapalli et al. (1996) and Lu and Likos (2004) reported that there is a direct correspondence between the nonlinear nature of the peak shear strength envelope, with respect to increasing matric suction, and the soil-water characteristic curve (SWCC). Within the regime of relatively low suction, and prior to the air-entry pressure, the soil pores remain essentially saturated, the failure envelope is virtually linear, and the beta angle φ^b is effectively equal to the friction angle φ'. As the soil becomes unsaturated, the reduction in the volume of pore-water effectively reduces the contribution of suction toward increasing shear strength.

This effect is more pronounced as the net normal stress increases, as observed in Figure 2-20 (a). Matric and total suction states, as well as pore-fluid temperature, are expected to have as critical an impact on peak and residual shear strength properties of compacted clayey soils with air-entry values considerably higher than that of a silty clayey sand. As previously mentioned, the scarcity of experimental evidence of this kind has been the chief motivation for this proposed research work.

2.2.5.2 Effect of temperature in shear strength behavior of soil

Even though this section is mainly developed to consider previous work on shear strength, some references that deal with volumetric changes and compressibility are mentioned. The purpose is to emphasize that most of the research available in the literature, regarding thermo-hydro-mechanical behavior of soil consider volume changes more than strength of the materials.

In this section, some previous work regarding the influence of temperature in the strength behavior of soils is reported. Most of the research in this field consider mainly tests in modified triaxial cell, isotropic cell, and consolidation tests. Other references also present some results from shear test, swelling and shrinkage, water infiltration, water retention, infiltration tests, thermal gradient, and thermohydraulic cell.

Lloret and Villar (2006) study the thermo-hydro-mechanical behavior of bentonite in a project called FEBEX (Full-scale High Level Waste Engineered Barriers). They studied these clayed soils through fabric characterization, water retention, permeability, swelling capacity, mechanical behavior, the influence of salinity and the effect of temperature. They concluded that the behavior of the clay may be explained taking into account the changes in its double-level structure, micro and macro.

The transfers between intra-aggregate adsorbed water – of density higher than that of free water – and inter-aggregate free water could explain most of the features related to the temperature and salinity changes.

Francois et al. (2007) presented a unified thermo-mechanical experimental study on a remoulded unsaturated sandy silt, which was carried out in two thermo-hydro-mechanical (THM) cells, one isotropic and one oedometric. In figure 2-21, a schematic shows the main components of both equipment used for the experimental program.

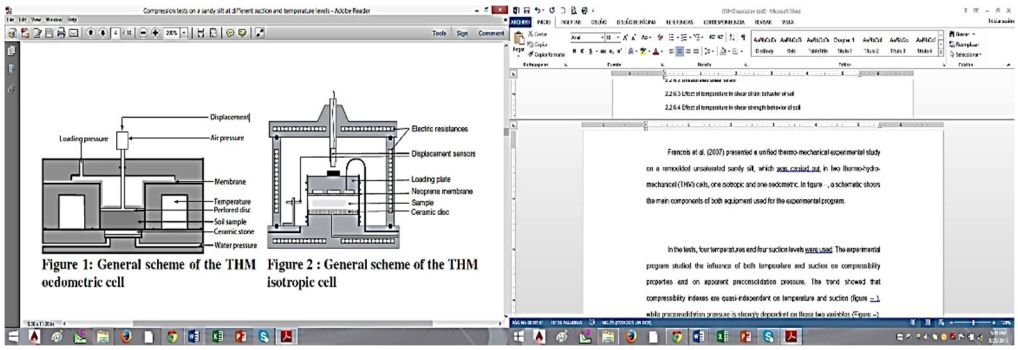

(a) (b)

Figure 2-21. General schemes of the equipment used in this study: (a) THM oedometric cell, (b) Isotropic cell.

In the tests, four temperatures and four suction levels were used. The experimental program studied the influence of both temperature and suction on compressibility properties and on apparent preconsolidation pressure. The trend showed that compressibility indexes are quasi-independent on temperature and suction (figure 2-22), while preconsolidation pressure is strongly dependent on these two variables (Figure 2-23). It is possible to see that apparent preconsolidation pressure decreases with temperature, but increases with suction, which seems to be coherent.

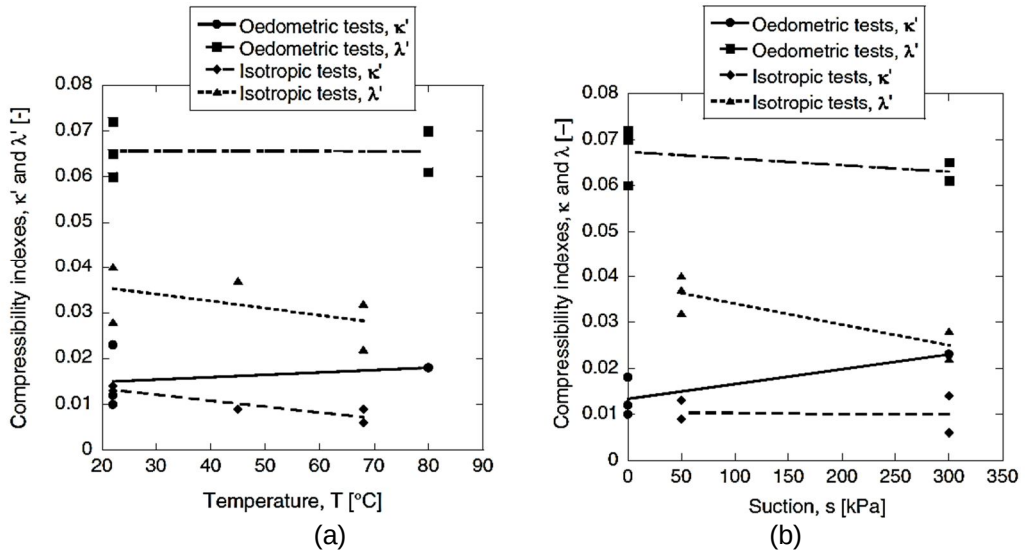

Figure 2-22. Effect of temperature and suction on compressibility indexes

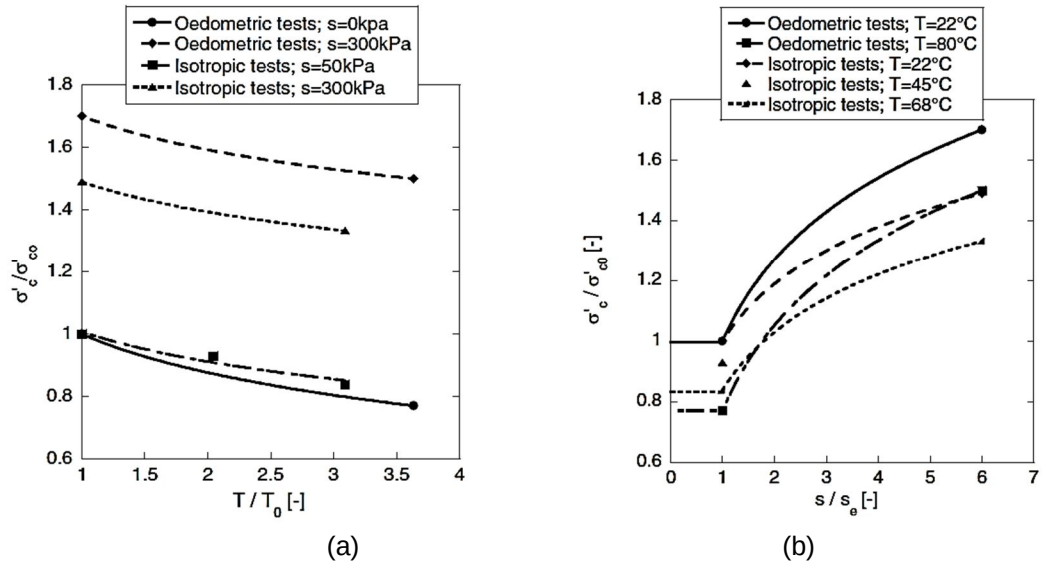

Figure 2-23. Effect of temperature and suction on apparent preconsolidation pressure: (a) Evolution of the apparent preconsolidation pressure with temperature, (b) Evolution of the apparent preconsolidation pressure with suction (Francois et al., 2007).

Seiphoori, Ferrari and Laloui (2011) presented an innovative double cell triaxial system developed for better understanding of the complex thermo-hydro-mechanical behaviour of soils. In addition to the conventional triaxial mechanical testing, the equipment is aimed to perform suction controlled tests under wide range of temperature and confining pressure. Suction controlled tests are implemented by the axis translation as well as vapor techniques to control the matric and total suction. They present an analytical approach to calibrate the force-displacement and volume change of the system under high axial loading, and calibrated the equipment using solid polyvinyl chloride (PVC). They demonstrated the efficiency of the approach in order to formulate the force-displacement and volume change relationships in closed form equations. Even though the equipment shows an interesting approach, they did not report any result of tests in soils. Figure 2-24 presents a picture of the equipment and figure 2-25 shows an explanation of its components.

Figure 2-24. THM triaxial system (Seiphoori, et al., 2011)

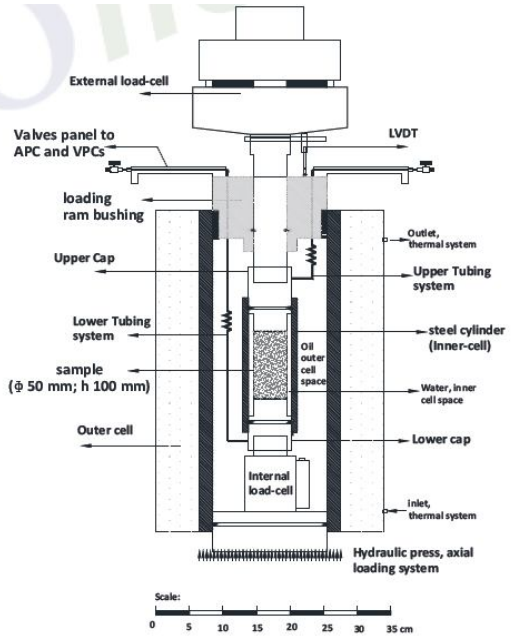

Figure 2-25. Schematic cross sectional view of the double-cell system (Seiphoori, et al., 2011)

Tang (2013) used an isotropic cell to investigate the thermal volume change behavior of opalinus clay (Switzerland) under suction controlled and isotropic pressure conditions.

The isotropic cell developed by Tang et al. (2007) (figure 2-26) for studying the thermo-mechanical behavior of unsaturated expansive clays was used. The isotropic pressure applied on the soil specimen is controlled by a volume/pressure controller. This later is equally used to monitor the soil volume change from the water exchange with the cell.

From these results, in unsaturated state, heating under low pressure induced an immediate thermal dilation followed by a thermal contraction. The contraction is to be linked to the release of pore water.

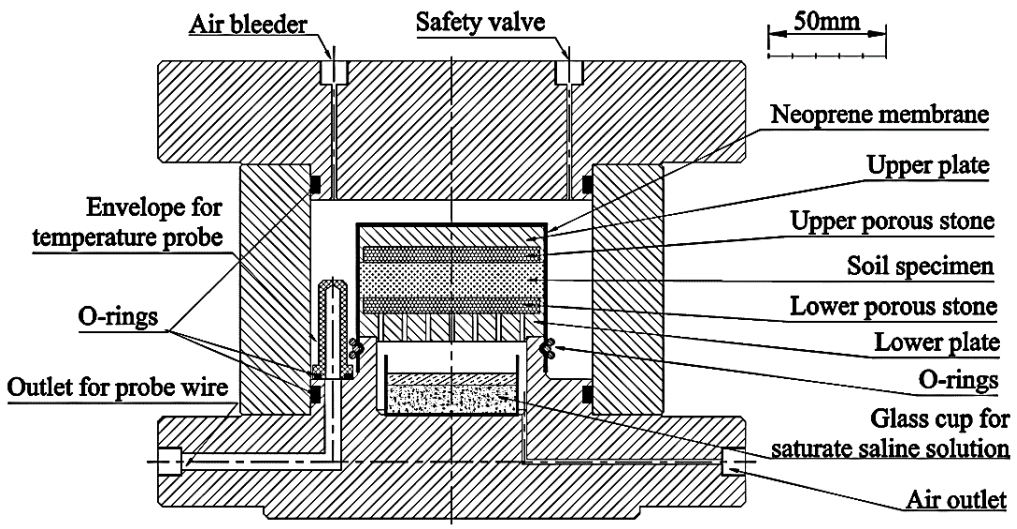

Figure 2-26. Basic scheme of the suction-temperature controlled isotropic cell (after Tang et al., 2007)

Zhou C (2013) performed an experimental study of the resilient modulus in unsaturated soils at different temperatures. A newly developed suction and temperature controlled cyclic triaxial apparatus was used to carry out three series of cyclic triaxial tests and investigate the resilient modulus. Suction levels from 0 to 250 kPa and temperatures of 20°C and 40°C. Figure 2-27 presents a picture of the device.

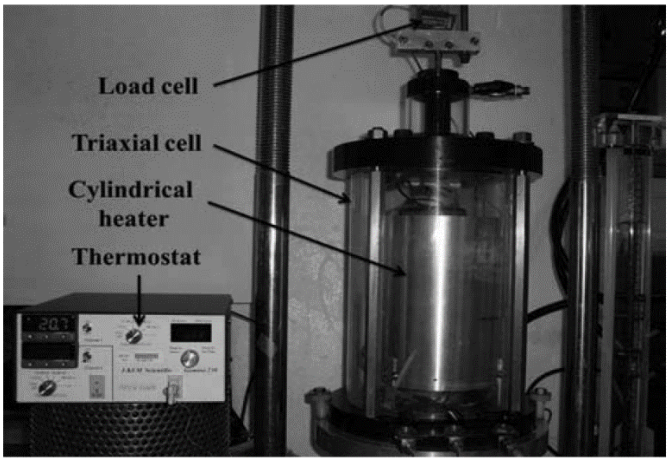

Figure 2-27. Suction and temperature controlled cyclic triaxial apparatus (Zhou C., 2013)

The soil used was a completely decomposed tuff from Hong Kong. Figure 2-28 and figure 2-29, present, respectively, the normalized resilient modulus as a function of number of load applications and as a function of the cyclic stress. In these two figures "W" means wetting, "D" means drying, and "T" means temperature. So, each curve represents a specimen resulting from a combination of these variables.

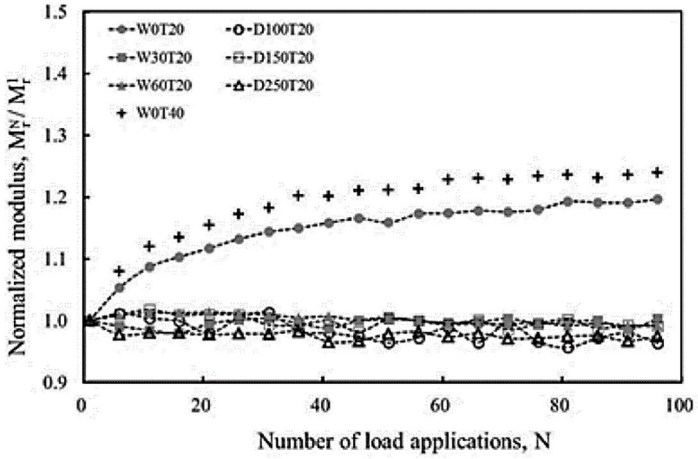

Figure 2-28. Relationship between normalized resilient modulus and number of load applications (Zhou C., 2013)

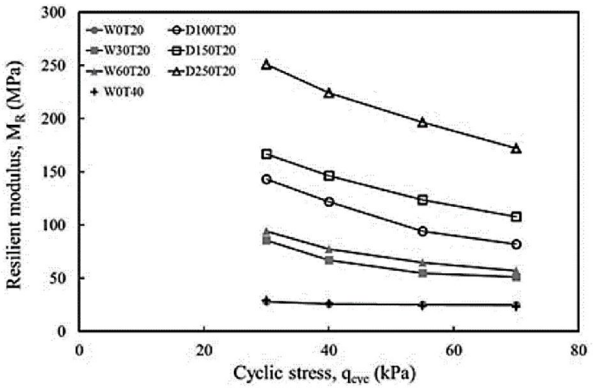

Figure 2-29. The influence of cyclic stress on resilient modulus at different suction and temperature conditions (Zhou C., 2013)

From these plots, the author concludes that resilient modulus increases significantly with suction. In addition, resilient modulus is almost insensitive to cyclic loads at values of suction higher than zero. Finally, for a given stress level, the increase of the normalized resilient modulus with increase in the number of load applications is more significant at higher temperatures with zero suction. This last conclusion may be explained by the fact that yielding stress of soil is smaller at higher temperatures.

Serri, Romero, Lloret, Suriol and Alonso (2013), designed a new apparatus that maintains the annular shape of the ring shear and capable of studying fast sliding processes promoted by heat induced friction. The apparatus was constructed based on a landslide case in Vajont and has been accepted as an explanation for the high velocity reached in this real case. The prototype could reach up to 30 Km/h along the landslide surface and vertical stresses up to 3 MPa.

The design of this complex prototype required the use of simulation-aided techniques to help interpreting thermo-hydro-mechanical coupled processes, which involve changes of pore water pressure in the shear band being heated.

They proposed a numerical solution for the case, and reported that shear strength vanishes at elapsed times around 10 seconds for relatively small shear band thickness (below 10 mm) and low permeability (10^{-13} to 10^{-11} m/s). Figure 2-30 shows the equipment developed and schematics of it. Figure 2-31, presents a zoom of the annular platen

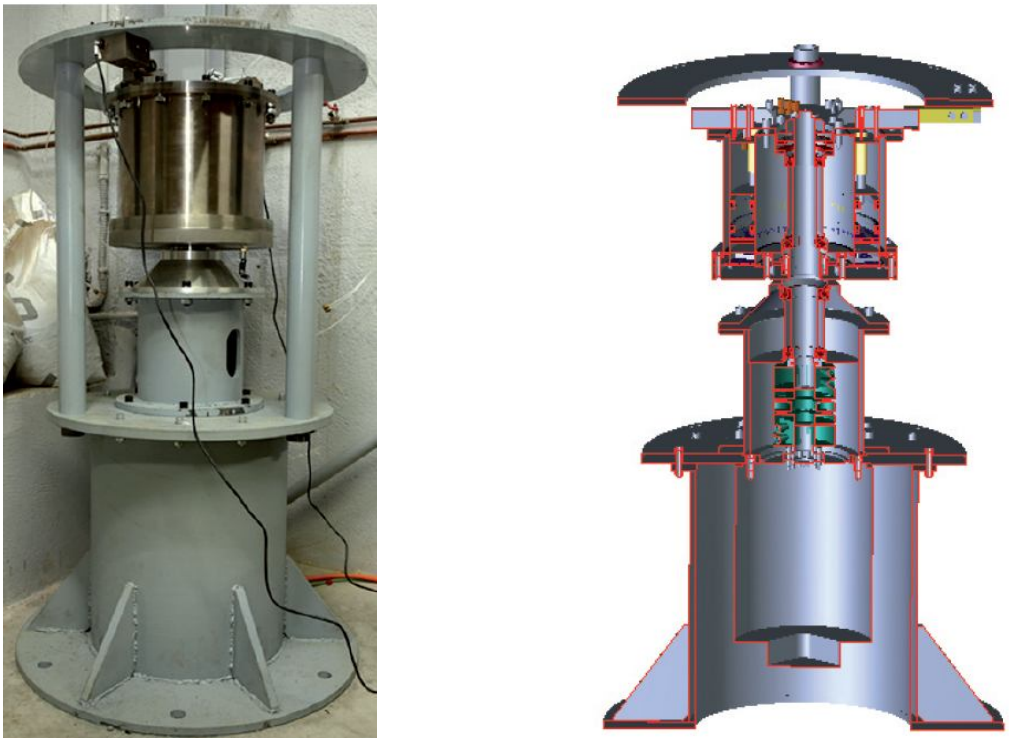

(a) (b)

Figure 2-30. New fast ring shear apparatus (Serri et al., 2007)

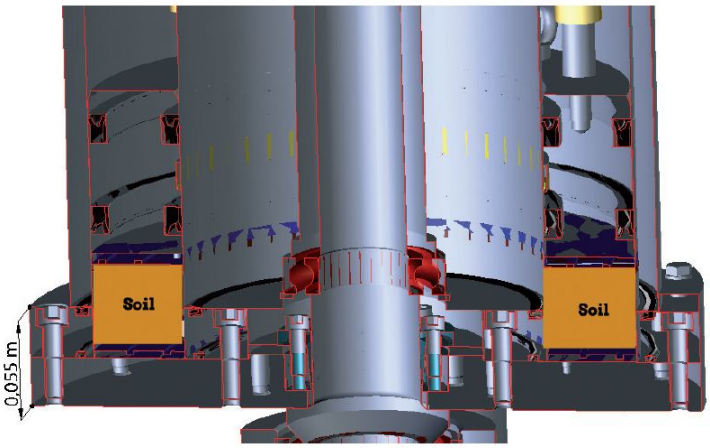

Figure 2-31. New fast ring shear apparatus: zoom of the annular sample (Serri et al., 2007)

This approach to the thermo-hydro-mechanical behavior of soils in a ring shear apparatus was developed for saturated conditions (as in the Vajont landslide case).

So far, research advances in the literature show that, the strength of soils increase with suction and normal stresses or confining pressures and with suction stresses. But strength decreases with an increasing temperature. Also, there are no research advances available that explain the thermo-hydro-mechanical behavior of unsaturated soils. This work focuses on that.

Chapter 3

Modifications to Test Procedures in the Ring Shear Apparatus

All the laboratory testing performed in this project consists of measuring the thermo-hydro-mechanical behavior of soils. In the previous chapter, the axis translation technique and the constant water technique were explained as the two approaches used to consider the influence of suction in the strength of unsaturated soils. This will be thoroughly explained in the following chapters. Besides, in order to try to get the best possible approach to understand this thermo-hydro-mechanical behavior, the equipment had to consider the thermal effects. Therefore, the following chapters will also explain how temperature controllers were adapted to the equipment to consider this.

In order to achieve good results, the procedures both to prepare the samples and to perform the tests, is fundamental. This chapter is devoted to explain how, based on previous work, and understanding some flaws and difficulties resulting from them, a new technique to prepare the samples and a better way to approach to the actual strength behavior of the materials were used during this work.

3.1 Compaction Procedure

In order to get the required unit weight of the sample that is located in between the top and bottom platen of the ring shear apparatus, the sample was compacted to a certain height calculated as a function of the volume.

After the sample was prepared and poured into the bottom platen of the ring shear, the top platen is set on the top of it, the compaction procedure is performed. At this point, two methods are to be explained. The monotonic force in the triaxial frame and the stress controlled compaction via axial actuator in the ring shear apparatus.

3.1.1 Monotonic Compaction Via the Triaxial Frame

Once the sample is between the platens of the ring shear apparatus, the sample is compacted in the triaxial frame that is possible to see in figure 3-1, where a monotonic force is applied to a deformation controlled force of 0.9 mm/min (the low speed is to avoid disturbance of the sample). When the sample reaches the required height, is transported to the ring shear and the test is started through the conventional way.

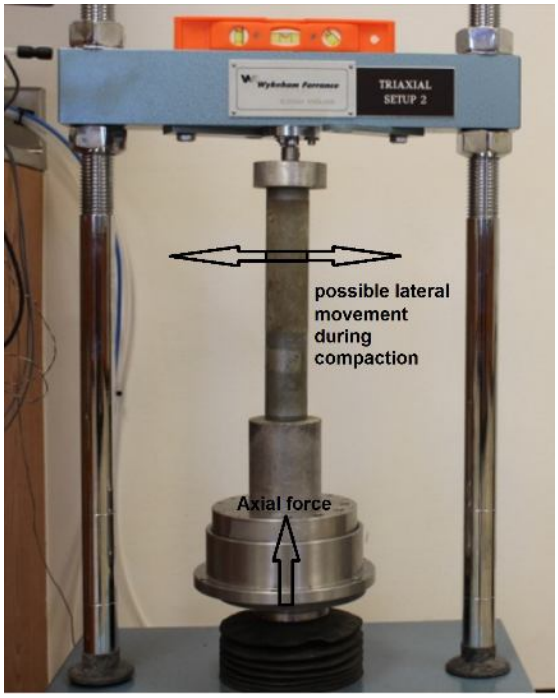

Figure 3-1. Triaxial frame used for monotonic compaction

3.1.2 Stress Controlled Compaction Via the Ring Shear Apparatus Vertical Load Shaft

The ring shear apparatus is a device capable of applying a stress to the sample until it gets the desided height (as a function of the volume), and consequently, the required unit weight of the sample.

The specimen is set in place, the same way as it is set to start the test. Then, a normal stress of 100 kPa (in this case) is applied to the sample via the axial actuator (that is also used to consolidate the soil sample), until it gets the required height. Figure 3-2 shows the axial actuator. Then, the normal stress is set to zero. Aprroximately two hours later, during which the sample is fixed and will not suffer volume changes, the test can be started also following the regular procedures from current and previous works. This method can be seen in figure 3-2. Figure 3-2 (a) presents the actual actuator that applies the normal stress. It is possible to see that this actuator can only move in the vertical direction, which guarantees that the compaction will not have any horizontal movement, and consequently, there will be no tilt during this process. Figure 3-2 (b) shows the bottom platen which goes located with the axial actuator in the middle of it.

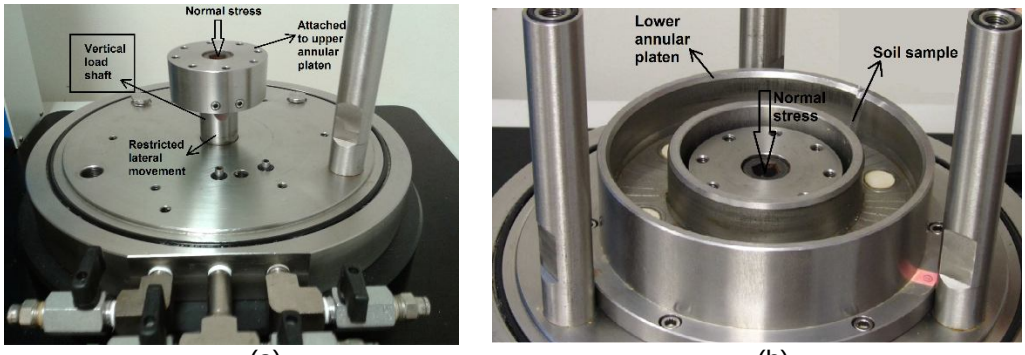

(a) (b)

Figure 3-2. Diagram of ring shear for application of normal stress

After bottom platen is located, the top platen is screwed to the axial actuator and compaction takes place (Figure 3-3). Figure 3-3 (a) shows the upper annular Platen (view of the porous stone that goes in contact with the soil sample), and figure 3-3 (b) shows the upper annular platen screwed to the vertical load shaft (ready for compaction)

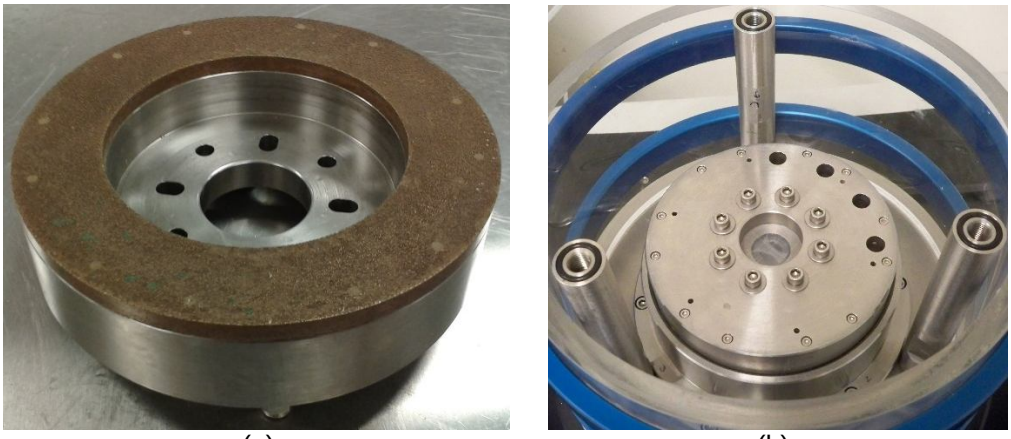

(a) (b)

Figure 3-3. Upper and lower annular platens before compaction

3.1.3 Comparison between compaction methods.

The idea of compacting directly inside the ring shear arose due to some flaws seen and experienced in the triaxial frame, as a consequence of current and previous work. The following paragraphs express two main reasons why compacting directly in the ring shear ended up being a much better method regarding technical and practical issues.

First, in the triaxial frame, due to limitations in the height of the sample and its dimensions (the height of the ring shear soil sample is small), some pieces needed to be added manually to reach the static pedestal in the top of the triaxial frame. This step is subject to human errors and can lead to some tilt in the compaction process. From the initial tests of this work, this was possible to prove. When the test was finished, lifting the top platen to remove the failed sample was difficult. The top platen was constantly stuck. When the sample was compacted directly in the ring shear apparatus, lifting the top platen was relatively easy.

Second, compacting in the triaxial frame, involved transportation of the sample to the frame (in order to compact) and the to the ring shear (in order to start the test).

This step could lead to disturbance of the sample and changes in the moisture content due to evaporation. Then, compacting directly in the ring shear apparatus is less sensitive to both transportation problems and moisture content losses, because the sample can be totally covered inside the ring shear chamber while it is compacted.

In general terms, this work recommends the use of the second compaction method. Compaction method in the ring shear minimizes: disturbance of the sample due to transportation, changes in moisture content due to evaporation, tilt in the failure surface (the axial actuator applies the normal stress in a guaranteed horizontal form).

3.2 Multi-Stage vs. Single-Stage Testing

This section will explain the basic ideas of performing tests via single-stage and multi-stage techniques, its differences and advantages of running tests via single-stage technique. The single-stage technique consists of consolidating the sample with a net normal stress, and after achieving the consolidation, shearing the sample under the same net normal stress until peak and failure strength is fully developed. Then, the specimen is removed and a new sample is places in order to start a new test with a different net normal stress.

The multi-stage technique consists of following the same procedure of single-stage technique, but using the sample without removing it from the ring shear apparatus. So, after the peak and residual strength has been fully developed under the first net normal stress, the shear stress is stopped and the net normal stress is increased until consolidation is achieved again, and shearing applied after that until peak and residual strength is developed again, and so on.

Every stage is a consolidation and consequent shearing of the sample, so for every stage, the peak and shearing failure parameters and conditions are linked to a particular net normal stress. There are no actual limit for the number of stages to be applied, but, and as it will be show in this work, the more stages, the more disturbed the soil is going to be after each one of them. The advantage of multi-stage testing is the short duration of the test compared to single-stage testing. The disadvantage is the change in geomechanical properties of soil after each stage. Figure 3-4 presents a schematic diagram of the stages of a ring shear test. Single stage consists of applying stages (a) and (b) only once, and multi-stage consists of applying these two stages several times, increasing the normal stress as many times as required.

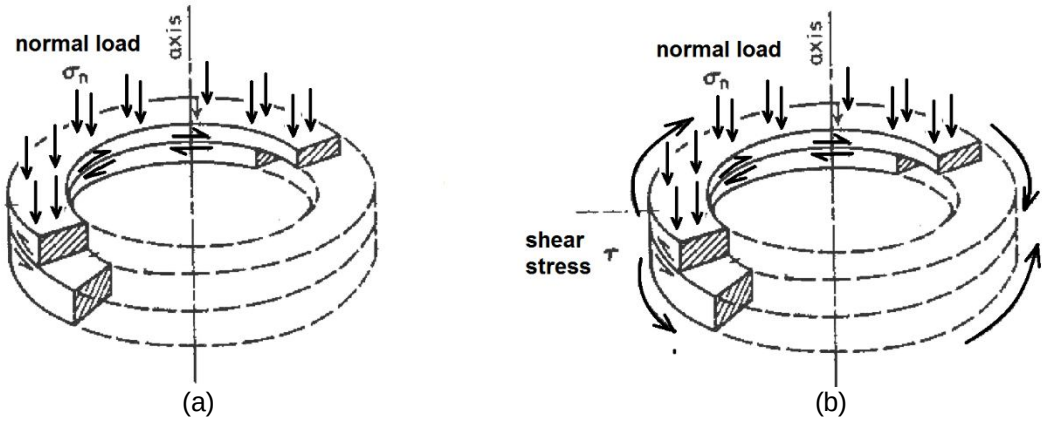

Figure 3-4. Schematic diagram of the ring shear testing consolidation and shearing stages.

3.2.1 Single-Stage Testing

Figure 3-5 shows a schematic diagram of several single-stage tests stress paths. The figure shows an example of a test performed in this project.

After assembling the test, a normal stress is applied through the top platen of the ring shear (for instance, $((\sigma_n - u_a) = 25$ kPa). As the soil of this project is a high plasticity clay (CH), the consolidation process took from two to three days.

Once consolidation is achieved, the shear stress is applied is applied until peak and residual states are reached (calibrated to a speed of 0.023°/min). This is one single-stage. Each arrow in figure represents one single-stage test.

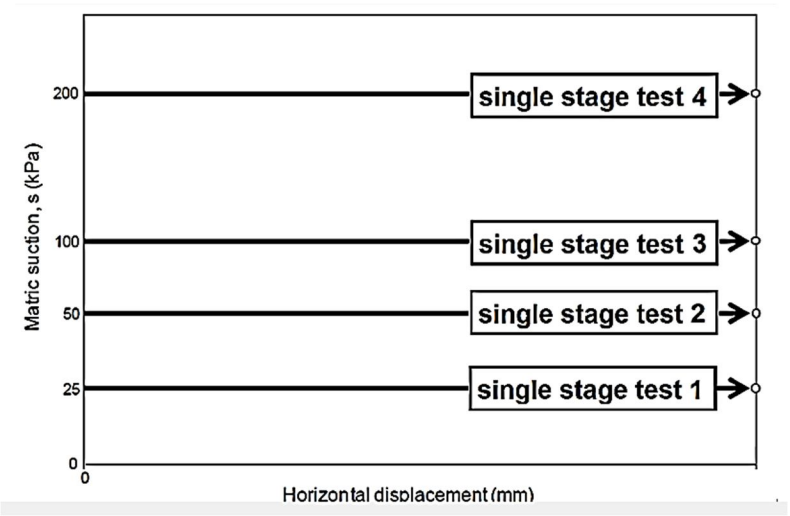

Figure 3-5. Single-stage testing.

3.2.2 Multi-Stage Testing

Figure 3-6, shows a schematic diagram of a multi-stage test stress path. Equally, this figure presents a representation of a test performed during this project. After assembling the test, a value of matric suction is applied (for instance, $(u_a-u_w) = 25$ kPa). Under this value of matric suction, all the stages are going to be performed. So, net normal stresses of $(\sigma_n - u_a) = 25, 50, 100, 200$ kPa will represent the four stages of this multi-stage test.

After a net normal stress of 25 kPa is applied and consolidation is achieved, shearing stresses are applied until peak and residual states are fully reached and guaranteed. Then, the following net normal stress of 50 kPa is applied until consolidation is again achieved, and shear stress is applied until peak and residual states are reached again.

The same procedure is followed for the other two stages. Again, it is possible to conclude that in each stage, consolidation, and shearing peak and residual states and parameters are linked to a net normal stress. In the figure the four arrows represent only one multi-stage test.

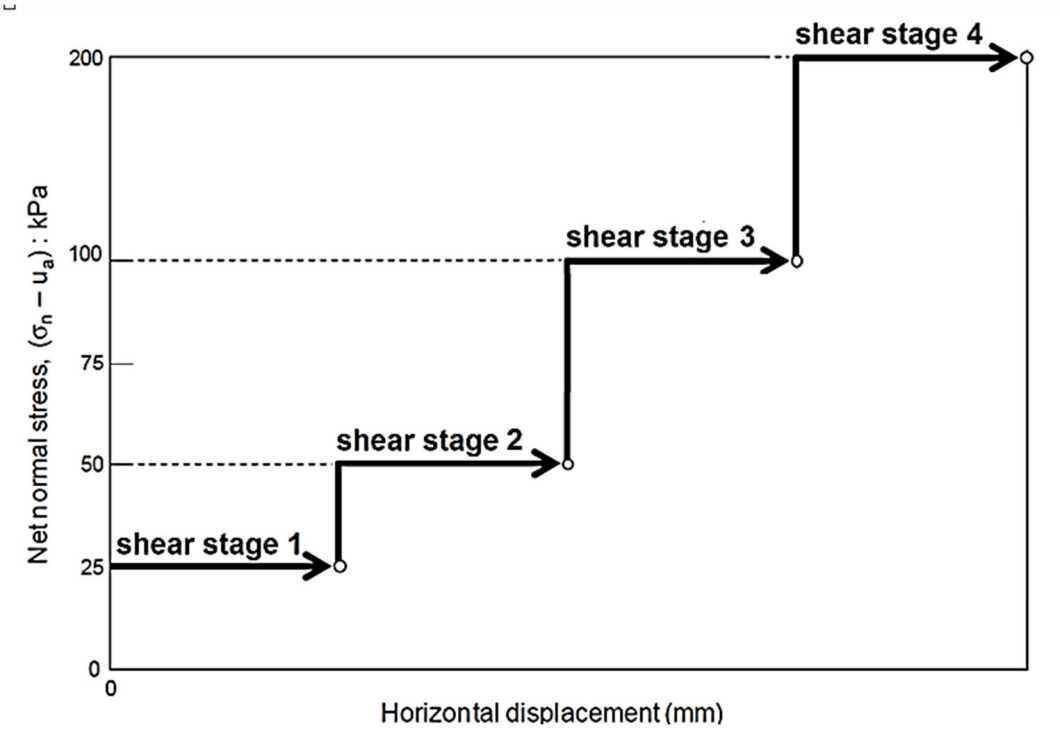

Figure 3-6. Multi-stage testing.

3.2.3 Comparison between Single-Stage and Multi-Stage

Figure 3-7 and figure 3-8, present, respectively multi-stage and single-stage performed during this project. The same soil was used, both figures show curves for a matric suction of ($u_a - u_w$) = 25 kPa and net normal stresses ($\sigma_n - u_a$) = 25, 50, 200 kPa.

All the official tests in this work, both with axis-translation and constant water techniques, were performed as single-stages tests. This was because it was possible to find out that in multi-stage tests, after the first stage, the soil is does not have the same mechanical properties. That is possible to conclude when in second and third stage, peak strength is almost the same as residual strength.

This behavior is possible to explain because after the first stage the soil already failed and reaches a state close to residual. In addition, in single-stage tests, the shear stress vs. Equivalent horizontal displacement starts from the same initial conditions, so "the behavior of the material only depends on the actual strength properties, an not on the previous stage". Finally, by performing single-stage, the stress-strain behavior of the clayed soil is closer to the actual behavior of this type of soil, noticing a clear difference between the peak and residual behavior.

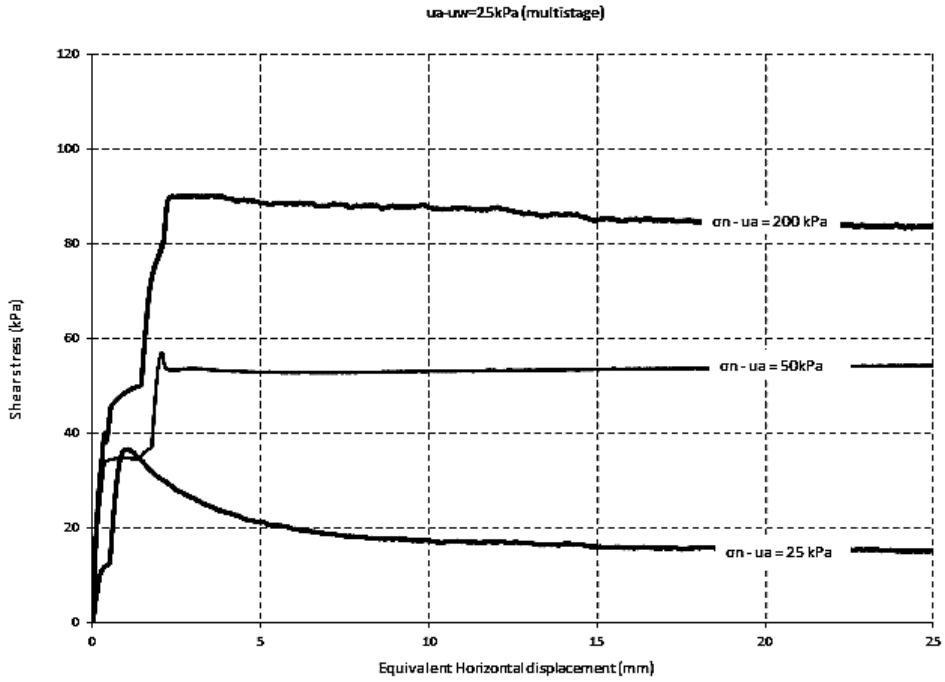

Figure 3-7. Multi-stage test in high plasticity clay (CH) used for this project

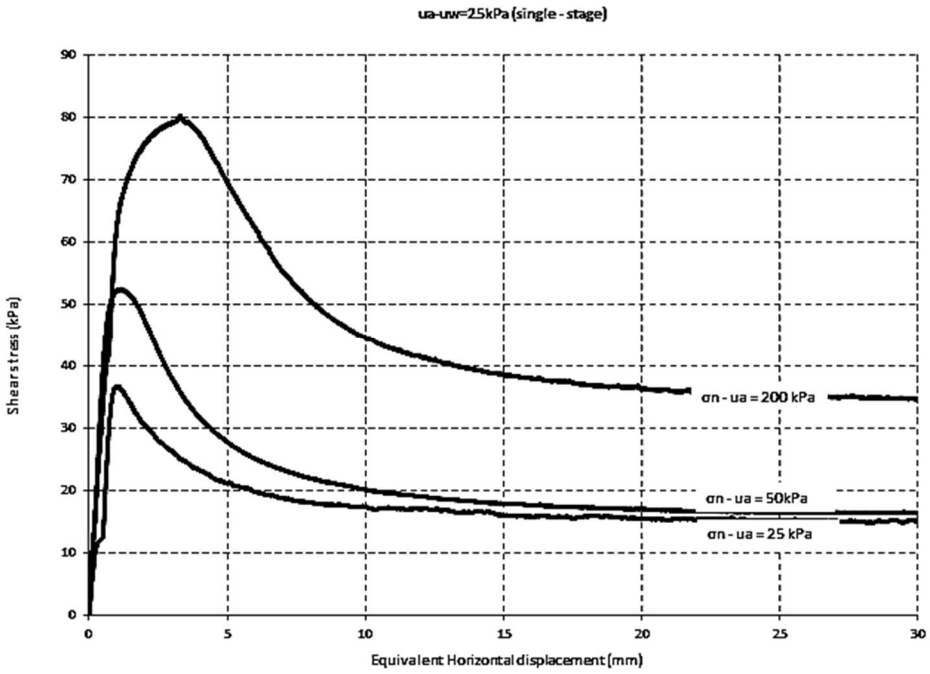

Figure 3-8. Single-stage tests in high plasticity clay (CH) used for this project

Chapter 4

Temperature Controller System for Servo/suction Controlled Ring Shear Apparatus

Velosa (2011) presents a thorough, rigorous and detailed explanation of the Servo/suction Ring Shear Apparatus used in this work. This section will explain the basic components of the device in order to introduce the Thermo Servo/suction-controlled Ring Shear Apparatus.

4.1 Servo/suction Controlled Ring Shear Apparatus

The novel ring shear apparatus has two independent servo-controlled apparatus: a pneumatic actuator for the application of normal loads (up to 8000 N) and an electromechanical rotary actuator for the application of monotonic torque (up to 113 N-m).

Figure 4-1, shows a general view of all the components of the suction controlled ring shear apparatus. It presents three principal modules: (1) Main cell with the system for axial and shear actuators (normal and torque loads); (2) Data acquisition and process control (DA/PC) system with software for real-time measurement of normal stresses, shear stresses, angular deformations, and torque loads; (3) PCP-15U suction control panel for application of air pressure (when axis-translation technique is used).

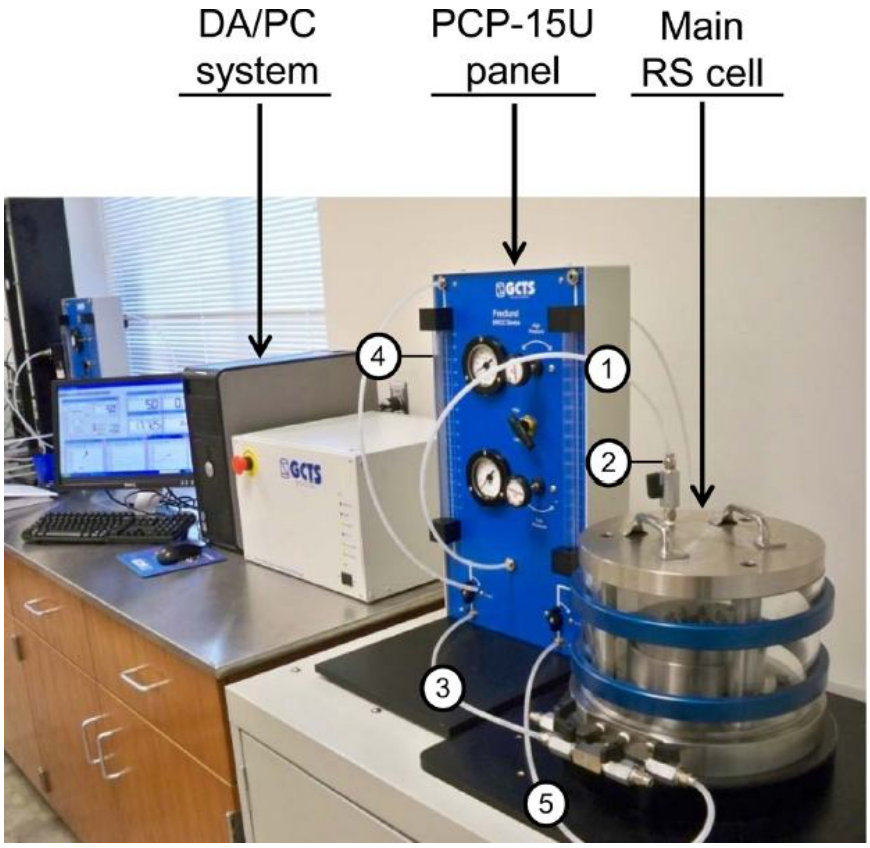

Figure 4-1. General view of suction-controlled ring shear test layout (Hoyos et al., 2011)

In this figure, items (1) and (2) represent how the air pressure is supplied from the PCP-15U panel to the main cell, item (5) shows a flushing line that connects to the core base of the main cell (flushing as a technique to avoid air bubbles in the system and allow a correct application of the axis-translation technique), and items (3) – (4) complete the flushing system (when there is no more water level change, equilibrium of suction is achieved)

4.1.1 Main Ring Shear Cell

Figure 4-2, presents an isometric view of the main cell, including the servo-controlled axial load an torque application systems, with all of the following: (1) top cover plate; (2) confining cell with 1000 kPa air pressure capacity; (3) bottom base plate; (4) rotary stainless steel upper annular platen; (5) fixed stainless steel lower annular platen; (6) vertical load shaft; (7) Model SWT 10-2K-B000 combined axial force and torque transducers (from Tovey Engineering); (8) Model FHA-40C-160-US-250 electromechanical rotary actuator (from Harmonic Dr. System) for torque application up to 113 N-m; (9) Model D-16-F-BF pneumatic actuator (from MB Marsh Bellofram) for axial load application up to 8000N; (10) linear variable differential transformer (LVDT) for monitoring of soil vertical deformation.

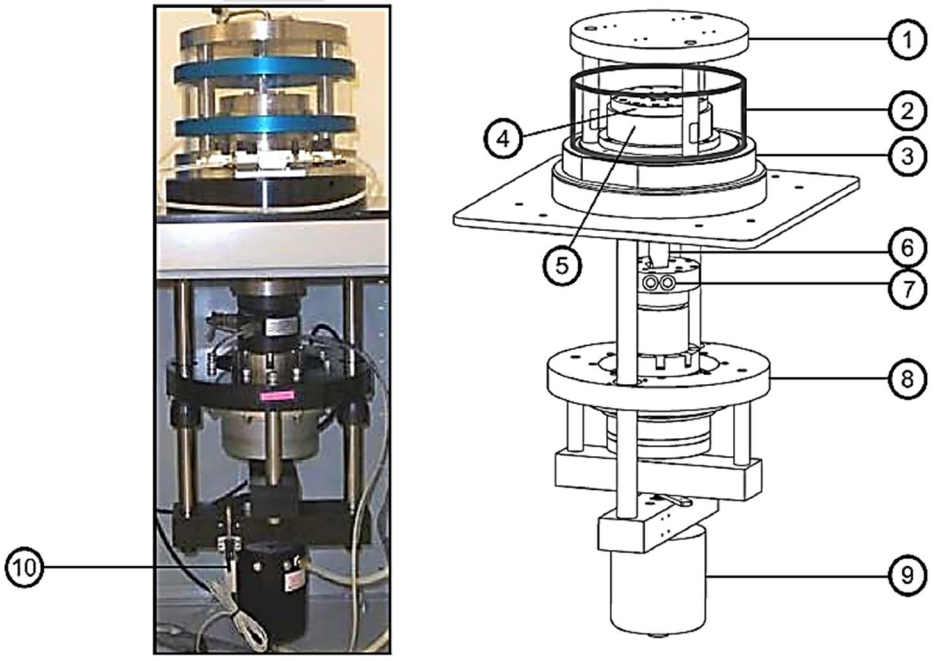

Figure 4-2. Isometric view of main cell and servo-controlled normal load and torque application systems (Hoyos et al., 2011)

4.1.2 Upper and lower annular platens

Figure --, present the upper and lower annular platens where the soil sample is placed. Figure 4-3 (a) shows the upper platen, which during the test, goes, fixed to the actuator that applies axial load (axial pneumatic actuator) and consequently shear load (electromechanical rotary actuator). Figure 4-3 (b) shows the lower annular platen which is fixed to the ring shear device and where the soil specimen is placed.

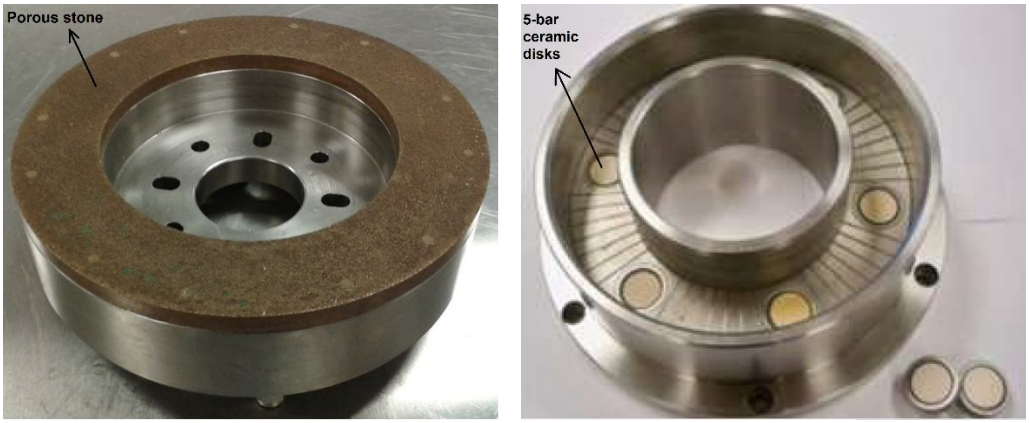

(a) (b)

Figure 4-3. Upper and lower annular platens with 5-bar ceramic discs.

4.1.3 PCP – 15U Panel

As shown in figure 4-1, a Model PCP – 15U pressure panel (from GCTS) is used for application and control of air pressure at the top of the sample, featuring dual pressure regulators and gauges for precise control of matric suction. Air pressure is applied to the main cell and transmitted to the soil specimen through the porous stone (figure 4-3 (a)) that is attached to the upper annular platen and is in contact with the soil sample (failure surface) during the test.

4.1.4 DA/PC System

As shown in figure 4-1, the DA/PC system consists of: Model SCON-1500 digital servo controller and acquisition system, model DSB-11 universal signal conditioning board for load cells and LVDT, performance/data reduction software, and model IBM PC unit.

4.1.5 Step-by-Step General Setting Up Procedure

An orderly step-by-step setting up procedure was established as follows: (1) All actuators and DA/PC system are switched on to allow the instruments to come into equilibrium and minimize the influence of temperature offsets; (2) a small piece of wet filter is placed over the top of each high-air-entry (HAE) ceramic disk, prior to specimen compaction, to ensure phase continuity between the pore-water in the soil and the water in the saturated disk. The sample is placed in the lower annular platen and compaction takes place (procedure explained in chapter 3); (3)

The vertical load shaft is brought up through a servo controller and the upper annular platen affixed to the top of the piston shaft (4) If axis-translation is used, then, all drainage and flushing lines are filled with de-aired water and flushed several times to avoid any trapped air in the whole system; (5) The main ring shear cell is installed and the top cover plate affixed to the cell; (6) a pore-air pressure line from the PCP-15U panel is connected to the cover plate via a quick connector; (7) The sample is then subjected to single-stage or multi-stage testing procedure.

If the test follows constant water technique instead of axis-translation technique (to measure suction influence in soil strength) steps (4) to (6) are avoided and the moisture content of the sample (based on its SWCC) is the parameter that will control suction.

4.2 Thermo-servo/suction Controlled Ring Shear Apparatus

So far, this chapter has explained the Servo/suction controlled ring shear apparatus capable of measuring peak and residual shear strength in the soil specimen. In order to include the variable of temperature, the device needed to be modified. This section of the chapter is committed to explain the changes made to the ring shear in order to consider the influence of both suction and temperature in the peak and residual strength behavior of the material at the same time.

The main reason to include temperature, as a variable in the behavior of the soil is to take into account the dramatic changes in temperature consequence of season changes. In this work, three values of temperature were used: 20°C, 30°C, and 40°C. As it is possible to see, the trend was to increase the temperature above the average temperature of 20°C, and one of the most important reasons to choose these values, was that in states like Texas, summer is the season when the most drastic temperature changes occur.

4.2.1 Modifications to the Ring Shear Apparatus to Adapt the Temperature Controller

Figure 4-4, presents a panoramic view of the new Thermo-servo/suction-controlled ring shear apparatus. Right below the PCP – 15U panel (that applies air pressure to the main cell and the soil sample), the HTC-250 controller box is located. This unit controls the temperature that goes the main cell, the fan, and the thermocouple that measures the applied temperature.

Figure 4-4. Panoramic view of the Thermo-servo/suction controlled Ring Shear Apparatus

Figure 4-5, presents a zoom to the connections that go from the Ring shear main cell to the HTC-250 controller box. Here it is possible to see that the unit controls all the process of application of temperature to the main cell, and particularly to the soil sample.

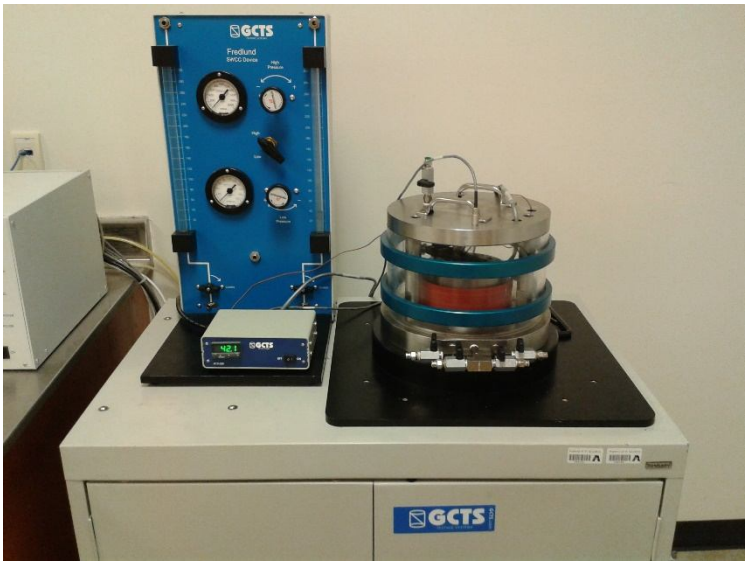

Figure 4-5. Zoom to the connections from the Ring Shear Main Cell to the controller box.

Figure 4-6 presents the HTC-250 controller box. The unit can apply a maximum Temperature - 70°C (158 °F), it has a heating Power of 180W, the input Voltage goes from 110V to120V AC and the input Current is 2 Amps maximum.

Figure 4-6. HTC-250 Controller box.

Figure 4-7, shows the backside of the HTC-250 controller box. This is to explain in detail the connections that go from this unit to the top cap of the ring shear main cell. Figure 4-8, shows the backside of the HTC-250 with all the connections plugged (during a test)

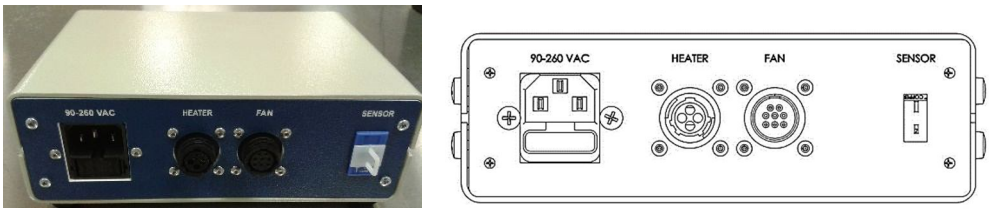

(a) (b)

Figure 4-7. Backside of the HTC-250 controller box.

Figure 4-8. Backside of the HTC-250 controller box during a test.

Figure 4-9 is a zoom to the connector that goes from the thermocouple to the sensor in the backside of the HTC-250 controller box. Red wire connects to the negative terminal on the connector

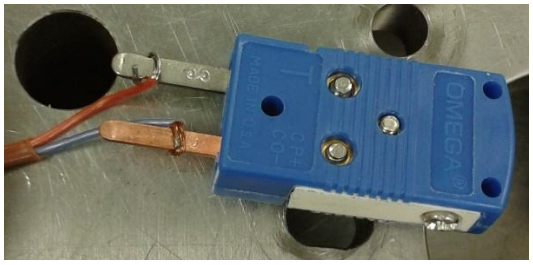

(a)

(b)

Figure 4-9. Connector that goes from the thermocouple to the HTC-250 controller box.

Figure 4-10, shows an outside view of ring shear main cell the top cover with the modifications due to the temperature controller unit.

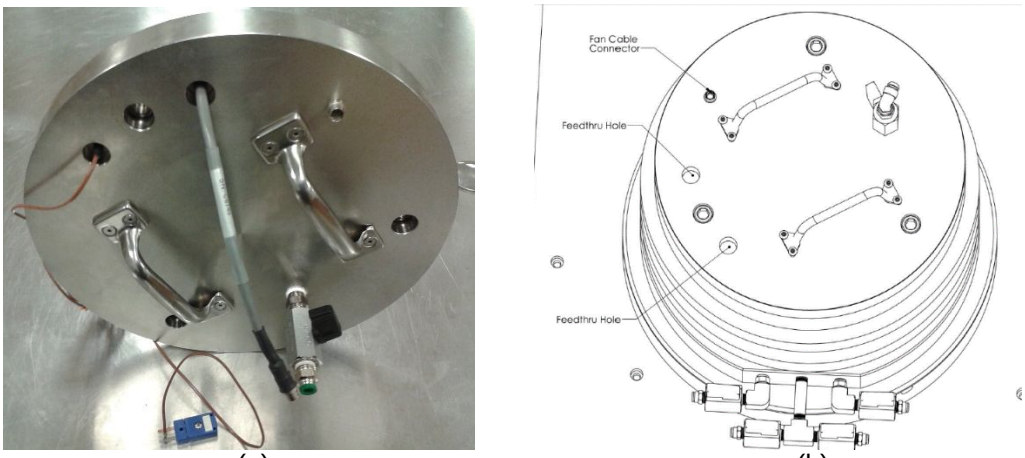

(a) (b)

Figure 4-10. Connections from HTC-250 controller box to the outside top cover of the ring shear main cell.

Figure 4-11, shows pictures of the upper and lower annular platens with the changes made in order to apply and control temperature to the soil specimen. Figure 4-11 (a) shows the upper annular platen with heater cable, heater connector and heater band; Figure 4-11 (b) shows the upper annular platen with connection for thermocouple

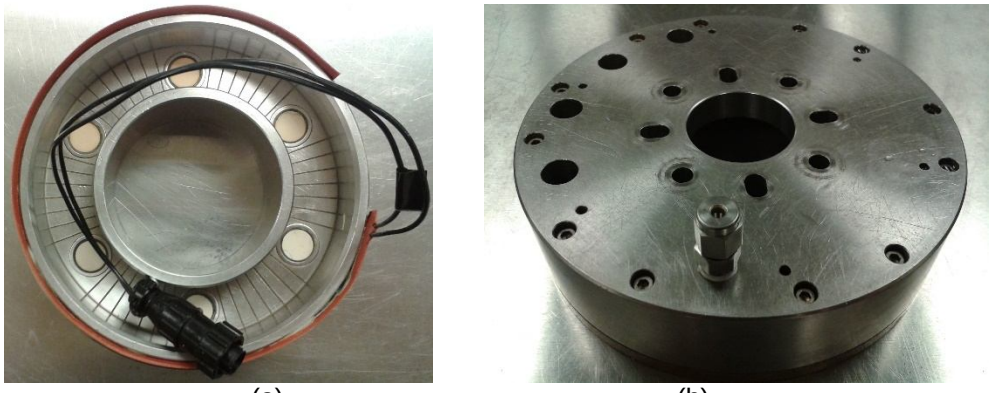

(a) (b)

Figure 4-11. Ring Shear Annular platens with modifications for application of temperature.

Figure 4-12, presents the connections from the inside part of the ring shear top cover to the lower annular platen (heater connection) and the upper annular platen (thermocouple). The function of the heater cable connection is to apply the temperature to the lower annular platen, and consequently, to the soil specimen. The function of the thermocouple is to measure and guarantee that the required temperature is actually being applied to the soil specimen. Figure 4-12 (a) is a general view of the connections, figure 4-12 (b) is a detailed schematic diagram of the heater and thermocouple connection, and a view of the fan.

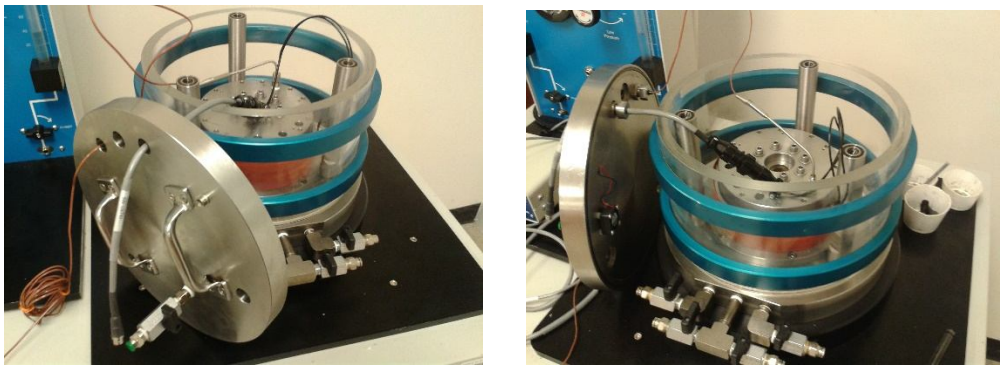

(a) (b)

Figure 4-12. Temperature controller connections inside the main cell

Figure 4-13 (a), shows the lower annular platen with the modification due to the heater connection, and figure 4-13 (b), presents a detailed view of the upper and lower annular platens with the modifications due to the temperature controllers.

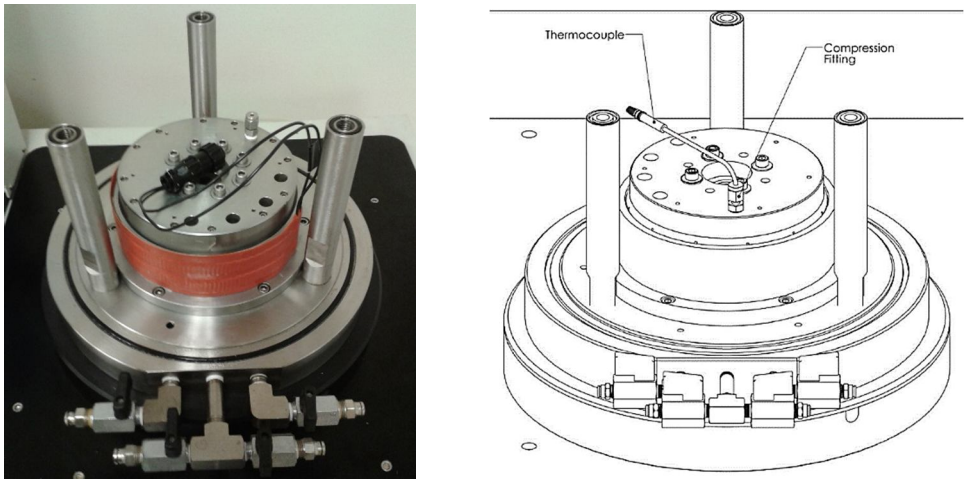

(a) (b)

Figure 4-13. Temperature controller connections insider the ring shear main cell.

4.2.2 Step-by-step Procedure for the Application of Temperature to the Test

This section explain the procedure to both adapt the temperature controller system to the ring shear and to run a test applying and controlling temperature. In this work, all the tests were performed through the constant water technique, but if the axis-translation technique is to be used, the procedure is analogous.

4.2.2.1 Assembly of the temperature controller system

The step-by-step procedure to adapt the temperature controller system to the servo/suction controlled ring shear apparatus is as follows: (1) The soil sample is prepared and poured into the lower annular platen following the same procedure as previous work without controlling temperature, but taking care of putting soil in contact with the heater cable and heater band (figure 4-14). (2) Assemble specimen and attach top platen to the loading shaft, (3) Insert thermocouple compression fitting and tighten to lock in place (for steps (2) and (3), see figure 4-15)

(4) Feed the heater feedthrough cable through a feedthrough hole in the cell top and screw the threaded fitting into the port hand tight, (5) Install the thermocouple connector on the end of the feedthrough cable (as mentioned before, the red wire connects to the negative terminal on the connector), (6) Continue with the assembly and closing the cell for standard ring shear testing, (7) Connect the fan cable to the connector mounted on the top of the cell, (8) Connect the heater cable to the heater feedthrough cable coming through the cell top, and (9) Connect the cables to the back of the HTC-250 controller box. Figure 4-16, presents the final assembly of the thermo-servo/suction controlled ring shear apparatus ready to start a test.

Figure 4-14. Sample preparation and placement into the lower annular platen

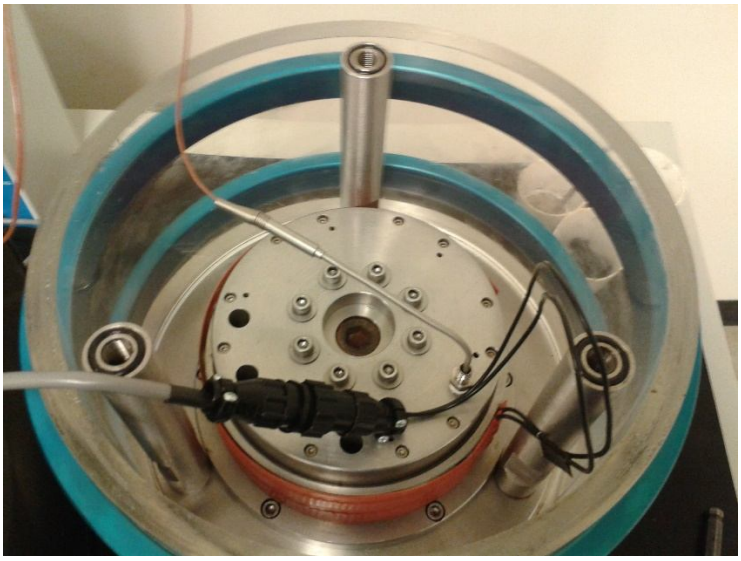

Figure 4-15. Assembly of the thermocouple and the heater cable

Figure 4-16. Final assembly of the temperature controller system before the start of a test.

4.2.2.2 Start of a thermo-servo/suction controlled ring shear test

Once the whole system is ready to start a test, including compacted sample, the procedure is as follows: (1.a) If constant water technique is used, turn on the HTC-250 controller box, (1.b) if axis-translation is used, wait until equilibrium of suction is achieved and then turn on the controller box, (2) Set the required temperature and auto tune it (the controller box will confirm when the required temperature is already calibrated – follow instructions manual), (3) at the same time, apply the net normal stress (commonly the temperature calibration is reached before consolidation of the sample is done), and (4) Once consolidation is done (make sure that temperature keeps calibrated and constant), apply shear stress to the sample (0.023°/min).

Chapter 5

Experimental Program

This chapter is committed to show the entire experimental program performed during this project in order to investigate strength-strain behavior of high plasticity clayed soil (CH). To achieve this, two techniques were used: axis-translation technique and constant-water technique (both of them previously explained).

For the axis-translation technique, only the ring shear apparatus was used, for both multi-stage and single-stage testing procedures, considering net stress and matric suction as variables, and a constant temperature of 20°C. A total of 19 tests, 6 multi-stage and 13 single-stage tests were performed.

For the constant-water technique, the ring shear apparatus was used. For the ring shear, a total of 22 tests were performed, via single-stage procedures, considering net stress, matric suction (as a function of moisture content, the constant-water technique) and temperature as variables.

The following tables will show the experimental program performed for both axis-translation technique (multi-stage and single-stage) and constant-water technique.

Table 5-1 shows tests from 1 to 6 performed using axis-translation technique via multi-stage testing procedures. The table shows all the tests performed. Later it will be possible to see that not all of the stages are presented in the plots. This was due to problems related with multi-stage test results in the ring shear for this type of soils. In the table it is possible to see that matric suction and net stress are the variables used (temperature is constant).

Table 5-1. Experimental variables for Multi-stage ring shear testing via axis-translation technique

MULTI-STAGE TESTING - AXIS-TRANSLATION - RING SHEAR		
Test No.	**ua-uw (kPa)**	**σ-ua (kPa)**
1	25	25
		50
		100
		200
2	50	25
		50
		100
		200
3	75	25
		50
4	100	25
		50
		100
		200
5	200	25
		50
		100
		200
6	300	25
		50

Table 5-2 shows tests from 7 to 18 performed using axis-translation technique via single-stage testing procedures (actually 20 tests were performed, but the torque capacity was exceeded in two of them).

The table shows all the tests performed. In this case, all the results were used in the plots, showing that single-stage testing procedures yield much better results for these type of soils subjected to large deformations. Once again, matric suction and net stress are the only variables used.

Table 5-2. Experimental variables for Single-stage ring shear testing via axis-translation technique

SINGLE-STAGE TESTING - AXIS-TRANSLATION - RING SHEAR		
Test No.	**ua-uw (kPa)**	**σ-ua (kPa)**
7	25	50
8	25	100
9	25	200
10	50	50
11	50	100
12	50	200
13	100	50
14	100	100
15	100	200
16	200	50
17	200	100
18	300	50

Table 5-3 shows tests A to AA (27 tests) performed in the ring shear apparatus using Constant-water technique, and via single-stage testing procedures. Multi-stage testing procedures were not used in this las experimental program, due to the problems seen in the axis-translation technique both during the tests and in the results (plots). In this table, it is possible to have a third variable, the temperature.

So, different to the two variables controlled with the axis-translation technique, now there are three variables: net stress, matric suction (controlled with the moisture content from SWCC), and temperature.

Table 5-3. Experimental variables for Single-stage ring shear testing via constant-water technique

SINGLE-STAGE TESTING - CONSTANT WATER - RING SHEAR			
TEST	**σn (kPa)**	**w (%) (as a function of matric suction from SWCC**	**T (°C)**
A	25	33 (Ua-Uw=25kPa)	20
B	25	33 (Ua-Uw=25kPa)	30
C	25	33 (Ua-Uw=25kPa)	40
D	25	28 (Ua-Uw=100 kPa)	20
E	25	28 (Ua-Uw=100 kPa)	30
F	25	28 (Ua-Uw=100 kPa)	40
G	25	21 (Ua-Uw=200 kPa)	20
H	25	21 (Ua-Uw=200 kPa)	30
I	25	21 (Ua-Uw=200 kPa)	40
J	100	33 (Ua-Uw=25kPa)	20
K	100	33 (Ua-Uw=25kPa)	30
L	100	33 (Ua-Uw=25kPa)	40
M	100	28 (Ua-Uw=100 kPa)	20
N	100	28 (Ua-Uw=100 kPa)	30
O	100	28 (Ua-Uw=100 kPa)	40
P	100	21 (Ua-Uw=200 kPa)	20
Q	100	21 (Ua-Uw=200 kPa)	30
R	100	21 (Ua-Uw=200 kPa)	40
S	200	33 (Ua-Uw=25kPa)	20
T	200	33 (Ua-Uw=25kPa)	30
U	200	33 (Ua-Uw=25kPa)	40
V	200	28 (Ua-Uw=100 kPa)	20

In the previous tables, the range of variables were shown. For the ring shear tests via multi-stage axis-translation technique, matric suction values of (u_a-u_w) = 25, 50, 75, 100, 200, and 300 kPa, and net stresses of (σ - u_a) = 25, 50, 100, 200 kPa, were used. In table 5-1, some values do not appear either because the torque capacity was exceeded or because the plots were not producing good results and multi-stage testing procedure was replaced for single-stage.

For ring shear tests via single-stage axis translation technique, the same variables were used. In table 5-2, it is possible to see that the value of net stress (σ - u_a) = 25 kPa was not performed. This was because the first stage of each multi-stage test was used in the final results of the single-stage experimental program. This will be thoroughly explained in the next chapter.

For the ring shear tests via single-stage constant-water technique, the following variables were used: (u_a-u_w) = 25 kPa (w=33%), 100 kPa (w=28%), and 200 kPa (w=21%); σ_n = 25, 50, 100, 200 kPa; and temperatures of T; and temperatures of T° = 20°C, 30°C and 40°C. These values of temperature were chosen due to local changes in weather conditions.

The material used during this project is as convenient as challenging in terms of the purposes established from the beginning of this experimental program. As it is widely known, the ring shear device was initially developed to measure peak and residual shear strength of clayed soils subjected to large deformations. There is some previous work in the same device used during this work, but some limitations with the variables leaded to keep on working with the same material, and is one of the reasons that inspired this following experimental program that will be thoroughly explained throughout this chapter. Table 5-4 shows the material used during this project and its basic properties.

Table 5-4. Characteristics and properties of the material used in this work

CHARACTERISTICS OF MATERIAL	
Sampling Location:	Highway US 287 S, beside St. Paul Overpass in Waxahachie, TX
Name:	High plasticity clay
Soil classification - USCS:	CH
Liquid Limit, LL:	67
Plastic Limit, PL:	29
Gs:	2.7
γ d:	14.18 KN/m3
w (insitu)	33%
Observations:	Sample recovered from failed slope at shallow depths of 3.05 meters from ground surface

5.1 Servo/suction –Controlled Ring Shear Testing Via Axis-Translation Technique

This section will show all the test results produced via both multi-stage and single-stage tests using axis-translation technique. Then, a comparison between the results produced by the two procedures will be done in order to justify the use of single-stage results for the analysis of results.

5.1.1 Multi-stage Testing

It was possible to see in the previous section, that tests 1 through 6 were performed using multi-stage via axis translation technique. This section will show the results that were produced from these tests. As mentioned in the previous section, not all the curves in the plots were used to be analyzed in this section, because not all the combination of net stresses and matric suction values yielded coherent results.

Later in this work, it will be explained that multi-stage testing in clays under large deformations does not produce the expected results, and that is why single-stage testing started to be used after test 6, yielding much better results.

5.1.1.1 General steps of multi-stage testing via axis translation technique

The procedure to run a multi-stage test in the ring shear apparatus is the same as that performed in previous work. Once the sample has been already compacted, and the ring shear device ready to start a test, air pressure was applied and flushing process is carried out in order to remove all air bubbles that may be inside the system. This is a fundamental step in the axis-translation technique, which allows to assume that pore-water pressure is close to atmospheric and that pore-air pressure is actually the matric suction ($u_a - u_w$). This flushing process will let the test achieve the equilibrium of suction, when the water level in the PCP-15U panel does not change anymore. Velosa (2011) has a detailed explanation of this process.

As during this work, high plasticity clay was tested, the equilibrium of suction took approximately 4 to 5 weeks, depending on the applied air pressure (the higher the air pressure, the more time it took to get equilibrium). This long lasting process occurred because of the low permeability of the tested material.

Then, once the equilibrium of suction was achieved, the net normal stress ($\sigma - u_a$) is applied and a plot “axis deformation vs. time” controls the consolidation of the sample. The software let the test have a real time plot of every stress applied

After consolidation, and under the same net normal stress, shearing stage is applied. The ring shear apparatus is calibrated to apply a shear stress at a speed of 0.023°/min.

Also, in real time it is possible to plot shear stress and torque, as a function of angular deformation and/or time. So, it can be guaranteed that both peak and residual states are reached.

Once, residual strength is achieved, a new and higher net normal stress is applied, and consolidation and shearing behavior reached as explained in the previous paragraph.

The number of stages and variables used is up to the scope of the project. The only consideration to take into account is that this ring shear device has a torque capacity of 113 N-m, so it is important not to exceed this value.

During this project, it was possible to realize that the ring shear is capable to stop the test before the combination of net stress and matric suction is going to exceed the torque capacity. Then, this work was committed to use a wider range of variables compared to previous projects that involved this device. It was possible to realize that at two combination of variables, the torque capacity was about to be reached and the software aborted the test. It was at $(u_a - u_w)$ = 300 kPa with $(\sigma - u_a)$ = 100 kPa, and at $(u_a - u_w)$ = 200 kPa with $(\sigma - u_a)$ = 200 kPa. That is why these two stages are not shown in this chapter.

5.1.1.2 Multi-stage test results, matric suction as a function of several net normal stresses

This section will show the multi-stage tests the way they were actually performed. Each figure represents one multi-stage test performed via axis-translation technique. Figure 5-1, shows the first multi-stage test performed during this work (test 1: $(u_a - u_w)$ = 25 kPa with $(\sigma_n - u_a)$ = 25, 200 kPa).

The test was actually performed including net normal stresses (σ_n - u_a) of 50 and 100 kPa, but for these two stages results were not coherent, so they were not included. The initial intention was to perform the test again and analyze possible mistakes, but, and as it will be seen in following figures, this non-coherent behavior at some stress states kept on happening during all the multi-stage tests. That is why, tests were not repeated and instead, the multi-stages testing procedure was finally changed to single-stage.

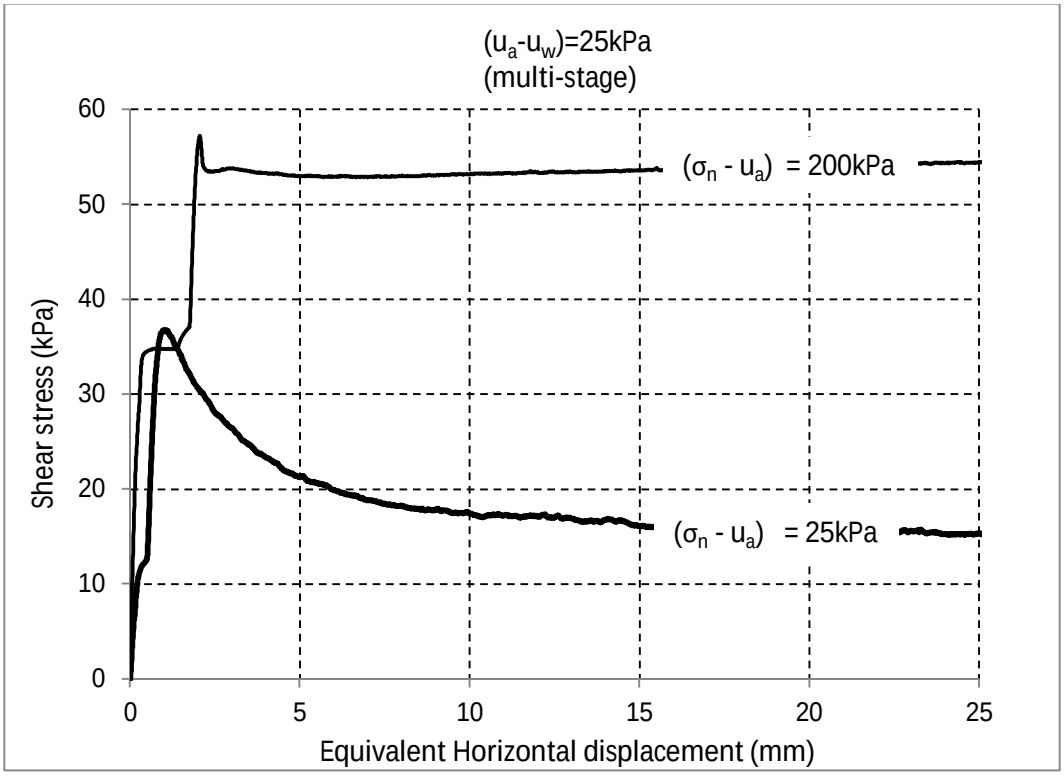

Figure 5-1. Multi-stage test 1 via axis-translation technique

In this figure, results show expected curves in terms of net stress. The higher the net stress, the higher the peak and residual strength of the clayed soil. However, the trend of the second stage had a different behavior compared to the first stage in terms of peak and residual shear stress values.

For the first stage, the difference between peak and residual is clear and the curve has an expected smooth behavior typical of this type of soil. For the second stage, the behavior is different. The peak shear stress is still higher than the residual shear stress, but the difference is very low. Peak and residual shear strength are close. This represented the start of an important conclusion that was drawn from this research project. After the first stage, the sample already failed and its geomechanical properties are not the same as when it was initially prepared. Then, the behavior tends to be different. This happens with the other multi-stage tests, as it is possible to see in the following figures.

Figure 5-2 shows the second multi-stage test performed during this work (test 2: $(u_a – u_w)$ = 50 kPa with $(\sigma_n - u_a)$ = 25, 50, 100, 200 kPa). In this test, all the stages were possible to be plotted. From this test, this difference in peak and residual shear stress values for each stage, when comparing the first stage with the following stages is high (as seen in test 1, peak shear stress value is close to the residual shear stress). Besides, analyzing the peak shear stresses, it is possible to see that for a net normal stress of 25 kPa the peak shear strength is higher than for a net normal stress of 50 kPa and 100 kPa, which is not supposed to happen (this behavior can also be seen in the following multi-stage tests). Finally, regarding the residual shear stress values, this test show expected results, as the higher the net normal stress applied is, the higher the residual shear stress also is.

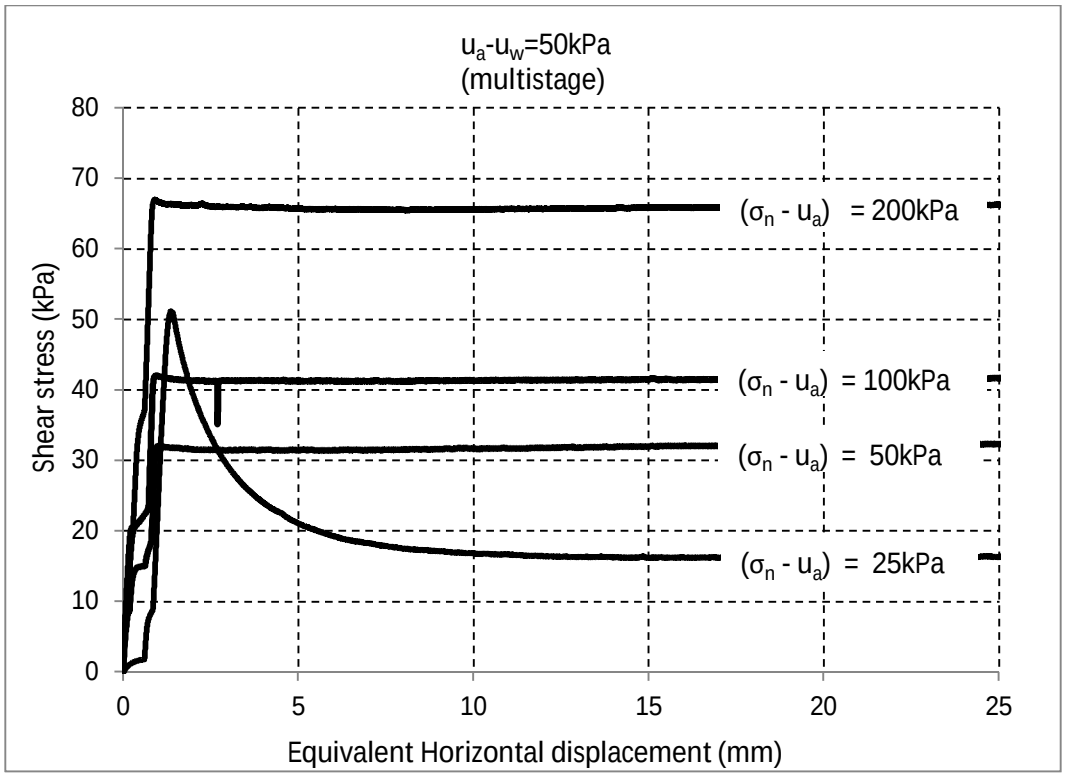

Figure 5-2. Multi-stage test 2 via axis-translation technique

Figure 5-3, shows the third multi-stage test performed during this work (test 3: (u_a – u_w) = 75 kPa with (σ_n - u_a) = 25, 50 kPa). In this test, for net normal stresses of 100 and 200 kPa, plots did not yield coherent results.

For this value of matric suction, a similar behavior seen in test 1 happens, regarding the difference between peak and residual shear stress values (comparing first stage with the following one). Besides, as seen in test 2, the first stage shows a higher peak shear stress for a net stress of 25 kPa compared with a net normal stress of 50 kPa, which is not expected to happen. This test shows flaws seen in tests 1 and 2.

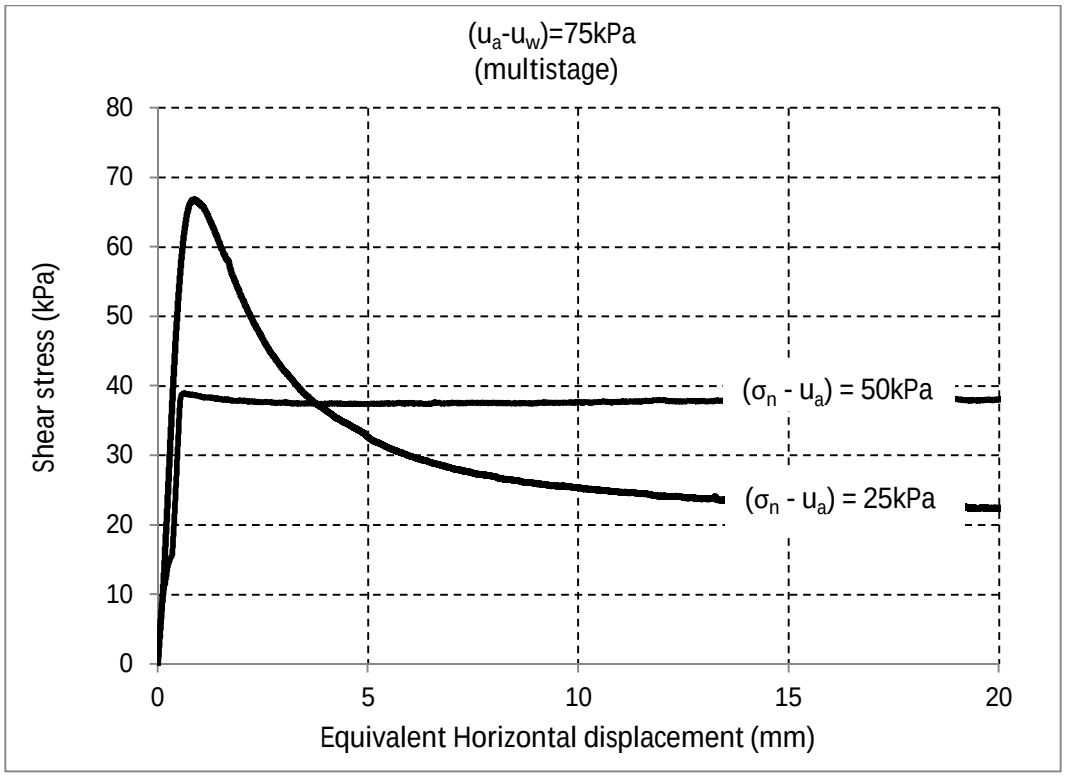

Figure 5-3. Multi-stage test 3 via axis-translation technique.

Figure 5-4, shows the multi-stage test 4 (($u_a - u_w$) = 100 kPa with ($\sigma_n - u_a$) = 25, 50, 100, 200 kPa). This test yielded similar results to those seen in test 2. Factors like: difference from peak to residual shear stresses when comparing first stage with the following stages, higher peak shear stress for a net normal stress of 25 kPa compared to net normal stress of 50 kPa (which is still not expected), and finally, residual stresses show coherent results (higher residual strength for higher net normal stresses.

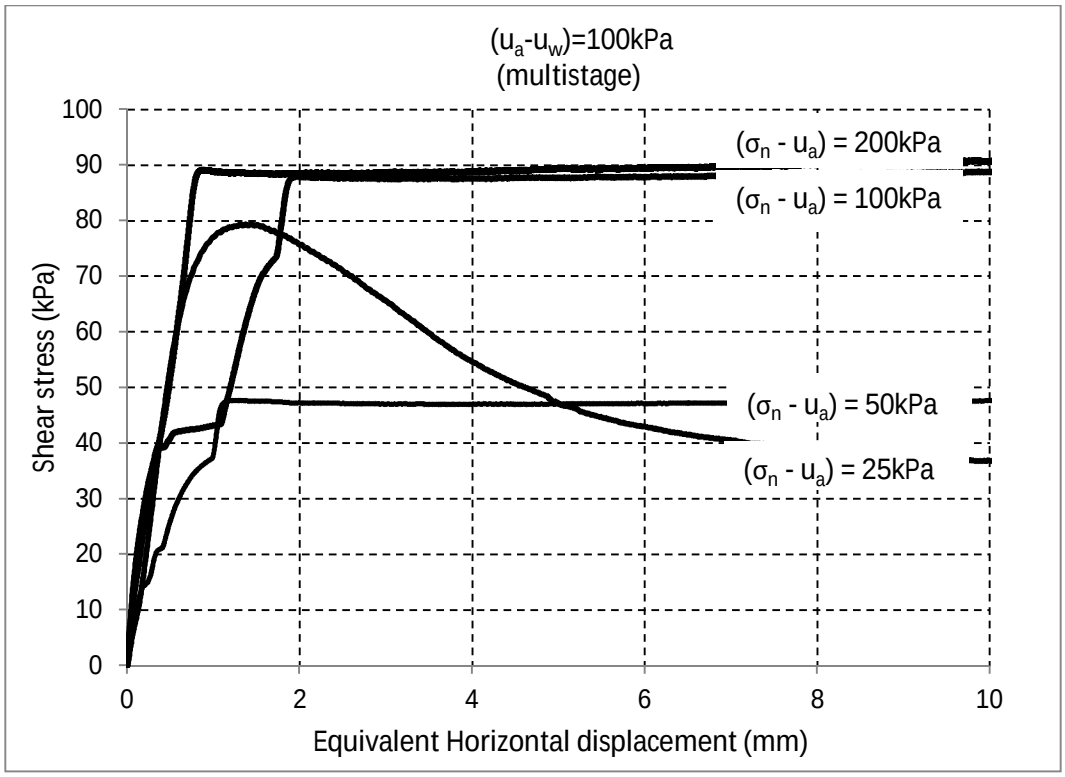

Figure 5-4. Multi-stage test 4 via axis-translation technique

Figure 5-5, shows the multi-stage test 5 (($u_a - u_w$) = 200 kPa with ($\sigma_n - u_a$) = 25, 50, 100 kPa). For this test, as mentioned before, for a matric suction of ($u_a - u_w$) = 200 kPa and a net normal stress of ($\sigma_n - u_a$) = 200 kPa, the torque capacity was exceeded. That is why this curve is not shown.

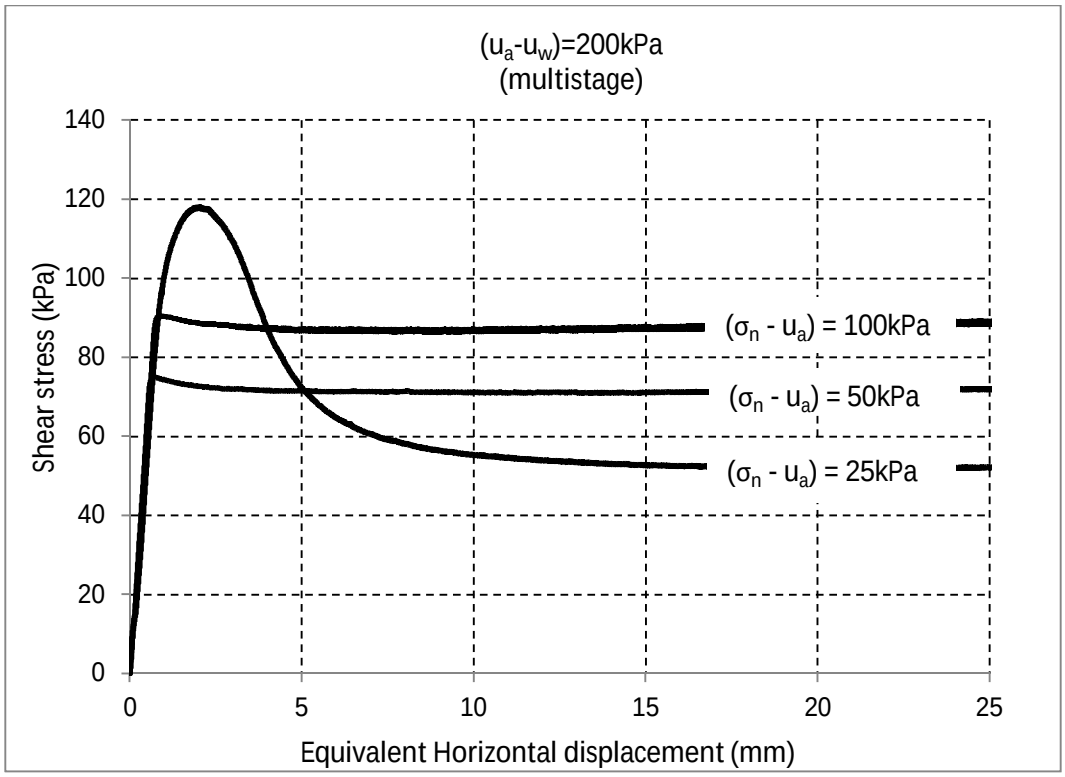

Figure 5-5. Multi-stage test 5 via axis-translation technique

And finally, Figure 5-6, shows the multi-stage test 6 ($(u_a - u_w)$ = 300 kPa with $(\sigma_n - u_a)$ = 25, 50 kPa). Also, results and comments are similar to those of tests 1 to 5. Also, similar to test 5, for net normal stresses equal or higher than 100 kPa, the torque capacity was exceeded, so the curve did not produce any good results.

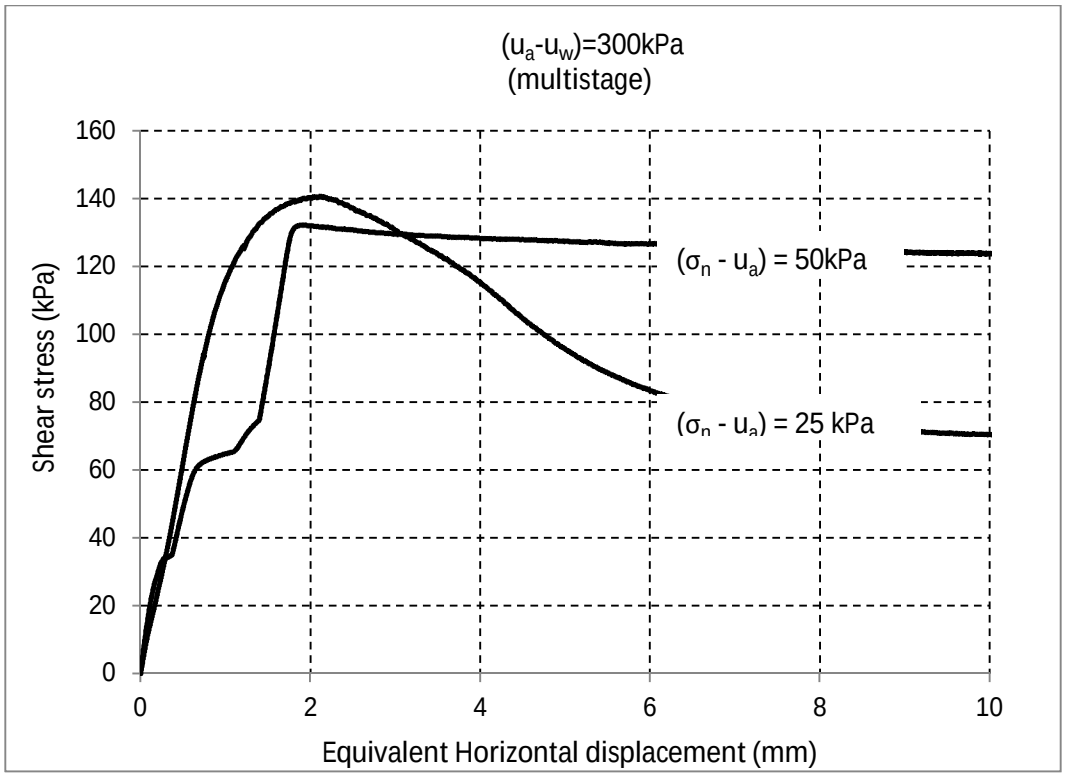

Figure 5-6. Multi-stage test 6 via axis-translation technique

In general terms, these 6 multi-stage tests show very good results for the initial stage of each test, presenting a clear difference between the peak and the residual behavior of the clayed soil. Later, it will be possible to see that by single-stage tests, a much better approach to the actual behavior of a high plasticity clay is possible to have.

5.1.1.3 Multi-stage test results, net normal stress as a function of several matric suction values

For the sake of analyzing the effect of matric suction in the strength of the soil, the following figures in this section, have plots for constant net normal stresses and several values of matric suction.

It is important to mention that for a net normal stress (σ_n - u_a) = 25 kPa, the figure is not shown in this part of the document. It will be explained in the following section that analyzes the single-stage tests. This is because the first stage of multistage tests 1 to 6, were used for the single-stage testing. This is coherent if it is analyzed that the first stage of a multi-stage test is exactly like a single-stage test. This first stage has no influence from the following stages. In the following section, it will be seen that the results are coherent and are what is expected to have as the peak and residual strength of a clayed soil like the one used in this project.

Figure 5-7, shows, for a constant net normal stress of (σ_n - u_a) = 50 kPa, curves for matric suction of (u_a – u_w) = 25, 50, 75, 100, 200, and 300 kPa. The results show curves from the second stage in every multistage test (after first stage or (σ_n - u_a) = 25 kPa). Results show an increase in both peak and residual shear strength with the increase in matric suction, which is an expected behavior. Here, the difference between peak and residual shear stress for each curve is low because, as mentioned at the beginning of this paragraph, they are results from a second stage.

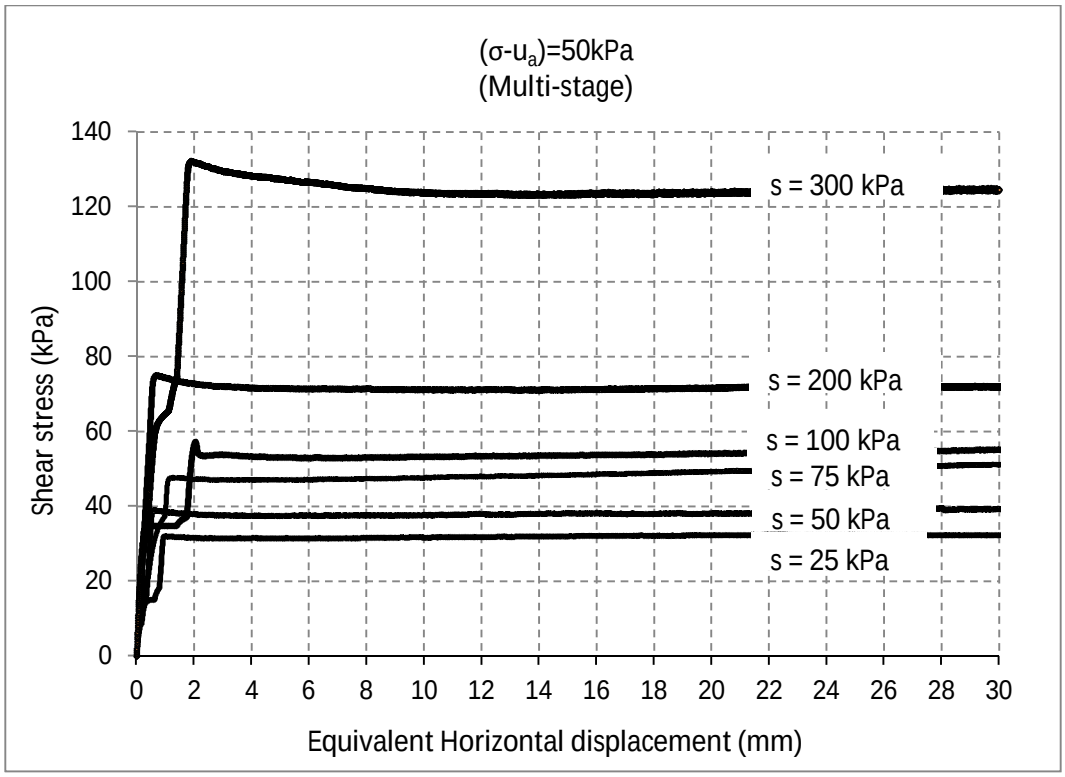

Figure 5-7. Multi-stage testing via axis-translation technique for a net stress of 50 kPa

Similarly, figure 5-8, presents for a net normal stress of $(\sigma_n - u_a)$ = 100 kPa, several values of matric suction $s = (u_a - u_w)$ = 50, 100, and 200 kPa. In this case, the situation is similar. The only observation would be that for matric suction values of 100 kPa and 200 kPa, the residual shear stress is very similar.

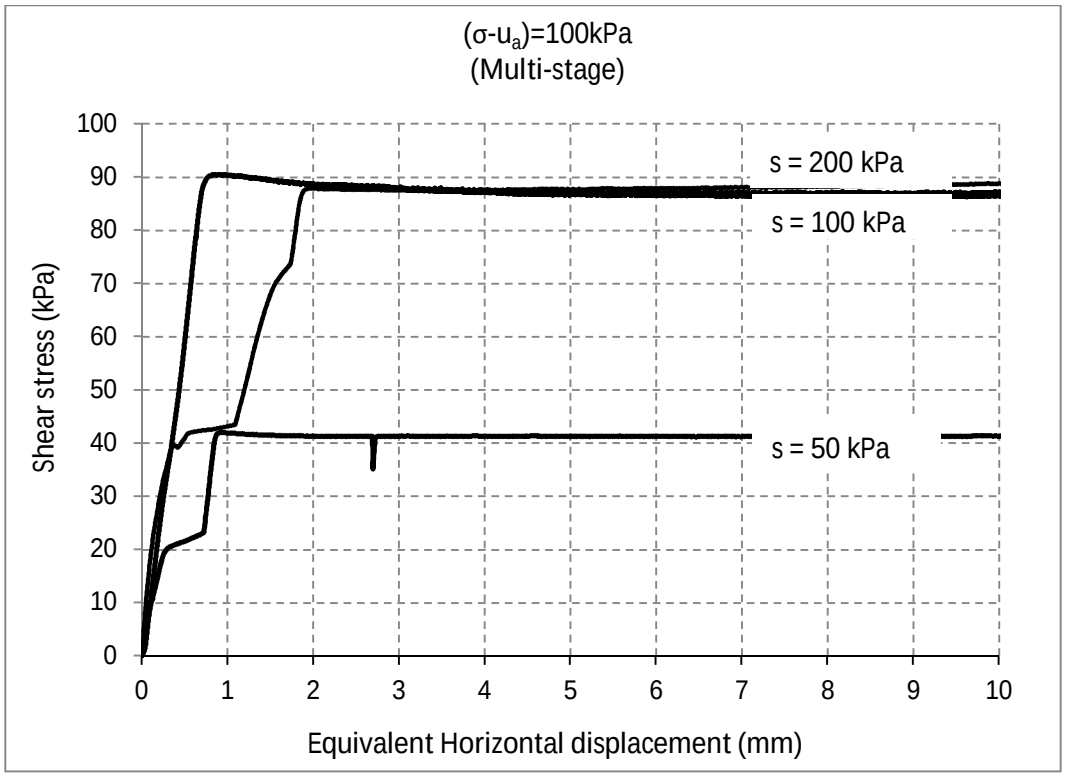

Figure 5-8. Multi-stage testing via axis-translation technique for a net stress of 100 kPa

And finally, figure 5-9, shows for a net normal stress of $(\sigma_n - u_a)$ = 200 kPa, several values of matric suction $s = (u_a - u_w)$ = 25, 50, and 100 kPa. A curve for matric suction of 200 kPa is not presented because, as said before, this combination of stresses causes the device to exceed its torque capacity.

In general terms, for these three previous figures, the suction shows, as expected, an increase in both peak and residual strength of the soil. However, the behavior of the curves in terms of the difference between the peak and residual shear stress values, because it is too low.

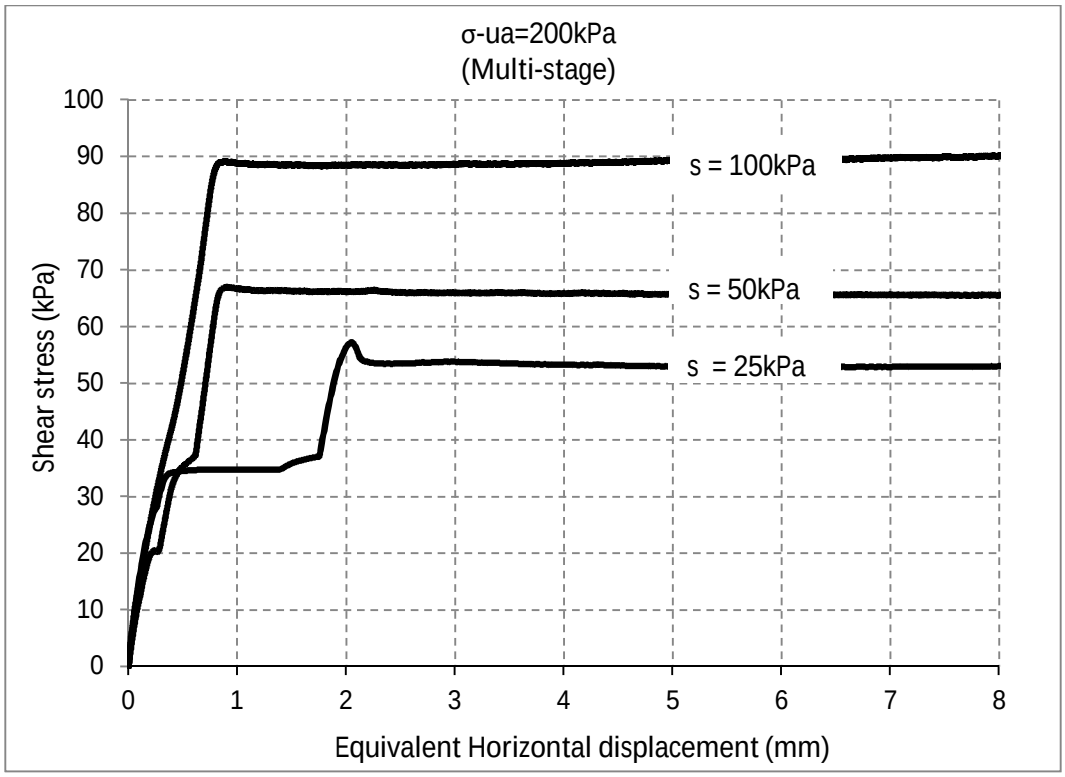

Figure 5-9. Multi-stage testing via axis-translation technique for a net stress of 200 kPa

5.1.2 Single-stage Testing

Based on the difficulties and flaws found on multi-stage testing procedures for the particular case of high plasticity clays subjected to large deformations, after test number 6, the decision was to start running single-stage tests. The main reason to do this change in the experimental program has a strong background, and the results that this project presents, support it.

In the previous section, it was explained that after the first stage, the soil sample already failed, and consequently, the soil properties change.

Then, even though the net normal stress applied increases and the shearing process is achieved under a higher normal stress, the peak and residual behavior is going to be different. Proof of this is the fact that in the previous section, those plots showing curves for different net normal stress at a constant matric suction, present the same behavior comparing the first stage with the following ones. This is, the first stage shows a smooth curve that has a clear peak stress and a drop in the curve that leads to a very different value of residual stress compared with the peak one. Nevertheless, the following stages show a peak stress that is higher than the residual stress as expected, but both values are very close.

This behavior can lead to conclude that the soil sample already had a failure surface in the first stage, and even though the sample is receiving different and higher net normal stresses, the shear stresses occur in the same failure surface.

Due to this proposed criteria, this section is committed to show why, plotting each curve with a different sample, will let the peak and residual strength of the specimen start from the same initial conditions, and consequently will show different results only based on the different state of stresses applied.

5.1.2.1 General steps of single-stage testing via axis translation technique

The procedure followed to perform a single-stage test is very similar to that one followed to perform a multi-stage test. This is, the preparation of the sample, the equilibrium of suction (which takes around 4 to 5 weeks because of the soil tested and depending on the air pressure applied), the first consolidation of the sample, and the first shearing stage, are the same for both type of tests.

The difference lies in the procedure after the first shearing stage, which, by the way, in a single-stage test, is actually the only one stage. After this single shearing stage is achieved, the net normal stress, the shear stress and the air pressure (matric suction) are set to zero, and the sample is removed in order to start a new test.

It is important to mention that the equilibrium of suction is the same regardless the type of test performed. The time required for equilibrium is only a function of the applied air pressure. Therefore, it is more time consuming to perform single-stage than multi-stage tests, because in a multi-stage, the equilibrium of suction is reached just once, for a number of stages that is always more than one, while for a single stage, equilibrium must be reached for only on stage. The following results will show that, even though single-stage are long lasting tests, they are totally worth it.

5.1.2.2 Single-stage test results, matric suction as a function of several net normal

To be consistent with the plots shown in multi-stage results, and in order to compare both techniques, the following plots will show shear-strain behavior of the soil for a constant matric suction and different net normal stresses. Unlike multi-stage analysis, each one of the curves in each plot is a different single-stage.

It is very important to mention that in these single-stages tests, the first stage was taken from each multi-stage test. As it will be seen, the first stage of all the multi-stage tests show a very high consistency with the rest of the single-stage tests in terms of peak and residual strength. This behavior did not happen during multi-stage testing, where after the first stage, and even though the net stress was increased, the peak strength decreased, which is not a coherent conclusion.

Figure 5-10, presents single-stage tests performed for a matric suction of (u_a- u_w) = 25 kPa and several values net normal stresses. From this figure, it is possible to see that the first stage (which was taken from the first stage of the multi-stage test 1) is very consistent with the following single-stage tests in terms of peak and residual shear strength. Besides, the shape of the curves is very similar from one to another and is actually the behavior that a high plasticity clayed soil should have. The consistency is also proved when the increase in the net normal stress generates an increase in both the peak and residual strength.

This initial figure shows that preparing new samples for each test, and trying to let the specimen have the same initial conditions in terms of its geomechanical properties and in terms of initial stresses, yield much better and coherent results than running tests with samples that have different initial conditions due to previous stages (different geomechanical properties and different stress history).

Finally, regarding the difference between residual shear strength from one curve to another, regarding the first three curves (net normal stresses of 25, 50 and 100 kPa), compared to the curve for net normal stress of 200 kPa, it is possible to say that, in order to be a fully consistent behavior of residual strength, the difference in residual shear stresses among all the curves should be similar. A positive conclusion from this is that, even though this difference in behavior is happening to the last test, still is coherent because for higher net normal stresses, residual stress values are also higher.

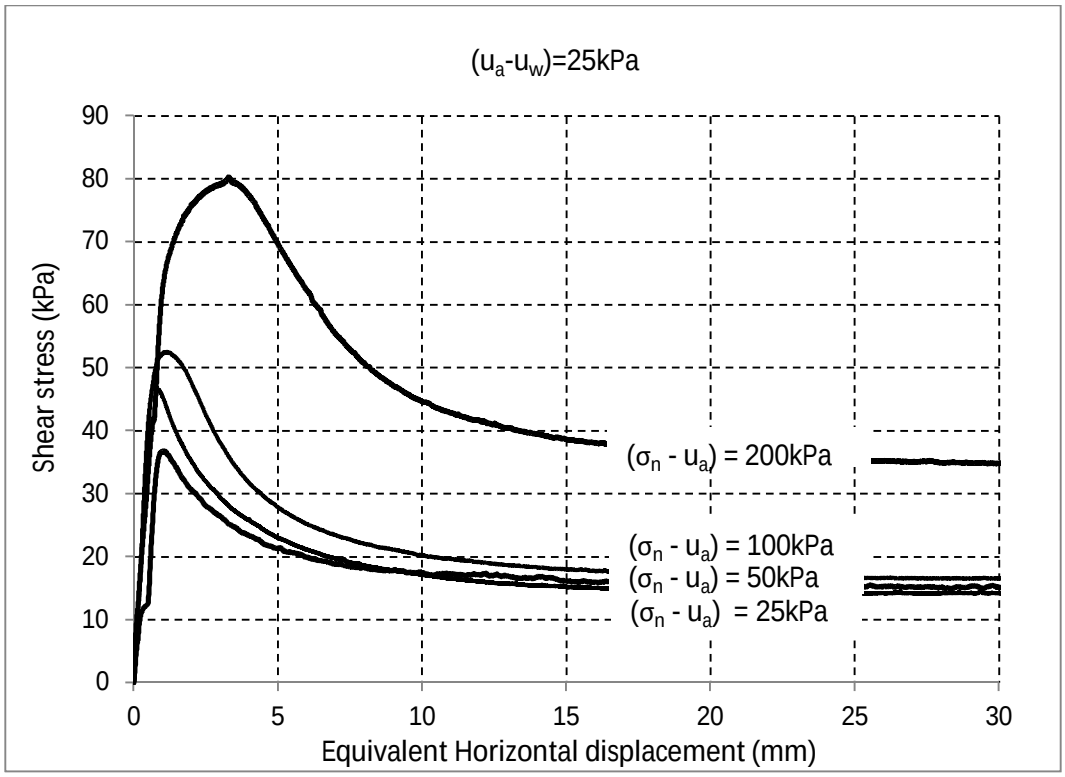

Figure 5-10. Single-stage tests via axis-translation technique for a matric suction of 25 kPa

Figure 5-11, presents single-stage tests performed for a matric suction of (u_a- u_w) = 50 kPa and several values net normal stresses. From this figure, it is possible to see that the first stage (which was taken from the first stage of the multi-stage test 2), just as in the previous figure, is consistent with the following single-stage tests regarding peak and residual strength. In general, all the curves in the figure present coherent results in terms peak strength, residual strength, difference between peak and residual stresses, increase in strength due to the increase in net normal stress.

Besides, compared with previous work in which tests were performed compacting the sample in the triaxial frame, the curves are now smoother. This is an important conclusion, particularly knowing that each one of these curves have approximately 15,000 to 16,000 readings of shear stress vs. angular deformation.

This figure shows one of the best results of the entire experimental program. This is because the difference between the peak shear strength from one curve to another is similar, and the same behavior occurs among residual shear strength values.

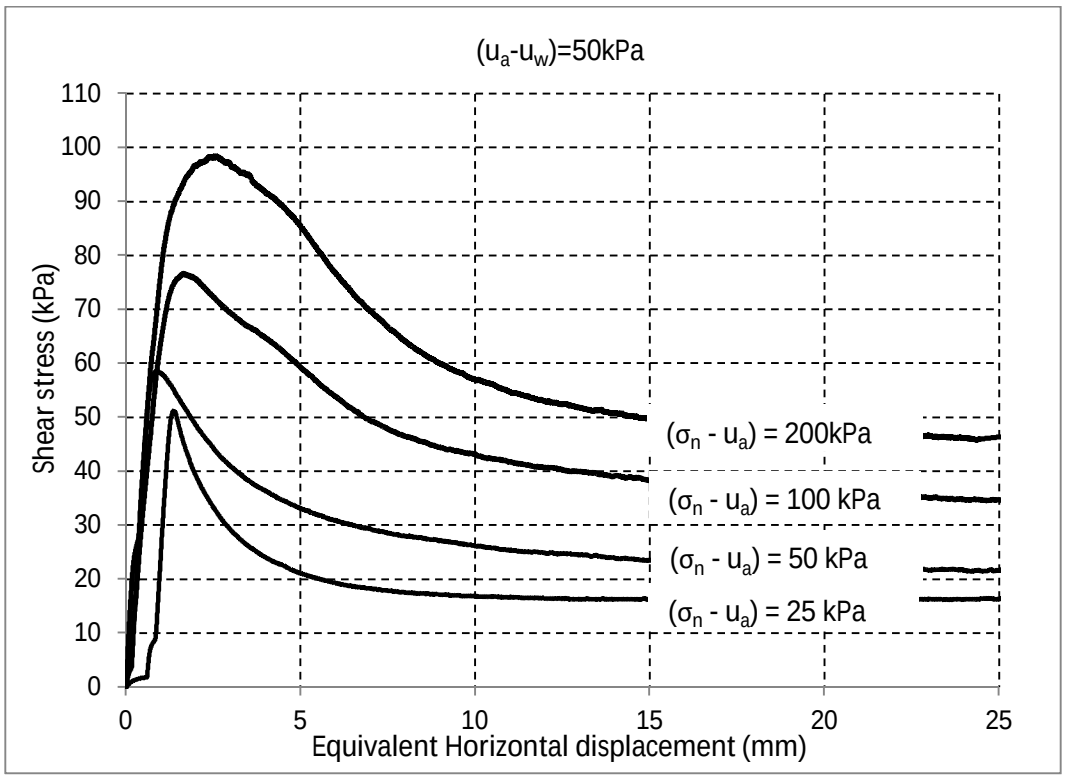

Figure 5-11. Single-stage tests via axis-translation technique for a matric suction of 50 kPa.

Figure 5-12, shows single-stage tests performed for a matric suction of (u_a- u_w) = 100 kPa and several values of net normal stresses. Here, it is possible to see that the first stage (which was taken from the first stage of the multi-stage test 4), is also consistent, regarding the increase in net normal stresses of the following single-stage tests plotted, and in terms of peak and residual stress values. In this figure, for net normal stresses of 25 and 50 kPa, the residual shear strength is virtually the same. In this particular case, this is not a common behavior, and residual shear stress should be higher for a higher net normal stress. Here, if it is emphasized that a CH soil like this one, is a complex soil to work with, this behavior may happen. A good result from this is the fact that the residual shear stress value for a net normal of 25 kPa is not higher than for a net normal stress of 50 kPa.

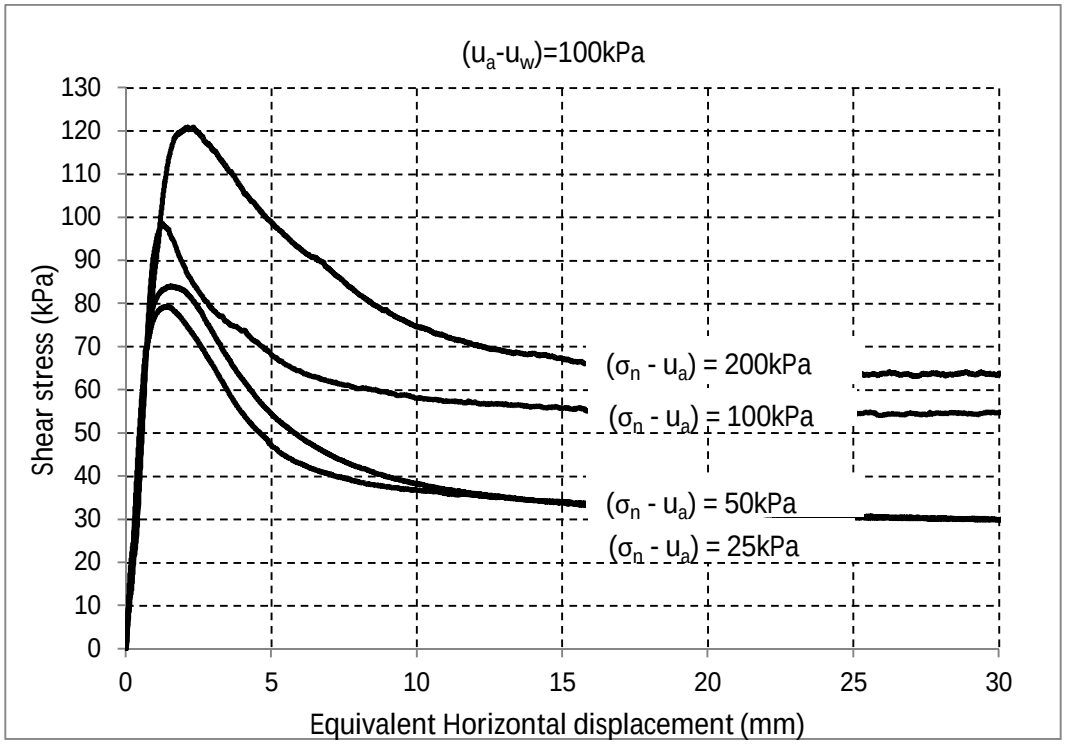

Figure 5-12. Single-stage tests via axis-translation technique for a matric suction of 100 kPa

Figure 5-13, shows single-stage tests performed for a matric suction of (u_a- u_w) = 200 kPa and several values of net normal stresses. Once again, the first stage (taken from the first stage of the multi-stage test 5). A curve for net normal stress of 200 kPa was not presented, as mentioned previously, because for this combination of stresses, the torque capacity of the equipment was exceeded. The test for this particular curve was actually performed, but, at a certain point the equipment itself stopped the test.

In spite of that, the three curves plotted, still show excellent behavior in terms of peak and residual strength, the difference shear stress values among all of them, and an increase in strength due to an increase in net normal stress.

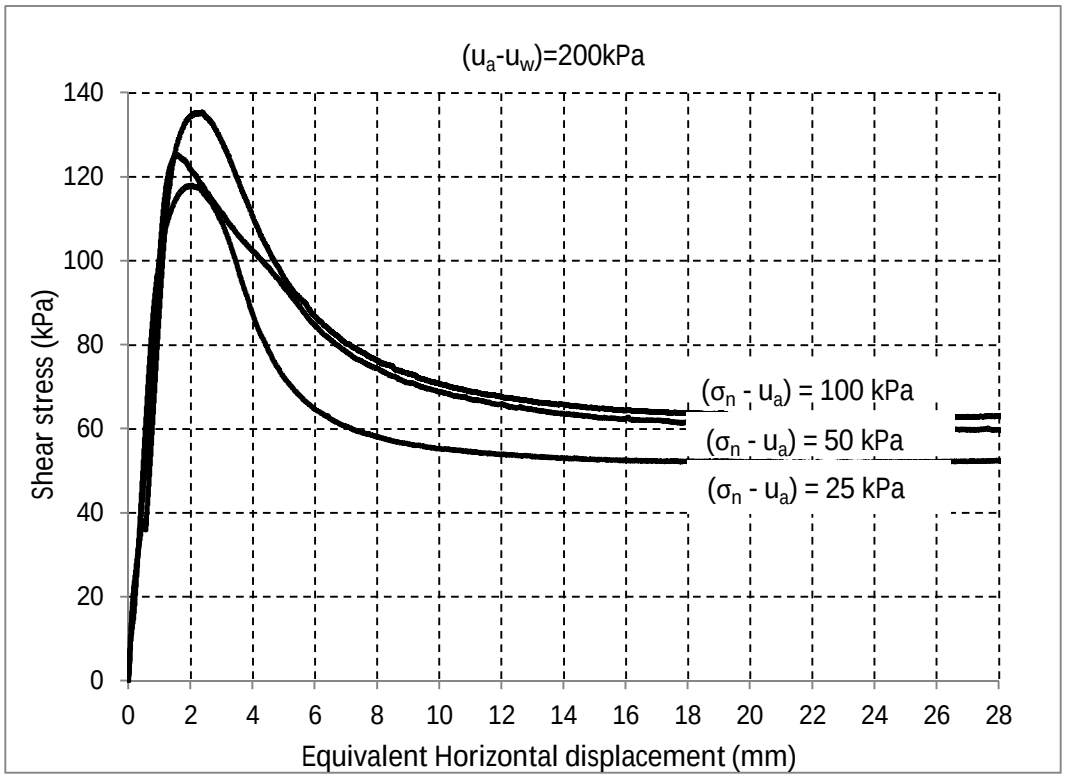

Figure 5-13. Single-stage tests via axis-translation technique for a matric suction of 200 kPa.

Figure 5-14, shows single-stage tests performed for a matric suction of (u_a- u_w) = 300 kPa and several values of net normal stresses. Once again, the first stage (taken from the first stage of the multi-stage test 6). Curves for net normal stresses of 100 kPa or higher were performed but not presented, because, the torque capacity of the equipment was exceeded again.

Even though this figure only shows two curves, due to the mentioned torque capacity limitations, results are still consistent and for higher net normal stress, the results show higher peak and residual strength values, and the curves are smooth and have a similar trend.

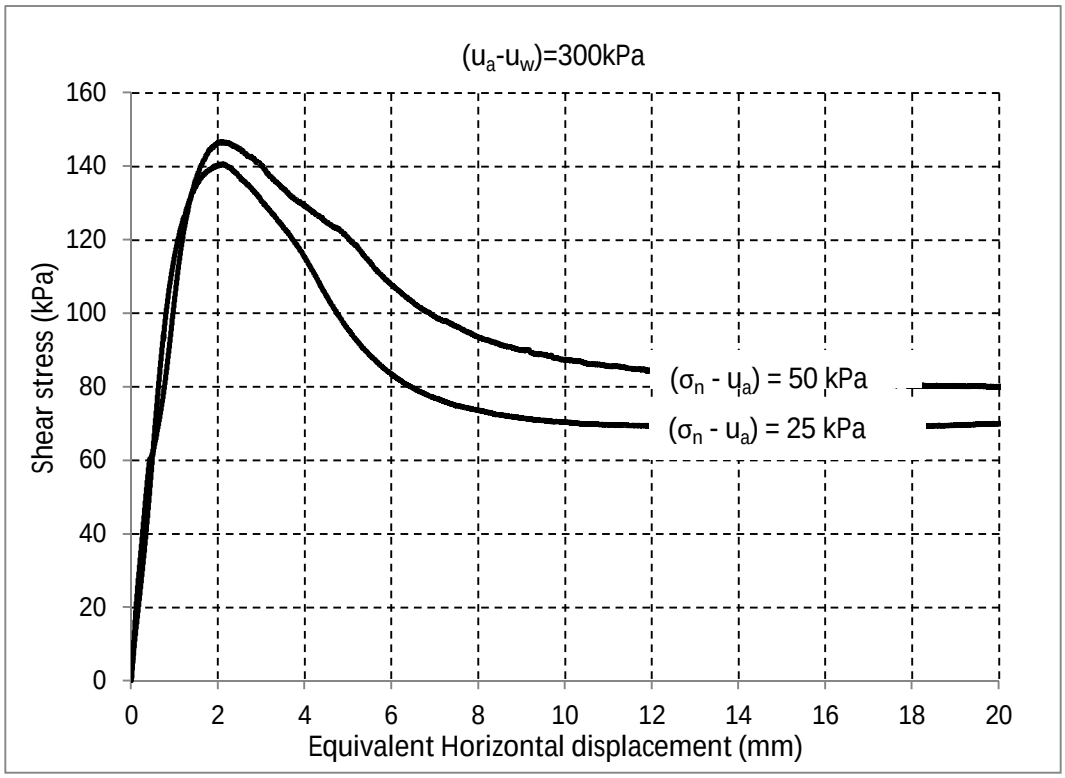

Figure 5-14. Single-stage tests via axis-translation technique for a matric suction of 300 kPa.

As partial concluding remarks based on these single-stage testing program, several positive insights can be highlighted. For a high plasticity clay, and in order to measure its peak and residual behavior in an equipment like the ring shear apparatus, which allows large deformations with no limit (before guaranteeing residual behavior has been reached), single-stage tests are a good option. The only flaw that can be mentioned so far, is that the tests take more time than multistage-testing, but the advantages highly outweigh the variable time.

Among the advantages of single-stage tests, some of them can be mentioned: smooth curves that show a clear difference between peak and residual behavior, consistent behavior among all stages in terms of this difference, guarantee that for each curve, the soil has virtually the same initial geomechanical properties and the same stress history (which is actually the compaction procedure). This last advantage is the most important one, because it allows comparing the curves for specimens under the same conditions. If the soil samples used have different properties and/or previous applied stresses, a comparison between them makes no real sense.

5.1.2.3 Single-stage test results, net normal stress as a function of several matric suction values

The previous was aimed to show and explain the advantages of single-stage testing procedures to test CH soils subjected to large deformations in the ring shear apparatus. The difference between the peak and residual shear strength behavior was clear, the curves were smooth (which is not easy because the software makes thousands of readings for each curve or test and the equipment is very sensitive), and the increase in net normal stress generated an increase in shear strength as it was expected.

This section presents the same single-stage tests of the previous section, but now each figure has curves under a constant net normal stress ($\sigma_n - u_a$) and for several values of matric suction ($u_a - u_w$). The main objective of this following plots is to show that the consistency was not only proved for several net normal stresses under a constant matric suction value, but also when an increase in matric suction is applied.

Figure 5-15, shows, for a constant net normal stress ($\sigma_n - u_a$) = 25 kPa, curves of several values of matric suction ($u_a - u_w$). This figure is particularly important, because it is presenting the first stage of all the six multi-stage tests. This explains that the soil in the first stage has initial conditions in terms of geomechanical properties and initial stress conditions, so the behavior of the curve is only a function of the soil properties and the applied "matric suction-net normal" stresses. Here, there is no influence of previous stresses and/or shearing processes.

The consistency is clear, the behavior of peak and residual shear stresses show an important difference (which is supposed to occur in a clayed soil), the trend of all the curves is similar, and of quite importance, the increase in matric suction, generates an increase in shear strength.

Due to the plot scale, for matric suctions of 25 kPa and 50 kPa, residual strength values seem to be equal, but they are not. Values are close, and in the following chapter, when failure envelopes are going to be studied and analyzed, the difference will be seen.

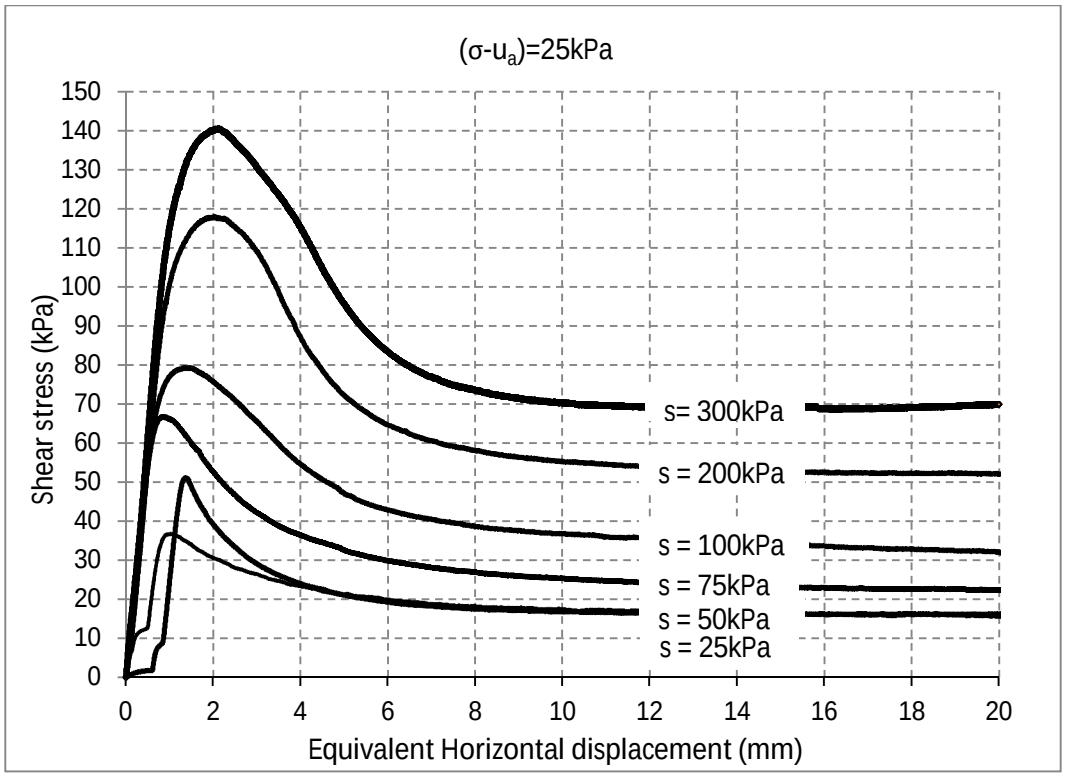

Figure 5-15. Single-stage test (first stage of multi-stage tests 1 to 6) for a net stress of 25 kPa

Figure 5-16 shows, for a constant net normal stress ($\sigma_n - u_a$) = 50 kPa, curves of several values of matric suction $s = (u_a - u_w)$. In this case, all the curves were tests performed with single-stage procedures. No multi-stage curves were included here, because a net normal stress of 50 kPa implies a second stage of a multi-stage test, which belongs to a sample that already failed.

Once more, the trend of the curves is very similar, and the correspondence between increase in matric suction and peak-residual strength is as expected.

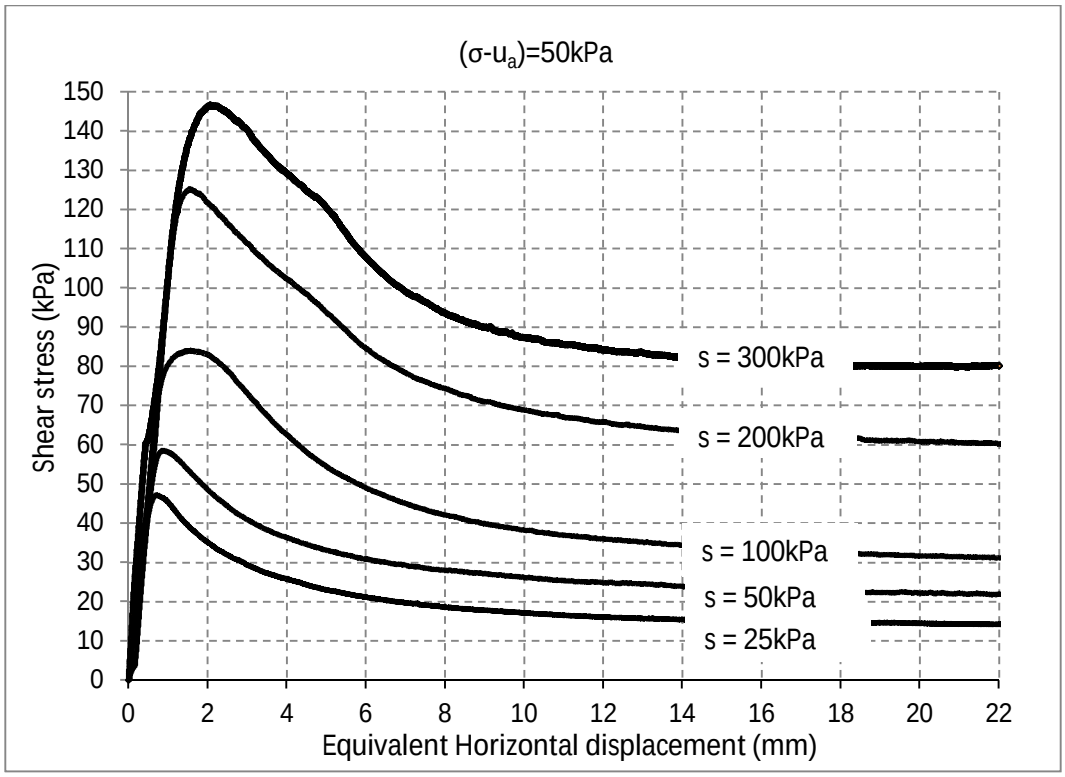

Figure 5-16. Single-stage test via axis-translation technique for a net stress of 50 kPa.

Figure 5-17, shows, for a constant net normal stress ($\sigma_n - u_a$) = 100 kPa, curves of several values of matric suction s = ($u_a - u_w$). As in the previous figure, all the curves were tests performed with single-stage procedures. For this value of net stress, once again peak and residual shear strength behavior keep on showing coherent results in terms of trends, difference between peak and residual values, and increase in strength due to an increase in matric suction.

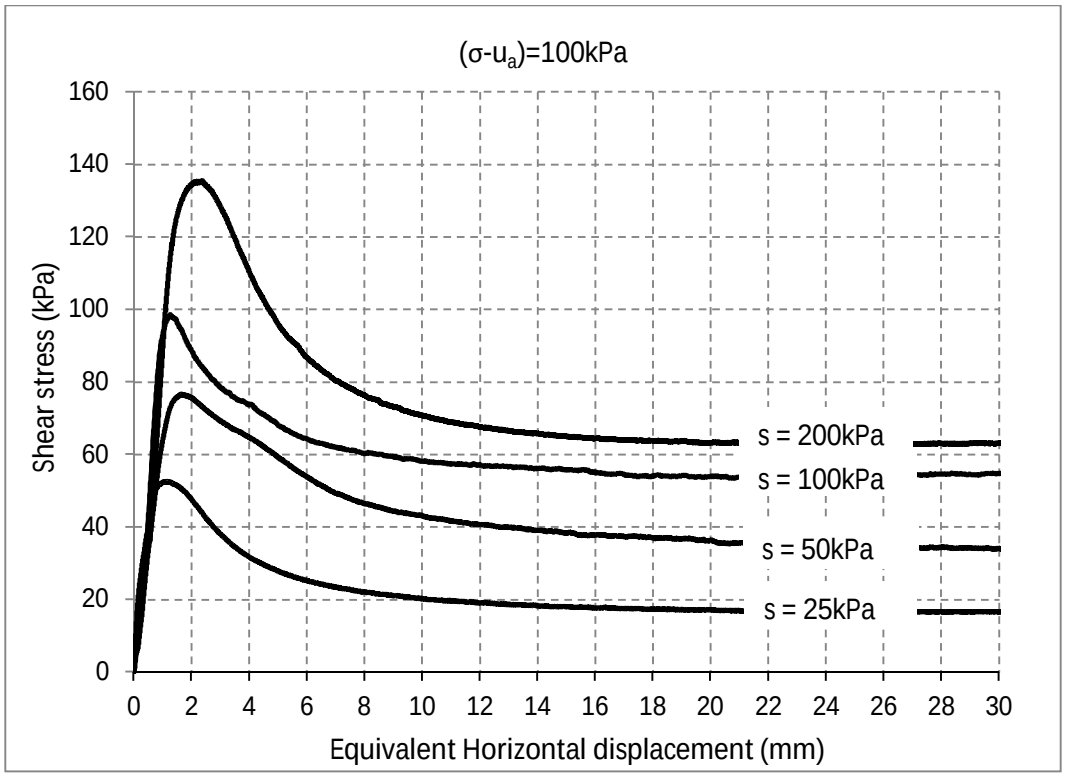

Figure 5-17. Single-stage test via axis-translation technique for a net stress of 100 kPa.

Finally, figure 5-18, shows, for a constant net normal stress ($\sigma_n - u_a$) = 200 kPa, curves of several values of matric suction s = ($u_a - u_w$). In this las case, there are only three curves. This occurs because, and as mentioned before, for a combination of net normal stress of 200 kPa and matric suction of 200 kPa, the torque capacity is exceeded, so the equipment and its software stopped the test at a certain point before reaching this torque capacity. So, this particular test was actually run, but it does not show representative results.

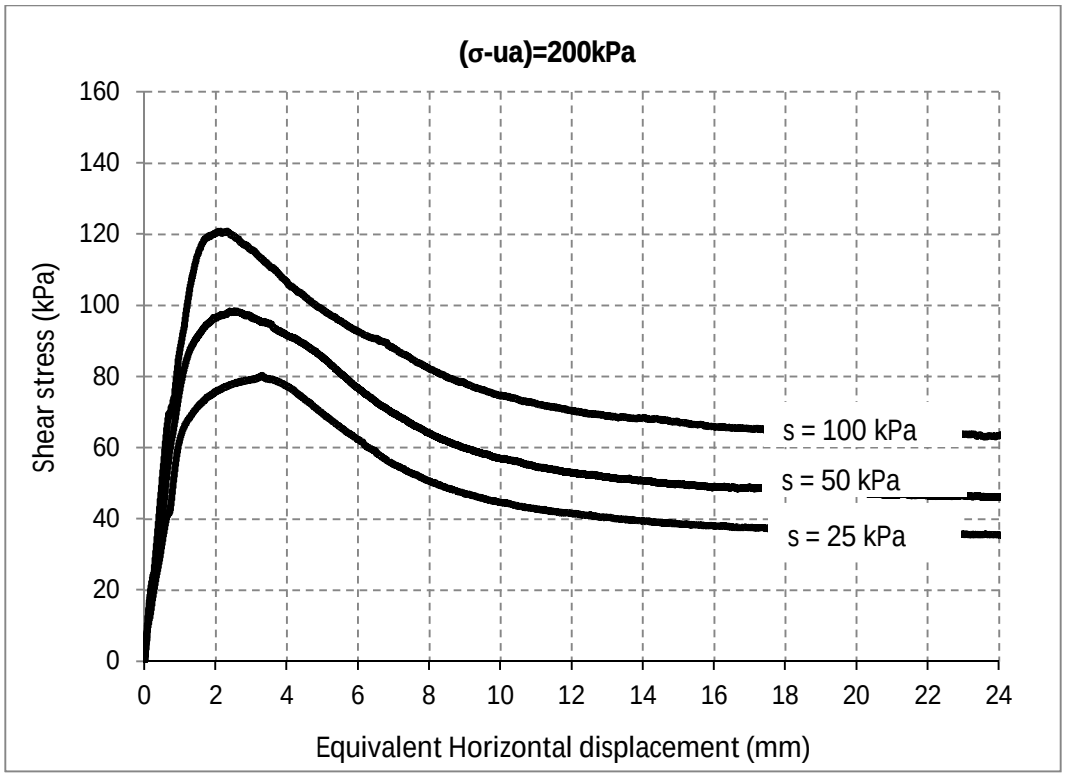

Figure 5-18. Single-stage test via axis-translation technique for a net stress of 200 kPa.

Even though the last single-stage test was not possible to be finished, the three other curves show the coherent and consistent results that have been shown throughout the entire single-stage testing program. Similar trends, coherent peak and residual strength behavior in terms of matric suction increase, and smooth curves that present a clear difference between the peak and the residual strength.

As concluding remarks, it is possible to mention that single-stage testing procedures could overcome the flaws and difficulties previous work results, which by the way, helped a lot to notice the advantages of these new proposed techniques.

Besides, single-stage tests also helped to get much better results, particularly with this challenging type of complex soil, that is not only highly plastic, but also a low permeability one which equilibrium of suction takes a long time and which is subjected to large deformations in the ring shear apparatus.

In the following chapter, where the analysis of definitive results are presented, it will be possible to see that results from both the first stage of multi-stage tests and all the single-stage tests were the ones used to achieve and draw conclusions about peak and residual shear strength of this CH soil.

5.1.3 Comparison Between Multi-stage and Single-stage Testing

For the sake of being clear, specific and thorough to explain the reasons mentioned above, regarding the advantages of working with a single-stage technique for the assessment and measurement of peak and residual shear strength in clayed soils subjected to large deformation, this section is devoted to graphically present and compare the two techniques that intend to achieve this goal.

The following two subsections will present the entire experimental program performed, using axis-translation technique. This is tests 1 through 6 (multi-stage) and test 7 through 18 (single-stage).

For the multi-stage tests, it is important to mention that all the tests were performed, but not all the curves were presented, because they were not representative. On the other hand, for the single-stage tests, all the curves yielded good results and are shown. Only two tests were not shown for the single-stage part of the experimental program, and it was because they both exceeded the torque capacity (as mentioned in previous sections).

These two tests were for: net normal stress ($\sigma_n - u_a$) = 100 kPa under matric suction ($u_a - u_w$) = 300 kPa; and for net normal stress ($\sigma_n - u_a$) = 200 kPa under matric suction ($u_a - u_w$) = 200 kPa.

5.1.3.1 Matric suction as a function of several net normal stresses

The following five figures will show the shear strength behavior of the analyzed material, each figure showing, for a constant value of matric suction ($u_a - u_w$), the behavior for several values of net normal stress ($\sigma_n - u_a$).

Figure 5-19, presents multi-stage vs. single stage tests for a matric suction of ($u_a - u_w$) = 25 kPa and net normal stresses of ($\sigma_n - u_a$) = 25, 50, 100, and 200 kPa (single-stage), and ($\sigma_n - u_a$) = 25, and 200 kPa (multi-stage). For the multi-stage tests, two stages ($\sigma_n - u_a$) = 50, and 100 kPa) are stages that were actually performed, but they were not presented, as mentioned before, because they were not representative regarding the shear strength behavior. This is, the curves reached the peak, then dropped slightly to residual and then went up again to values that were even greater than the peak value.

This is one of the reasons why this project suggests single-stage testing procedures and considers a multi-stage test, a non-reliable one, particularly when working with clayed soils.

Now, regarding the curves shown in the figure, it is possible to see that for a net normal stress ($\sigma_n - u_a$) = 200 kPa, the single-stage curve gives a higher peak shear strength and a lower residual shear strength compared to the multi-stage curve. This leads to several comments.

First, the single-stage test yielded a higher peak shear strength, probably because the initial conditions of the sample did not have any previous shearing and failure stages, so the geomechanical properties (strength-strain properties) do not have any influence from a previous stress state (stress history), contrary to the multi-stage test which in this case had three previous failure stages. This may be the reason for the lower peak shear strength in the multi-stage test.

Second, the single-stage test shows a smooth trend and a clear difference from peak to residual behavior, which is actually expected in this soil type. The multi-stage test shows a peak and a residual, but the difference between them is not very clear and besides, the curve intends to increase after about 15 mm of equivalent horizontal displacement until a point at which it seems to virtually reach the value of peak shear strength. This may occur because of two reasons. One could be that the sample already failed in previous stages (in the same failure surface), so the peak strength is lower to a point where it is close to residual strength. Another reason could be that the sample is suffering a “softening behavior” after the stages, so after each stage, the curve tries to go from a “brittle” behavior to a “ductile” behavior, even though it is good to clarify that at the end of each curve, the residual stress does not get to a similar value for these two curves.

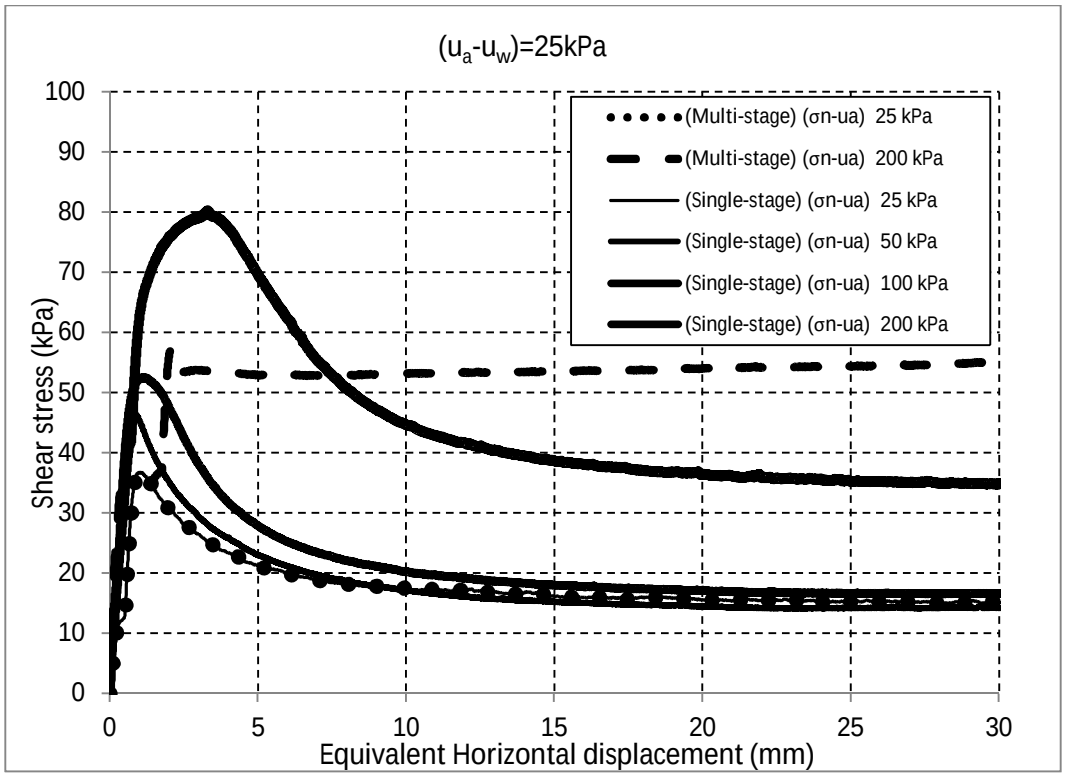

Figure 5-19, Multi-stage vs. single-stage testing for a constant matric suction of 25 kPa

Figure 5-20, presents multi-stage vs. single stage tests for a matric suction of (u_a – u_w) = 50 kPa and net normal stresses of (σ_n – u_a) = 25, 50, 100, and 200 kPa (multi-stage and single-stage). As it is possible to see, in this case, all the stages reached good results in the multi-stage test. In terms of the strength behavior, the trend is very similar when comparing both techniques. The single-stage test still shows a clear difference and a smooth drop from peak to residual strength, and a higher peak shear strength values in all the stages (stages that represent the four values of net normal stresses applied). On the other hand, the multi-stage test keeps showing a very low difference between the peak and residual strength values, and the residual strength is higher than that resulting from the single-stage test.

In these curves from the multi-stage test, the closeness between peak and residual shear stress values is even more visible, and the both peak value and the point where the curve starts trying to search residual are not clear.

Finally, only regarding multi-stage test, and comparing the first stage with the second one, the peak shear strength is higher for 25 kPa than for 50 kPa of net normal stresses. This behavior is not supposed to be like this, because the higher the net normal stress is, the higher the shear strength should be. From this comment, it is fundamental to emphasize that when comparing this first stage of the multi-stage test with the other single-stage tests, the behavior is very consistent.

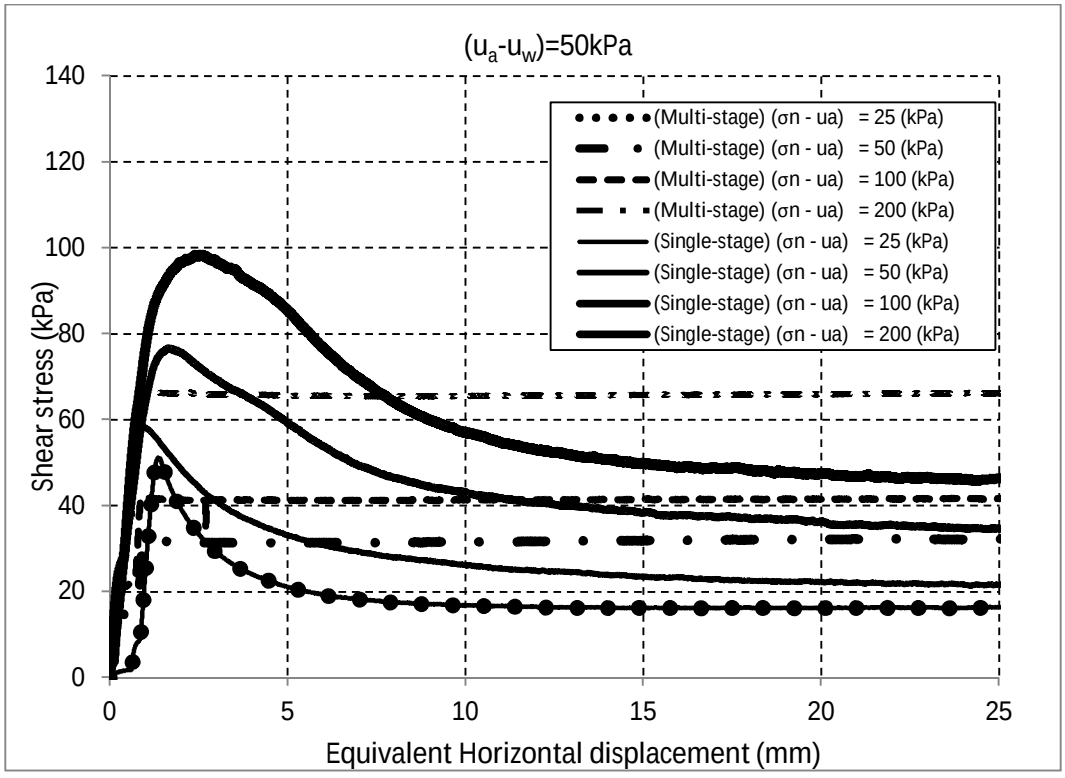

Figure 5-20. Multi-stage vs. single-stage testing for a constant matric suction of 50 kPa

Figure 5-21, presents multi-stage vs. single stage tests for a matric suction of (u_a – u_w) = 100 kPa and net normal stresses of (σ_n – u_a) = 25, 50, 100, and 200 kPa (multi-stage and single-stage). The behavior and differences here are similar to those seen and commented on previous figure for matric suction of 50 kPa and net normal stresses ranging from 25 to 200 kPa. Some comments can be made about the figure that reinforce the potential advantage and reliability of performing single-stage tests.

In the single-stage tests, for net normal stresses of 25 kPa and 50 kPa, the residual shear strength is almost the same. It should not occur, but at least the residual shear strength for a net normal stress 25 kPa is not higher than that one for 50 kPa of it.

In the multi-stage test, for a net normal stress of 100 kPa, besides the peak shear stress is not clear, it is lower than the residual shear stress, which is not a coherent result.

Finally, just for the sake of explaining the short length of the multi-stage test stage for net normal stress of 200 kPa, it is possible to say that it the test was stopped because it had the same behavior as the curve for net normal stress of 100 kPa, and at an approximately equivalent horizontal displacement of 11 mm, the residual shear stress had already exceeded the peak shear stress.

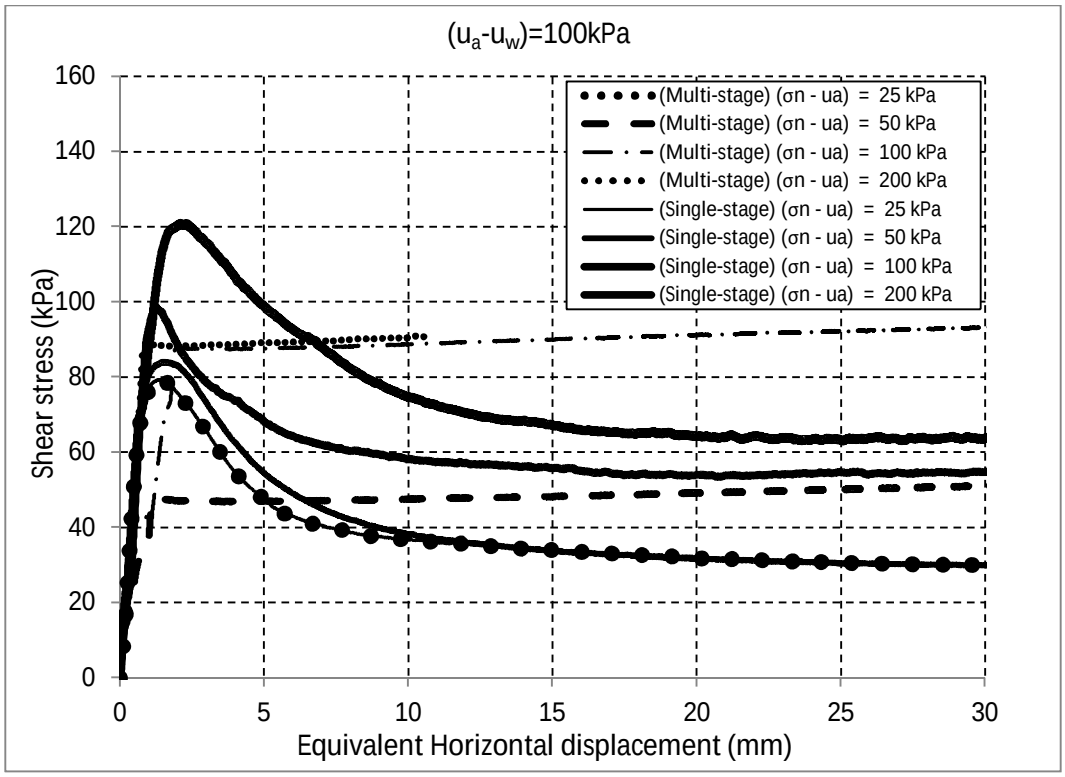

Figure 5-21. Multi-stage vs. single-stage testing for a constant matric suction of 100 kPa

Figure 5-22, shows multi-stage vs. single stage tests for a matric suction of (u_a – u_w) = 200 kPa and net normal stresses of (σ_n – u_a) = 25, 50, and 100 kPa (multi-stage and single-stage. The behavior is still the same. In the multi-stage test, the peak shear stress of the first stage ((σ_n – u_a) =25 kPa) is now higher not only than the peak shear stress of second stage ((σ_n – u_a) =50 kPa) but also than that one of ((σ_n – u_a) =100 kPa), which is still more concerning if the objective is to draw coherent conclusions. Then, when comparing this first stage of multi-stage with the other ones from single-stage tests, the results are the expected ones (just as it happened in the previous figure for a matric suction of 100 kPa).

Finally, in this figure, curves for net normal stress of 200 kPa are not presented neither for the multi-stage test nor for the single-stage tests. This is because under this combination of net normal stress and matric suction values, the torque capacity is exceeded.

The multi-stage test was actually performed for this combination of stresses ((u_a – u_w) = 200 kPa and (σ_n – u_a) = 200 kPa), and at this point, the capacity of the torque was reached for the first time. Then, for the single-stage test, this combination of stresses was not considered.

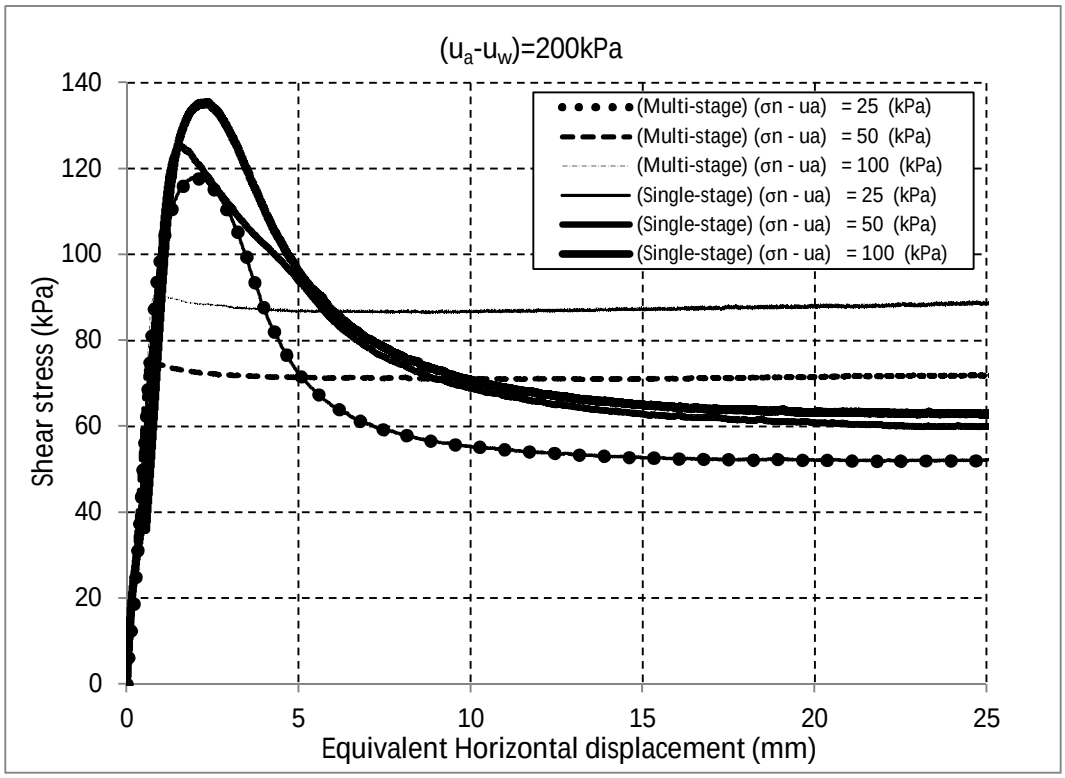

Figure 5-22. Multi-stage vs. single-stage testing for a constant matric suction of 200 kPa

Figure 5-23, shows multi-stage vs. single stage tests for a matric suction of ($u_a - u_w$) = 300 kPa and net normal stresses of ($\sigma_n - u_a$) = 25, and 50 kPa (multi-stage and single-stage. Curves for net normal stresses of 100 kPa and higher could not be shown due to the torque capacity limitation mentioned previously. Similar to the last figure, the multi-stage test was performed for a net normal stress of 100 kPa, and it exceeded the capacity of the torque once again, so for the single-stage test, this stage was not considered.

Even though this figure has only two curves, the figure is conclusive and both the peak and residual shear strength behavior are still similar to that seen in previous figures.

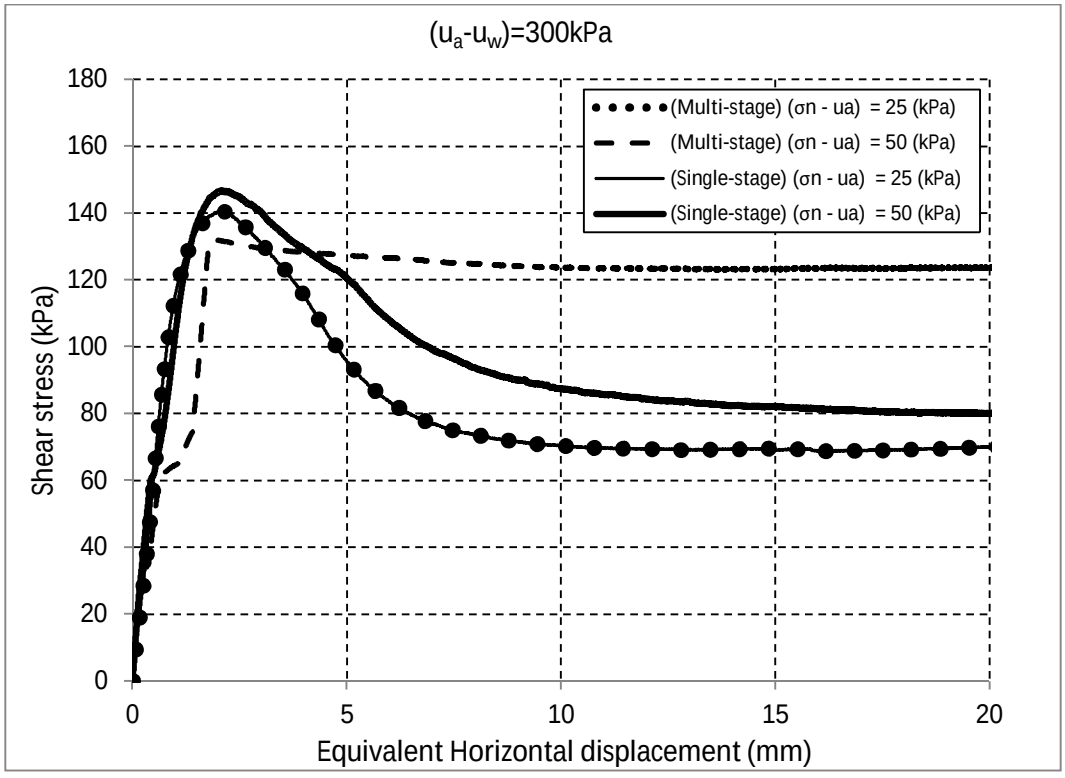

Figure 5-23. Multi-stage vs. single-stage testing for a constant matric suction of 300 kPa

From the five figures presented and analyzed in this section, some comments are required to be done. Single-stage testing seem to fit well when performing tests in such complex soils as high plasticity clays (CH). The curves show an important difference between peak and residual shear strength, an increase in shear strength with the increase in matric suction and net normal stress, and the curves are smooth and very consistent one from another when increasing either the net normal stress (constant matric suction) or the matric suction (net normal stress constant). In addition, none of the tests that were performed as single-stage, were rejected, and gave good results. Only those two mentioned tests that exceeded the torque capacity were not used for this work, but that does not depend on the used technique to perform the tests.

On the other hand, multi-stage tests showed several disadvantages and limitations, and this entire chapter was committed to show, explain, and analyze that. In multi-stage testing, the peak shear strength was not very different from the residual one, after the first stage, the residual shear stress reached and sometimes exceeded the peak shear stress, and some curves gave non-consistent results (so they were not presented in this work).

5.1.3.2 Net normal stress as a function of several matric suction values

The following three figures will show the shear strength behavior of the analyzed material, each figure showing, for a constant value of net normal stress ($\sigma_n - u_a$), the behavior for several values of matric suction ($u_a - u_w$). A figure for a constant net normal stress of 25 kPa was not presented because there are no curves to compare as the first stage of multi-stage was used for single-stage testing. These following figures are aimed to confirm the advantages of a single-stage testing procedure, seen from another perspective. The concluding remarks to be made are similar.

Figure 5-24, presents the shear strength behavior for a constant net normal stress of ($\sigma_n - u_a$) = 50 kPa and matric suction values ($u_a - u_w$) ranging from 25 kPa to 300 kPa. In the case of single-stage testing, once again, the plots show higher peak stress values and lower residual stress values compared to multi-stage testing, they show an important difference in behavior from peak to residual, and a consistent drop from peak to residual and comparable with the other stages is seen in all the tests. Then, in the case of multi-stage testing, the limitations are also the same, the peak is not clear, the difference between peak and residual is very low, and for large deformations, the residual stress values reach and even overcome the peak stress values.

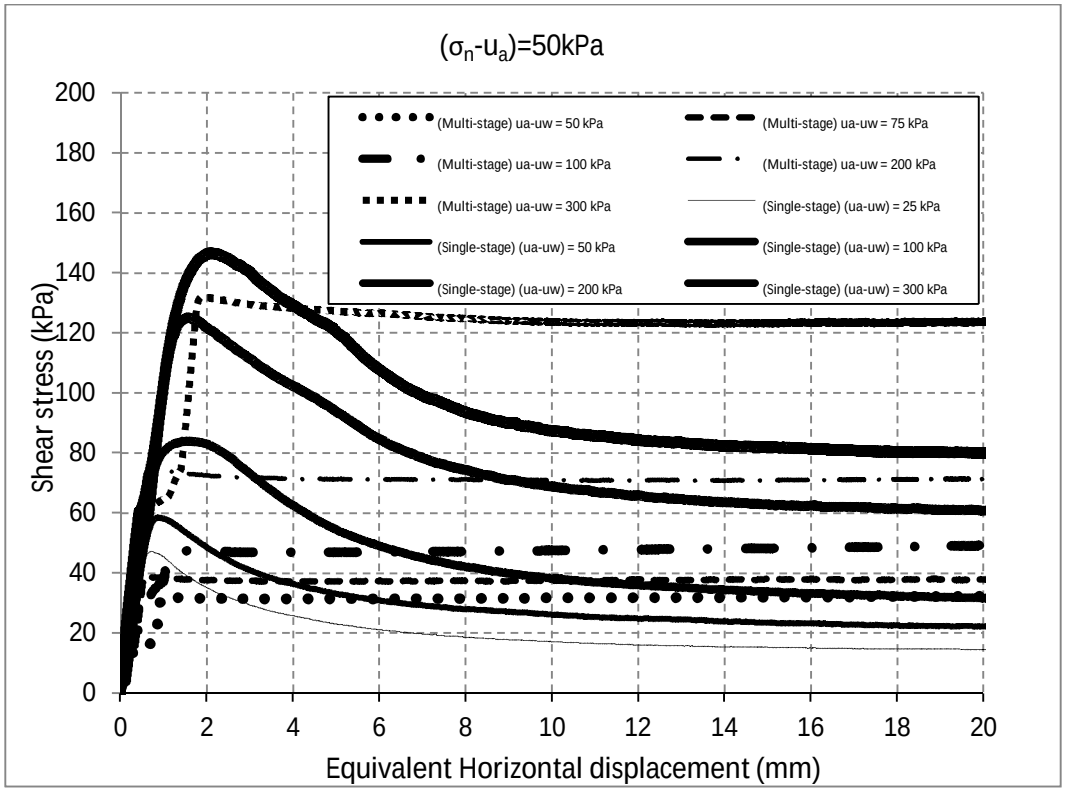

Figure 5-24. Multi-stage vs. single-stage testing for a constant net normal stress of 50 kPa.

Figure 5-25, presents the shear strength behavior for a constant net normal stress of ($\sigma_n - u_a$) = 100 kPa and matric suction values ($u_a - u_w$) ranging from 25 kPa to 200 kPa. In this figure, even though, there is an increase in the net normal stress, the behavior and the concluding comments are similar to those done in the previous figure. Single-stage tests keep on yielding plots that are more reliable. The multi-stage test keeps on having problems to show a clear peak stress and a clear difference and/or drop from peak to residual stress.

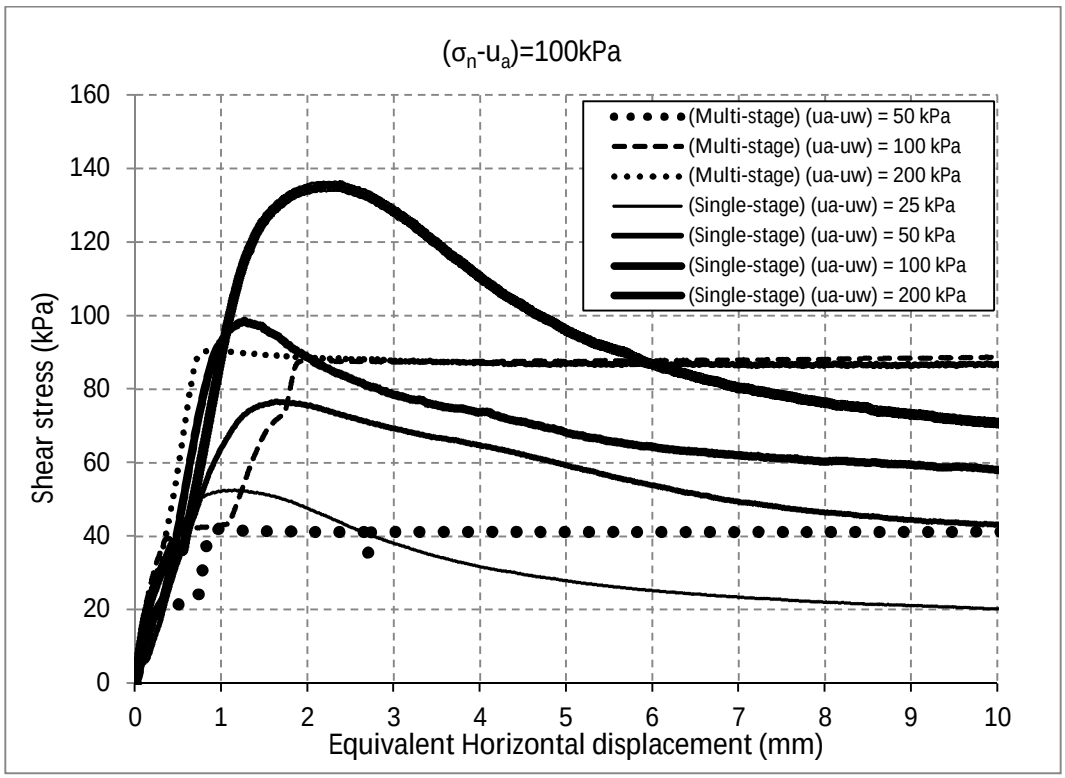

Figure 5-25. Multi-stage vs. single-stage testing for a constant net normal stress of 100 kPa.

Finally, figure 5-26, presents the shear strength behavior for a constant net normal stress of $(\sigma_n - u_a)$ = 200 kPa and matric suction values $(u_a - u_w)$ ranging from 25 kPa to 100 kPa. In this case, in terms of the highest net normal stress applied during this experimental program, the reliability that is possible to have when running a single-stage test is again presented. Both the advantages of single-stage testing performance and results and the difficulties of multi-stage testing results have been a constant throughout the entire experimental program, and this las figure is not the exception. Then, based on all the results presented in this chapter using axis-translation technique, the next chapter will show the analysis of results using only the first stage of the multi-stage tests and all the single-stage tests.

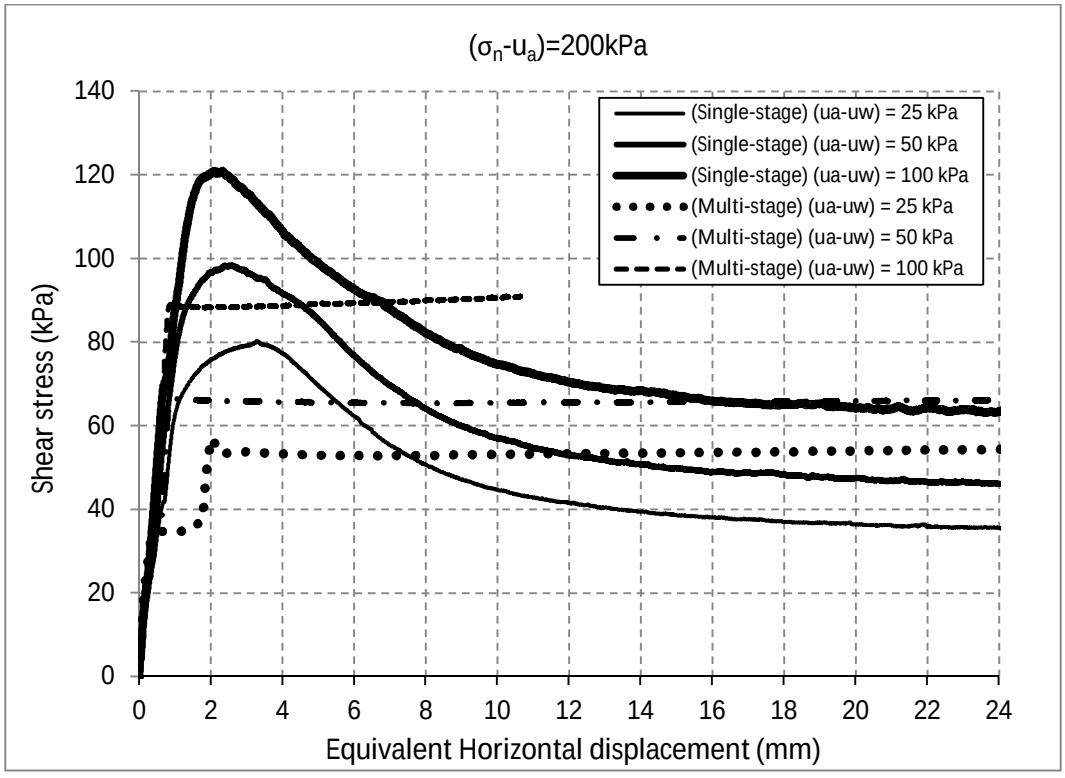

Figure 5-26. Multi-stage vs. single-stage testing for a constant net normal stress of 200 kPa

5.2 Thermo-servo/suction-Controlled Ring Shear Testing Via Constant-Water Technique

According to the SWCC of the soil, for matric suction values of 25, 100, and 200 kPa, it corresponds moisture contents of 33, 28 and 21% respectively, so with those values samples were prepared and tests were performed. Figure 5-27 shows the SWCC curve that corresponds to the soil used during this project.

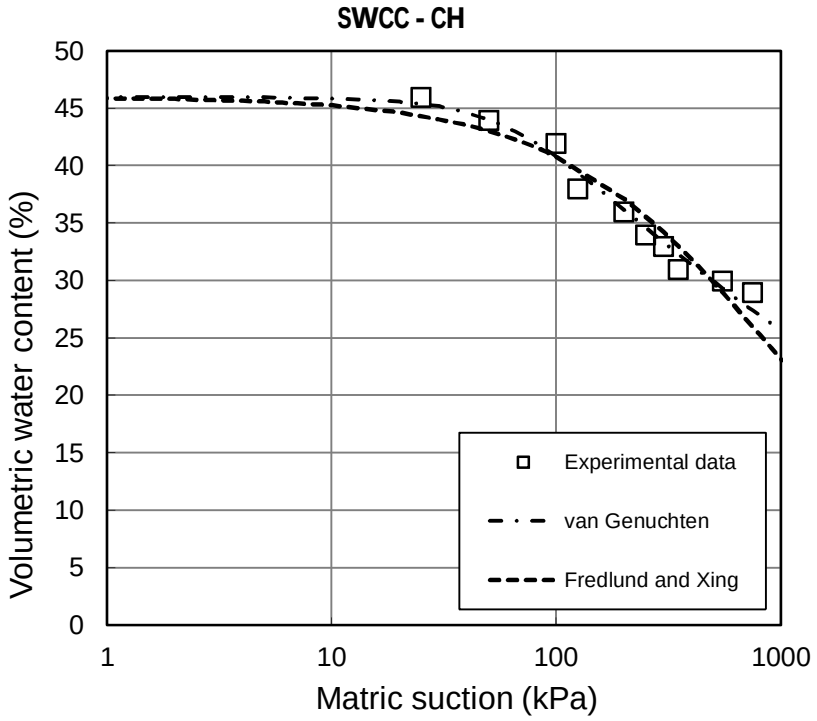

Figure 5-27. Soil-water characteristic curve for the soil used during this project

With the constant-water technique, several values of temperature were used in order to study the influence of temperature and suction on the strength behavior of soil simultaneously.

5.2.1 Net Normal Stress vs. Matric Suction for several values of temperature

A combination of net normal stresses and matric suction values (moisture content from SWCC) for several values of temperature were used to perform tests in the ring shear apparatus. This section will show the results from the tests, which variables were shown at the beginning of this chapter.

Fig 5-28 presents for a net normal stress of σn=25kPa and a matric suction of 200 kPa (w=21%), curves for shear stress vs. equivalent horizontal displacement at temperatures of 20°C, 30°C, 40°C. From the figure it is possible to see that for an initial increase in temperature (30°C), the peak shear strength increases. Then for a temperature of 40°C, the shear strength drops.

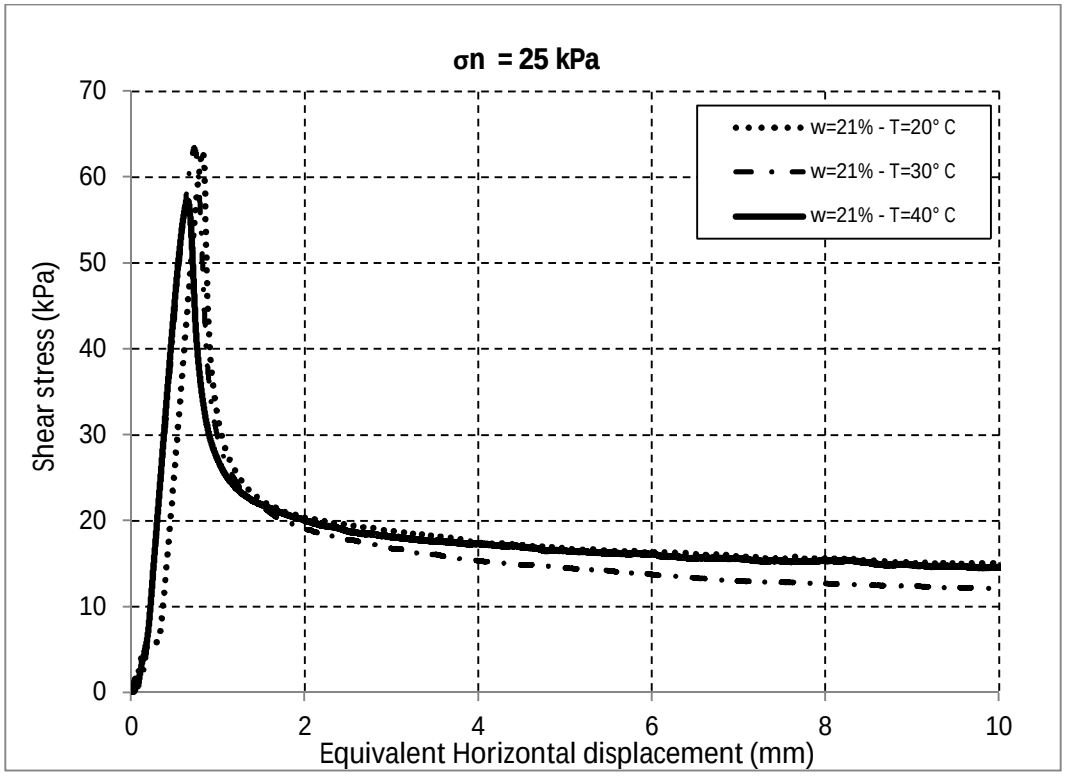

Figure 5-28. Peak and residual Shear Strength for a net normal stress of 25 kPa as a function of suction and temperature.

From the previous figure, figure 5-29 presents the variation of peak and residual shear strength with the increase in temperature. Here it is more clear the change in shear strength. The peak shear strength, as mentioned in the previous figure increases and the decreases. On the other hand, the residual shear strength decreases and then increases. It is important, in terms of the residual shear strength that this behavior occurs for a low net normal stress.

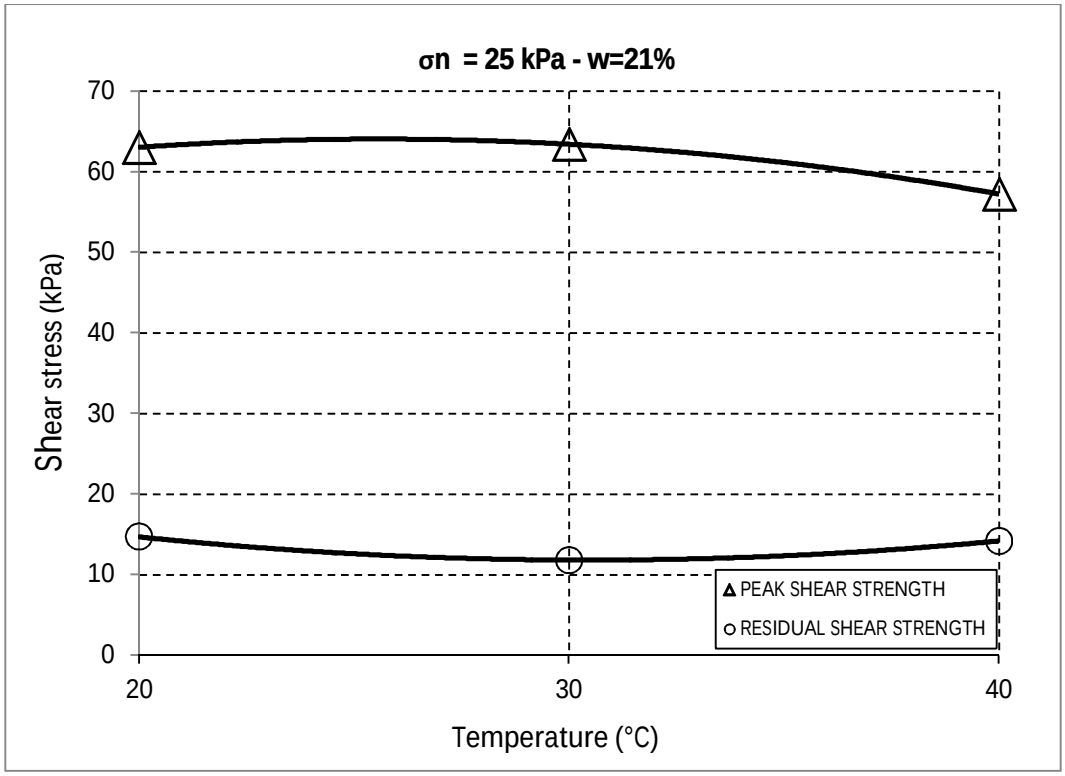

Figure 5-29. Peak and residual Shear Strength as a function of Temperature for a net normal stress of 25 kPa and matric suction of 200 kPa (w=21%)

Figure 5-30 shows for a net normal stress of σn=25kPa and a matric suction of 100 kPa (w=28%), curves for shear stress vs. equivalent horizontal displacement at the same different temperatures of the previous figure. Again It is possible to see that for an initial increase in temperature (30°C) , the peak shear strength increases. Then for a temperature of 40°C, the shear strength drops. In this case the change in peak strength is more notorious.

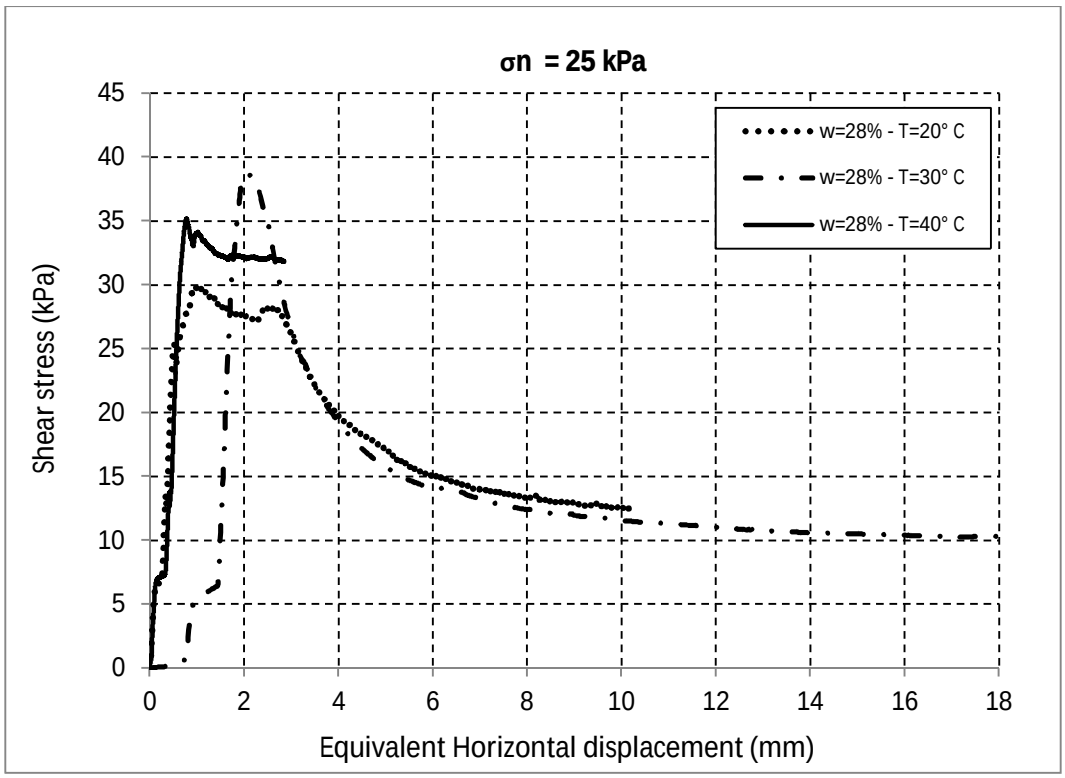

Figure 5-30. Shear Stress vs Equivalent Horizontal displacement for a net normal stress of 25 kPa, a matric suction of 100 kPa (w=28%) and temperatures of 20°C, 30°C, 40°C.

From the previous figure, figure 5-31 presents the variation of peak and residual shear strength with the increase in temperature. The peak shear strength, as mentioned in the previous figure increases and the decreases. On the other hand, the change in residual shear strength is more dramatic, it decreases for 30°C. Then, for 40°C, there is an important increase in residual shear strength compared with the previous plot for matric suction of 200 kPa.

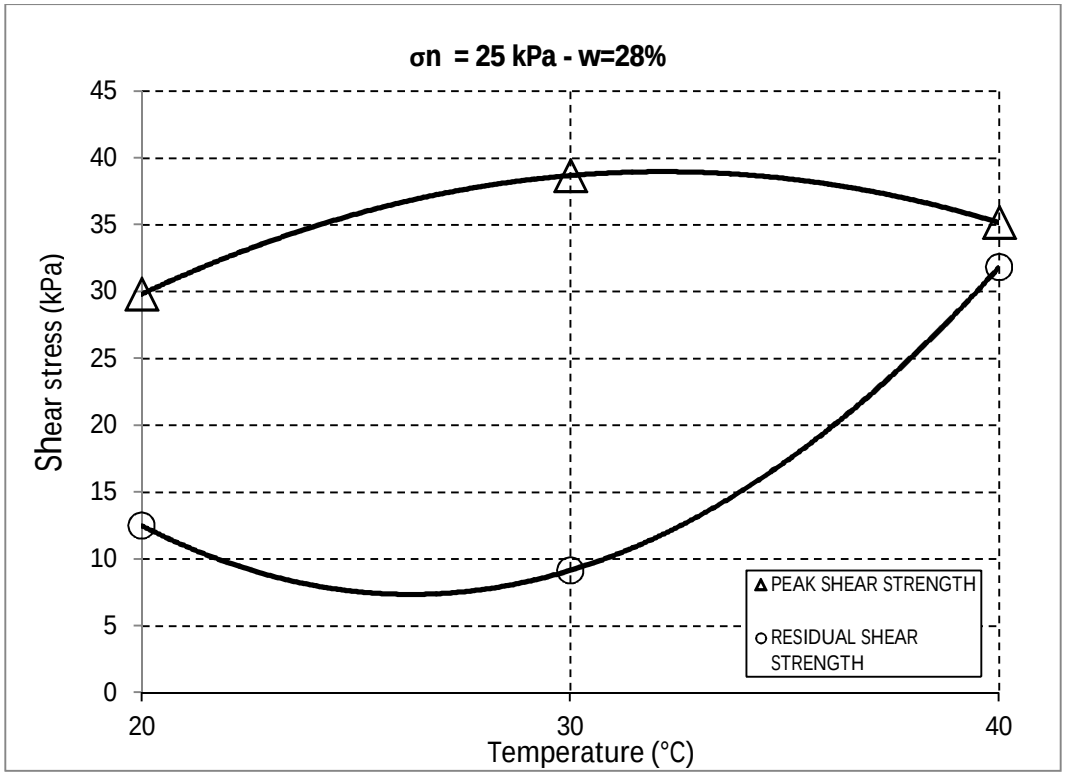

Figure 5-31. Variation of peak and residual Shear Strength as a function of Temperature for a net normal stress of 25 kPa and matric suction of 100 kPa (w=28%)

Figure 5-32 shows for a net normal stress of σn=25kPa and a matric suction of 25 kPa (w=33%), curves for shear stress vs. equivalent horizontal displacement with the variation of temperature. Again It is possible to see that for an initial increase in temperature (30°C) , the peak shear strength increases. Then for a temperature of 40°C, the shear strength shows an even more notorious drop.

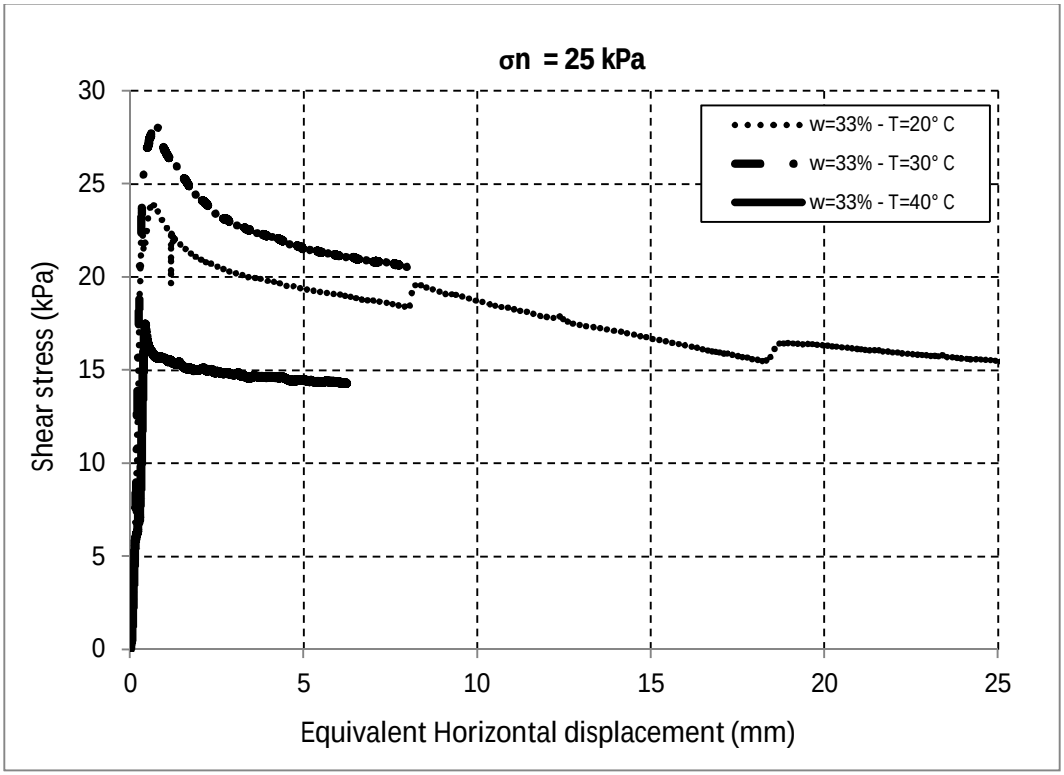

Figure 5-32. Shear Stress vs Equivalent Horizontal displacement for a net normal stress of 25 kPa, a matric suction of 25 kPa (w=33%) and temperatures of 20°C, 30°C, 40°C.

Figure 5-33 shows the variation of peak and residual shear strength with the increase in temperature.

The peak shear strength, as mentioned in the previous figure increases and then decreases. In this case, the residual shear strength has a different behavior, as it increases and then decreases. It is possible to define that the low value of matric suction may have affected this important change.

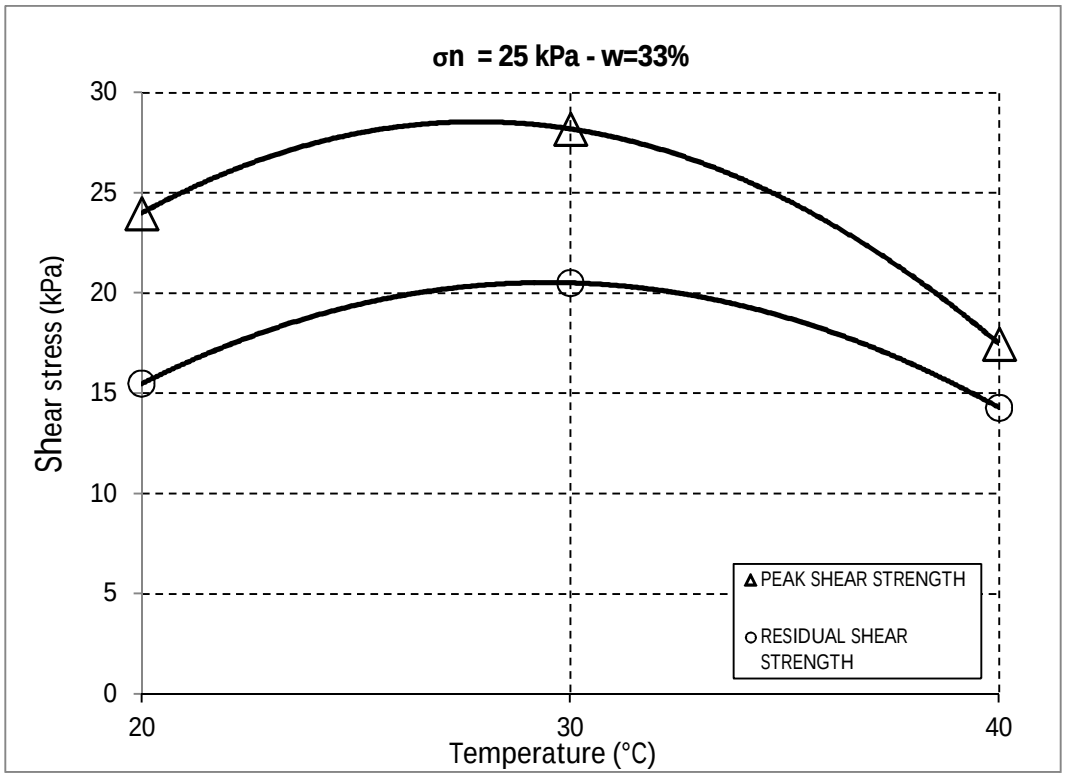

Figure 5-33. Variation of peak and residual Shear Strength as a function of Temperature for a net normal stress of 25 kPa and matric suction of 25 kPa (w=33%)

Figure 5-34 shows for a net normal stress of σn=100kPa and a matric suction of 200 kPa (w=21%), curves for shear stress vs. equivalent horizontal displacement with the variation of temperature. Now, as there is an important increase in the net normal stress, the behavior is different.

The peak shear strength decreases for 30°C, and then increases for a temperature of 40°C. It is notorious that the behavior is opposite to what happened for a net normal stress of 25 kPa.

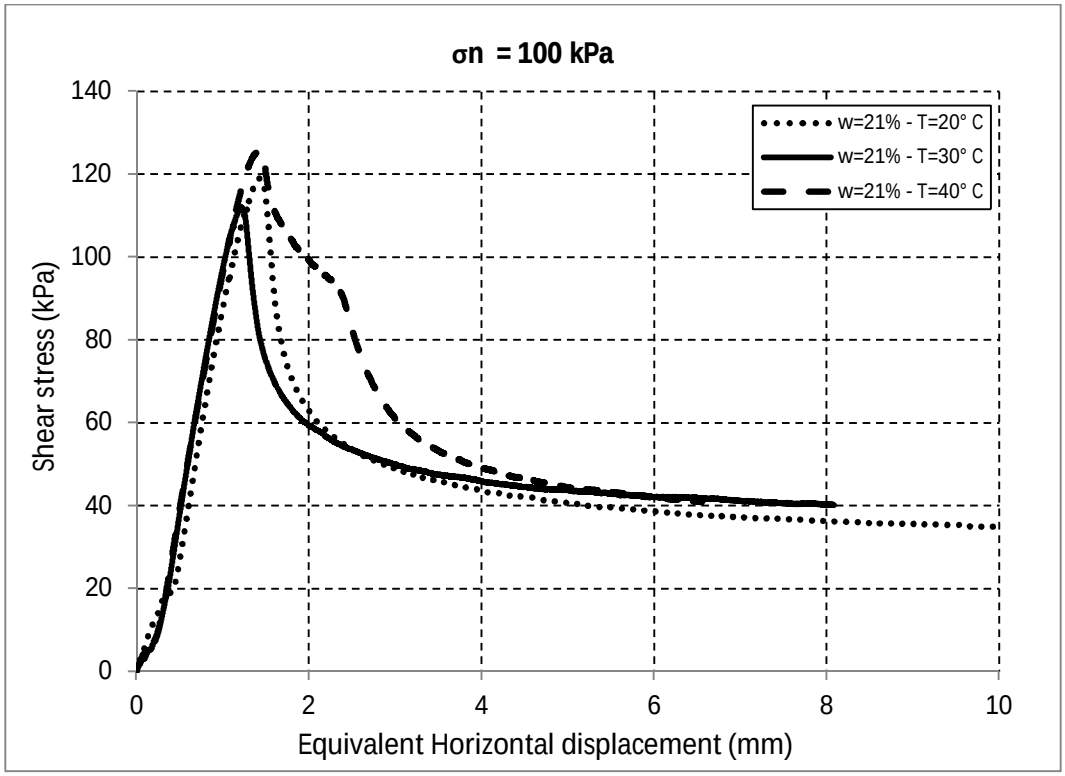

Figure 5-34. Shear Stress vs Equivalent Horizontal displacement for a net normal stress of 100 kPa, a matric suction of 200kPa (w=21%) and temperatures of 20°C, 30°C, 40°C.

Figure 5-35 shows the variation of peak and residual shear strength with the increase in temperature. The peak shear strength, as mentioned in the previous figure decreases and then increases. In this case, the residual shear strength shows a slight change in its behavior. It increases and then decreases, but it is not dramatic.

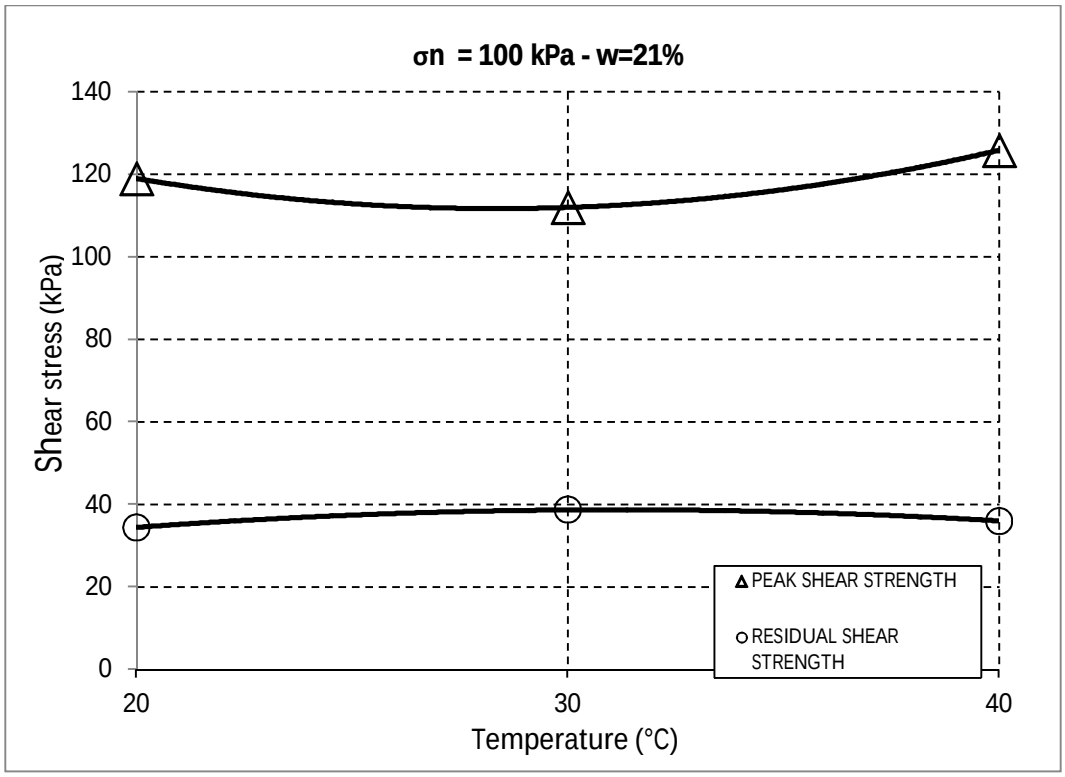

Figure 5-35. Variation of peak and residual Shear Strength as a function of Temperature for a net normal stress of 100 kPa and matric suction of 200 kPa (w=21%)

Figure 5-36 shows for a net normal stress of σn=100kPa and a matric suction of 100 kPa (w=21%), curves for shear stress vs. equivalent horizontal displacement with the variation of temperature. Again, because of the important increase in the net normal stress, the peak shear strength decreased and finally increased with the increase in temperature.

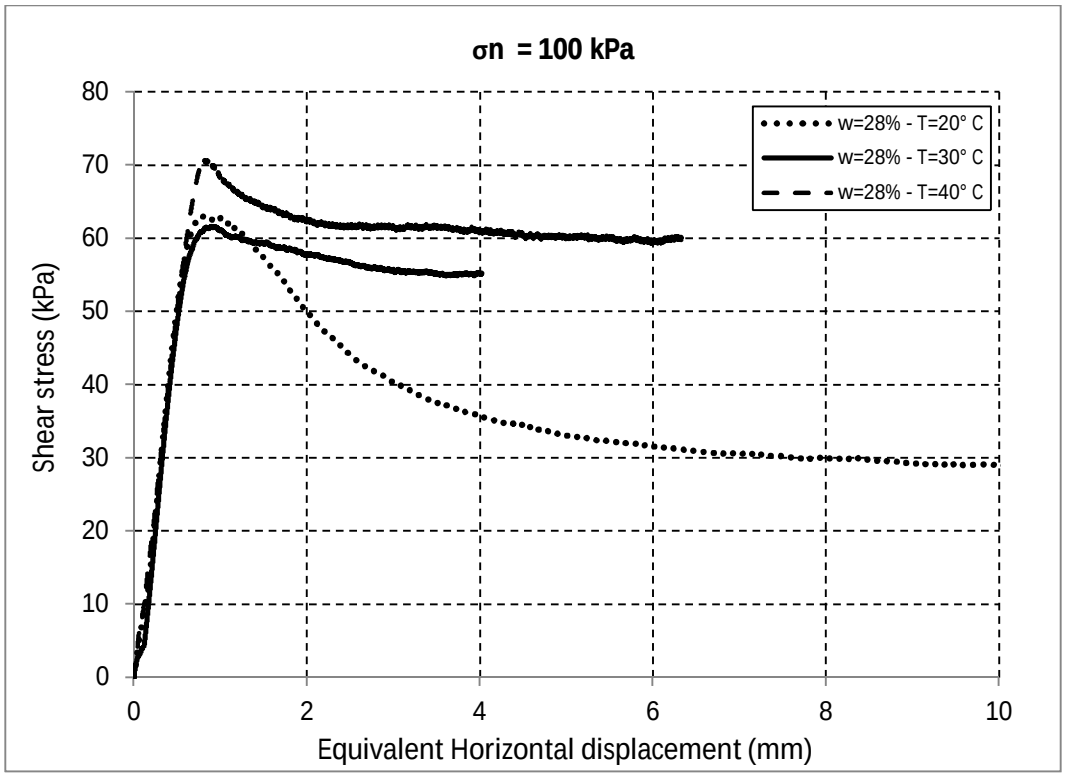

Figure 5-36. Shear Stress vs Equivalent Horizontal displacement for a net normal stress of 100 kPa, a matric suction of 100kPa (w=28%) and temperatures of 20°C, 30°C, 40°C.

Figure 5-37 shows the variation of peak and residual shear strength with the increase in temperature. The behavior of the peak shear strength, decreases and then increases. This is coincidental with the same normal stress of the previous plot (100 kPa). The residual shear strength has a similar behavior to the previous plot too, but in this case, it is more notorious, because for a temperature of 40°C, it ends up with an important increase.

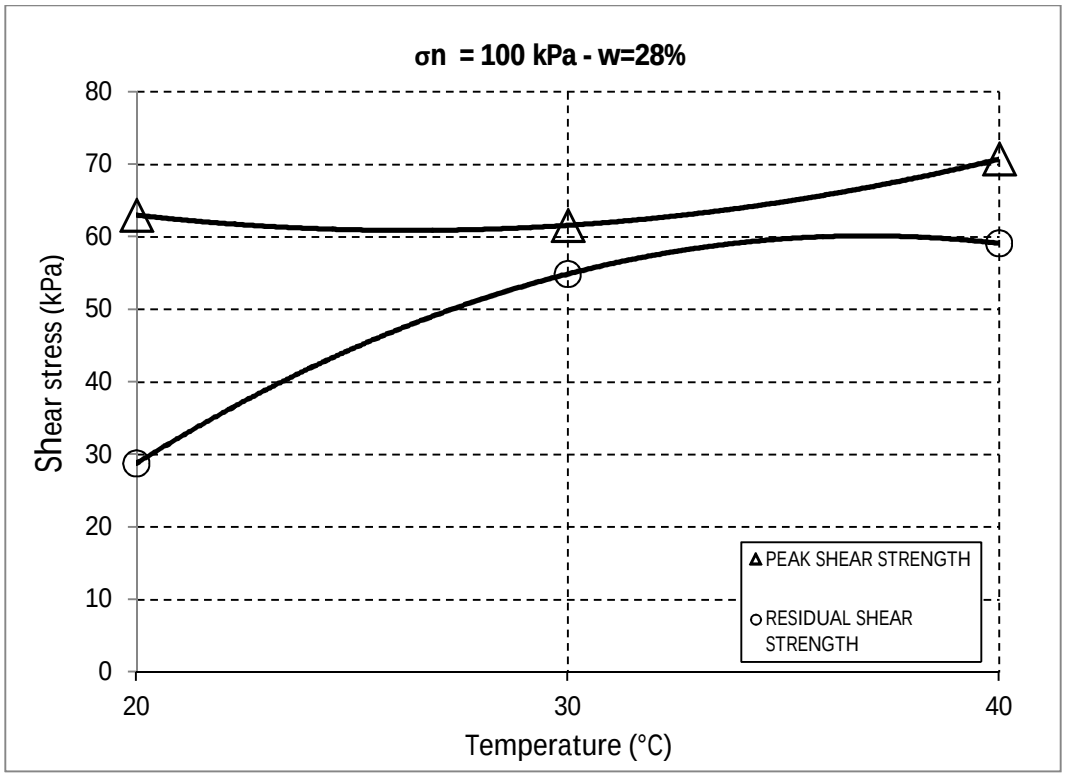

Figure 5-37. Variation of peak and residual Shear Strength as a function of Temperature for a net normal stress of 100 kPa and matric suction of 100 kPa (w=28%)

Figure 5-38 shows for a net normal stress of σn=100kPa and a matric suction of 25 kPa (w=33%), curves for shear stress vs. equivalent horizontal displacement with the variation of temperature. The behavior of the peak shear strength follows the same trend as the other two plots for net normal stress of 100 kPa. It decreases for 30°C, and then increases for 40°C.

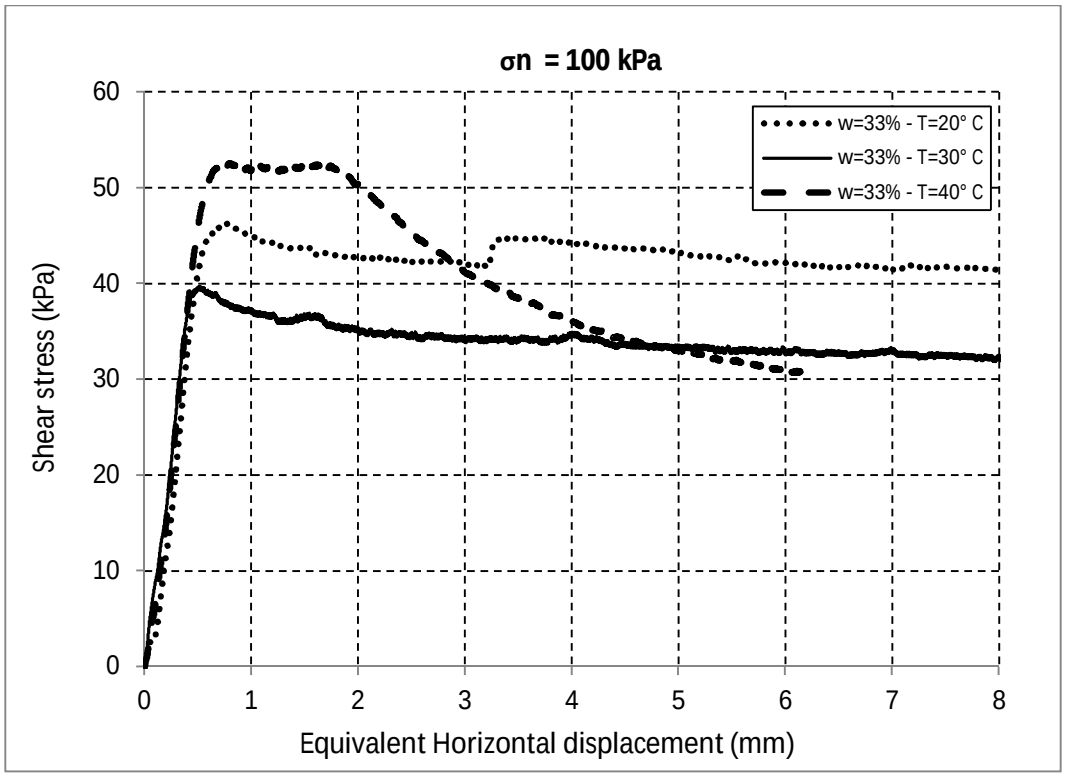

Figure 5-38. Shear Stress vs Equivalent Horizontal displacement for a net normal stress of 100 kPa, a matric suction of 25kPa (w=33%) and temperatures of 20°C, 30°C, 40°C.

Figure 5-39 shows the variation of peak and residual shear strength with the increase in temperature. The peak shear strength, as mentioned in the previous figure decreases and then increases. Once again, as it happened for a net normal stress of 25 kPa, the residual shear strength shows an important decrease for a low value of matric suction (25 kPa).

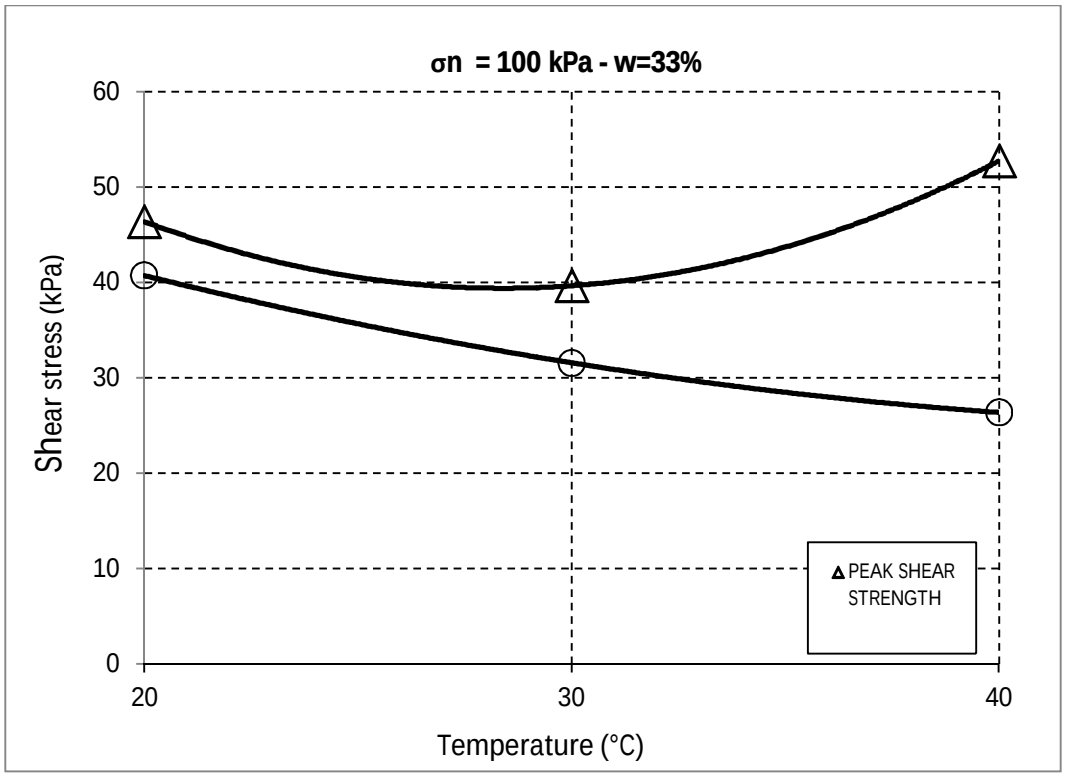

Figure 5-39. Variation of peak and residual Shear Strength as a function of Temperature for a net normal stress of 100 kPa and matric suction of 25 kPa (w=33%).

Figure 5-40 shows for a net normal stress of σn=200kPa and a matric suction of 25 kPa (w=33%), curves for shear stress vs. equivalent horizontal displacement with the variation of temperature. The behavior for a net normal stress of 200 kPa has a similar behavior to the one for a net normal stress of 100 kPa. It decreases for 30°C, and then increases for 40°C.

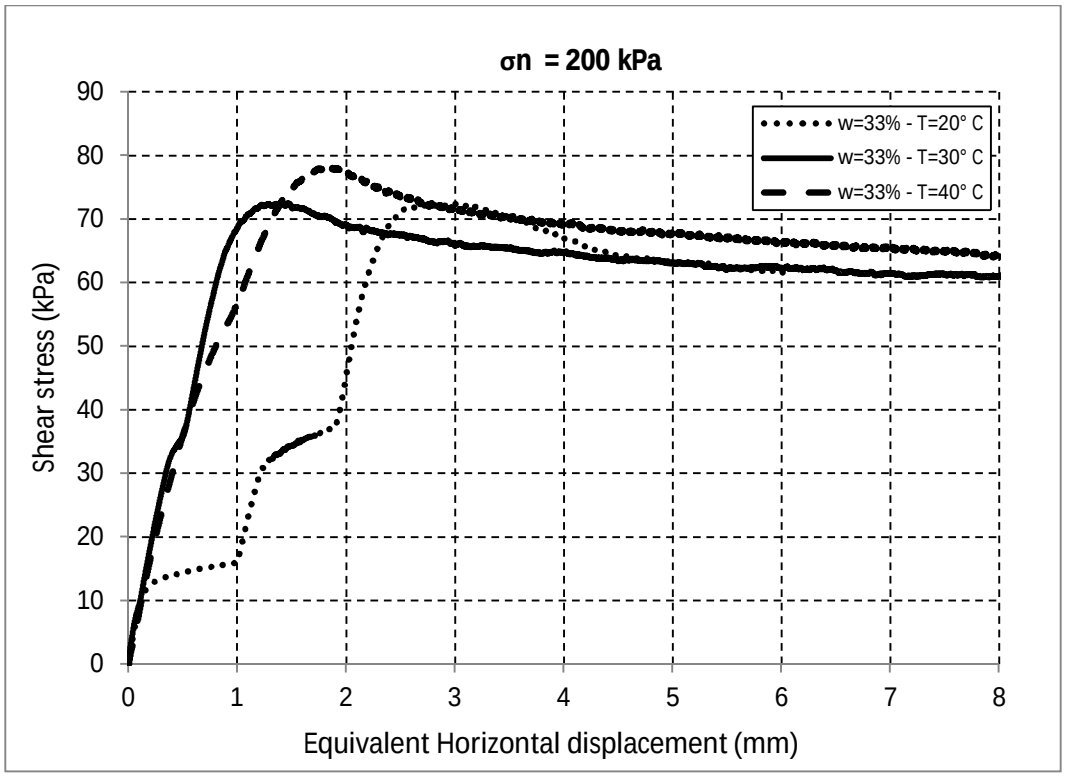

Figure 5-40. Shear Stress vs Equivalent Horizontal displacement for a net normal stress of 200 kPa, a matric suction of 25kPa (w=33%) and temperatures of 20°C, 30°C, 40°C.

Figure 5-41 shows the variation of peak and residual shear strength with the increase in temperature. For this combination of stresses, both the peak and residual shear strength show a similar behavior. There is a slight decrease for 30°C, and then, a slight increase for 40°C.

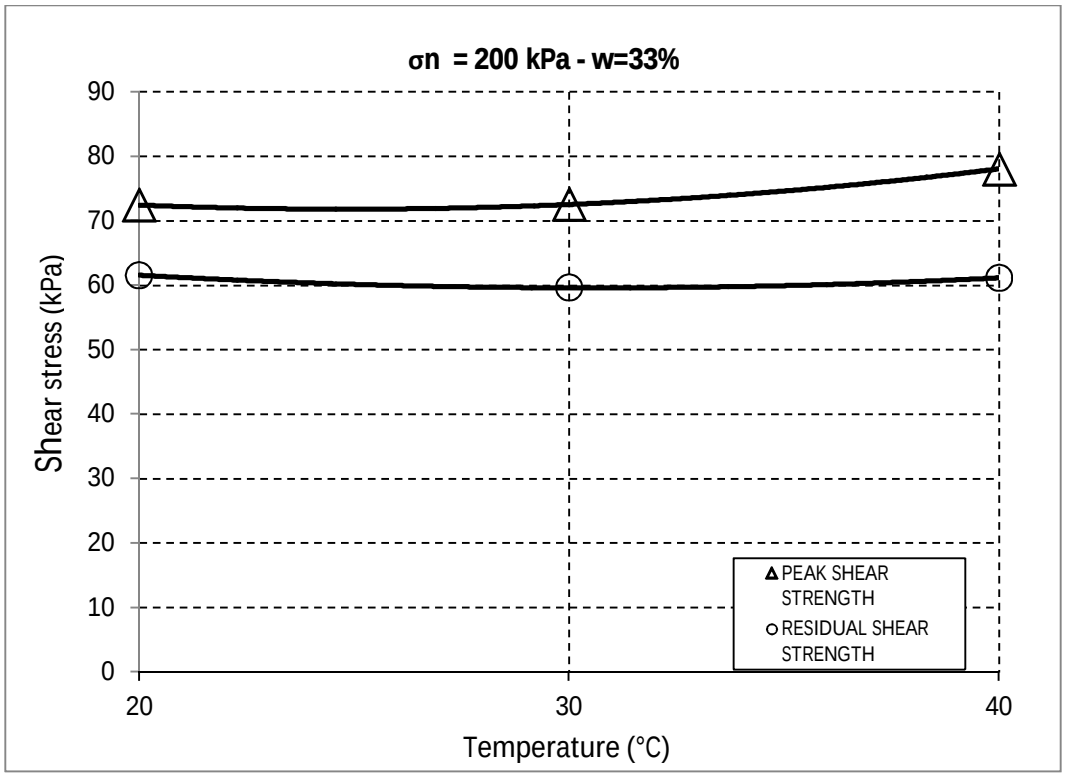

Figure 5-41. Variation of peak and residual Shear Strength as a function of Temperature for a net normal stress of 200 kPa and matric suction of 25 kPa (w=33%).

Chapter 6

Analysis of Results

This chapter presents and analyzes the entire experimental program presented in chapter 5. Peak and residual shear strength behavior is investigated through envelopes which are shown in terms of the interaction among shear stress, net normal stress and matric suction, and both using axis-translation technique and constant water technique.

It is mandatory to define that during this chapter, all the single-stage tests were used, and only the first stage of the multi-stage tests were also used.

6.1 Unsaturated Shear Strength Behavior Via Axis-translation Technique

First, peak and residual failure envelopes, in terms of a constant value of matric suction and several values of net normal stresses, are going to be analyzed. Each figure will have a different value of matric suction, and in each figure, it will be possible to see how the shear strength decreases after failure, specially the strength related to cohesion forces. Failure envelopes will have a linear behavior as they follow the Mohr-Coulomb criterion.

Second, peak and residual envelopes, in terms of a constant value of net normal stress and several values of matric suction, are going to be analyzed. In this case, each figure will present a different value of net normal stress, and for each figure, there will also be a decrease in the envelope (consequence of a decrease in shear strength). Two approaches of the envelopes will be shown and studied.

The initial and commonly followed linear behavior as a first trial, and a second one that considers that the envelope diminishes its slope after a certain increase in shear stress and/or matric suction (as presented by several authors in the available literature).

Finally, the influence of suction in the shear strength of soil will be studied by plotting several envelopes in a same graph (both shear stress vs. net normal stress, and shear stress vs. matric suction).

Figure 6-1, shows, for a matric suction value of $(u_a - u_w)$ = 25 kPa, and net stresses of $(\sigma_n - u_a)$ = 25, 50, 100, and 200 kPa, the peak and residual failure envelopes in a shear stress vs. net normal stress plot, following the Mohr-Coulomb criterion.

From this figure, an initial important conclusion can be drawn. The peak shear strength is visibly higher than the residual one, which is a common behavior in highly plastic clayed soils like those that were used during this work. This decrease in strength is mainly due to cohesion forces, more than to frictional forces. While the intercept of cohesion decreases from 32 kPa to 9 kPa (less than a third part of the peak cohesion), the friction angle only changes from 13.37° to 6.69°, (approximately a half of the strength, in terms of frictional component). This is an expected behavior, because the finer the soil is, the more cohesion forces and the less frictional forces it has.

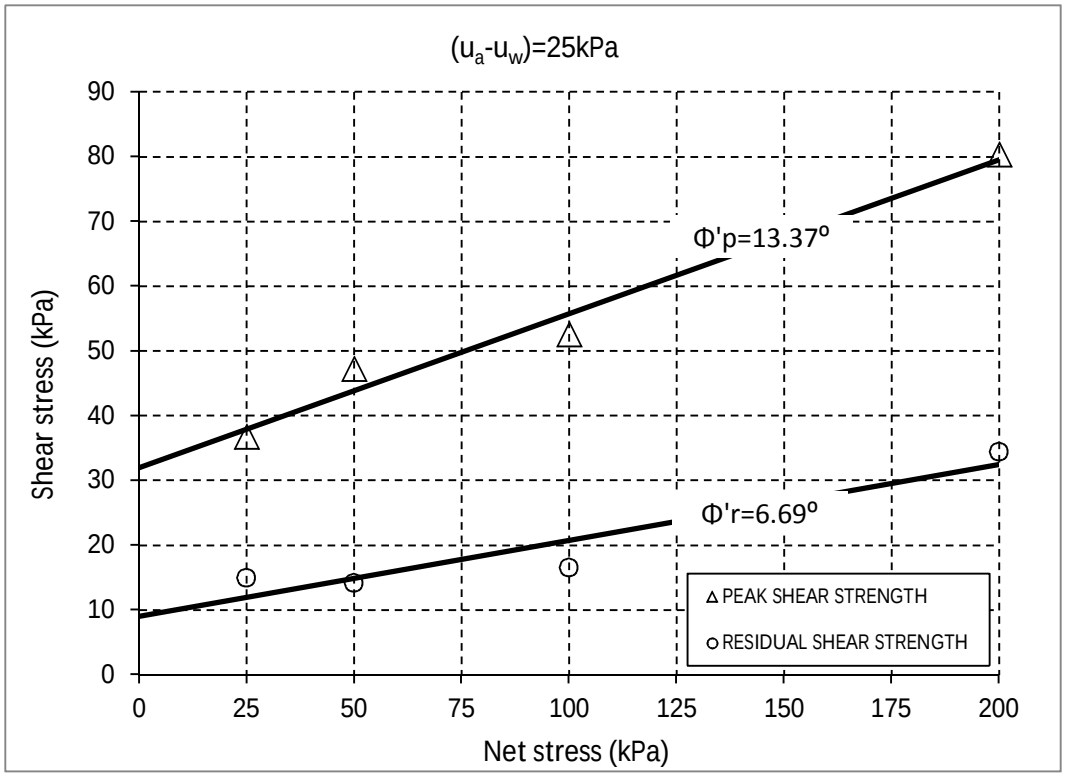

Figure 6-1. Mohr-Coulomb failure envelope, for a matric suction value of ($u_a - u_w$) = 25 kPa, and net stresses of ($\sigma_n - u_a$) = 25, 50, 100, and 200 kPa.

Figure 6-2 shows the peak and residual failure envelopes for a matric suction value of ($u_a - u_w$) = 50 kPa, and net stresses of ($\sigma_n - u_a$) = 25, 50, 100, and 200 kPa. In this case, for an increased value of matric suction, the shear strength behavior is similar to the previous value of matric suction of 25 kPa. The main component of strength that decreases after failure is cohesion, changing from 46 to 13 kPa. This decrease in cohesion is not as dramatic as in the previous figure, but it is still almost to a third part of the peak value. And, again, the friction angle decreases from peak to residual approximately one half of the peak value.

If this figure is compared with the previous one, it is possible to conclude that the increase in matric suction gave the soil an additional strength to both the peak and residual failure envelopes. This increase in strength due to the influence of matric suction is seen in both the cohesion and friction angle, but again, this increase is more notorious in the intercept of cohesion. Then, so far, the decrease in shear strength from peak to residual, and the increase in shear strength with the increase in matric suction is mainly due to cohesion forces.

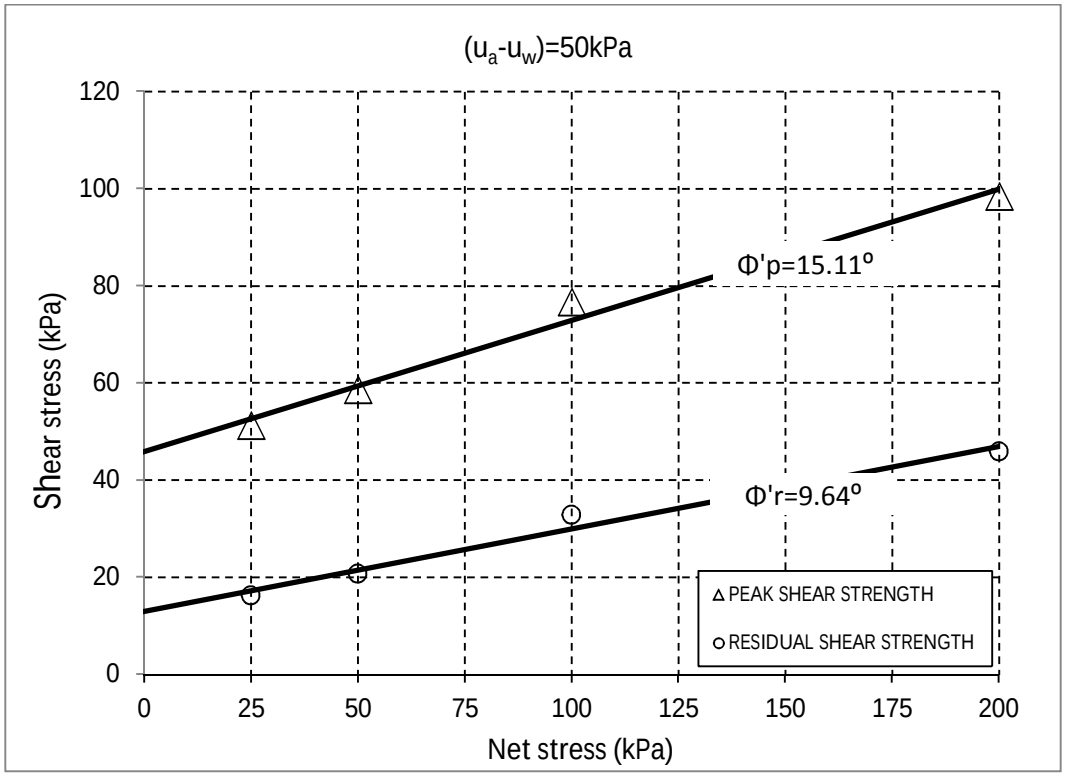

Figure 6-2. Mohr-Coulomb failure envelope, for a matric suction value of ($u_a - u_w$) = 50 kPa, and net stresses of ($\sigma_n - u_a$) = 25, 50, 100, and 200 kPa.

Figure 6-3, shows the peak and residual failure envelopes for a matric suction value of ($u_a - u_w$) = 100 kPa, and net stresses of ($\sigma_n - u_a$) = 25, 50, 100, and 200 kPa. In general terms, the strength keeps on increasing with the increase in matric suction, as expected. This increase in both peak and residual shear strength is mainly due to cohesion. The friction angle remains slightly constant compared to previous values of matric suction. The correlation between the experimental points and the failure envelope is high and both the peak and residual failure envelopes are virtually parallel.

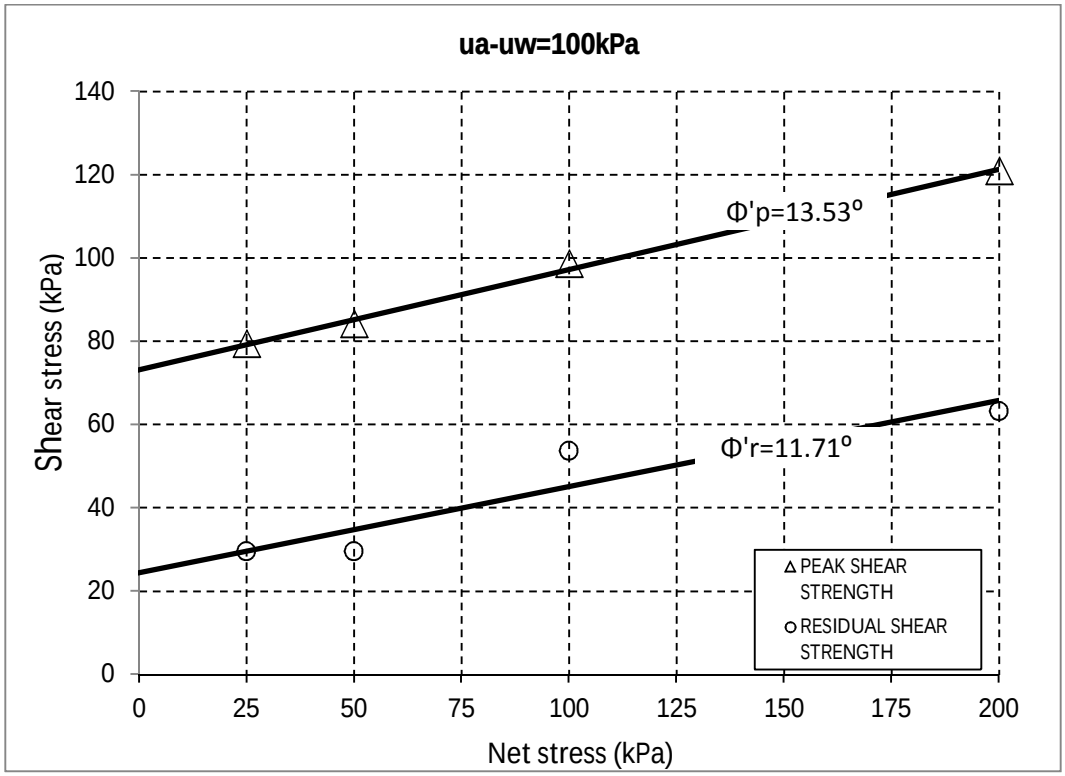

Figure 6-3. Mohr-Coulomb failure envelope, for a matric suction value of ($u_a - u_w$) = 100 kPa, and net stresses of ($\sigma_n - u_a$) = 25, 50, 100, and 200 kPa.

Figure 6-4 shows the peak and residual failure envelopes for a matric suction value of ($u_a - u_w$) = 200 kPa, and net stresses of ($\sigma_n - u_a$) = 25, 50, and 100 kPa. Friction angle remains slightly constant compared to the previous plots, even though they are somewhat lower, cohesion keeps on increasing and the correlation is still good even when an additional experimental point for a net stress of 200 kPa was not possible to have due to the capacity of the torque in the ring shear apparatus.

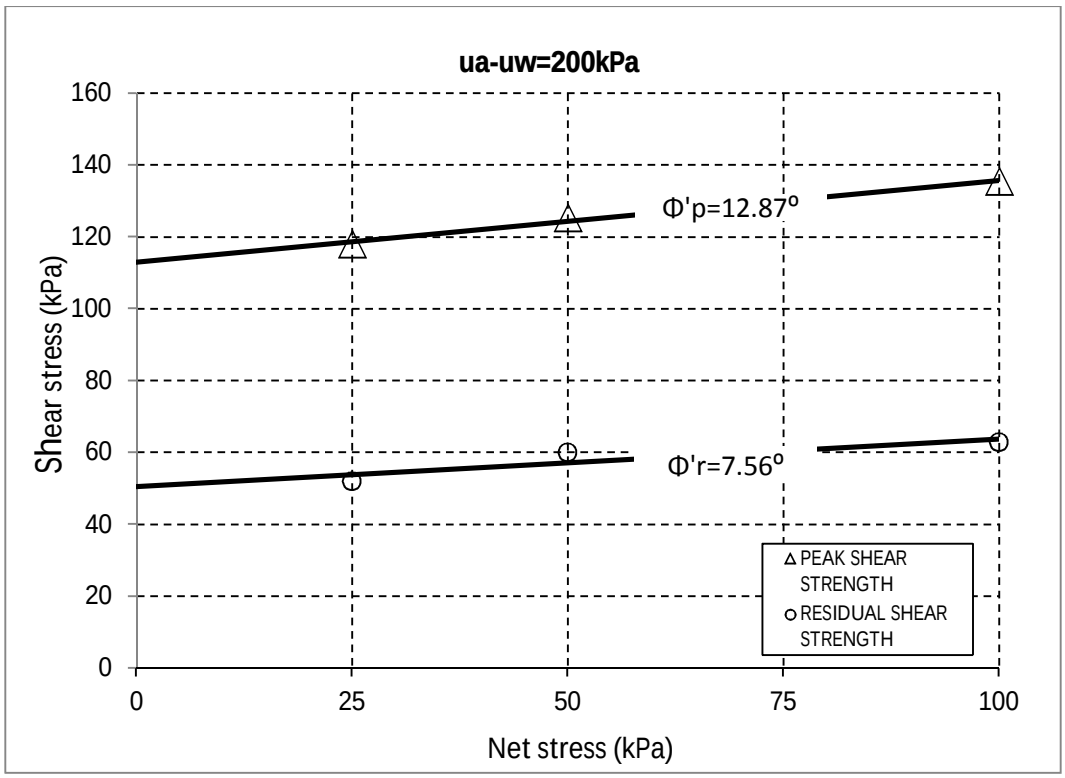

Figure 6-4. Mohr-Coulomb failure envelope, for a matric suction value of ($u_a - u_w$) = 200 kPa, and net stresses of ($\sigma_n - u_a$) = 25, 50, and 100 kPa.

Figure 6-5 shows the peak and residual failure envelopes for a matric suction value of ($u_a - u_w$) = 300 kPa, and net stresses of ($\sigma_n - u_a$) = 25, and 50 kPa. Friction angle increased notoriously to almost the double of the previous results. In this case for each envelope, there are only two experimental points, also because the torque capacity of the equipment was exceeded, so drawing a precise conclusion in this case is difficult. At least another experimental point would be necessary. In spite of that, the experimental points that were possible to get, give virtually parallel envelopes and an increase in both peak and residual strength compared to previous failure envelopes that have lower values of matric suction.

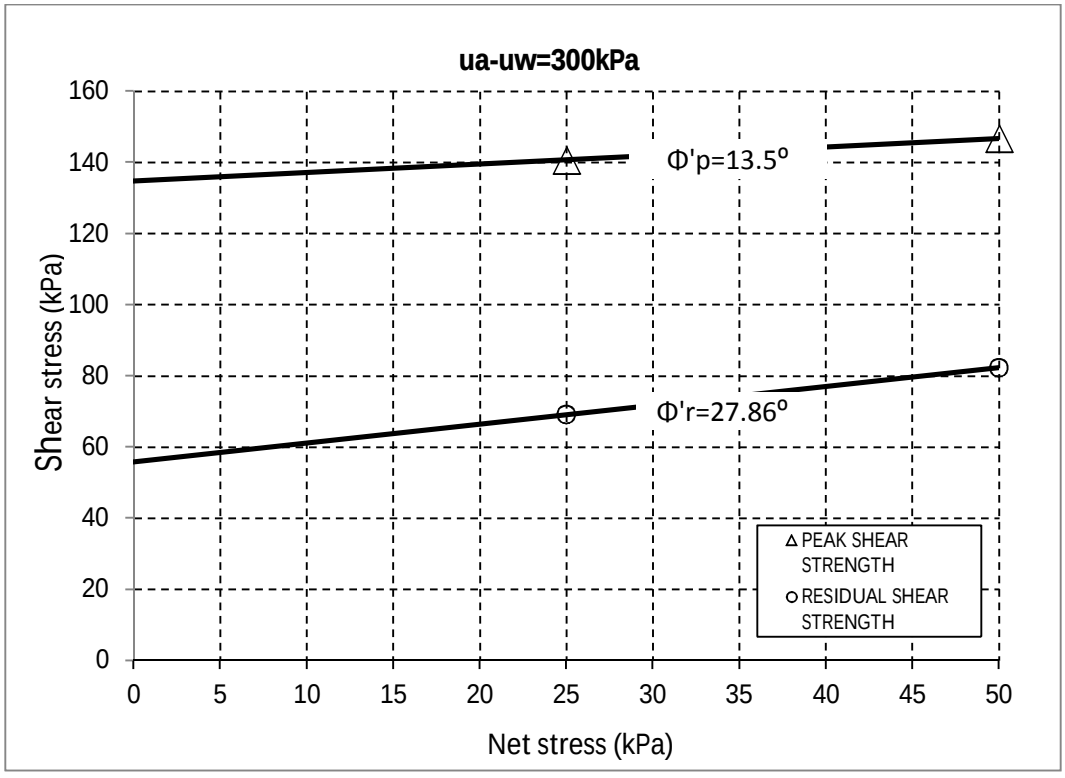

Figure 6-5. Mohr-Coulomb failure envelope, for a matric suction value of ($u_a - u_w$) = 200 kPa, and net stresses of ($\sigma_n - u_a$) = 25, 50, and 100 kPa.

The same set of tests can be plotted in terms of the shear strength and the matric suction. The following figures will present the peak and residual envelopes related with matric suction.

Figure 6-6, shows the peak and residual envelopes related with matric suction for a net stress of $(\sigma_n - u_a)$ = 25 Kpa and matric suction values of $(u_a - u_w)$ = 25, 50, 75, 100, 200, and 300 kPa. The internal friction angle related with suction is relatively high for the peak envelope. It is important to notice that a linear relationship among the experimental points was plotted.

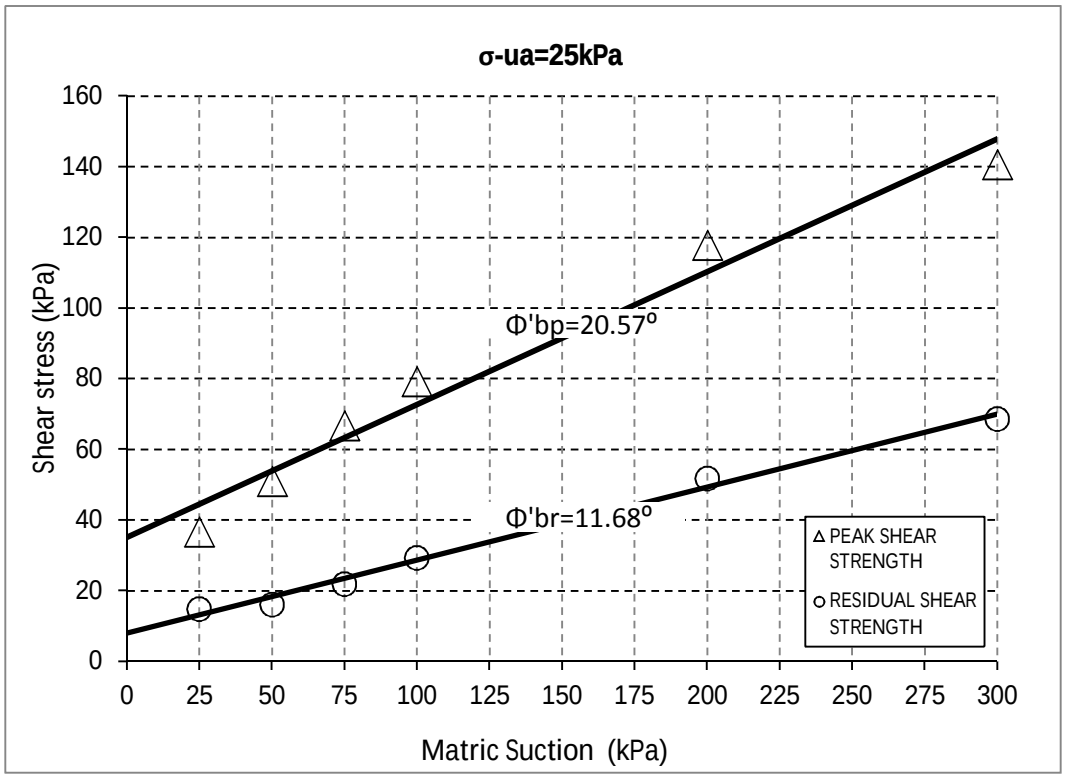

Figure 6-6. Failure envelope as a function of Shear stress and matric suction for a net stress of $(\sigma_n - u_a)$ = 25 Kpa and matric suction values of $(u_a - u_w)$ = 25, 50, 75, 100, 200, and 300 kPa.

Now, and as it was mentioned in chapter 2, several authors have proved through experimental work, that for high values of matric suction the value of "Φ'b" starts to decrease, which implies that the slope of the envelope is not linear.

Figure 6-7, shows the peak and residual envelopes related with matric suction for a net stress of $(\sigma_n - u_a)$ = 25 Kpa and matric suction values of $(u_a - u_w)$ = 25, 50, 75, 100, 200, and 300 kPa, now showing the nonlinearity of the peak and residual failure envelope. It is possible to notice that the experimental data and the envelopes have a high correlation.

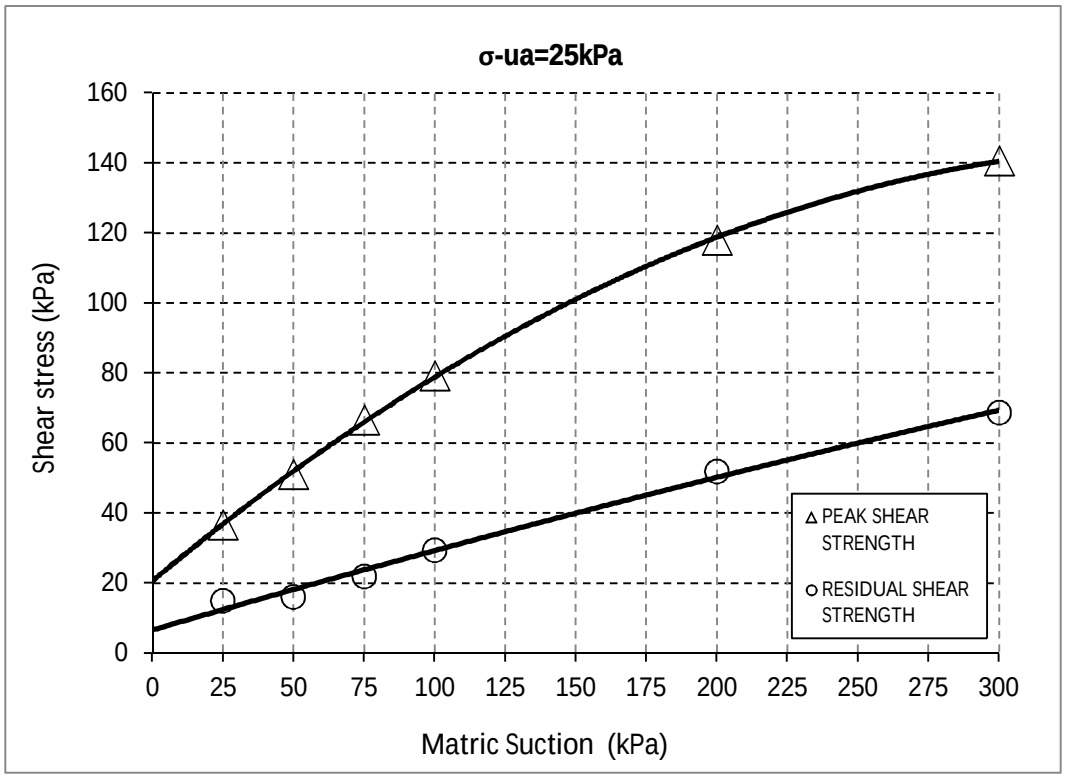

Figure 6-7. Nonlinearity of the Failure envelope as a function of Shear stress and matric suction for a net stress of $(\sigma_n - u_a)$ = 25 Kpa and matric suction values of $(u_a - u_w)$ = 25, 50, 75, 100, 200, and 300 kPa.

Figure 6-8 shows the peak and residual envelopes related with matric suction for a net stress of ($\sigma_n - u_a$) = 50 Kpa and matric suction values of ($u_a - u_w$) = 25, 50, 100, 200, and 300 kPa. The internal friction angle related with matric suction for both peak and residual failure envelopes, is very similar to those obtained for a net stress of ($\sigma_n - u_a$) = 25 Kpa . The figure shows a linear relationship between the experimental data. An increase in cohesion can be observed.

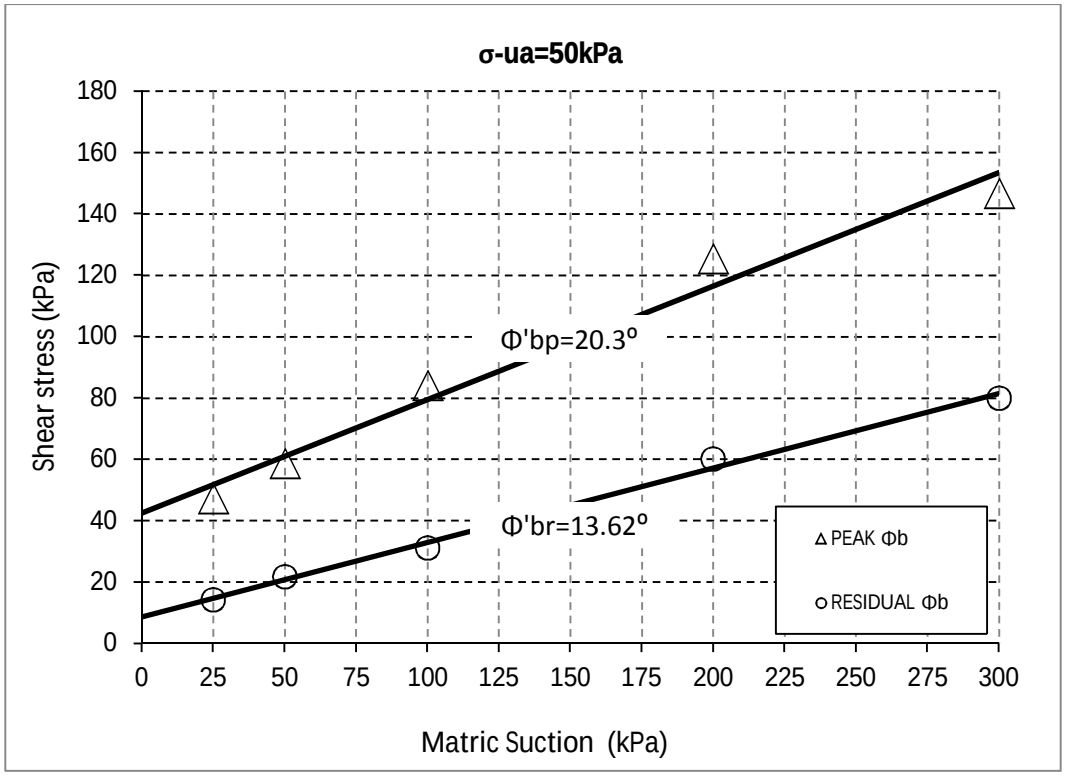

Figure 6-8. Failure envelope as a function of Shear stress and matric suction for a net stress of ($\sigma_n - u_a$) = 50 Kpa and matric suction values of ($u_a - u_w$) = 25, 50, 100, 200, and 300 kPa

Figure 6-9 shows the nonlinear behavior of the peak and residual failure envelopes related with matric suction for a net stress of ($\sigma_n - u_a$) = 50 Kpa and matric suction values of ($u_a - u_w$) = 25, 50, 100, 200, and 300 kPa. Again, It is possible to notice that the experimental data and the envelopes have a high correlation.

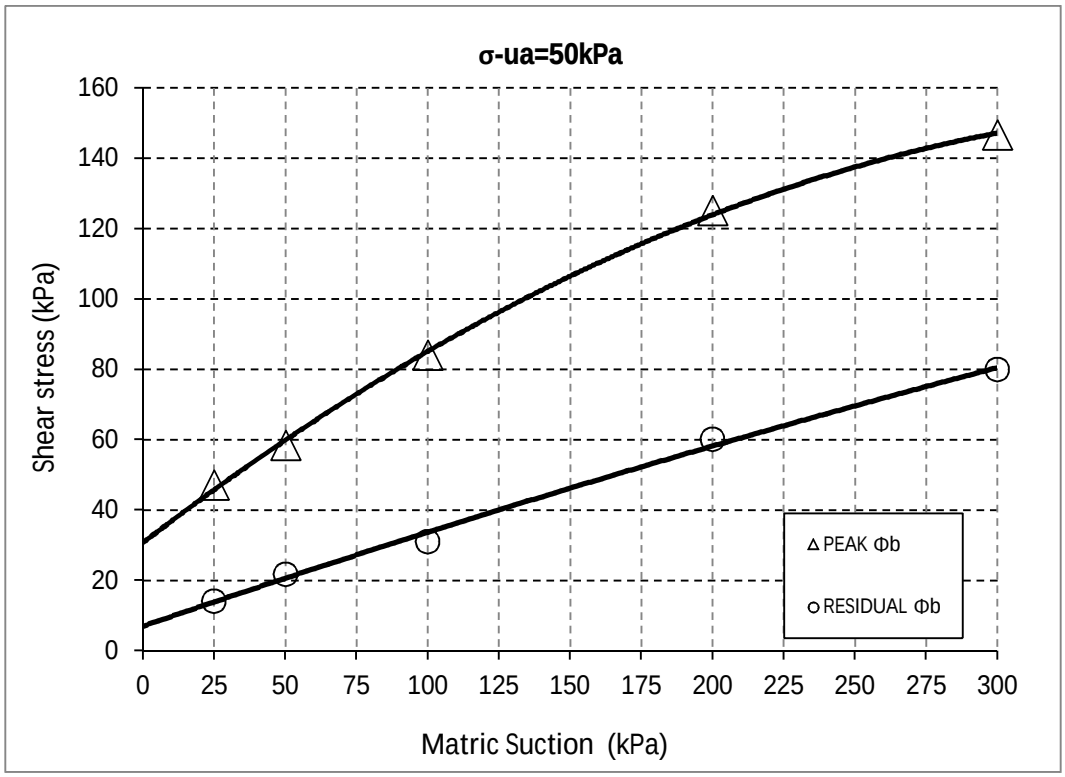

Figure 6-9. Nonlinearity of the Failure envelope as a function of Shear stress and matric suction for a net stress of ($\sigma_n - u_a$) = 50 Kpa and matric suction values of ($u_a - u_w$) = 25, 50, 100, 200, and 300 kPa.

Figure 6-10 shows the peak and residual envelopes related with matric suction for a net stress of ($\sigma_n - u_a$) = 100 Kpa and matric suction values of ($u_a - u_w$) = 25, 50, 100, and 200 kPa. The internal friction angle related with matric suction for both peak and residual failure envelopes, remains relatively constant, and cohesion keeps increasing with the increase in net normal stress as expected.

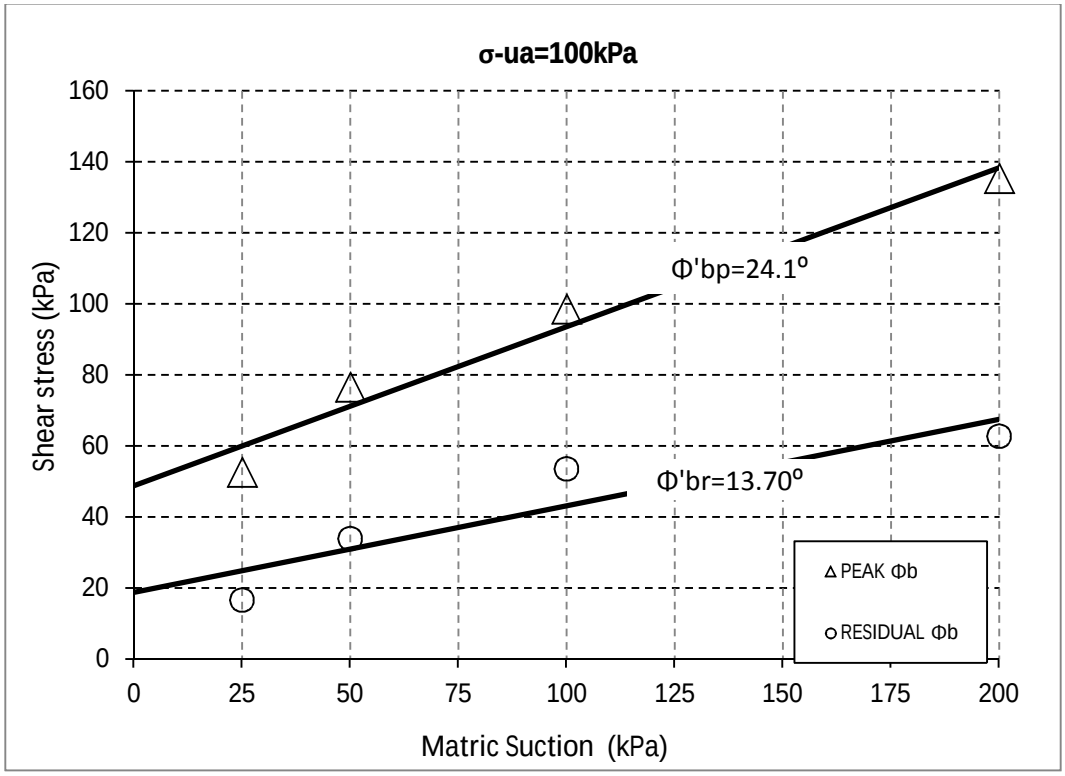

Figure 6-10. Failure envelope as a function of Shear stress and matric suction for a net stress of ($\sigma_n - u_a$) = 100 Kpa and matric suction values of ($u_a - u_w$) = 25, 50, 100, and 200 kPa.

Figure 6-11, shows the nonlinear behavior of the peak and residual failure envelopes related with matric suction for a net stress of ($\sigma_n - u_a$) = 100 Kpa and matric suction values of ($u_a - u_w$) = 25, 50, 100, and 200 kPa. Again, It is possible to notice that the experimental data and the envelopes have a high correlation. In this case, the nonlinearity is more notorious in the residual failure envelope.

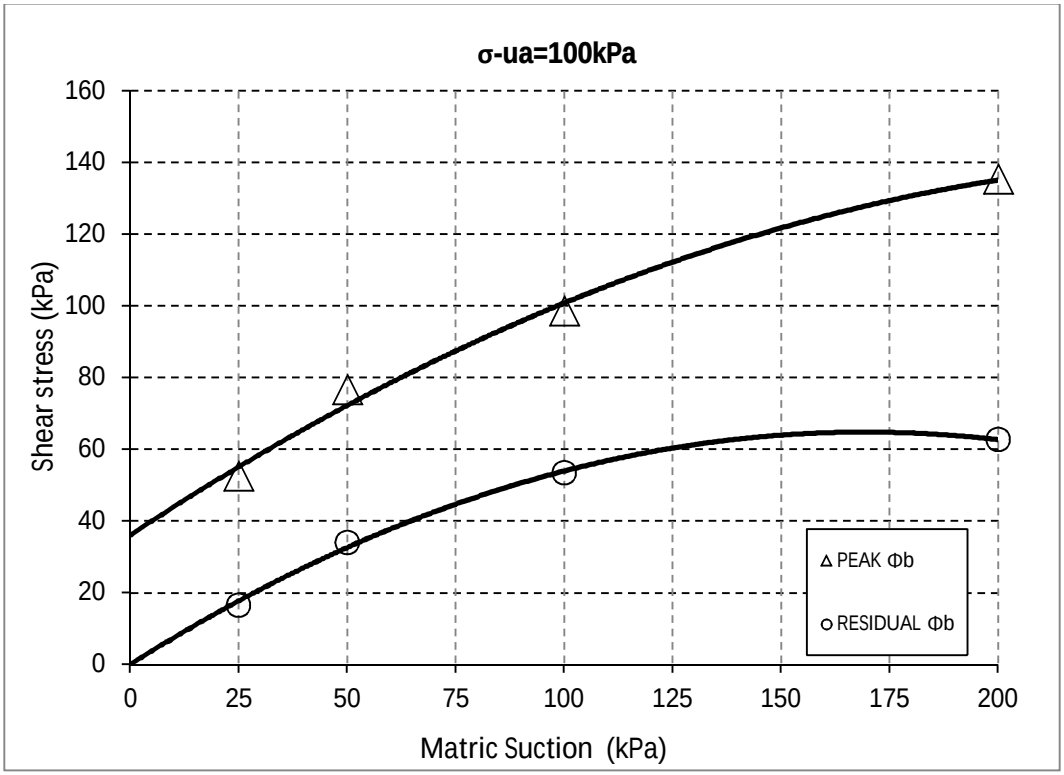

Figure 6-11. Nonlinearity of the Failure envelope as a function of Shear stress and matric suction for a net stress of ($\sigma_n - u_a$) = 100 Kpa and matric suction values of ($u_a - u_w$) = 25, 50, 100, and 200 kPa.

Figure 6-12 shows the peak and residual envelopes related with matric suction for a net stress of ($\sigma_n - u_a$) = 200 Kpa and matric suction values of ($u_a - u_w$) = 25, 50, and 100 kPa. The internal friction angle related with matric suction for both peak and residual failure envelopes, has an important increase, and cohesion keeps increasing with the increase in net normal stress as expected.

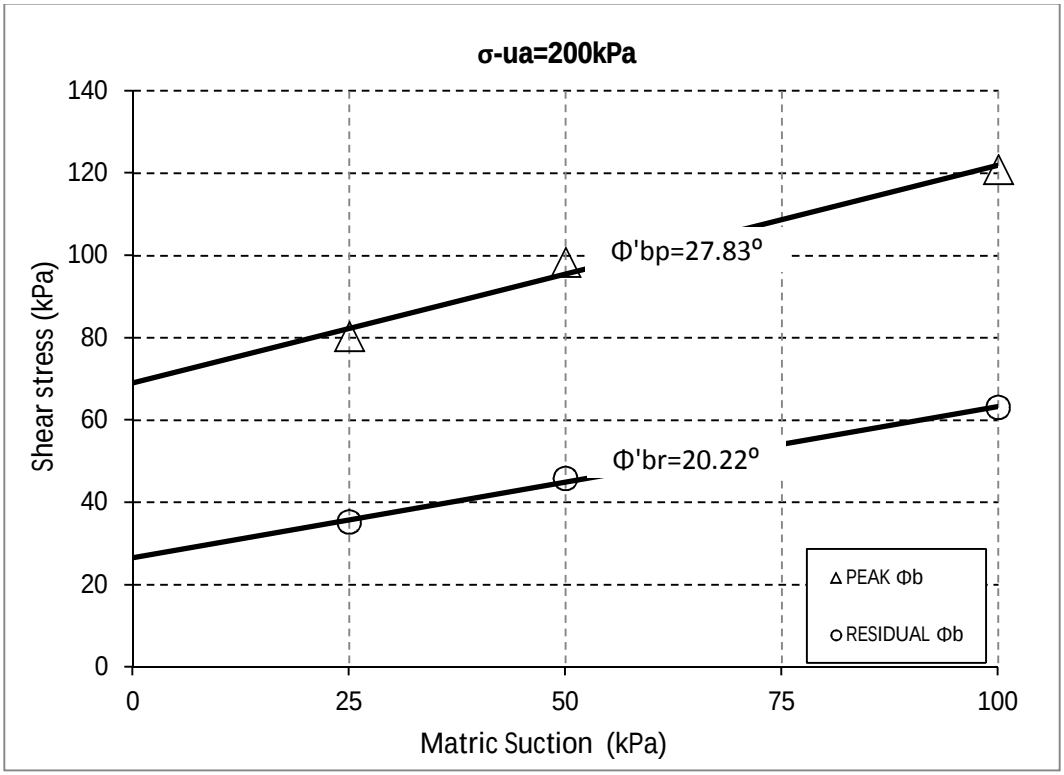

Figure 6-12. Failure envelope as a function of Shear stress and matric suction for a net stress of ($\sigma_n - u_a$) = 200 Kpa and matric suction values of ($u_a - u_w$) = 25, 50, and 100 kPa.

Figure 6-13 shows the nonlinear behavior of the peak and residual failure envelopes related with matric suction for a net stress of $(\sigma_n - u_a)$ = 200 Kpa and matric suction values of $(u_a - u_w)$ = 25, 50, and 100 kPa. Again, It is possible to notice that the experimental data and the envelopes have a high correlation. In this case, the nonlinear behavior is similar to that observed for net stresses of 25 and 50 kPa.

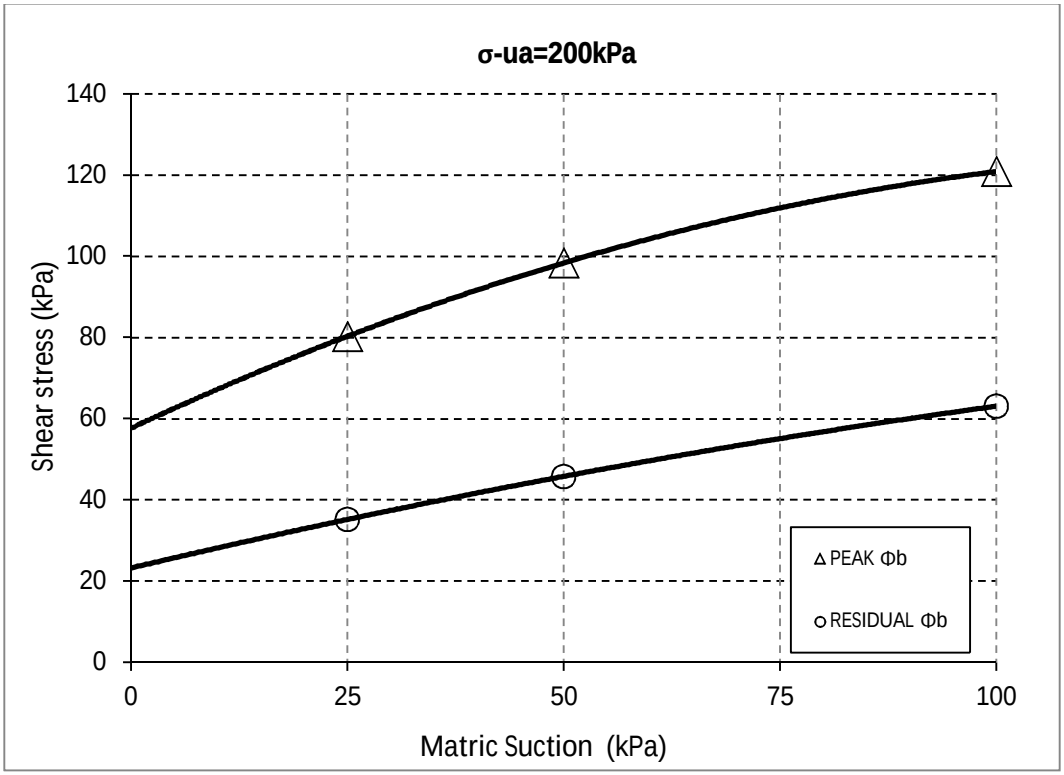

Figure 6-13. Nonlinearity of the Failure envelope as a function of Shear stress and matric suction for a net stress of $(\sigma_n - u_a)$ = 200 kPa and matric suction values of $(u_a - u_w)$ = 25, 50, and 100 kPa.

Figure 6-14 presents a summary and comparison of the peak failure envelopes presented in the previous figures, as a function of several values matric suction. The results show consistency in terms of matric suction and shear strength.

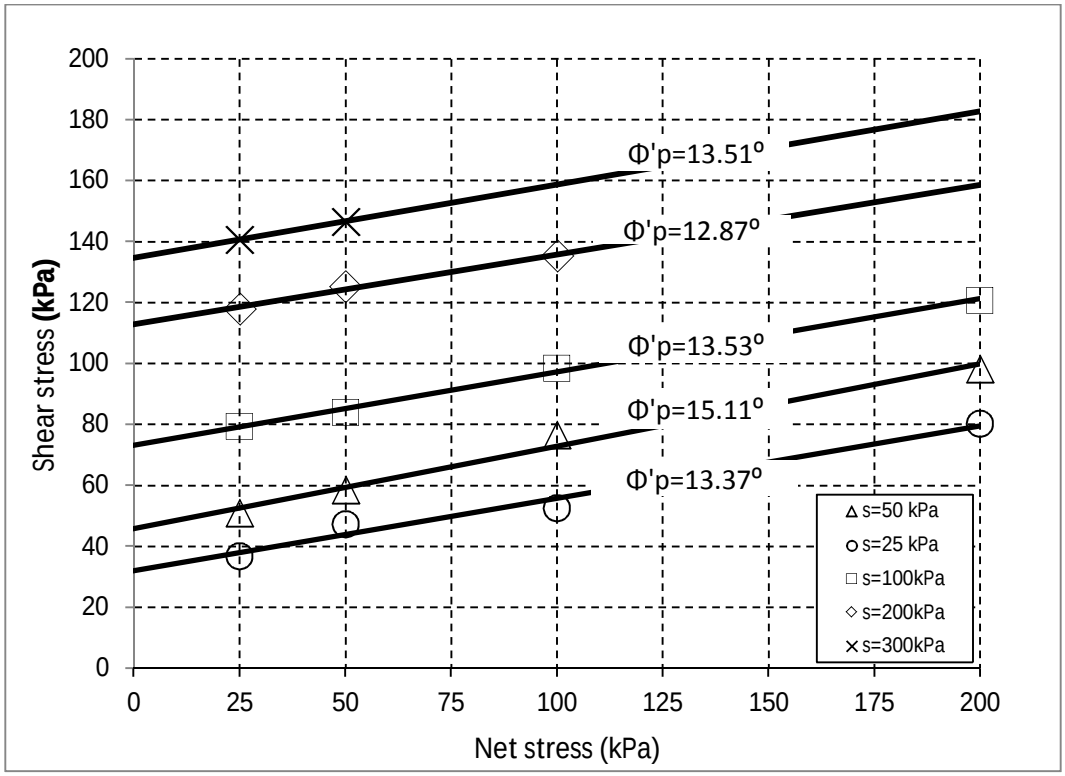

Figure 6-14. Peak failure envelopes as a function of matric suction.

Figure 6-15, presents a summary and comparison of the residual failure envelopes presented in the previous figures, as a function of several values of matric suction. The results show consistency in terms of matric suction and shear strength. Only for a matric suction of 300 kPa, there is an important difference in the slope with respect to the other failure envelopes. In this case, there are only two experimental points, and then it is difficult to draw precise conclusions.

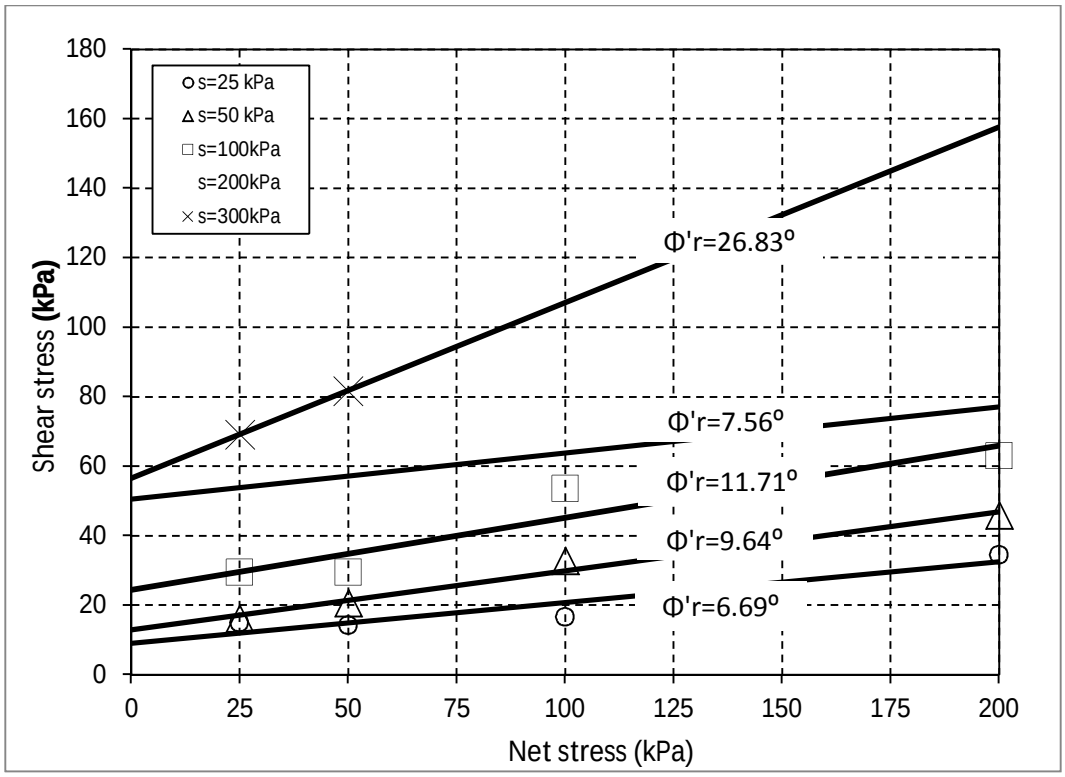

Figure 6-15. Residual failure envelopes as a function of matric suction

Figure 6-16 presents a summary and comparison of the peak failure envelopes in terms of the matric suction and as a function of several net stresses presented in the previous figures. The results show consistency in terms of net stress and shear strength. In this case, the linear approach is shown.

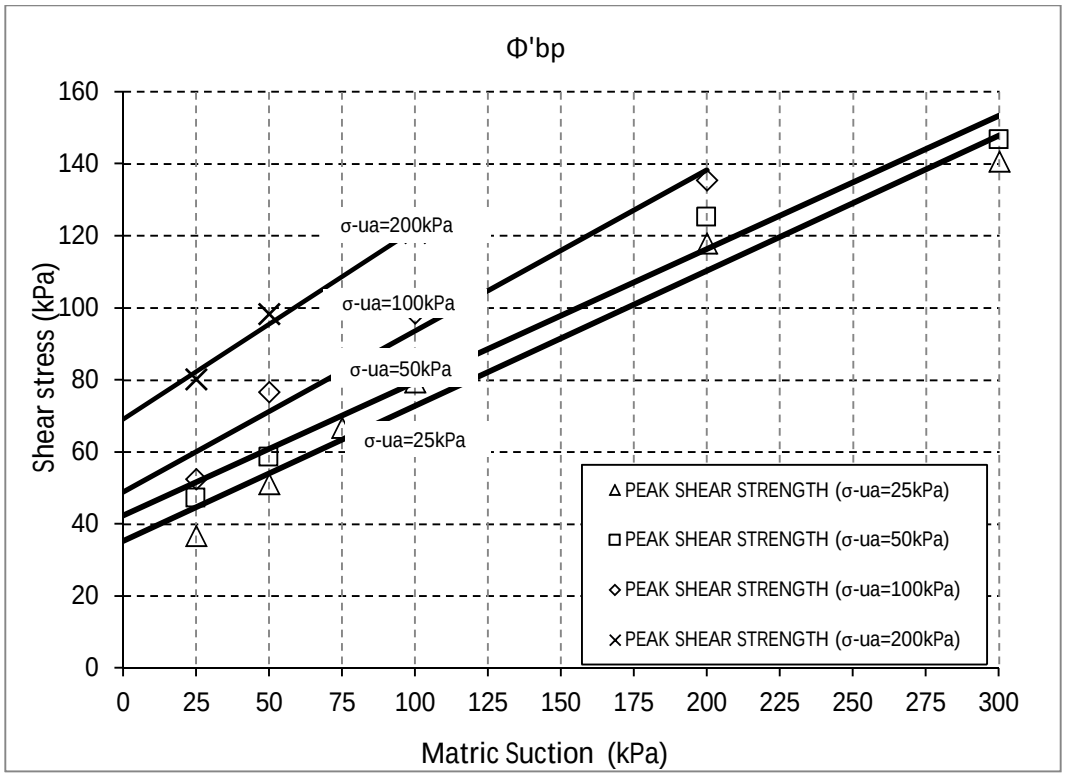

Figure 6-16. Peak failure envelopes in terms of matric suction and as a function of net stress

Figure 6-17 presents a summary and comparison of the nonlinear peak failure envelopes in terms of the matric suction and as a function of presented in the previous figures, as a function of several values of net stress. The results show consistency in terms of net stress and shear strength.

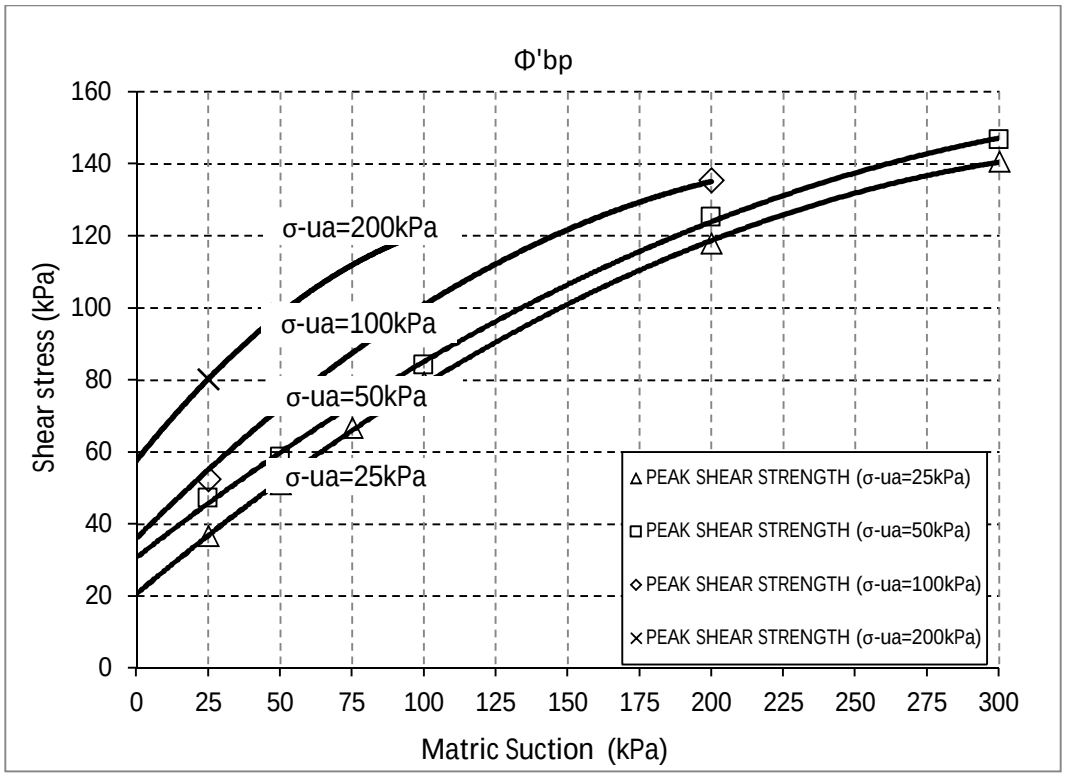

Figure 6-17. Nonlinear Peak failure envelopes in terms of matric suction and as a function of net stress

Figure 6-18 presents a summary and comparison of the residual failure envelopes in terms of the matric suction and as a function of several net stresses presented in the previous figures,. The results show consistency in terms of net stress and shear strength. In this case, the linear approach is shown.

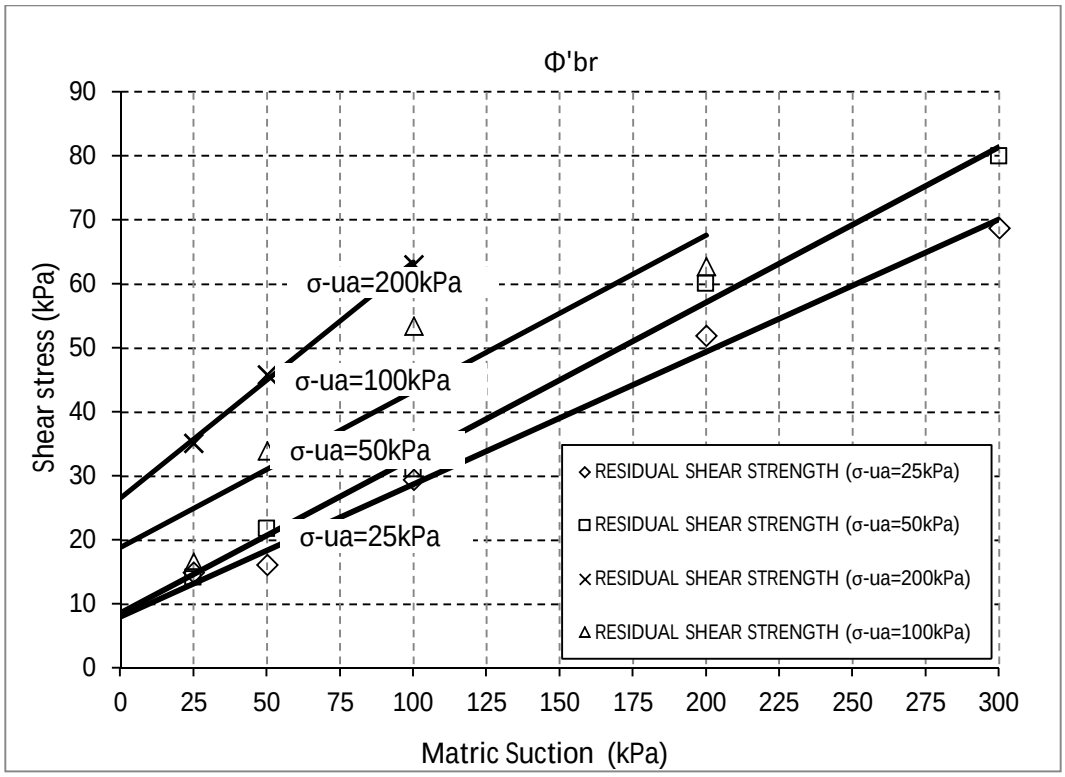

Figure 6-18. Residual failure envelopes in terms of matric suction and as a function of net stress

Figure 6-19 presents a summary and comparison of the nonlinear residual failure envelopes in terms of the matric suction and as a function of presented in the previous figures, as a function of several values of net stress. The results show consistency in terms of net stress and shear strength

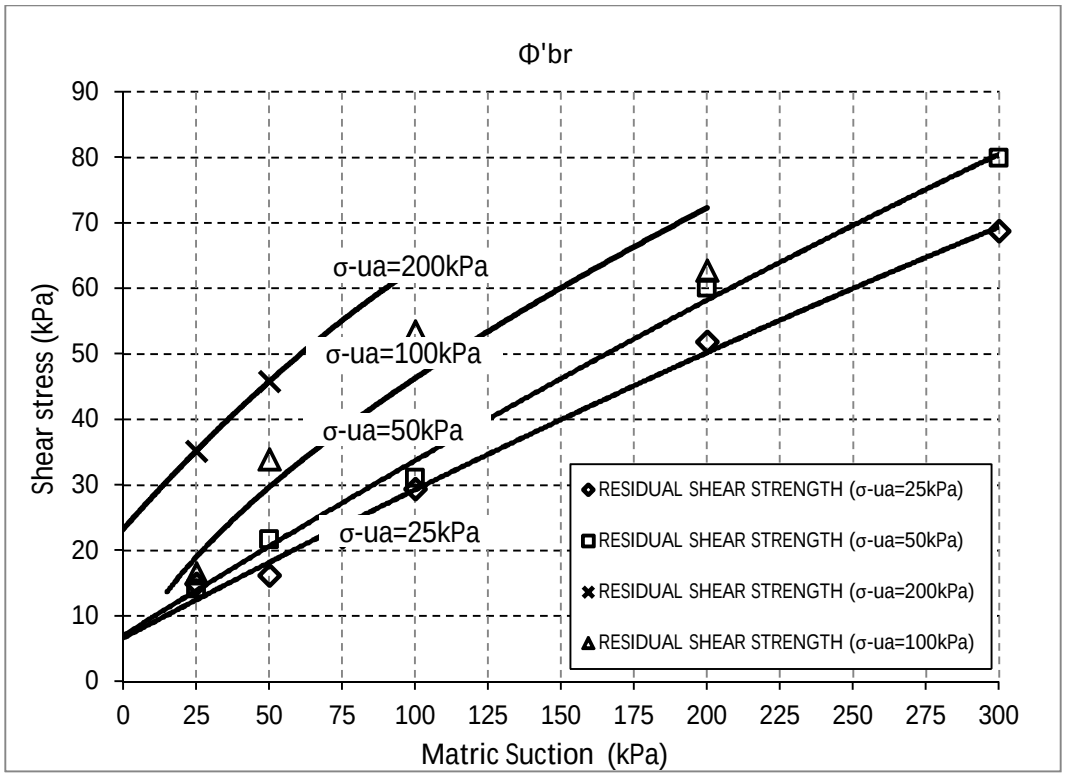

Figure 6-19. Nonlinear Residual failure envelopes in terms of matric suction and as a function of net stress

6.2 Unsaturated Shear Strength behavior Via Constant-Water Technique and the effect of temperature

This section will show peak and residual failure envelopes and the effect of temperature in the shear strength, considering the net stress and the matric suction as variables.

Figure 6-20 presents peak and residual failure envelopes in terms of matric suction for several values of temperature and a net normal stress of 25 kPa. In this case, it is possible to see how, with the increase in temperature, there is an increase in strength, but then there is a drop in the failure envelope for a temperature of 40°C

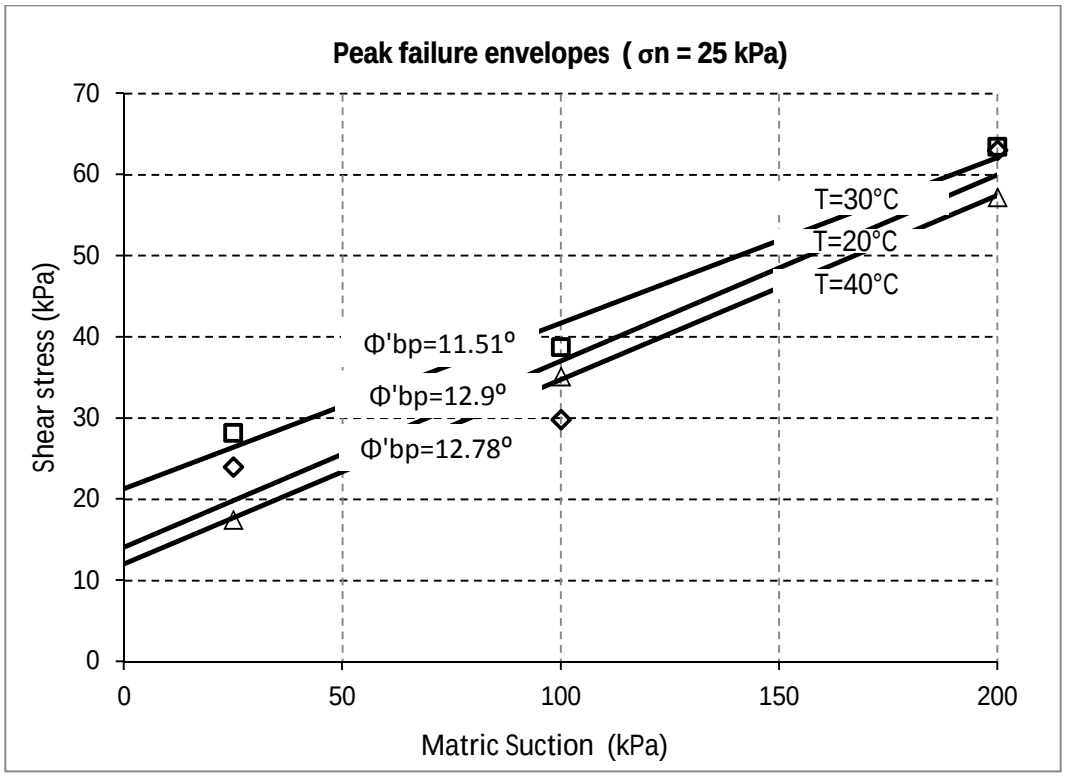

Figure 6-20. Peak failure envelopes in terms of matric suction for several values of temperature and a net normal stress of 25 kPa

Figure 6-21 shows peak and residual failure envelopes in terms of matric suction for several values of temperature and a net normal stress of 100 kPa. In this case, it is possible to see how, with the increase in temperature, there is an decrease in strength, but then there is an increase in the failure envelope for a temperature of 40°C.

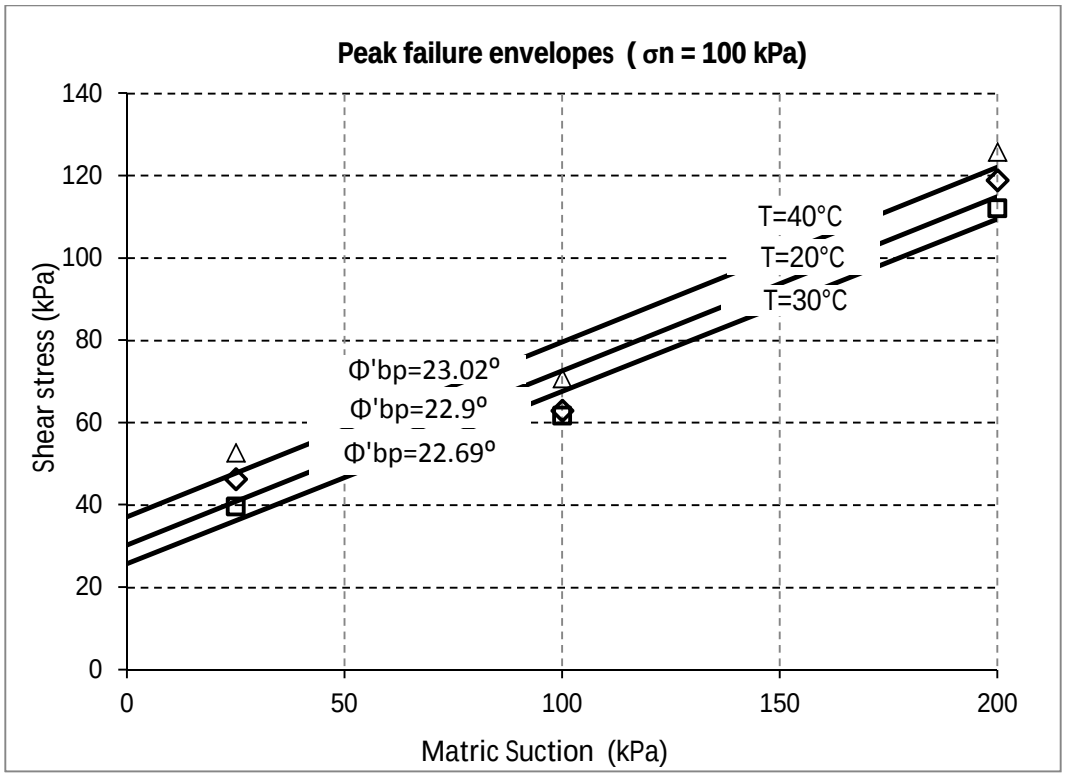

Figure 6-21. Peak failure envelopes in terms of matric suction for several values of temperature and a net normal stress of 100 kPa

6.3 Comparison of Axis-translation and Constant-water techniques results

This section is committed to compare the two methods for considering the effect of matric suction in the strength of soil. During this project, the axis-translation technique was only used for an average temperature of 20°C, and the constant-water technique was used for several temperatures. Then, in order to compare, only those results for an average temperature obtained with the constant-water technique will be considered.

Figure 6-22 presents the shear stress vs. equivalent horizontal displacement for both methods, and for a net normal stress of 25 kPa. Results obtained with constant-water technique, give lower results, both peak and residual. One of the most important reasons is that axis-translation was performed as a drained test, so the net normal stress allows drainage and also allows particles to get close together. Constant-water was performed as an undrained test, in order to keep the moisture content constant and the matric suction constant, then there is some compression but not as much as in a drained test.

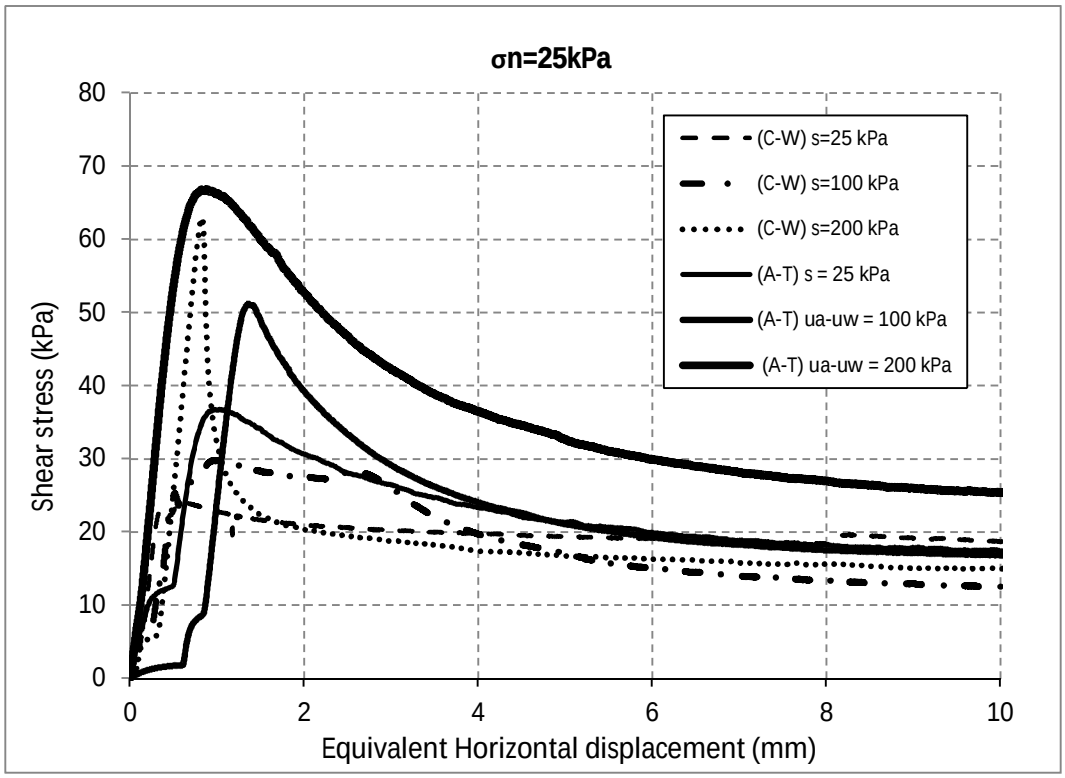

Figure 6-22. Comparison between axis-translation and constant-water techniques for a net normal stress of 25 kPa

Figure 6-23 presents the shear stress vs. equivalent horizontal displacement for both methods, and for a net normal stress of 100 kPa. Results obtained with constant-water technique, give lower results, both peak and residual as well. The reason mentioned for the previous plot applies for this case too. The drained behavior of the axis-translation technique gives more strength to the soil.

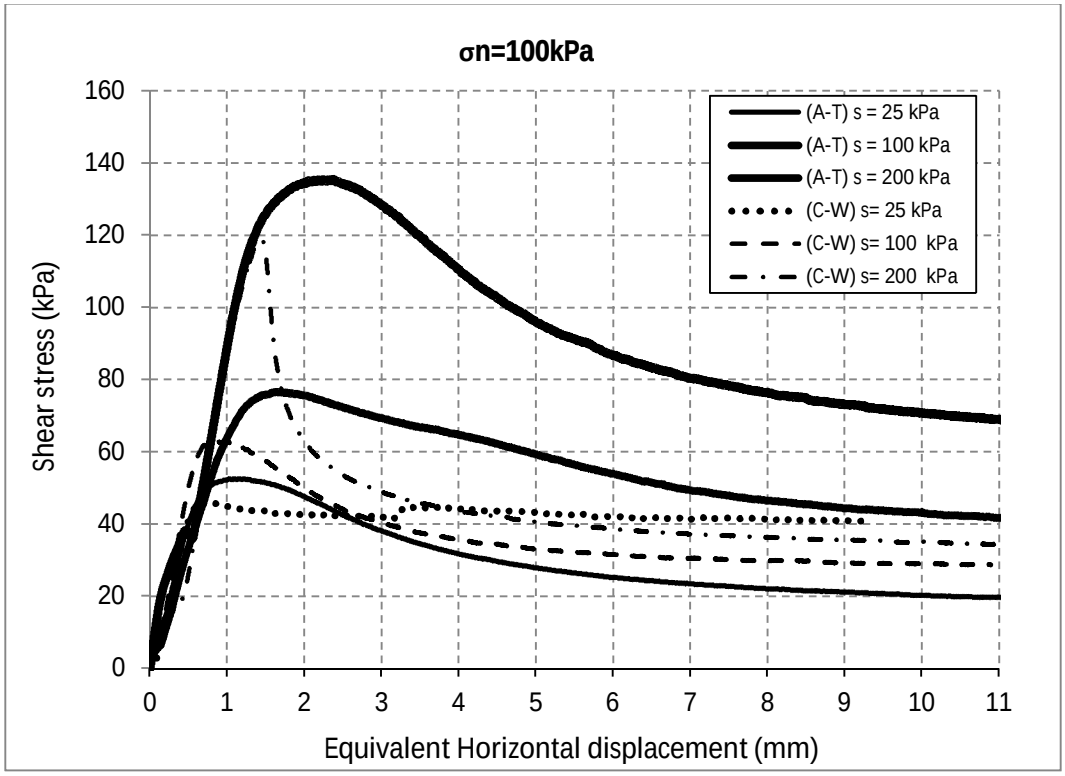

Figure 6-23. Comparison between axis-translation and constant-water techniques for a net normal stress of 100 kPa

Chapter 7

Conclusions and Recommendations

7.1 Summary

This work is committed to give a step in the study of unsaturated soils. In every construction project, foundation design, slope stability, tunneling design, pavement design, the engineer has to deal with unsaturated soils, particularly in tropical countries where water level is close to ground surface. Above ground water level, there is a process called capillarity, which causes the soil to suffer suction stresses that increases its strength. This additional strength is not commonly considered in the design of structures.

This project studied high plasticity clays in a novel suction controlled ring-shear apparatus, which measures both peak and residual strength of soils under large deformations. The soil sample is thicker than that one used in the Bromhead ring shear apparatus. Besides, in order to consider the season changes of the environment, a temperature controller was adapted to the device to consider both the effect of suction and temperature in the strength of soil at the same time.

During the process of performing the tests, ways to prepare the sample were discussed in order to get better results. Techniques to perform the test were also tried and compared to analyze the best way to approach to the real behavior of clayed soils in the field. The following section will summarize the main conclusions from this work and will make some recommendations for future research projects.

7.2 Conclusions and Recommendations for Upcoming projects

The main conclusions and recommendations of this project are as follows

Compaction of the sample: The process of compacting the sample is of quite importance in order to get good results. The top annular platen of the ring shear in contact with the sample must be horizontal to avoid the effect of wall friction with the bottom annular platen and to guarantee that the sample is actually in full contact with the top annular platen. Previously, the sample was compacted in the triaxial frame that is shown in this document. During this project, the initial tests were performed in this frame, and the conclusion was that an inclination was produced between the top and bottom annular platens because the triaxial frame allows some lateral movement. The ring shear apparatus is a stress controlled apparatus that applies a constant deformation to the sample and does not allow lateral deformation, so it guarantees the horizontality of the failure surface. The recommendation from this experience is to keep on using the ring shear to compact the sample until the desired thickness is achieved.

Multi-stage vs. Single stage testing: a section of this project is dedicated to analyze the difference of testing the sample under multi-stage or single-stage procedures. The conclusion was that in a multi-stage test, the sample becomes a different material after the first stage, and the shear stress vs. equivalent horizontal deformation curves show the difference. After the first stage, the sample already failed and then, even though it is subjected to a different net normal stress, the sample has a lower shear strength. This is why, in a multi-stage test, the stages after the first one, show a peak shear strength that is close to the residual, and sometimes the residual tends to be higher. This means that the soils is becoming brittle. The recommendation

here is that, even though it takes more time, single stage testing is a better way to approach to the real strength of the soil.

Control of temperature: most of the work done in the laboratory considering the effect of temperature and suction at the same time has been performed using a modified triaxial equipment, an isotropic cell or an oedometer. The results from these previous work have focused on volumetric changes, effects on preconsolidation pressure, among others, but none of them have directly focused on measuring the combined effect of temperature and suction on strength parameters. This project worked on an approach and some conclusions can be drawn. For a relatively high net normal stress the temperature, even though it tended to decrease, it ended up increasing the strength. On the other hand, for a higher net normal stress, even though it tended to increase, it ended up decreasing the strength of the material. Suction stresses and changes in temperature are processes that occur all the time in the field, and they are complex to study, but if more research is committed to keep on trying to find out the real effect of these two variables in the strength of the soil, better conclusions can be done.

Axis-translation vs constant-water techniques: a section of this work was also dedicated to investigate the difference of these two ways to control matric suction in the laboratory, and some conclusions were also drawn from it. Regarding the work performed in the ring shear apparatus, axis-translation was performed as a drained test, during which the consolidation process is allowed in a better way, the particles get together and the strength increases. On the other hand, during the constant-water technique, the test was performed as an undrained process in order to keep the moisture content constant, so the compression of the sample occurs but not in the same way. That is why when comparing the two techniques, with the axis-translation technique, the peak shear

strength was higher. The recommendation is that depending on what happens in the field or which process is being searched, drained or undrained, is how the test should be performed.

Appendix A

Residual Beta Angle vs Matric Suction

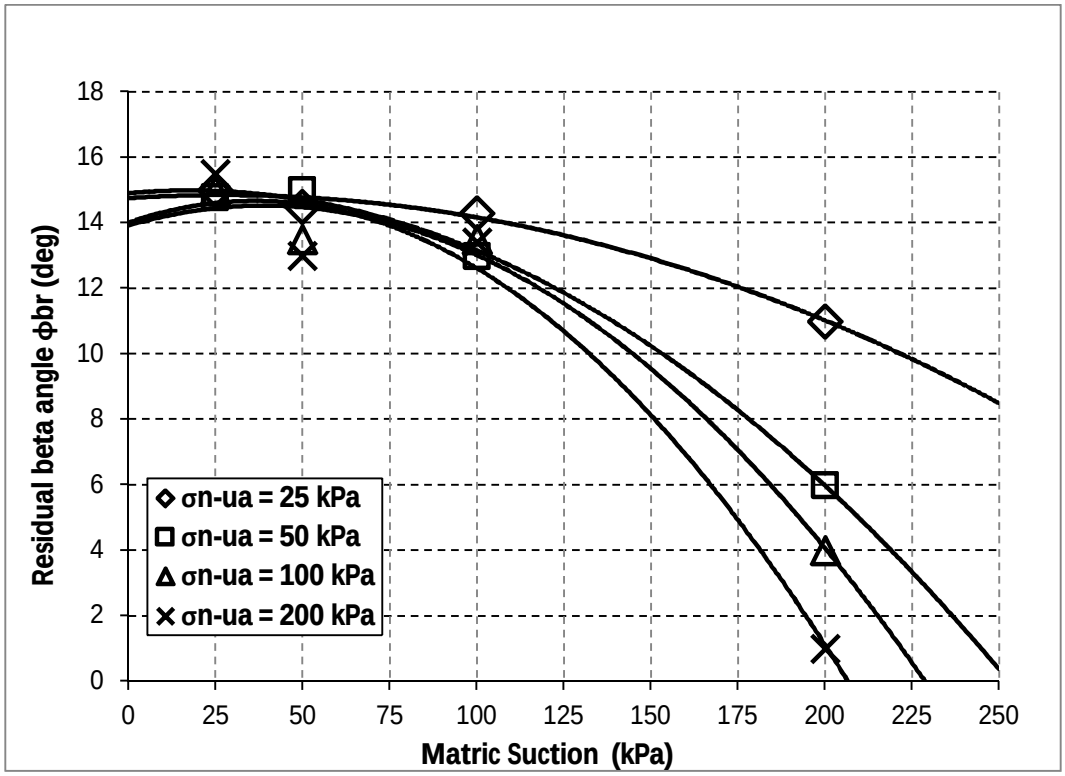
Residual beta angle ϕbr (deg)
Matric Suction (kPa)
σn-ua = 25 kPa
σn-ua = 50 kPa
σn-ua = 100 kPa
σn-ua = 200 kPa
0
2
4
6
8
10
12
14
16
18
0
25
50
75
100
125
150
175
200
225
250

Appendix B

Single Stage Stress Paths

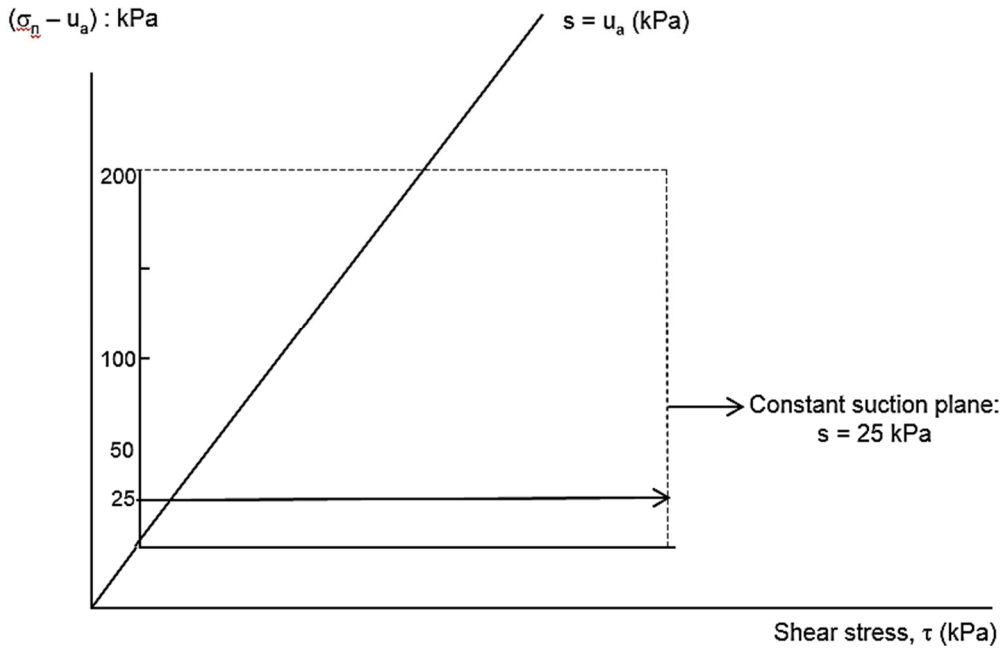
(σn – ua) : kPa
s = ua (kPa)
200
100
50
25
Constant suction plane:
s = 25 kPa
Shear stress, τ (kPa)

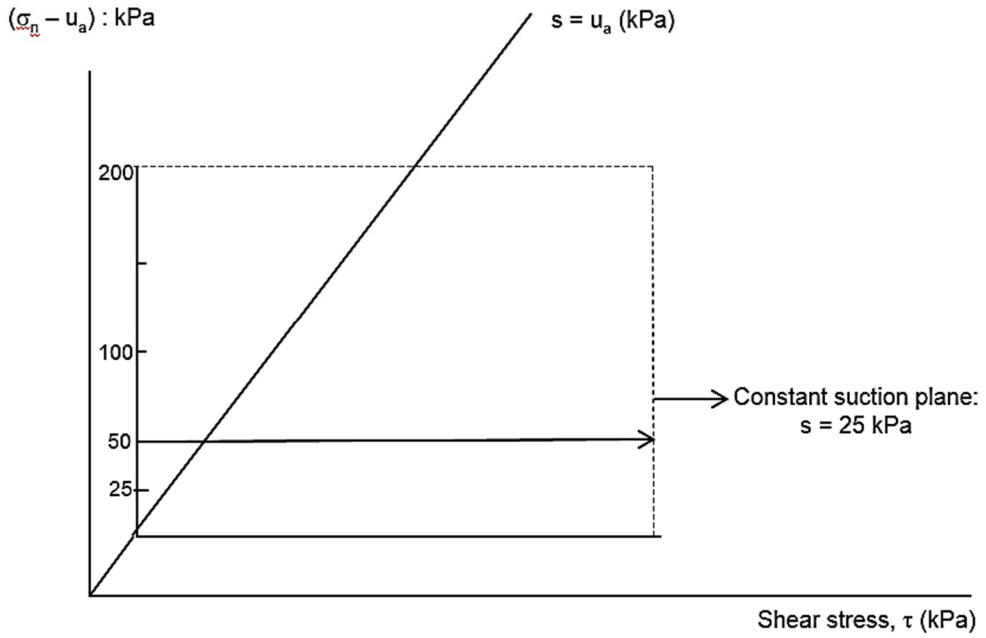
$(\sigma_n - u_a)$: kPa
$s = u_a$ (kPa)
200
100
50
25
Constant suction plane:
s = 25 kPa
Shear stress, τ (kPa)

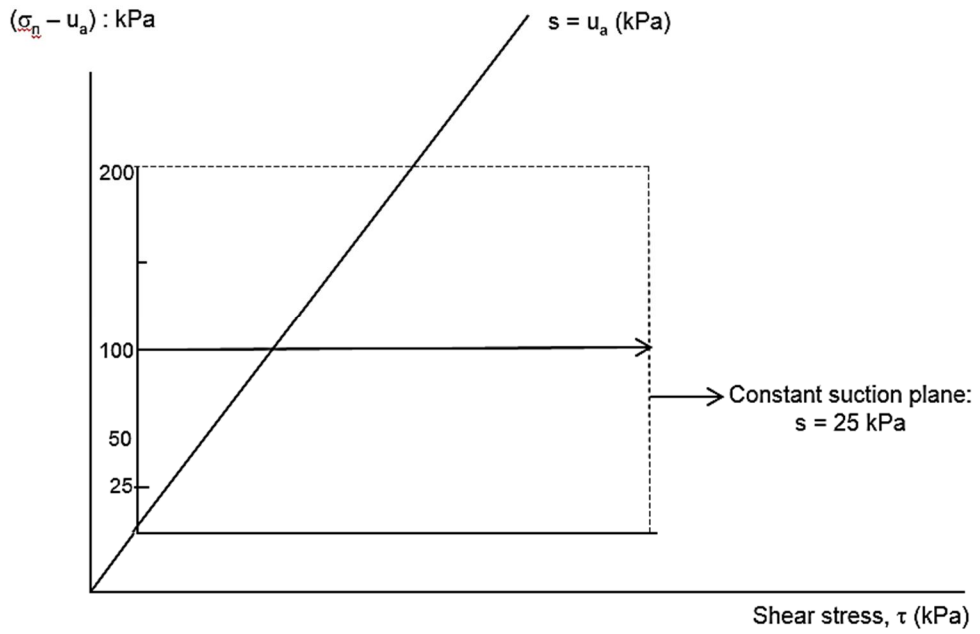
(σn – ua) : kPa
s = ua (kPa)
200
100
50
25
Constant suction plane:
s = 25 kPa
Shear stress, τ (kPa)

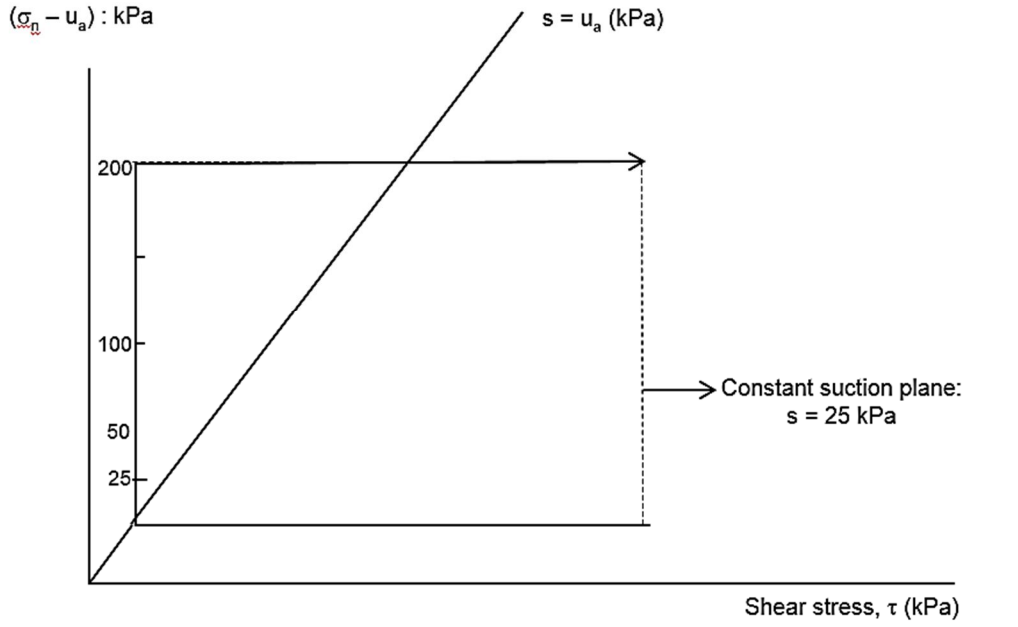
$(\sigma_n - u_a)$: kPa
$s = u_a$ (kPa)
200
100
50
25
Constant suction plane:
s = 25 kPa
Shear stress, τ (kPa)

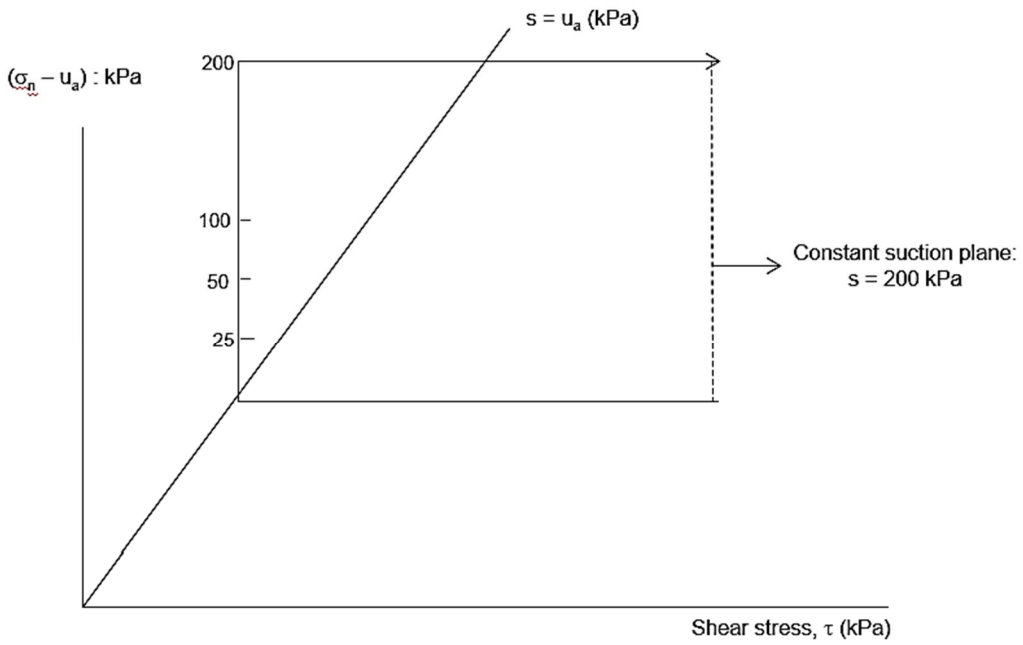
s = u_a (kPa)
(σ_n – u_a) : kPa
200
100
50
25
Constant suction plane:
s = 200 kPa
Shear stress, τ (kPa)

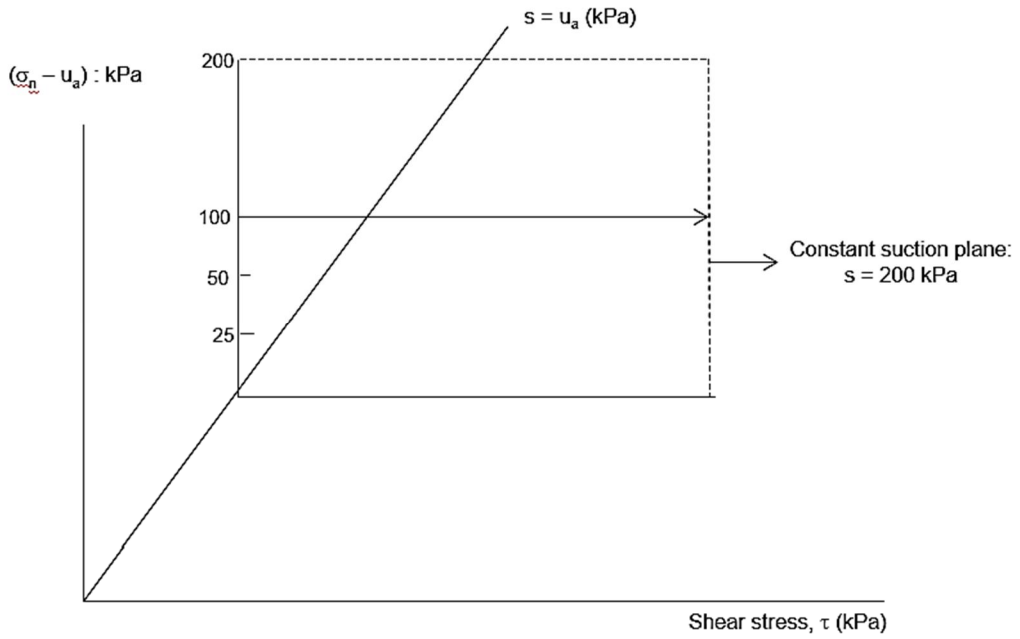
s = u_a (kPa)
(σ_n – u_a) : kPa
200
100
50
25
Constant suction plane:
s = 200 kPa
Shear stress, τ (kPa)

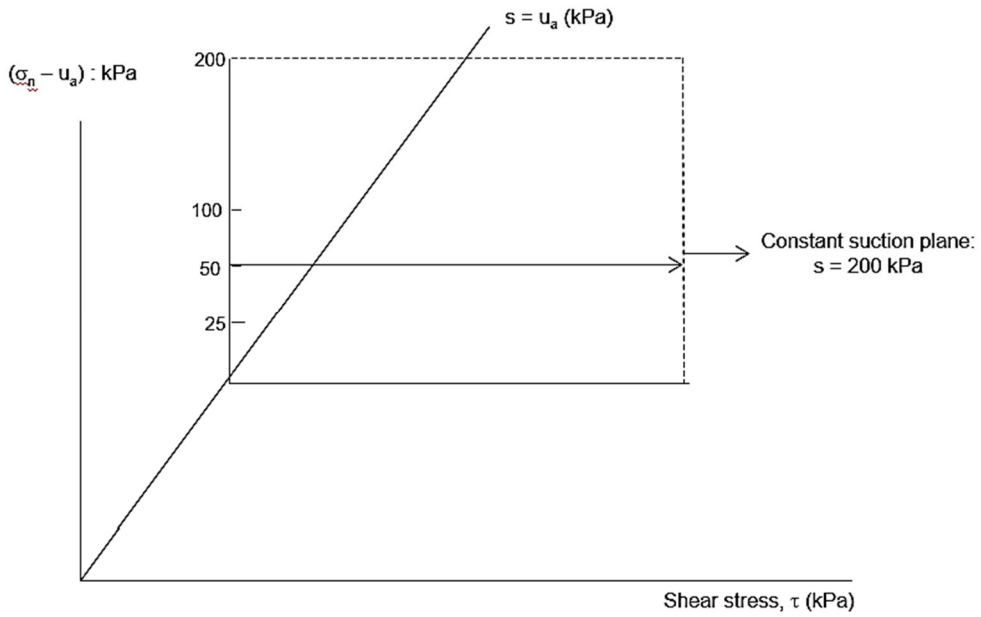
s = u_a (kPa)
(σ_n – u_a) : kPa
200
100
50
25
Constant suction plane:
s = 200 kPa
Shear stress, τ (kPa)

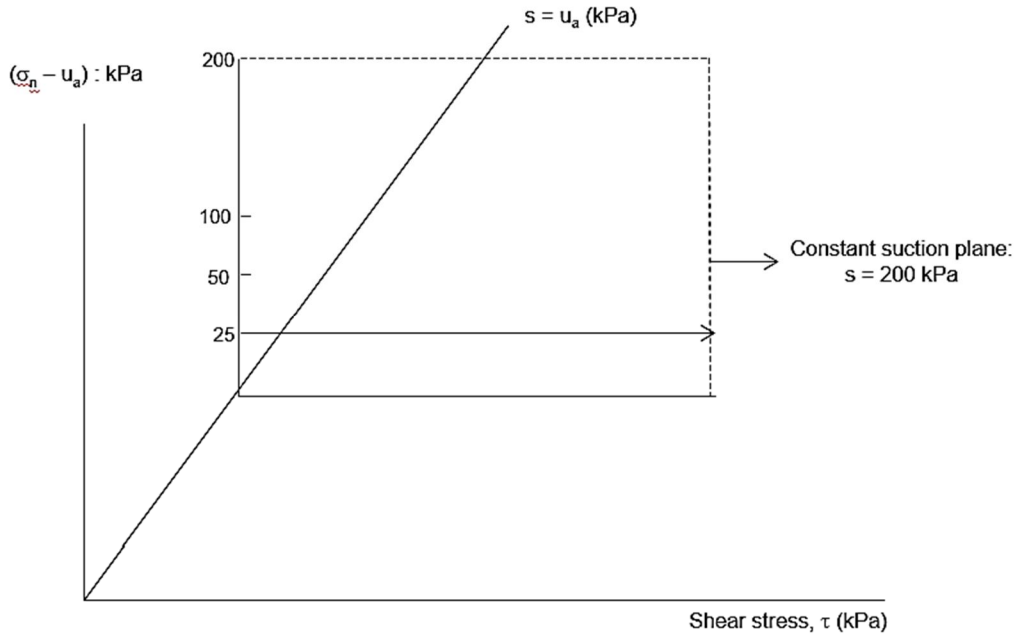
s = u_a (kPa)
(σ_n – u_a) : kPa
200
100
50
25
Constant suction plane:
s = 200 kPa
Shear stress, τ (kPa)

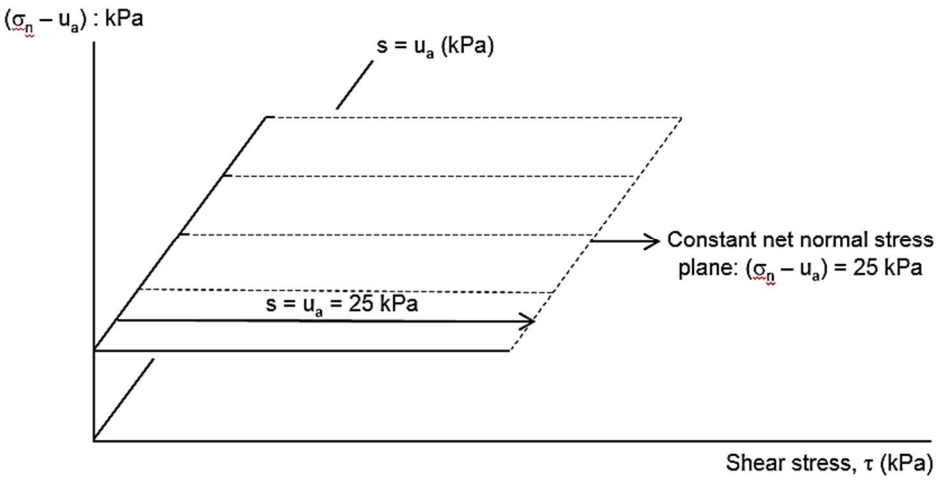
$(\sigma_n - u_a)$: kPa
$s = u_a$ (kPa)
Constant net normal stress plane: $(\sigma_n - u_a) = 25$ kPa
$s = u_a = 25$ kPa
Shear stress, τ (kPa)

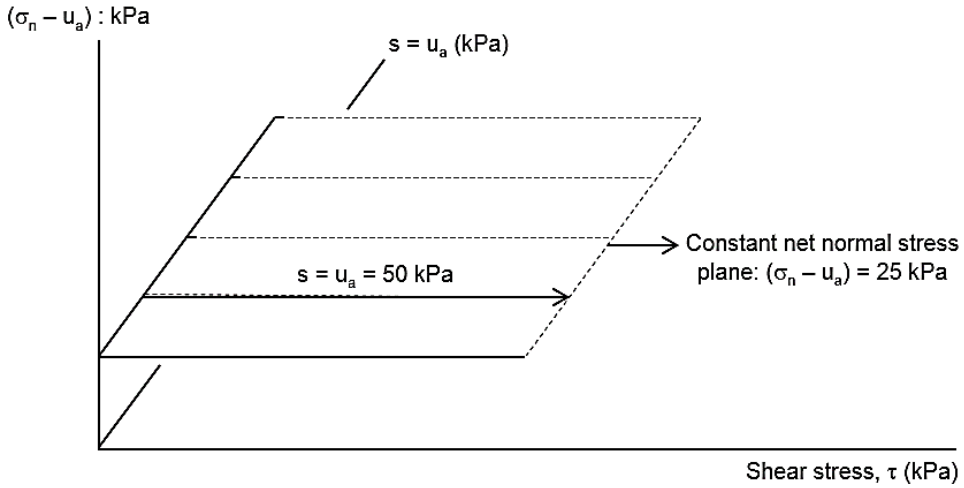
$(\sigma_n - u_a)$: kPa
$s = u_a$ (kPa)
$s = u_a$ = 50 kPa
Constant net normal stress plane: $(\sigma_n - u_a)$ = 25 kPa
Shear stress, τ (kPa)

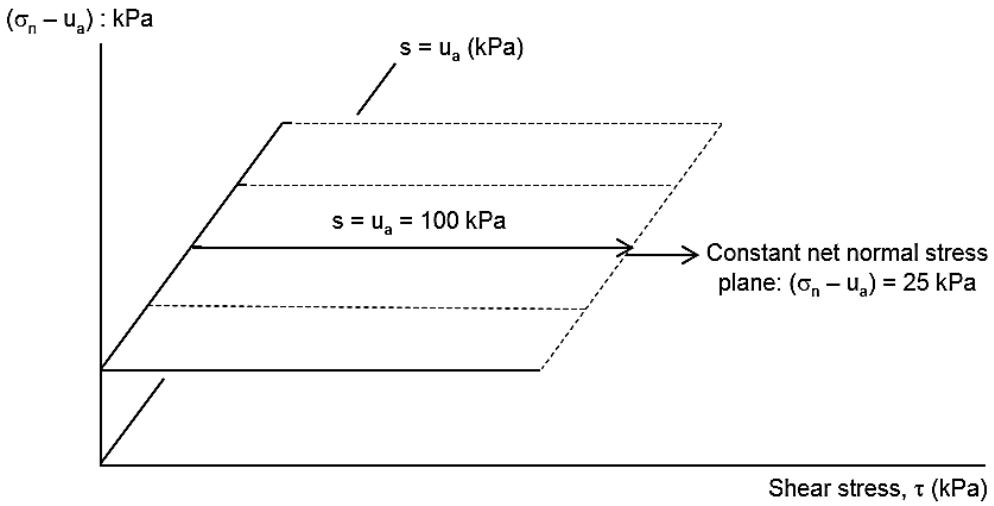
$(\sigma_n - u_a)$: kPa
$s = u_a$ (kPa)
$s = u_a$ = 100 kPa
Constant net normal stress plane: $(\sigma_n - u_a)$ = 25 kPa
Shear stress, τ (kPa)

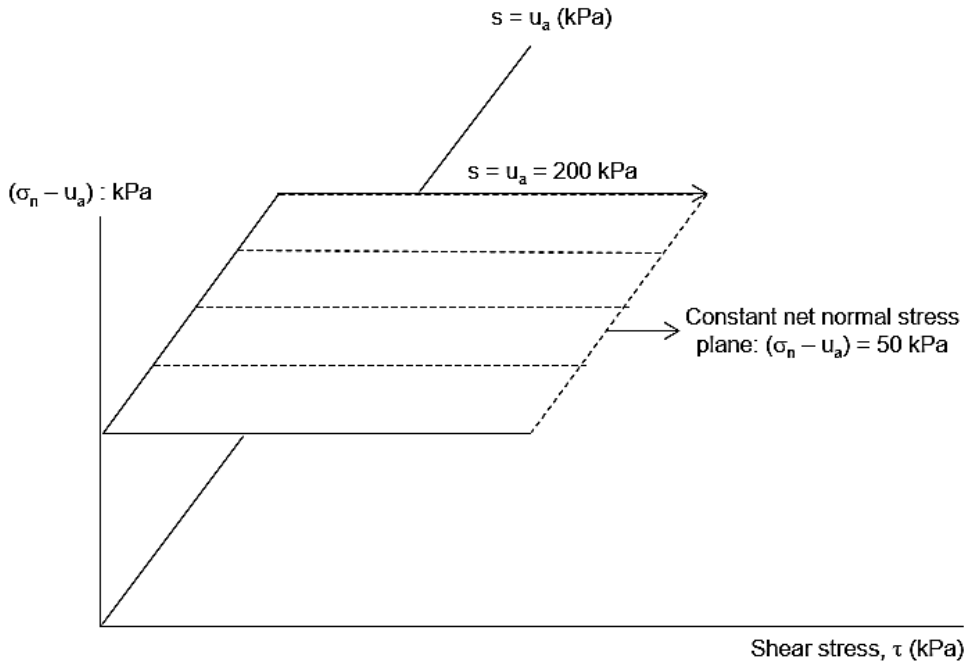
s = u_a (kPa)
s = u_a = 200 kPa
(σ_n – u_a) : kPa
Constant net normal stress plane: (σ_n – u_a) = 50 kPa
Shear stress, τ (kPa)

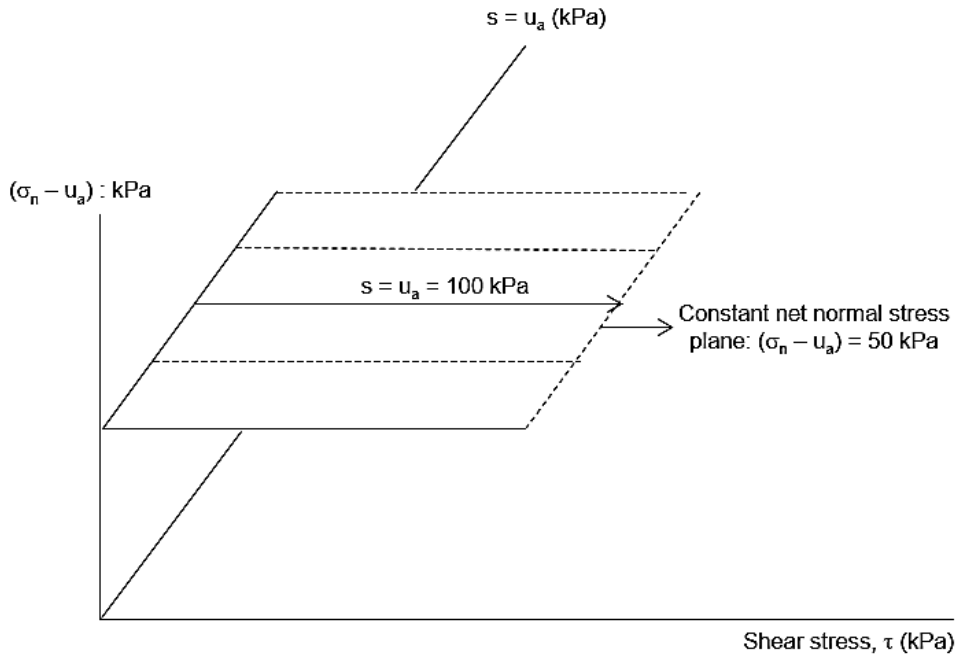
s = u_a (kPa)
(σ_n – u_a) : kPa
s = u_a = 100 kPa
Constant net normal stress plane: (σ_n – u_a) = 50 kPa
Shear stress, τ (kPa)

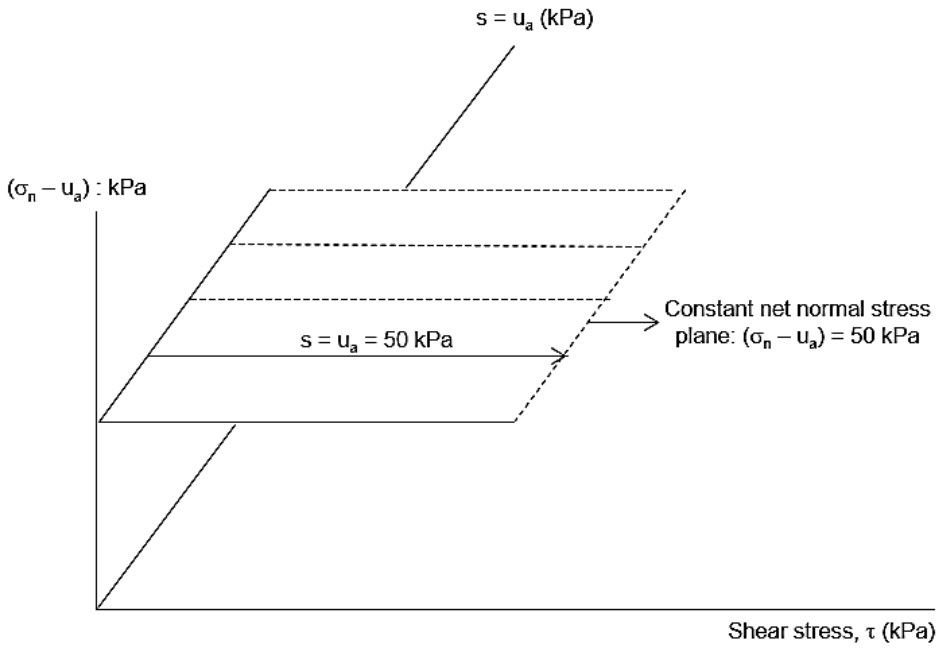
s = u_a (kPa)
(σ_n – u_a) : kPa
s = u_a = 50 kPa
Constant net normal stress plane: (σ_n – u_a) = 50 kPa
Shear stress, τ (kPa)

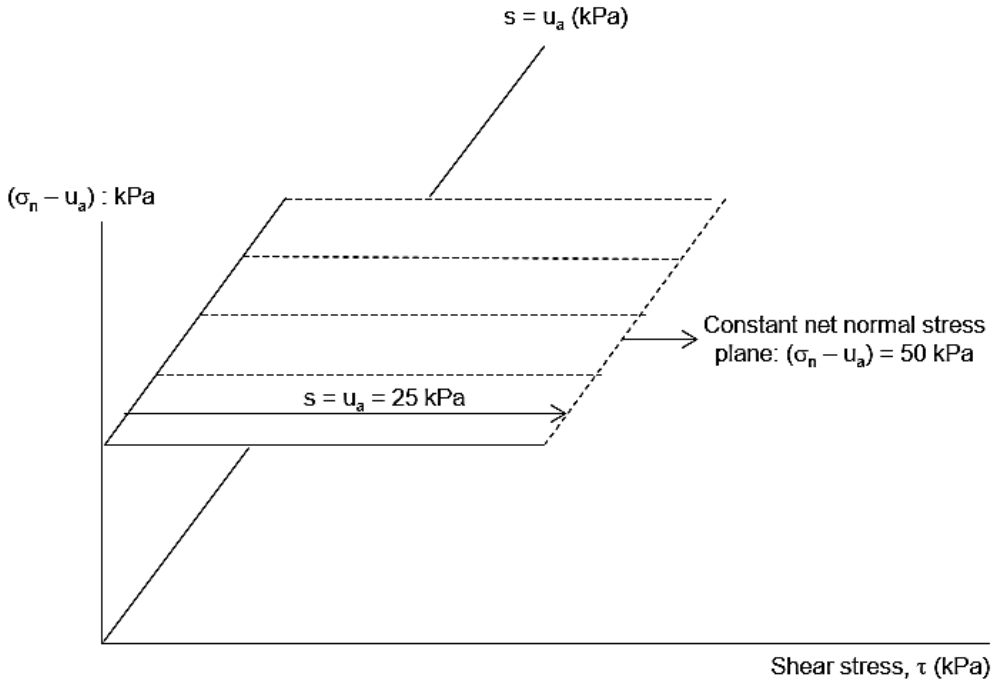
s = u_a (kPa)
(σ_n – u_a) : kPa
Constant net normal stress plane: (σ_n – u_a) = 50 kPa
s = u_a = 25 kPa
Shear stress, τ (kPa)

Appendix C

Typical Failure Surfaces

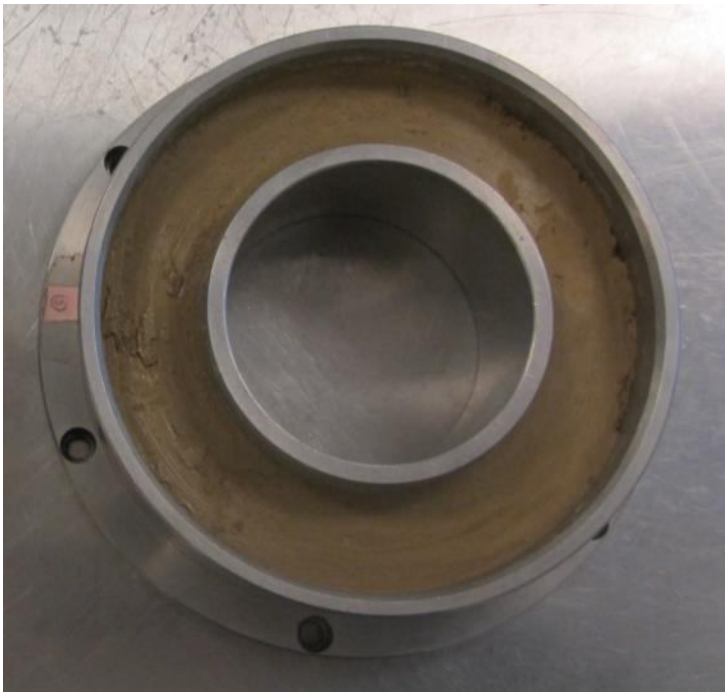

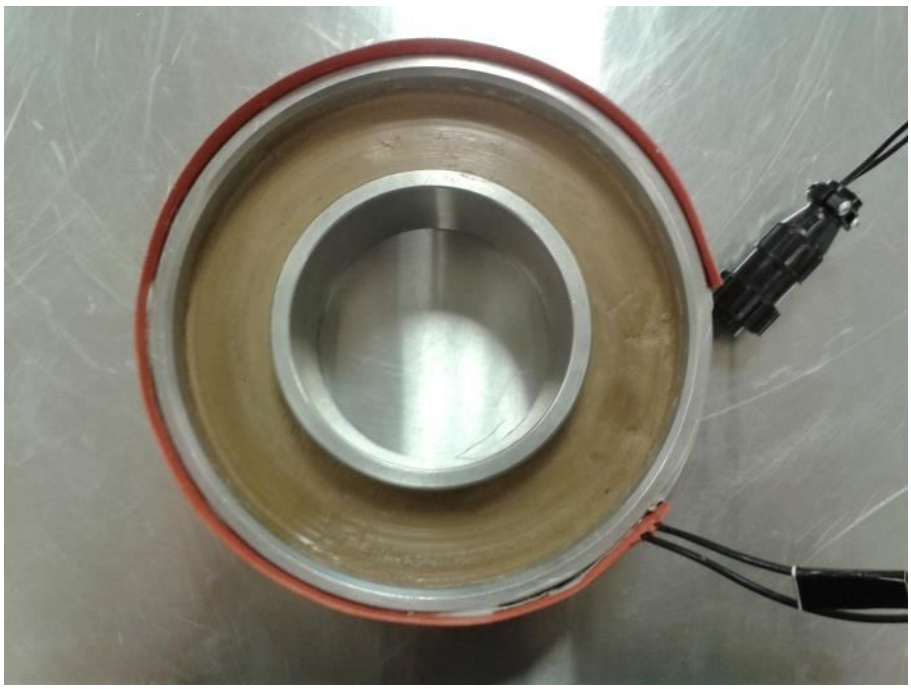

References

- Alonso, E.E., Gens, A., and Josa, A. (1990). “A constitutive model for partially saturated soils.” Géotechnique, 40(3), 405- 430.
- A. Lloret, M.V. Villar (2007). “Advances on the knowledge of the thermo-hydro-mechanical behavior of heavily compacted “FEBEX Bentonite” Physics and Chemistry of the Earth 32, 701–715.
- ASTM Standard D7608-10. “Standard Test Method for Torsional Ring Shear Test to Determine Drained Fully Softened Shear Strength and Nonlinear Strength Envelope of Cohesive Soils (Using Normally Consolidated Specimen) for Slopes with No Preexisting Shear Surfaces,” ASTM International.
- ASTM Standard D6467-06a. “Standard Test Method for Torsional Ring Shear Test to Determine Drained Residual Shear Strength of Cohesive Soils,” ASTM International.
- Ali Seiphoori, Alessio Ferrari and Lyesse Laloui (2011). “An advanced calibration process for a thermo-hydro-mechanical triaxial testing system”. Deformation Characteristics of Geomaterials : Proceedings of the Fifth International Symposium on Deformation Characteristics of Geomaterials, Is-seoul, 1-3.
- Anh-Minh Tang and Yu-Jun Cui (2005). “Controlling suction by vapour equilibrium technique at different temperatures, application to the determination of the water retention properties of MX80 clay”. Canadian Geotechnical Journal, 42(1): 287-296.
- Anh-Minh Tang, Yu-Jun Cui, Nathalie Barnel (2007). “ A new isotropic cell for studying the thermo-mechanical behavior of unsaturated expansive clays”. Geotechnical Testing Journal 30,(5) 341-348.

- Anuchit Uchaipichat (2005). “Experimental investigation and constitutive modeling of Thermo-Hydro-Mechanical coupling in unsaturated soils”. PhD Dissertation. School of Civil and Environmental Engineering The University of New South Wales. Sydney, New South Wales, Australia.
- Baldi, G., Hueckel, T., and Pellegrini, R. (1988). “Thermal volume changes of mineral-water system in low-porosity clay Soil.” Canadian Geotechnical Journal, 25, 807-825.
- Bergenstahl, L., Gabrielsson, A., and Mulabdic, M. (1994). “Changes in soft clay caused by increases in temperature.” Proc., 13th International Conference on Soil Mechanics and Foundation Engineering, Comptes-rendus, New Delhi, January 5-10, 1637-1640.
- Bishop, A.W., Alpan, I., Blight, G.E., and Donald, I.B. (1960). “Factors controlling the shear strength of partially saturated cohesive soils.” Proc., ASCE Research Conference on the Shear Strength of Cohesive Soils, Boulder, 503-532.
- Blatz, J.A., and Graham, J. (2000). “A system for controlled suction in triaxial tests.” Géotechnique, 50(4), 465-478.
- Blatz, J.A., and Graham, J. (2003). “Elastic plastic modeling of unsaturated high-plastic clay using results from a new triaxial test with controlled suction.” Géotechnique, 53(1), 113-122.
- Bourne-Webb, P., Amatya, B., Soga, K., Amis, T., Davidson, C., and Payne, C. (2009). “Energy pile test at Lambeth College, London: Geotechnical and thermodynamic aspects of pile responses to heat cycles.” Géotechnique, 59(3), 237-248.

- Brandl, H. (2006). “Energy foundations and other thermo-active ground structures.” Géotechnique, 56(2), 81-122.
- Bromhead, E.N. (1979). “A simple ring shear apparatus.” Ground Engineering, 12(5), 40-44.
- B. François, S. Salager, M.S. El Youssouf, D.Ubals Picanyol, L. Laloui, C. Saix (2007). “Compression tests on a sandy silt at different suction and temperature levels”. American Society of Civil Engineers, Geotechnical Special Publication GSP 157, Computer Applications in Geotechnical Engineering – GeoDenver, 1-10.
- Cai, G.-Q., Zhao, C.-G., and Liu, Y. (2010). “Temperature effects on soil-water characteristic curve of unsaturated soils.” Rock and Soil Mechanics, 31(4), 1055-1060.
- Campanella, R.G., and Mitchell, J.K. (1968). “Influence of temperature variations on soil behavior.” J. Soil Mech. and Found. Div., 94(SM3), 9-22.
- Cekerevac, C., and Laloui, L. (2004). “Experimental study of thermal effects on the mechanical behaviour of a clay.” IJNAMG, 28, 209-228.
- De Gennaro, V., Pande, G.N., and Lerat, P. (2002). “Stability problems in soil-structure interfaces: Experimental observations and numerical study”. International Journal of Geomechanics, 2(12), 175-203.
- Delage, P., Sultan, N., and Cui, Y.-J. (2000). “On the thermal consolidation of Boom clay.” Canadian Geotechnical Journal, 37, 343-354.
- Demars, K.R., and Charles, R.D. (1982). “Soil volume changes induced by temperature cycling.” Canadian Geotechnical Journal, 19, 188-194.
- E. Romero, M.V. Villar, A. Lloret (2005). “Thermo-hydro-mechanical behavior of two heavily overconsolidated clays”. Engineering Geology 81, 255–268.

- E.Romero, Li Xiangling (2006). “Thermo-hydro-mechanical characterization of opholie backfill mixture”. Chinese Journal of Rock Mechanics and Engineering 25, (4), 733-740.
- Francois, B., and Laloui, L. (2010). “An oedometer for studying combined effects of temperature and suction on soils.” Geotechnical Testing Journal, 33(2), 112-122.
- Fredlund, D.G. (1987). “Soil suction monitoring for roads and airfields.” Symposium on the State-of-the-Art of Pavement Response Monitoring Systems for Roads and Airfields, Sponsored by the U.S. Army Corps of Engineers, Hanover, NH, March 6-9, 1989.
- Fredlund, D.G., Morgenstern, N.R., and Widger, R.A. (1978). “The shear strength of unsaturated soils.” Canadian Geotechnical Journal, 15(3), 313-321.
- F. Collin, X.L. Li, J.P. Radu, R. Charlier (2002). “Thermo-hydro-mechanical coupling in clay barriers”. Engineering Geology 64, 179–193.
- Garga, V.K., and Infante Sedano, J.A. (2002). “Steady state strength of sands in a constant volume ring shear apparatus”. Geotechnical Testing Journal, 25(4), 414-421.
- Graham, J., Tanaka, N., Crilly, T., and Alfaro, M. (2001). “Modified Cam-Clay modeling of temperature effects in clays.” Canadian Geotechnical Journal, 38, 608-621.
- Groger, T., Tuzun, U., and Heyes, D. (2003). “Modeling and measuring of cohesion in wet granular materials”. Powder Technology, 123, 203-215.
- Hilf, J.W. (1956). “An investigation of pore water pressure in compacted cohesive soils.” Technical Memorandum No. 654, United States Department of Interior, Bureau of Reclamation, Design and Construction Division, Denver, CO.

- Hoyos, L.R., Velosa, C.L., and Puppala, A.J. (2011). “A servo/suction-controlled ring shear apparatus for unsaturated soils: development, performance, and preliminary results.” Geotechnical Testing Journal, ASTM, 34(5), 413-423.
- Hueckel, T., and Pellegrini, R. (1992). “Effective stress and water pressure in saturated clays during heating-cooling cycles.” Canadian Geotechnical Journal, 29, 1095-1102.
- Infante Sedano, J.A., Vanapalli, S.K., and Garga, V.K. (2007). “Modified ring shear apparatus for unsaturated soil testing.” Geotechnical Testing Journal, ASTM, 30(1), 1-9.
- Iverson, N.R., Baker, R.W., and Hooyer, T.S. (1997). “A ring-shear device for the study of till deformation: Tests on tills with contrasting clay contents”. Quaternary Science Reviews, 16, 1057-1066.
- Jones, D.R.V., and Dixon, N. (1998). “Shear strength properties of geomembrane/geotextile interfaces”. Geotextiles and Geomembranes, 16, 45-71.
- Kamai, T. (1998). “Monitoring the process of ground failure in repeated landslides and associated stability assessments”. Engineering Geology, 50, 71-84.
- Karakouzian, M., and Hudyma, N. (2002). “A new apparatus for analog modeling of clay smears”. Journal of Structural Geology, 24(5), 905-912.
- Kuntiwattanakul, P., Towhata, I., Ohishi, K., and Seko, I. (1995). “Temperature effects on undrained shear characteristics on clay.” Soils and Foundations, 35(1), 427-441.
- Laloui, L., Nuth, M., and Vulliet, L. (2006). “Experimental and numerical investigations of the behavior of a heat exchanger pile.” IJNAMG, 30, 763-781.
- Likos, W.J., and Wayllace, A. (2010). “Porosity evolution of free and confined bentonites during interlayer hydration.” Clays and Clay Minerals, 58(3), 399-414.

- Likos, W.J., and Lu, N. (2006). “Pore scale analysis of bulk volume change from crystalline swelling in Na^{+}- and Ca^{2+}-smectite.” Clays and Clay Minerals, 54(4), 516-529.
- Likos, W.J., and Lu, N. (2003). “Automated humidity system for measuring total suction characteristics of clay.” Geotechnical Testing Journal, ASTM, 26(2), 178-189.
- Likos, W.J., and Lu, N. (2002). “Water-vapor sorption behavior of smectite-kaolinite mixtures.” Clays and Clay Minerals, 50(5), 553-561.
- Lloret, A., Villar, M.V., Sanchez, M., Gens, A., Pintado, X., and Alonso, E.E. (2003). “Mechanical behavior of heavily compacted bentonite under high suction changes.” Géotechnique, 53(1), 27-40.
- Lu, N., Godt, J.W., and Wu, D.T. (2010). “A closed-form equation for effective stress in unsaturated soil.” Water Resources Res. 46: 14 pp.
- Lu, N., and Likos, W.J. (2004). *Unsaturated soil mechanics*, John Wiley & Sons, Hoboken, N.J.
- McCartney, J.S. (2011). “Issues involved in using temperature to improve the mechanical behavior of unsaturated soils.” *Unsaturated Soils: Theory and Practice*, Kasetsart University, Proceedings of the 5th Asia-Pacific Conference on Unsaturated Soils, November 14-16, 2011, Pattaya, Thailand, Eds: A. Jotisankasa, A. Sawangsuriya, S. Soralump, and W. Mairaing, 6 pp.
- Mancktelow, N.S., Arbaret, L., and Pennacchioni, G. (2002). “Experimental observations on the effect of interface slip on rotation and stabilization of rigid particles in simple shear and a comparison with natural mylonites”. Journal of Structural Geology, 24, 567-585.

- Meehan, C.L., Brandon, T.L., and Duncan, J.M. (2007). “Measuring drained residual strength in the Bromhead ring shear.” Geotechnical Testing Journal, ASTM, 30(6), 1-8.
- Merchán, V., Romero, E., and Vaunat, J. (2011). “An adapted ring shear apparatus for testing partly saturated soils in the high suction range.” Geotechnical Testing Journal, ASTM, 34(5), 433-444.
- Merchán, V., Vaunat, J., Romero, E., and Meca, T. (2008). “Experimental study of the influence of drying on the residual friction angle of clays.” Proc., First European Conference on Unsaturated Soils, Durham, U.K., Eds: D.G. Toll, C.E. Augarde, D. Gallipoli, and S.J. Wheeler, CRC Press, 423-428.
- Nishimura, T., and Fredlund, D.G. (2003). “A new triaxial apparatus for high total suctions using relative humidity.” Proc., 12th Asian Regional Conference on Soil Mechanics & Geotechnical Engrg., Singapore, vol. 1, 65-68.
- Olsen, H.J. (2002). “Laboratory measurement of soil mechanical parameters for an annually mouldboard ploughed versus unploughed soil.” Soil & Tillage Research, 64, 263-274.
- Romero, E., Della Vecchia, G., and Jommi, C. (2011). “An insight into the water retention properties of compacted clayey soils.” Géotechnique, 61(4), 313-328.
- Romero, E., Hoffmann, C., Castellanos, E., Suriol, J., and Lloret, A. (2005). “Microstructural changes of compacted bentonite induced by hydro-mechanical actions.” Proc., International Symposium on Large Scale Field Tests in Granite, Sitges, Spain, *Advances in Understanding Engineered Clay Barriers*, Eds: E.E. Alonso and A. Ledesma, Taylor & Francis Group, London, 193-202.
- Romero, E., Gens, A., and Lloret, A. (2003). “Suction effects on a compacted clay under non-isothermal conditions.” Géotechnique, 53(1), 65-81.

- Sabatini, P.J., Elias, V., Schmertmann, G.R., and Bonaparte, R. (1997). *Geotechnical Engineering Circular Number 2: Earth Retaining Systems*. Washington, D.C.
- Stark, T.D., Choi, H., and McCone, S. (2005). "Drained shear strength parameters for analysis of landslides." J. of Geotechnical and Geoenv. Engrg., 131(5), 575-588.
- Shinohara, K., and Golman, B. (2002). "Dynamic shear properties of particle mixture by rotational shear test". Powder Technology, 122, 255-258.
- Stark, T.D., and Eid, H.T. (1997). "Slope stability analyses in stiff fissured clays". Journal of Geotechnical and Geoenvironmental Engineering, 123(4), 335-343.
- Stark, T.D., and Contreras, I.A. (1996). "Constant volume ring shear apparatus". Geotechnical Testing Journal, 19(1), 3-11.
- Stark, T.D., and Poeppel, A.R. (1994). "Landfill liner interface strengths from torsional-ring-shear tests". Journal of Geotechnical Engineering, 120(3), 597-617.
- Stark, T.D., and Eid, H.T. (1994). "Drained residual strength of cohesive soils". Journal of Geotechnical Engineering, 120(5), 856-871.
- Stark, T.D., and Vettel, J.J. (1992). "Bromhead ring shear test procedure". Geotechnical Testing Journal, 15(1), 24-32.
- Tang, A.M., Cui, Y.-J., and Barnel, N. (2008). "Thermo-mechanical behaviour of a compacted swelling clay." Géotechnique, 58(1), 45-54.
- Uchaipichat, A., Khalili, N., and Zargarbashi, S. (2011). "A temperature controlled triaxial apparatus for testing unsaturated soils." Geotechnical Testing Journal, 34(5), 424-432.

- Uchaipichat, A., and Khalili, N. (2009). “Experimental investigation of thermo-hydro-mechanical behaviour of an unsaturated silt.” Géotechnique, 59(4), 339-353.
- Vanapalli, S.K., Fredlund, D.G., Pufahl, D.E., and Clifton, A.W. (1996). “Model for the prediction of shear strength with respect to soil suction.” Canadian Geotechnical Journal, 33(3), 379-392.
- Vaunat, J., Merchán, V., Romero, E., and Pineda, J. (2007). “Residual strength of clays at high suctions.” Proc., Second International Conference on Mechanics of Unsaturated Soils, Weimar, Germany, vol. 2, 151-162.
- Vaunat, J., Amador, C., Romero, E., and Djeren-Maigre, I. (2006). “Residual strength of a low plasticity clay at high suctions.” Proc., Fourth International Conference on Unsaturated Soils, Carefree, Arizona, vol. 1, 1279-1289.
- Villar, M.V., and Lloret, A. (2004). “Influence of temperature on the hydro-mechanical behaviour of a compacted bentonite.” Applied Clay Science, 26(14), 337-350
- Wang, G., Sassa, K., and Fukuoka, H. (2003). “Downslope volume enlargement of a debris slide-debris flow in the 1999 Hiroshima, Japan, rainstorm.” Engineering Geology, 69, 309-330.
- Wang, Y., and Kwong, J. (2002). “Shear strength of soils containing amorphous clay-size materials in a slow-moving landslide.” Engineering Geology, 65, 293-303.
- Wang, F.W., Sassa, K., and Wang, G. (2002). “Mechanisms of a long-runout landslide triggered by the August 1998 heavy rainfall in Fukushima Prefecture, Japan.” Engineering Geology, 63, 169-185.

- Watry, S.M., and Lade, P.V. (2000). “Residual shear strengths of bentonites on Palos Verdes Peninsula, California.” Geotechnical Special Publication No. 101, Geo-Institute of the ASCE, 323-342.

Biographical Information

Jairo Edmundo Yepes Heredia was born in Pasto, Colombia on October 10, 1981. He earned his B.S. degree in Civil Engineering from the “Universidad Nacional de Colombia”, in Manizales, Colombia in January 2006. In August 2006, he started his graduate studies in the Geotechnical Engineering section of the “Universidad Nacional de Colombia”, in Bogota, Colombia, where he earned a M.Sc. degree in Geotechnical Engineering. In summer 2011, he was started his graduate studies at The University of Texas at Arlington, as a doctoral student. Mr. Yepes has completed all the requirements for the Degree of Philosophy Doctor in Civil Engineering in November 2015, graduated in December 2015, and therefore he earned his degree at UTA.